ISSN-0571-7112

ԱՍՏՂԱՖԻԶԻԿԱ
АСТРОФИЗИКА

ТОМ 38 НОЯБРЬ, 1995 ВЫПУСК 4

Выходит с 1965 г.
на русском и английском языках

"АСТРОФИЗИКА" - научный журнал, издаваемый Национальной Академией наук Республики Армения. Журнал печатает оригинальные статьи по физике звезд, физике туманностей и межзвездной среды, по звездной и внегалактической астрономии, а также статьи по областям науки, сопредельным с астрофизикой. Журнал предназначается для научных работников, аспирантов и студентов старших курсов.

«ԱՍՏՂԱՖԻԶԻԿԱ»-ն գիտական հանդես է, որը հրատարակում է Հայաստանի Հանրապետության Գիտությունների Ազգային ակադեմիան։ Հանդեսը տպագրում է ինքնատիպ հոդվածներ աստղերի ֆիզիկայի, միգամածությունների և միջաստղային միջավայրի ֆիզիկայի, աստղաբաշխության և արտագալակտիկական աստղագիտության, ինչպես նաև աստղաֆիզիկային սահմանակից բնագավառների գծով։ Հանդեսը նախատեսված է գիտական աշխատակիցների, ասպիրանտների և բարձր կուրսերի ուսանողների համար։

FRENCH-ARMENIAN ASTRONOMICAL COLLOQUIUM

The first Colloquium between French and Armenian astronomers in frame of collaboration between astronomers of both countries took place on September 29 - October 4, 1995 in Byurakan Astrophysical Observatory of the National Academy of Sciences of the Republic of Armenia.

The purpose of the meeting first of all was to discuss the main topics of researches of astronomers in both countries to promote further effective collaboration between them. This was the reason that the subject of the Colloquium was very wide including the results of various kind of investigations from stars to galaxies and galaxy systems. Some of reports were reviews of own works of the authors.

Welcome speeches were held by academician Victor Ambartsumian, by the president of the Armenian National Academy of Sciences, academician Fadey Sarkissian and by the Ambassador of France in Armenia M-me France d'Harting.

The present issue of "Astrofizika" is devoted to the reports given at the Colloquium. The articles are arranged according to the programme of the Colloquium. The posters are collected at the end of the issue.

We are grateful to Drs. H.Harutyunian, R.Kandalian, A.Mickaelian for their valuable contribution in the editorial work of the issue.

The organization of the colloquium as well as this publication became available thanks to financial support of CNRS (PICS no247), MESR (programme PARCECO), AFACS (Association Franco-Armenienne pour la Cooperation Scientifique), Observatoire de Paris, CNFA. We would like to express our thanks to them for their encouraging support.

L.V.Mirzoyan, A.T.Kalloghlian
The editors

LADIES AND GENTLEMEN

This is to welcome all participants of the French-Armenian Colloquium on Astrophysics. It is difficult to imagine any other scientific discipline which is in larger degree connected with the international cooperation. In this final decade of our century the significance of such cooperation has increased enormously. New ideas and new conceptions are propagating from one country to another with enormous speed which accelerates the progress of astronomy very strongly.

I wish to all of you successful work and good health.

Victor Ambartsumian
1995, September 29
Byurakan

АСТРОФИЗИКА

ТОМ 38 НОЯБРЬ, 1995 ВЫПУСК 4

THE OPTICAL OBSERVATIONS OF FLARE STARS IN THE GALAXY

L.V.MIRZOYAN, V.V.HAMBARIAN, A.T.GARIBJANIAN, A.L.MIRZOYAN

Byurakan Astrophysical Observatory

The observations of flare stars in the Galaxy are considered. The UV Ceti type stars of the solar vicinity and the flare stars in star clusters and associations have almost the same properties. The differences between them are connected with the age. Flare stars are one of richest populations in the Galaxy. The evolutionary path for all flare stars is the same.

1. *Introduction.* Stellar evolution is connected with nonstationary states of stars and stellar groups. This regularity was confirmed when in 1947 Ambartsumian [1] discovered ***stellar systems of a new type - stellar associations***. For the first time it has been established that the star formation process is continuing in the Galaxy.

In 1949 a new type flaring variables are discovered (UV Cet type) among red dwarf stars of solar vicinity. The flares of the UV Cet type stars are similar to outbursts of novae, but happened very frequently.

The observation of Joy and Humason [2] of the spectrum of UV Cet showed that its flare was conditioned by the intensification of its continuum, which was unexpected phenomenon. At present about 100 stars of this type are discovered [3].

Ambartsumian [4] noted that the UV Cet type flare stars showed emission lines and UV-excess during their flares i.e. they are physically similar to the T Tau stars.

However, the T Tau type stars are very young stars, while UV Cet type stars are much older ones. This discrepancy was explained after by Haro and Morgan [5] who detected the first flare stars in the Orion association, which had higher luminosites.

The discovery of flare stars of different ages [see 6,7] allowed to explain the observed differences between their parameters (luminosity, connection with diffuse matter etc.) as a result of their evolution.

In this paper the main results of the study of flare stars in star clusters and associations and in general galactic star field obtained in the Byurakan Astrophysical Observatory are presented.

2. *The UV Cet type flare stars of solar vicinity.* The UV Cet type red dwarf flare stars of solar vicinity have too lower luminosities and are observed separately by photoelectric method.

The physical properties (frequencies, colours, random distribution of flares, forms of light curves, spectral peculiarities and others) of the UV Cet type flare stars were known owing to photometric and spectral observations by Gershberg and Chugainov, Kunkel, Cristaldi and Rodono, Moffett, Moffett and Bopp(see, [6,7]).

However, the evolutionary importance of flare stars was revealed only after the detection of flare stars in star clusters and associations.

3. *The flare stars in star clusters and associations.* The existence of flare stars in associations and then in star clusters has decisive significance for the problem of evolution of red dwarf stars.

For the detection of flare stars of higher luminosities in stellar systems the photographic method with wide-field telescopes is used which allowed to detect at once all enough powerful stellar flares taking place during observations [8]. This search is generally realized by the method of stellar chains. With increasing of exposure time for each image of a star in the chain the time resolution of flare observations is decreasing strongly and the short, even large, flares are lost.

The analysis of this question based on the photoelectric observations of flares of the UV Cet type stars carried out by Moffett [9] showed, for example, that of 297 flares registered in the U-band only 21 and of 342 flares observed in the B-band non could be detected by the photographic method [10]*.

The discovery of numerous flare stars in star clusters and associations was established by photographic observations in the Asiago (Italy), Tonantzintla (Mexico) and Byurakan (Armenia) observatories. Soon the photographic search of flare stars in regions of stellar systems were began in the Abastumani (Georgia), Konkoly (Hungary) and Rozhen (Bulgaria) observatories (see, [6,7]).

4. *Significance of the discovery of red dwarf stars and their distribution in the Galaxy.* The discovery of the first flare star (UV Cet) showed its unusual properties, but it was impossible to predict the importance of this discovery for the problem of evolution of red dwarf stars.

Haro [8] was the first who understood the evolutionary status of flare stars. Taking into account observations he concluded that the T Tau stars are in average younger, than flare stars. Haro [8] suggested a hypothesis according to which flare stars present an evolutionary stage of red dwarf stars following the stage of T Tau type stars.

* *The first flare star in Byurakan Astrophysical Observatory was discovered in 1962, in Orion association [11].*

This hypothesis became a regularity of red dwarf stars evolution when Ambartsumian [12] showed that all or almost all red dwarf stars of lower luminosities in the Pleiades cluster must be flare stars.

From the view of evolutionary connection of the T Tau type stars and flare stars, as stages which pass red dwarf stars there are very important two facts: 1. the flare activity of some T Tau stars (see [13]), 2. the existence of the joint multiple systems of the Trapezium type containing the T Tau type and flare stars together [14]. It is naturally to suppose, that stars are formed in stellar associations, which corresponds to the observed space distribution of flare stars in the Galaxy. Namely, all flare stars having comparatively high luminosities are observed in star clusters and associations whereas the luminosities of flare stars are regulary decreasing, in average, with moving off from their "maternal" systems.

For example, during 180 hours photographic observations of general galactic field only one flare was detected, while in the Pleiades region one flare is observed in every 1-2 hours [6]. This is the reason that the flare activity can be considered as an evidence of the membership of a star in the nearby system. To determine the space distribution of flare stars of lower luminosities in the Galaxy the distribution of UV Cet type flare stars of solar vicinity was used. It has been shown that the results of photographic observations of stellar flares are in complete agreement with the assumption that the UV Cet type stars of solar vicinity are distributed almost uniformly in the galactic disk [10].

The portion of the UV Cet type flare stars among flare stars detected in regions of star clusters and associations is less than 10%.

5. *Some evidences indicating the physical and evolution similarity of all red dwarf flare stars.* We have some evidences in favour of the physical similarity of all red dwarf flare stars. The observations of flare stars show that there is no essential difference between light curves of the UV Cet stars and flare stars in associations and star clusters [15]. The colours of flare emission is practically the same for flares in both groups. Haro's [16] division of all observed flares into two groups by the flare rising time - "fast" and "slow" is general property of flares for all flare stars. The Herzsprung-Russell diagram is similar for both groups [13]. The energetic spectra of red dwarf flare stars in star clusters and associations are the natural continuation of the energetic spectra of the UV Cet type flare stars of the solar vicinity [17]. The flare frequencies of flare stars in the star clusters and associations are depend on their luminosities, in both cases. At last, the spectra of flare stars in the star clusters and associations and of the UV Cet type flare stars of solar vicinity are completely the same [18].

6. ***Variations in flare systems with their aging.*** Comparison of flare star systems of different ages show that the properties of flare stars change with aging. For example, the mean luminosities of them in systems of various ages are quite different.

Table 1 constitutes the results of photographic observations of flare stars in nearest star clusters and associations obtained mainly by the post-graduated students of the Byurakan observatory (I.Jankovicz, M.K.Tsvetkov, H.S.Chavushian, N.D.Melikian, A.S.Hojaev, R.Sh.Natsvlishvili, V.V.Hambarian) (see [6,7]). The total number of flare stars in them at present exceeds 2000.

Table 1

MEAN LUMINOSITIES AND AGES OF FLARE STARS IN THE NEAREST STELLAR SYSTEMS

System	n	M_{pg}	T(yr)
Orion	473	7.7	3×10^5
Cygnus(NGC 7000)	56	8.1	2×10^6
Monocerotis(NGC 2264)	29	6.3	6×10^6
TDC	58	9.1	10^7
Pleiades	191	9.7	7×10^7
Preasepe	14	10.1	4×10^8
UV Ceti region	16	10.0	10^8-10^{10}

Note- n-is the number of the used flare stars, M_{pg} - mean photographic magnitude and T(yr) -estimated age of the system in years. TDC - Taurus Dark Clouds.

Comparison of numbers presented in two last columns show the regular decrease of the mean luminosity of flare stars (Fig.1).

Only in NGC 2264 association the mean luminosity deviates from the normal correlation, which may be explained by errors in determination of distance or age of this system.

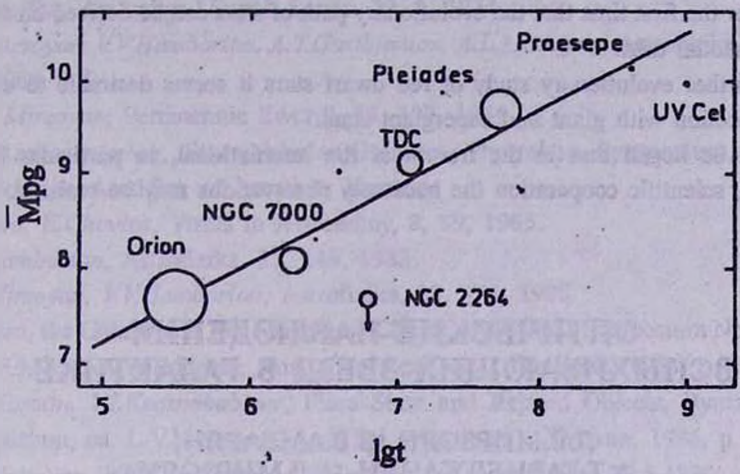

Fig.1. The observed correlation between the mean luminosity of flare stars in star clusters and associations with their aging.

It is seen that with aging of the system the mean luminosity of flare stars is regularly decreasing.

The observed correlation includes the observational selection: as farther is the system as larger is this selection. This selection can change the inclination of this correlation but not sharply. The correlation (M_{pg} , lgt) shows the real direction of variations of mean luminosities in stellar systems with aging (see [19]).

7. *Conclusion.* The optical observations of flare stars in the Galaxy, in particular in regions of star clusters and assotiations revealed the evolutionary importance of these stars in evolution of red dwarf stars.

There are evidences that the evolutionary path of red dwarf stars can be state on the base of observational data. Namely, it is very probable the following evolutionary path of these stars [7].

T Tau Stars - Flare Stars - Red Dwarf Stars of Constant Radiation.

The photographic observations showed that all flare stars are formed in star clusters and associations and then have left their "maternal" systems owing to their motions and disintegration of these systems. At the same time with the aging they continuously lost the flare activity and constitute the population of galactic disk. The UV Cet type flare stars are members of the disk population. This is the reason that the stars of lowest luminosities in the Galaxy are among flare stars.

It is for the first time that the evolutionary path of stars can be derived on the base of observational data.

For further evolutionary study of red dwarf stars it seems desirable to examine their connection with giant and supergiant stars.

It can be hoped that in the frames of the international, in particular French-Armenian, scientific cooperation the necessary observations may be realized.

ОПТИЧЕСКИЕ НАБЛЮДЕНИЯ ВСПЫХИВАЮЩИХ ЗВЕЗД В ГАЛАКТИКЕ

Л.В.МИРЗОЯН, В.В.АМБАРЯН,
А.Т.ГАРИБДЖАНЯН, А.Л.МИРЗОЯН

Обсуждены наблюдения вспыхивающих звезд в Галактике. Звезды типа *UV* Кита окрестности Солнца имеют почти одинаковые свойства, что и вспыхивающие звезды в звездных скоплениях и ассоциациях. Различия между ними связаны с возрастом. Вспыхивающие звезды являются одним из богатых звездных населений Галактики. Эволюционный путь одинаков для всех вспыхивающих звезд.

REFERENCES

1. *V.A.Ambartsumian*, Astrophysics and Stellar Evolution, Acad.Sci. Armenia, Yerevan, 1947.
2. *A.H.Joy, M.L.Humason*, Publ. Astron. Soc. Pacific, 61, 179, 1949.
3. *R.E.Gershberg*, Flare Stars of Small Masses, Nauka, Moscow, 1978.
4. *V.A.Ambartsumian*, Comm.Byurakan Obs., 13,3,1954.
5. *G.Haro, W.Morgan*, Astrophys.J., 118,16,1953.
6. *L.V.Mirzoyan*, Stellar Instability and Evolution, Armenian Acad.Sci., Yerevan, 1981.
7. *L.V.Mirzoyan*, Early stages of Stellar Evolution, Armenian Acad. Sci., Yerevan, 1991.
8. *G.Haro*, Non-Stable Stars, IAU Symposium No.3, ed.G.H.Herbig, Cambridge University Press, Cambridge, 1957, p.26.

9. *T.J.Moffett*, Astrophys.J.Suppl. Series. 29, 1, 1974.
10. *L.V.Mirzoyan, V.V.Hambarian, A.T.Garibjanian, A.L.Mirzoyan*, Astrofizika, 29, 44, 1988.
11. *L. V. Mirzoyan*, Peremennie Zwezdi, 15, 192, 1964.
12. *V.A.Ambartsumian*, Stars,Nebulae,Galaxies, Byurakan Symposium, ed. V.V.Sobolev, Acad.Sci. of Armenia, Yerevan.
13. *G.Haro, E.Chavira*, Vistas in Astronomy, 8, 89, 1965.
14. *V.V.Hambarian*, Astrofizika, 28, 149, 1988.
15. *L.V.Mirzoyan, V.V.Hambarian*, Astrofizika, 28, 375, 1988.
16. *G. Haro*, the Galaxy and The Magelanic Clouds, IAU-URSI Symposium No.20, eds. F.J.Kerr, A.W.Rodgess, Australian Acad. Sci., Canberra, 1964, p.30.
17. *S.A.Korotin, V.I.Krasnobabtsev*, Flare Stars and Related Objects, Byurakan Symposium, ed. L.V.Mirzoyan, Acad.Sci. of Armenia, Yerevan, 1986, p.147.
18. *L.V.Mirzoyan, V.V.Hambarian, A.T.Garibjanian*, Astrofizika, 33,5,1990.
19. *L.V.Mirzoyan*, "Flares and Flashes" IAU Colloquium No 151, eds. H.W.Durbeek, J.Greiner, R.E.Gershberg, Spinger-Verlag, 1995, p.55.

АСТРОФИЗИКА

ТОМ 38 НОЯБРЬ, 1995 ВЫПУСК 4

SPECTRAL SIGNATURES OF SOLAR STRUCTURES

Z.MOURADIAN

Observatoire de Paris-Meudon DASOP 92195 Meudon CEDEX France

A review on physical properties of various regions of the solar atmosphere is given for both quiet and active sun. More typical morphological and spectral features for each region are presented. Possible genetic relations between solar structures are indicated.

1. *Introduction.* The findings of research in the Solar atmosphere may help interpret the stellar spectra, at least for stars of spectral classes F and G.

Stellar atmospheres can be studied by scanning the surface of the star, using either the companion (in the case of double stars) or the stellar rotation as for Doppler-Zeeman Imaging methode (Semel,1995). For the long lived structures, stellar rotation introduces a modulation of the spectral features, in which case structures are considered to constant in time. In the present paper we shall propose a spectral method, in which the variation of spectral lines is studied generally in relation to the rotation of the star. We shall review specific spectral characteristics of certain solar structures, which can help in identifying the structures in the stellar atmosphere.

Traditionally, the Sun's atmosphere is divided into three layers - the photosphere, the chromosphere and the corona - and radially, into the Quiet and Active Sun. The two main phenomena which structure the solar atmosphere are the convection and the magnetic field, which guide the energy flow and/or the material flow, with higher efficiency in chromosphere and in corona. The existence and the variation of the Active Sun is due to the magnetic field. On the other hand, convection is the cause of the appearance of Photospheric Granulation, of Supergranulation, and probably of the Giant Cells (Unipolar Magnetic Regions).

In the following sections we shall mention - for a limited number of solar structures - a short morphological description, their origin (how they may be generated), their general properties, and their spectral characteristics. These may help in detecting these structures in the stellar atmosphere. We shall limit the present paper to the discussion of the visible spectrum.

In stellar atmospheres the structures may have different geometrical dimensions and small variations in physical characteristics with respect to the Sun. The differences observed between the stellar atmosphere and Solar quiet atmosphere, can be interpreted as differences in the physical conditions.

2. *Quiet sun.* The main characteristic of the quiet Sun is its homogeneity with regards to the spatial resolution expected from the rotation effect. An average model of the quiet atmosphere is given by the VAL-C model (Vernazza et al., 1981) in Fig. 1, which is always taken as reference for the quiet Sun atmosphere.

2.1. Photospheric Granulation. Morphology: Photospheric granules are the smallest convective elements of solar quiet atmosphere. They are irregular polygons. Granules are bright, surrounded by darker intergranules.

Origin: The granules are formed in the last 300 km of the convective zone, where convective instability occures because of hydrogen atom recombinations.

Physical Properties: The average granular diameter is 1000 km, and the distance between granules is around 2000 km. The upward velocity is ~0.5 km/s and the temperature jump relative to the intergranular material of 700 K. The granule - intergranule contrast is about 15%.

Spectral detection: The integrated solar spectrum, covering granules and intergranules, is revealed in a C-shaped distortion of spectral lines. The line width also shows variations with time, relative to the Solar Activity cycle (Livingston,1994).

2.2 Spicules. Morphology: Spicules are the fine structures of the solar chromosphere. At the limb they appear as inclined cylinders penetrating the corona. In fact, they are chromospheric plasma trapped in magnetic flux tubes and ejected into the corona.

Origin: Spicules form at the boundary of supergranules. Several models propose upward mechanism for the plasma. The most likely models are those based on the pinching of magnetic field.

Physical Properties: The geometrical dimensions are: height ~11000 km, diameter ~800 km; tilt of 30° with in respect to the local vertical. The upward velocity is 40 km/s; the temperature is about 10^4 K and the density 10^{11} cm^{-3} at 6000 km. There are roughly $7 \cdot 10^6$ spicules on the solar surface, i.e. covering 1% of the solar surface. Spicules continually feed the corona with plasma, which is partially lost through solar wind.

Spectral detection: The upward motion of the plasma and the optically thick Ca II K (3934Å) and H (3968Å) lines produce a higher intensity of the K2v or H2v

Table 1

INTENSITY RATIOS IN THE SOLAR SPECTRUM

Spectral line	Intensity ratio	Disk center	Irradiance
Ca II K	I(K2v)/I(K2r)	1.11	1.12
Ca II K	I(K2v)/I(K3)	1.62	1.72
Ca II H	I(H2v)/I(H2r)	1.10	1.07
Ca II H	I(H2v)/I(H3)	1.68	1.73
HI	$I_0(H\alpha)/I_0(H\beta)$	0.91	1.15
HI	$I_0(H\alpha)/I_0(H\gamma)$	1.03	1.01
HI	$I_0(H\alpha)/I_0(H\delta)$	1.12	0.77

components with respect to the K2r (H2r) or to K3 (H3) (see Table I). Another spectral signature of spicules is the emission of He I lines (5875 Å and 10830 Å).

2.3 Supergranulation. Morphology: Supergranulation is a convective feature of the photosphere, clearly showing the material flow from the center to the boundary. Between two adjacent supregranules we find the faculae (flocculis), which are the basis of the spicules. The distribution of flocculis on the surface gives the appearaence of a net, called chromospheric network.

Origin: Supergranulation is due to a convective instability in the convective zone, produced by the recombination of He I atoms.

Physical Properties: The diameter of a supergranule is around 30 000 km, and the lifetime is about one day.

Spectral detection: No direct detections possible, but the presence of spicules is a proof of the existence of the supergranules.

2.4 Quiet Corona. Morphology: The corona is the outerlayer of the solar quiet atmosphere. It is formed by a great number of arch shaped magnetic field tubes. Coronal Holes are regions of open magnetic field. Generally they are located on the solar magnetic pole.

Origin: The corona exists because the coronal arches are heated, but no generally accepted model exists for the heating mechanism; the Alfven Waves seem to be a good candidate (Ofman, 1994; 1995).

Physical Properties: The specific characteristics of the corona are its high temperature (10^6 K) and its low plasma density of about 10^8 cm^{-3} at the base and 10^5

cm^{-3} at four Solar radii. In Coronal Holes the temperature is ~1.6 10^6 K and the density one-third of the quiet corona. A strong temperature gradient (~10^{-2} °/cm) characterizes the transition region between chromosphere and corona.

Spectral detection: The intensity of the white-light corona is about 10^{-6} times that of the photosphere. The continuum spectrum is linear polarized. The spectral lines are due to forbidden transition, as FeXIV 5305Å, Fe X 6374Å. The chromosphere-corona transition provides a rich EUV solar spectrum.

2.5. Prominences. Morphology: The prominence, or filaments when seen on the disk, are the cool components of the corona. They have the appearance of a fine curtain suspended by the magnetic field over the photospere $B^{\prime\prime}=0$ line. They are well observed in H I Hα and Ca II K lines, 6563 Å and 3934 Å respectively. In visible solar spectrum the filament is in absorption mode while the prominence at the limb, is in emission.

Origin: The formation of the prominences by condensation of the coronal plasma under the effect of the magnetic field is not generally accepted.

Physical Properties: Prominences are about 50 000 km high, and ~5000 km thick.They may range from 10^4 to 10^5 km in length. The temperature is 6 000^0-10 000^0 K and the density of 10^{10} to 10^{11} cm^{-3}. The magnetic field is 5-25 G. Prominence may undergo ejection processes, in which case velocities of a few 10^2 km/s may be observed. This is followed by a Coronal Mass Ejection.

Spectral detection: The spectrum of a prominence is very similar to that of the chromosphere. The filament is in absorption in Hα, and invisible in Hγ. So the ratio of these two lines may be an indicator of filaments. The prominence has emission lines in K, Hα and He I 10830Å.

2.6. Global Magnetic Field. The Global Magnetic Field of the Sun is that of the quiet Sun, concentrated on supergranules boundaries. The magnetic field has the effect of a background field even if they are no Active Regions (see Kitt Peak National Observatory magnetic field dayly observations)

The Sun's magnetic flux varies with the Solar Activity. At the minimum, the flux is 8 G. It reaches to 20-25 G during the Sunspot maximum, due to the high number of active regions (Lean,1994).

3. *Active Sun.* Since the spatial distribution of active region being random, in certain limits, the solar rotation may introduce some modulation in spectral lines.

3.1. Sunspots. Morphology: Sunspots are dark limited areas of the photosphere. A sunspot consists of a dark "umbra" and a "penumbra", less dark. They are produced by strong magnetic fields. They exhibit a bipolar structure, nearly parallel to the equator. The magnetic polarity of the preceding spot and that of the following spot are

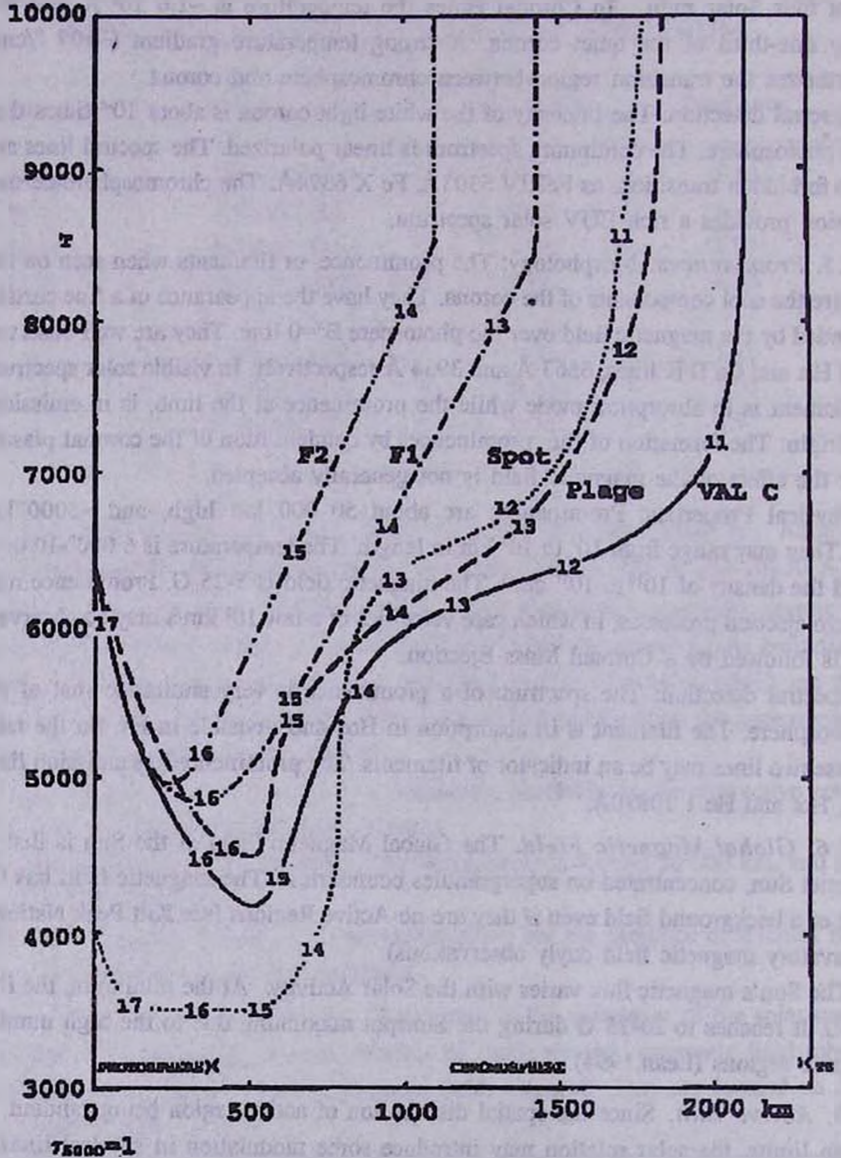

Fig. 1. Comparison of five models of solar armosphere structures: the Quiet Atmosphere (Val-C), the Facular Plage (Plage), the Sunspot (Spot), and Flares (F1 and F2). The numbers indicate the total number of hydrogen atoms.

opposite, and are of reverse polarity in either hemispheres. Sunspots accumulate in "Sunspot Groups".

Origin: *Sunspots are form* when magnetic field tubes are close up by the photospheric velocity field. The magnetic field concentration prevents the energy flux reaching the solar surface. Consequently, the photosphere is locally cool with respect to the environment.

Physical Properties: The spots are almost circular, and can extend to dimensions of one-twelfth the solar diameter. The magnetic field can reach 2 000-3 000 G, and sometimes even 5000 G. The effective temperature and the gas pressure are 0.7 and 0.4 times that of the quiet photosphere, respectively(the Fig. 1 gives the sunspot model of Avrett et al,1981). The average life-time of a sunspot is a few days to a week, but can also be as long as 3 months. The larger the umbra,the stronger the magnetic field and the cooler the temperature is (Bray and Loughhead, 1964).

Spectral detection: *As atmosphere of a sunspot* is cooler than that of the photosphere, the line spectrum is rich in molecular bands, and the continuum spectrum is close to that of stars of class dK0. The most characteristic molecular bands are (Sotirovski, 1971):

-C2 (0,0 band head 5165Å) absent in sunspot, present in the photosphere.

-CN (0,0 band head 3883Å) unchanged in sunspots and in the photosphere.

-MgH(0,0 band head 5212Å) more intense in sunspots than in the photosphere.

-TiO(0,0 band head 5166Å) strong in sunspots, and practically absent in the photosphere.

3.2. Facular Plage. Morphology: The facular plage, or Plage, is a structure of the high photosphere and chromosphere. It is hotter and brighter than the environment. It is composed of a great number of "Chromosphric grains". The plage surrounds the Sunspot group and appears before and disappears after it.

Origin: The medium intensity magnetic field transports the energy toward the surface and heats the facular plage.

Physical Properties: The magnetic field intensity is around 50 to 200 G, and the magnetic flux is 5-8 10^8 Mx. The magnetic structure is generally bipolar, but may also be multipolar. The diameter of the grains is less than 1000 km, and the temperature greater than 900 K (see Fig. 1 Plage model of Lemaire, 1981). Plage range in area from 5 to 20 times that of Sunspot Groups.

Spectral detection: The facular plages are quite visible in Ca II K and H lines and the brightast regions are visible in Hα. A good index for plage is the radio emission in 10.7 cm. Plages can also be identified by the ratio of hydrogen lines (Hiei et al., 1981).

3.3. Coronal Condensation. Morphology: Facular plages in the Active Region are continuous in altitude, with magnetic arches forming a "dome"- shaped structure, the "Coronal Condensation". The plage is in fact the cool end of the hot coronal arches.

Origin: The formation of Coronal condensation is related to that of the AR.

Physical Properties: The temperature is somewhat higher $T=3\cdot10^6$ K, and the electron density is aboud 10^{10} cm^{-3}. Coronal condensation can reach heights of 1/10 $R_\odot$.

Spectral detection: The corona of an Active Region shows a characteristic emission, the forbidden lines (Fe XIV 5303 Å, Ca XV 5694 Å), detected only at the solar limb. On the disk the active regions are "visible" in EUV spectrum, in soft X-rays or in microwaves.

3.4. The Active Region. Morphology: An Active Region (AR) is a configuration consisting of a Sunspot Group, surrounded by a facular plage, and often a filament separating plages of opposite magnetic polarities. Coronal arches, flares and associated phenomena are also components of the Active Region. From the magnetic point of view, an AR may be bipolar or complex (Semel et al., 1991).

Origin: Active Regions are formed by the emergence of magnetic fields close to Pivot Points (Mouradian et al.1987), which are small regions in rigid rotation.

Physical Properties: An Active Region can extend in longitudes of over 20-30°, nearly parallel to the equator. It is located in latitude bands of 10 to 30°, in either hemisphere. During the solar cycle ARs migrate from high latitudes (~35-40°), toward the equator. Often a number of Active Regions are grouped in a limited area, the "Complex of Activity" (Gaizuskas et al., 1983). At the birth of an Active Region, the first composant which appears is the compact and brilliant facular plage, then the Sunspot Group, and in the last phase the Filament. The decreasing phase starts with the disappearance of the Sunspots, then of the Facular Plage, and at the end that of the Filament.

Spectral detection: An Active Region is detected as the sum of its components.

3.5. Flares. Morphology: The Flare is a sudden energy release in the chromosphere and corona, lasting anywhere from a few minutes to one or two hours. The whole solar spectrum is concerned, from elementary particles, γ or X-rays to long radio wave-lengths. The Flare starts by a short "impulsive" phase of a few seconds, and continues with the "gradual" phase. They are generally located inside an Active Region or between two close ARs.

Origin: The source of energy release is the Active Region's corona. The magnetic field accelerates and guides the particles, which tumble down into the chromosphere or upper the photosphere. The magnetic complexity of the Active Region facilitates the release of big flares.

Physical Properties: The energy released by Flare can range up to 10^{28} to 10^{32} erg, and is often accompanied by a "Coronal Mass Ejection" (CME). A flare is formed by a number of "Flaring Arches" (Mouradian et al, 1983; Martine & Svestka, 1988). The plasma temperature rages from 10^4 to 10^7 K.

Spectral detection: The principal spectral lines (H_α, H_β, H_γ, H, K, 10830, among others) are in emission, their profiles are wide and the wings spread (Svestka, 1976). The flares producing accelerated particles induce X-rays and/or γ-rays. In very energetic flares, continuum spectrum emission, appears i.e. the "White Light Flares" (WLF). The spectra of WLF can be of two types (Machado et al., 1980): F1 and F2 (Fig. 1).

-Type I WLFs are the flares for which all the emission maxima are simultaneous. The Balmer jump may be from 0.1 to several times of the continuum. The Balmer lines are intense and broad, whereas the metallic lines are normally wide, as they are for non-WLF. A "blue excess" of the continuum may be detected for this type of flare. Type I flares belong to the F2 model (Fang & Ding, 1994).

-Type II WLFs are due to the H^- emission of the upper photosphere. The maxima of the various spectral features are not simultaneous. The Balmer jump is normal. Fang and Ding class the type II WLF as model F1 flares.

3.6. Coronal Mass Ejection. Morphology: Coronal mass ejection is a very faint long-scale structure, visible over the solar limb.

Origin: The corona plasma is pushed toward the outer corona triggered by a flare or a prominence disruption.

Physical Properties: CME generally covers up to 60° around the solar limb. The speed of ejection is of the order of 100 to 1200 km/s. Often coronal mass ejection is associated to type II or IV radio bursts. Some CME extend to 4.5 $R_\odot$.

Spectral detection: Coronal mass ejection is observed in white light at the Solar limb.

3.7. Solar Wind. Morphology: Solar Wind is a continuum flux of elementary particles toward the interplanetary space. It is a convective process in a divergent monopolar magnetic field.

Origin: Solar Wind emanates from Coronal Holes, principally those of North and South poles.

Physical Properties: The expansion velocity of the plasma is about 15 km/s. The two polar Coronal Holes will come together at a distance of 1 to 2 $R_\odot$ and will form a "Neutral Current Sheet", located around the equatorial plane. At 1 AU the velocity is 400 km/s, the density ~5 cm^{-3} and the T_{prot}~10^4 and T_{elect}~10^5 K. The magnetic field is $5 \cdot 10^{-5}$ G. The solar wind is divided into four alternative magnetic sectors: two high speed and two low speed.

Spectral detection: In the case of the Sun the detection is made in situ, by satellite.

3.8. Activity Cycle. Morphology: The Activity Cycle is an almost periodic variation of structures of the active Sun (Sunspot, Facular Plages, Flare, and so on). The number and importance of these structures vary roughly in phase.

Origin: All the structures participating in the activity cycle are of magnetic origin, so the evolution of the cycle is strongly related to that of the dynamo.

Physical Properties: An Activity Cycle occures between two minima. The increasing phase is more rapid than the descreasing, representing 1/4 and 3/4, respectively, of the total cycle duration. In the Solar case, the cycle is about 11 years for Sunspot numbers, but 22 years for the magnetic field cycle. Note also the longlasting cycle of 80-120 years. In the past, the Solar cycle has weakened, as in the 17th century,over a period of about 70 years. The magnetic flux grows from minimum to maximum by a factor of 2.5 to 3.

Spectral detection: The most sensitive spectral feature is the Ca II K line, due to the variation in the number of Facular Plages. Some other spectral lines also show intensity and width variations in phase with the Solar Activity (Livingston, 1994).

The autor is indebted to Drs. R. Boyer, T. Heristchi, I. Soru-Escaut, P.Sotirovski for helpful discussions.

СПЕКТРАЛЬНЫЕ ОСОБЕННОСТИ СОЛНЕЧНЫХ СТРУКТУР

З. МУРАДЯН

Дан обзор физических свойств различных областей солнечной атмосферы как для спокойного, так и для активного солнца. Для каждой области приведены наиболее характерные морфологические и спектральные оцобенности. Указаны возможные генетические связи между солнечными структурами.

REFERENCES

Allen C.W.:1973, "Astrophysical Quantities", The Athlone Press, London.

Avrett E.H.:1981, in "The Physics of Sunspot" L.E.Cram & J.H.Thomas (eds.) Sacramento Peak Observatory Conference, p. 235.

Badalyan O.G., Livshits M.A.: 1994, in "Solar Coronal Structures", V.Rusin, P.Heinzel, J.C.Vial (eds.), Veda Publ. House, Slovak Acad. of Sci, p.77.

Bouver S.D.: 1992, Solar Phys. 142, 368.

Boyer R., Henoux J.C., Sotirovski P.: 1971, Solar Phys. 19, 330.

Brey R.J., Loughhead R.E.: 1964, "Sunspors",Chapman and Hall Ltd., London.

Fang C. and Ding M.: 1994, Progress in Astronomy 12, 100.

Gaizauskas V., Harvey K.L., Harvey J.W., Zwaan C.: 1983, ApJ, 265, 1056.

Hiel E., Mouradian Z., Dumont S., Pecker J.C.: 1983, in "Active Phenomena in the Outer Atmosphere of the Sun and Stars", J.C.Pecker and Y.Uchida (eds.), Observatoire de Paris Ed., p. 272.

Lean J.: 1994, in "The Solar Engine and Its Influence on Terrestrial Atmosphere and Climate", E. Nesme-Ribes (ed.), NATO ASI Series, Springer-Vrelag, Berlin, p. 163.

Lemaire P.: 1981, Astron. Astrophys 103, 160.

Livingston W.: 1994, in "The Solar Engine and Its Influence on Terrestrial Atmosphere and Climate", E. Nesme-Ribes (ed.), NATO ASI Series, Springer-Vrelag, Berlin, p. 145.

Machado M.E., Avrett E.H., Vernazza J.E., Noyes R.W.: 1980, ApJ 242, 336.

Martin S.F., Svestka Z.: 1988, Solar Phys. 116, 91.

Mouradian Z., Martres M.J., Soru-Escaut I.: 19.., Solar Phys. 87, 309.

Mouradian Z., Martres M.J., Soru-Escaut I., Gesztelyi L.: 1987, Aston.& Astrophys 183, 129.

Mouradian Z., Soru-Escaut I.: 1991, Aston.& Astrophys. 251,649.

Ofman L., Davila J.M., Steinolfson R.S.: 1994, ApJ, 421, 360; 1995, ApJ, 444, 471.

Semel M.: 1995, in "3D Optical solarspectra Methodes in Astronomy", G.Compte and M.Marcelin (eds.), ASP Conference Siries 71, 340.

Semel M., Mouradian Z., Soru-Escaut I., Maltby P., Rees D., Makita M.: 1991, in "Solar Interior and Atmosphere", A.N.Cox, W.C.Livingston, M.S.Matthews (eds.), The Univ. of Arizona Press, Tucson, p. 844.

Sotirovski P.: 1971, Aston.& Astrophys. 14, 319.

Svestka Z.: 1976, "Solar Flares", D.Reidel Publ. Co.

Vernazza J.E, Avrett E.H., Loeser R.: 1981, ApJ Suppl., 45, 635.

АСТРОФИЗИКА

ТОМ 38 НОЯБРЬ, 1995 ВЫПУСК 4

SPECTRAL STUDIES OF YSO ENVELOPES AND COLLIMATED OUTFLOWS

T.Yu.MAGAKIAN, T.A.MOVSESSIAN

Byurakan Astrophysical Observatory,
National Academy of Sciences of Armenia

A short review of the studies of the young nebulous objects in the dark clouds in the Byurakan Observatory. The results of the prolonged observational programme, carried out mainly on the 6-meter telescope of SAO RAS, are described, and the relation of this programme with the methodology of study the non-stable phenomena, traditional for Byurakan, is pointed out.

1. *Introduction.* As the one of the most famous features of the Byurakan Astrophysical Observatory (BAO) always was the special interest for the non-stable astronomical phenomena it is quite understandable that young non-stable stars were (and are) in the focus of the attention of BAO for a long time. Here we shall present a short overview of the observational studies of young nebulous objects in the dark clouds in BAO during the whole history of the observatory and especially in the period of last twenty years.

2. *First studies and searches.* We can assume the classic papers of Ambartsumian [1,2] as the beginning of the studies of young nebulous objects in BAO. Shortly after that several photometric and polarimetric observational works, performed with the modest size telescopes of BAO, were published (for example, [3,4]). But very soon the direction of studies was changed to the preparation of lists of new objects, discovered on the maps of the Palomar Observatory Sky Survey (POSS). The total amount of the thus found nebulous objects in the dark clouds, even after the excluding the overlaps and already known nebulae, was surprisingly high. We shall describe here only the most significant lists.

The first list of 35 new cometary nebulae (CN) in the Taurus-Auriga dark clouds was prepared by Badalian [5], and even if it did not acquired much publicity, it is worth to mention that in this search some Herbig-Haro (HH) objects and collimated outflows were found independently and also for the first time the classification of CN in 4 morphological types was suggested. Much more popularity was gained by the list of CN by Parsamian [6] (which included in particular very interesting object P21). As the next step the lists of 130 new CN, HH and other nebulous objects of Gyulbudaghian and Magakian [7,8,9] should be considered. The list of 36 HH candidates [8] with some additional data was reprinted in [10], and the objects from this work (so-called GGD objects) in the following years became the target of the rather intense studies. The coverage of sky in this survey was quite high: the surveys of Bernes [11] and Cohen [12], published shortly after and conducted on the same principles, show significant overlap with GM objects. But even then not all the young nebulous objects, visible on the POSS maps, were discovered; subsequent works of Gyulbudaghian (see, for example [13,14]) added about 60 new objects.

In the recent years the surveys of young emission and reflection nebulae, based on POSS, were replaced in the world practice by the direct imaging with narrow-band filters, and many new very small and/or very faint objects were revealed by means of this technique. On the other hand, it should be noted that the greatly increased total number of CN, HH and other nebulous objects in the dark clouds suggests the necessity of a new general catalogue of such objects. This problem is only partly covered by the electronic catalogue of HH objects of Reipurth [15], and catalogue of CN, compiled by Parsamian and Petrossian [16] is somewhat outdated and not homogeneous.

It is quite clear that full-scale investigations must include not only the searches but the detailed observational studies as well. Due to the modest capabilities of the equipment available in BAO this kind of studies for a long time were restricted by several spectral observations, obtained with the large telescopes abroad. In accordance with the idea of Ambartsumian that some unusual features of CN could be connected with the instability of their core stars and the outflow phenomena, these researches were aimed mainly to the quest and investigation of different anomalies in the spectra of CN, which could be ascribed to the non-stable activity during the early stages of stellar evolution.

In fact, many of the unusual properties of CN (their shape, colours, variability, violation of the Hubble's relation for the reflection nebulae etc.; see, for example, [16]), which previously were thought to be connected with non-thermal emission and other effects of stellar instability, afterwards were naturally explained by the existence of the absorbing circumstellar disks. But the main idea about the role of anisotropic and directed outflows was true. Just these outflows, as we know presently, are responsible for the spectral peculiarities of the certain CN. (For the review of the anomalous spectra of CN see [17]).

In our opinion, the key object for the understanding the CN phenomenon as a whole is represented by the famous Hubble variable nebula NGC 2261. Indeed, it presents not only the classical features of CN (cometary shape with the young emission-line star in the head; bipolarity; variability; centrosymmetric polarization pattern with the indications of the presence of circumstellar dust disk), but also for the first time the spectral anomaly (the strengthening of the absorption lines in the spectrum of the nebula in comparison with that of the star) was found by Greenstein just for this object [18]. Other important steps were: the discovery of HH objects, located on the axis of the nebula [19]; the detailed study of the spectral anomalies and the idea of the existence of outflow from the central star [20,21]; and the most important one - the interpretation of these anomalies as the spectral asymmetry of the central source, caused by directed outflow [22].

The hypothesis about the collimated outflows from young stellar objects (YSO) was transformed to the established fact when these outflows were at last detected directly by Mundt and his coworkers [23,24].

3. *Observations of last twenty years*. In the 1975 the situation with the observational capabilities of BAO drastically changed when both the 2.6-meter telescope in Byurakan and 6-meter telescope of the Special Astrophysical Observatory (Russia) became operational. This offered new possibilities in the investigations of the young nebulous objects. Moreover, so large amount of the newly found objects literally was demanding the observations. Our observational programme was launched in 1976 and continues up to the present times. Of course, it was changing during these 20 years along with our understanding of the problem and the upgrading of the observational equipment as well. For all these years our programme is and remains the only one in the whole CIS aimed strictly to the studies of CN, HH and their interaction with interstellar medium. We shall briefly describe the stages of the programme and main observational results.

First studies of the new objects from Byurakan lists were performed in 1976-1985. For the morphological studies the direct images on 2.6-meter telescope were obtained. By those the new variable nebulae PV Cep and V1515 Cyg were discovered [25]. The spectral observations were carried out with one-dimensional IPCS on the 6-meter telescope. Many new emission stars and 10 HH objects were found. Especially interesting was the discovery of a new CN with anomalous spectrum - Ber 48 [26].

In 1985-1989 these exploratory observations were replaced by the detailed investigations of the optical jets and inner structures of HH objects with the long-slit equipment on the 6-meter telescope. As the most interesting results we can mention the revealing of the new optical jets CoKu Tau/1 [27] and L723 [28] and the studies of the structure and kinematics of many HH objects.

We continue the long-slit observations on 6-meter telescope up to now, but from 1989 also the new exciting possibility to observe the extended objects by means of three-dimensional spectroscopy, namely with multi-pupil field spectrograph (MPFS) became available. So our present observational programme is based both on the 2D and 3D spectral studies and encompasses the following directions.

a) Studies of shock waves in the jets and HH objects.

As the recent example, the studies in the NGC7129 star formation region could be mentioned [29,30]; for several objects complex H_α-emission profiles were found and their comparison with theoretical profiles was performed. For GGD35 and HH103 the maps of velocity components, compared to their proper motions, suggest unusual internal structures. Some new very faint HH objects, located in this field, for example HH105, were confirmed and their radial velocities obtained for the first time. We studied also the spectra of the faint emission-line stars in this field; especially interesting is the highly variable V350 Cep, for which the conspicuous spectral variations were revealed during the years of observations.

A detailed spectral analysis of the shock structure in the GM1-27 object was performed, using the long-slit spectra with a high spatial resolution [31]. The different behavior of various spectral lines inside the object suggests the presence of spatial stratification. It was concluded, that these observations enabled us to resolve not only the bow shock and Mach disk inside the HH object, but also the bow shock itself.

Just recently we obtained long-slit spectra for the very interesting, but little studied yet chains of HH objects in Orion, namely HH84, HH85, HH94. Strong variations of radial velocity and physical parameters are evident in several condensations; full reduction of the data is in progress.

The main conclusion is the following: the theory describes well the interaction of high-velocity jets and bullets with interstellar medium, but there exist very unusual observed cases, for which we must seek a more elaborated explanations (multiple shocks? unusual internal structure of cloudlets? very inhomogeneous surroundings?).

b) Studies of the sources of anisotropic outflows.

These investigations were performed with MPFS and are being continued.

A new source of an optical collimated outflow (Fig.1) was identified with the emission-line star LkH$_\alpha$225 [32,33]. Subsequent observations revealed a strong variability of the both components of this double star as well as conspicuous changes in the shape of the associated nebula. But we cannot deduce from the present data, which of the two stars excites the HH emission inside the nebula.

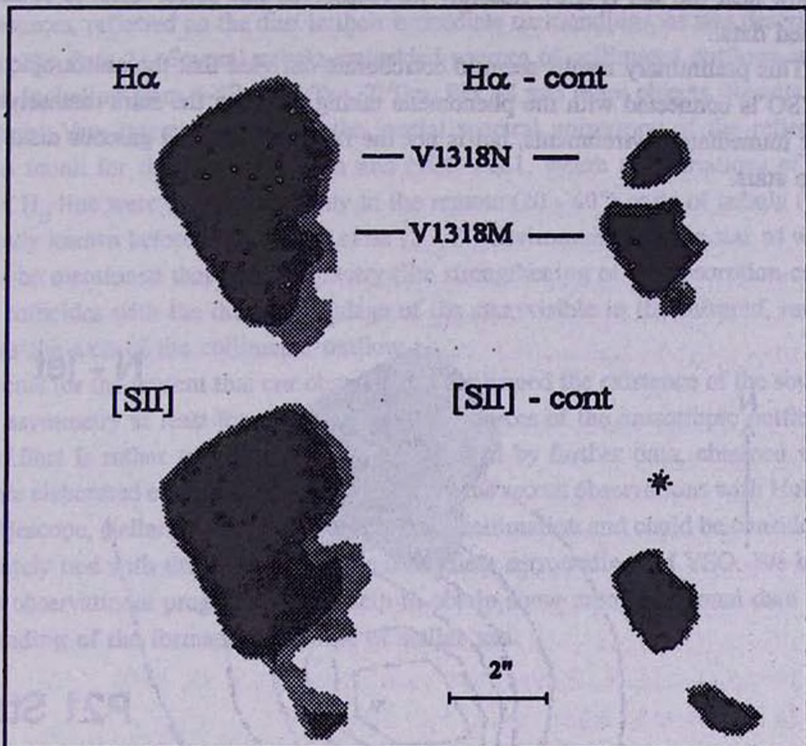

Fig 1. Images of LkH$_{\alpha}$ 225, restored from the spectra, obtained by multi-pupil field spectrograph (MPFS).

Also by means of the integral-field spectroscopy a small collimated jet was revealed near the faint YSO Haro 6-10 [34].

For the star in the apex of the cometary nebula Pars 21, deeply embedded in a circumstellar dusty envelope, and recently identified as a FU Ori-type object, the H$_{\alpha}$ absorption profiles have been studied. The undoubted asymmetry of the star image, observed in the red wing of this line, was revealed. This asymmetry is caused by the shift of the red wing of H$_{\alpha}$ absorption, ascribed to the anisotropy of the cool expanding envelope around the star. In reality we observe, of course, the spectrum of the star, reflected from various angles by different parts of the dusty stellar environment. It was possible also to reconstruct the shape of the both emission lobes of the collimated outflow near the star (Fig.2). Recently we reobserved this object again to obtain more refined data.

This preliminary results seem to corroborate our idea that the anisotropic activity of YSO is connected with the phenomena taking place on the stars themselves or in their immediate environments, but is not the result of dust and gaseous disks around these stars.

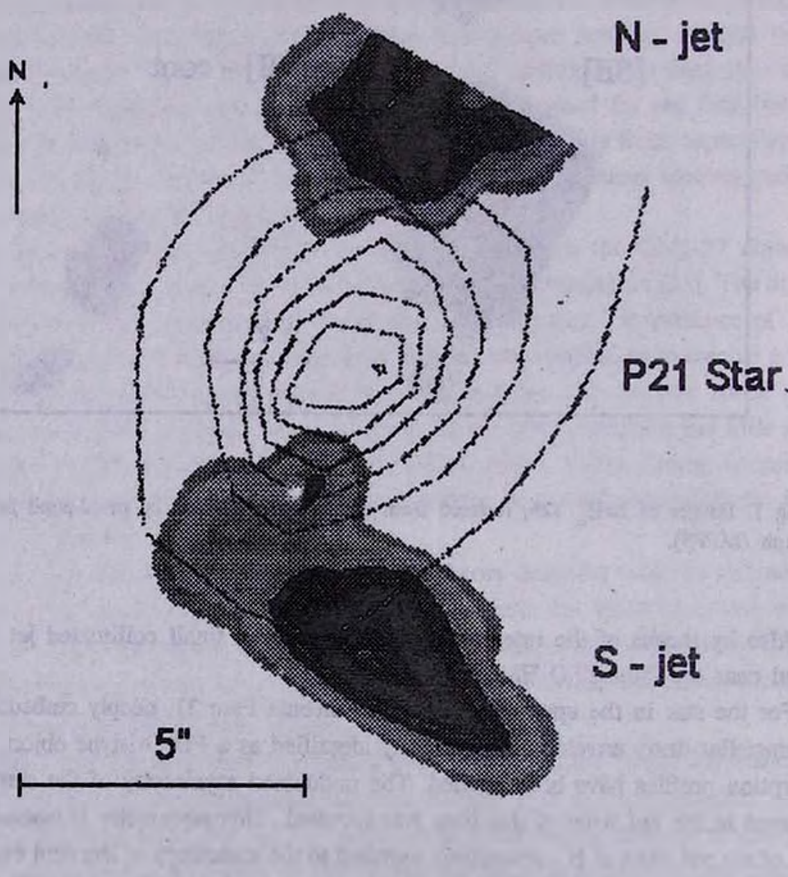

Fig 2. Emission lobes of the bipolar jet from P21 FU Ori-type star, restored from the MPFS spectra.

c) Studies of the reflected spectra of cometary nebulae.

We tried to apply the integral-field spectroscopy to analyze the spectra of the central sources, reflected on the dust in their immediate surroundings, as was described above for the Pars 21. Several nebula-embedded sources of collimated outflows were observed, including Haro 6-5B, CW Tau, T Tau, Ber 48 and other objects. Results are under study. Very interesting case of the spatial spectral anisotropy of the reflected light was found for the famous R Mon and NGC 2261, where the variations of the profile of H_α line were revealed not only in the remote (20 - 40") parts of nebula (this was already known before), but for the close (5 - 7") environments of the star as well. It should be mentioned that this asymmetry (the strengthening of the absorption component) coincides with the dusty appendage of the star, visible in the infrared, rather than with the axis of the collimated outflow.

It seems for the present that our observations confirmed the existence of the sought spectral asymmetry at least for the several stars - sources of the anisotropic outflows, but this effect is rather subtle and must be confirmed by further data, obtained with even more elaborated equipment. As was shown by the recent observations with Hubble Space Telescope, stellar jets indeed have very high collimation and could be considered as intimately tied with the processes in the immediate surroundings of YSO. We hope that this observational programme will help to obtain some more additional data and understanding of the formation and role of stellar jets.

СПЕКТРАЛЬНЫЕ ИССЛЕДОВАНИЯ ОБОЛОЧЕК И КОЛЛИМИРОВАННЫХ ПОТОКОВ МОЛОДЫХ ЗВЕЗДНЫХ ОБЪЕКТОВ

Т.Ю.МАГАКЯН, Т.А.МОВСЕСЯН

Краткий обзор исследований молодых туманных объектов в темных облаках в Бюраканской обсерватории. Описаны результаты продолжительной наблюдательной программы, выполняемой в основном на 6-метровом телескопе САО РАН, и отмечена взаимосвязь этой программы с традиционным для Бюракана методологическим подходом к изучению нестационарных явлений.

REFERENCES

1. *V.A.Ambartsumian*, Comm. BAO, 13, 1954.
2. *V.A.Ambartsumian*, Voprosy kosmogonii, 4, 76, 1955.
3. *E.Ye.Khachikian*, Comm. BAÎ, 25, 67, 1958.
4. *E.S.Parsamian*, Comm. BAÎ, 30, 51, 1962.
5. *G.S.Badalian*, Dokl. AS Arm.SSR, 31, 261, 1960.
6. *E.S.Parsamian*, Izv. AS Arm.SSR, ser. phys.-math., 18, 146, 1965.
7. *A.L.Gyulbudaghian, T.Yu.Magakian*, Pis'ma v AZh, 3, 113, 1977.
8. *A.L.Gyulbudaghian, T.Yu.Magakian*, Dokl. AS Arm.SSR, 64, 104, 1977.
9. *A.L.Gyulbudaghian, T.Yu.Magakian*, Astron.Tsirk. No.953, 1, 1977.
10. *A.L.Gyulbudaghian, Yu.I.Glushkov, E.K.Denisyuk*, Astrophys.J. (Letters), 224, 137, 1978.
11. *C.Bernes*, Astron.Astrophys. Suppl., 29, 65, 1977.
12. *M.Cohen*, Astron.J., 85, 29, 1980.
13. *A.L.Gyulbudaghian*, Pis'ma v AZh, 8, 232, 1982.
14. *A.L.Gyulbudaghian*, Astrofizika, 20, 631, 1984.
15. *B.Reipurth*, A general catalogue of Herbig-Haro objects, 1994.
16. *E.S.Parsamian, V.M.Petrossian*, Comm. BAÎ, 51, 3, 1979.
17. *T.Yu.Magakian, E.Ye.Khachikian*, Trudy GAISh, 60, 274, 1988.
18. *J.L.Greenstein*, Harvard obs. monographs, No.7, 19, 1948.
19. *G.H.Herbig*, Astrophys. J., 152, 439, 1968.
20. *J.L.Greenstein, M.A.Kazarian, T.Yu.Magakian, E.Ye.Khachikian*, Astrofizika, 12, 587, 1976.
21. *J.L.Greenstein, M.A.Kazarian, T.Yu.Magakian, E.Ye.Khachikian*, Astrofizika, 15, 615, 1979.
22. *B.F.Jones, G.H.Herbig*, Astron. J., 87, 1223, 1982.
23. *R.Mundt, J.Stocke, H.S.Stockman*, Astrophys. J. (Letters), 265, 71, 1983.
24. *R.Mundt, J.W.Fried*, Astrophys. J. (Letters), 274, 83, 1983.
25. *A.L.Gyulbudaghian, T.Yu.Magakian, A.S.Amirkhanian*, Pis'ma v AZh, 3, 162, 1977.
26. *T.Yu.Magakian, E.Ye.Khachikian*, Astrofizika, 28, 139, 1988.
27. *T.A.Movsessian, T.Yu.Magakian*, Astrofizika, 31, 501, 1989.
28. *T.A.Movsessian*, Pis'ma v AZh, 15, 131, 1989.
29. *T.Yu.Magakian, J.Boulesteix, M.Marcelin, E.Le Coarer*, Astron. Astrophys, 294, 928, 1994.
30. *T.Yu.Magakian, T.A.Movsessian*, AZh, 1996 (submitted).

31. *T.Yu.Magakian, T.A.Movsessian*, Astron. Astrophys., 295, 504, 1995
32. *T.Yu.Magakian, T.A.Movsessian*, IAU Colloq. No.149, "3D optical spectroscopic methods in astronomy", 292, 1995.
33. *T.Yu.Magakian, T.A.Movsessian, S.V.Dodonov, V.V.Vlasyuk*, Pis'ma v Azh,1996 (submitted).
34. *T.A.Movsessian, T.Yu.Magakian* (in preparation).

АСТРОФИЗИКА

ТОМ 38 НОЯБРЬ, 1995 ВЫПУСК 4

OBSERVATIONS OF STELLAR ASSOCIATIONS ON THE SPACE TELESCOPE GLAZAR

R.Kh.HOVHANNESSIAN[1], H.M.TOVMASSIAN[1,2], R.A.EPREMIAN[1]

1 Byurakan Astrophysical Observatory,
Armenia 378433. E-mail address: byur@mav.yerphi.am
2 INAOE, Puebla, Pue., M'exico

On the base of observations by Space Telescope Glazar at 1640A the distribution of early (O-B-A) type stars and absorption matter in the directions of 20 known OB associations have been investigated. The 44 stellar groups are found in these directions. The dust matter is distributed within these groups quite non-uniformly and patchy.It is absent in the space between these groups. It has been shown that 93 stars have dense circumstellar dust envelopes and the half of them are sources of IR-radiation (IRAS observations). Dust clouds exist in the directions of Per OB1, Aur OB1 and Car OB1 at the distances 460, 1000, 1000 pc, respectively. The 20 new stellar groups of OB types are found out.

The telescope Glazar was taken onto orbit around the Earth at 30 March 1987 installed on the board of astrophysical module *Kwant* of *Mir* Space Station.

The telescope has 1.3° field. The diameter of the main Ritchey-Chretien mirror is 40cm, and the focal length is 1.7m. The linear size of view-field is 40mm, the scale of images is nearly *2'/mm*, the angular resolution is about 20". The microchannal amplifier was used as a detector of ultraviolet radiation. The received information was registered on the photofilm Kodak 103a-G. The band-pass of the whole system is about 250A with a peak at 1640A. The pointing of the telescope towards the observed field is worked out by cosmonauts with the Mir Space Station, the stabilization system of which keeps the given orientation usually with an accuracy about 1'.

Regular observations with orbital telescope Glazar were carried out in August 1987 up to March of 1989. During that time 810 of early type stars were observed in the directions of 20 known stellar associations.

The results of these observations are presented in [1-9]. The limiting apparent magnitude at the wave length 1640A was 11^m at the beginning and decreased to 2.5^m during one and half years. Certainly the absorption is substantially greater at short wave-length than in V-band. The observations by Glazar at 1640A enabled us to find out groups of OB- and A-stars at various distances.

Therefore it is of more importance to determine the distances of stellar groups by the method of plots of variable extinction, i.e. by study of the dependence of modules $(m\text{-}M)_{1640}$ on color excesses $E(m_{1640}\ \text{-}V)$ of stars. This method was given in [7].

Table 1

RESULTS BASED ON OBSERVARTIONS BY GLAZAR

Stellar Association	Num. of Stars (in deg2)	Limit. Mag. at 1640A	Number and Distance of Groups in pc						Num. of Stars with Dust Envel.	Num.of Binary Stars	Num.of Unknown Stars
Cas OB1,2	18(19)	9.0	400	700					5(2)	5	1
Per OB1,3	42(12)	10.0	460*	850	1500	2600			6(4)		
Aur OB1,2	42(17)	8.2	600	1100	2000	3000			4(3)	3	
Ori OB1	102(30)	11.0	130	270	510	730	960?		23(10)	2	1
Gem OB1	13(7)	9.0	300	1100	2400?				5(2)	3	
Mon OB1,2	35(10)	9.0	250	600	1700				6(2)		10
CMa OB1	43(10)	9.0	320	570	1100				8(4)		
Pup OB1,2	159(24)	9.0	120	370	700	1250	2400	4000	5(4)	1	43
Vel OB1,2	71(15)	9.0	110	460	1700				5(4)	4	3
Car OB1,2	233(13)	8.5	560	1100	2000	4000	5600		12(10)		5
Sco OB1	22(8)	10.0	250	1700					5(3)		
Cyg OB1,3	30(9)	10.0	300	660**	1300				4(3)		

* - [13] and ** - [14].

By this investigation we find out [4,6-10] 44 stellar groups, the 20 of them were unknown. The 16 of them contain B3- and later B- type stars, while 4 contain also O-B2 type stars.

The distribution of the dust matter in these groups seemed to be non-uniform and patchy. We must point out that the dust is mainly found within groups being absent in the space between them.

It has been shown that 15 stars of A0-F4 spectral type are being binary systems, with the components of hot stars of sdO-sdB types.

The 93 stars with the assumed circumstellar dust envelopes are found out and 53 of them are sources of IR-radiation according to IRAS [11].

The linear sizes and the masses of dust envelopes are determined for 36 stars in the directions of Cas OB1-OB2, Per OB1 and Ori OB1 [12]. These parameters differ strongly: the radii are in the limits 130÷3250*a.u.*, and the masses are from $10^{-7} M_{\odot}$ up to $10^{-2} M_{\odot}$.

The 66 stars among observed objects are uncatalogued stars.

It has been shown that the interstellar absorption law differs from normal one within the Carina nebulae: R_{1640}=2.14 and R_V=4.0, while according to the normal law R_{1640}=1.75 and R_V=3.2-3.3.

The list of studied 20 stellar associations is given in Table 1, with names, numbers of observed stars in each association (where the fields in deg² are given in parentheses), limiting magnitude at 1640A, distances of groups (in pc) in directions of these associations, number of stars with the assumed circumstellar dust envelopes (the number of IRAS stars are given in parentheses), number of binary stars and numbers of unknown OB stars.

It is shown that two associations exist in direction Per OB1 (d= 1900-2300pc [15-18]), which are projected each on the other. The distance between them is 1000pc [10,13,19,20].

Dust clouds in the directions of Per OB1, Aur OB1 and Car OB1 exist at distances 460, 1000 and 1000pc, respectively.

НАБЛЮДЕНИЯ ЗВЕЗДНЫХ АССОЦИАЦИЙ НА КОСМИЧЕСКОМ ТЕЛЕСКОПЕ "ГЛАЗАР"

Р.Х.ОГАНЕСЯН, Г.М.ТОВМАСЯН, Р.А.ЕПРЕМЯН

По результатам наблюдений, выполненных на космическом телескопе "Глазар" на 1640А, исследовано распределение звезд ранних спектральных классов и поглощающей материи в направлениях 20 известных OB-ассоциаций. В направлениях этих ассоциаций обнаружены 44 звездные группировки. Пылевая материя распределена в объемах этих группировок весьма неравномерно и клочковато. Пыль отсутствует в пространстве вне этих группировок. Показано, что 93 звезды погружены, возможно, в сравнительно плотные околозвездные пылевые оболочки, половина которых является источником ИК-излучения (наблюдение IRAS). Показано, что существуют пылевые облака, в направлениях Per OB1, Aur OB1 и Car OB1, на расстояниях 460, 1000 и 1000 пк соответсвенно. Обнаружены 20 новых звездных группировок OB спектральных классов.

REFERENCES

1. *H.M.Tovmassian, Yu.M.Khodjayants, M.N.Krmoyan, A.L.Kashin, A.Z.Zakharian, R.Kh.Hovhannessian, M.A.Mkrtchian, G.H.Tovmassian, D.Huguenin, V.V.Bootov, Yu.V.Romanenko, A.J.Laveikin, A.P.Alexandrov,* Pisma v Astron. J., 14, 291,1988.
2. *H.M.Tovmassian, R.Kh.Hovhannessian, R.A.Epremian, D.Huguenin, S.I.Serova, V.G.Titov, M.Kh.Manarov*, Astrophys. Space Sci., 174, 279,1990.
3. *H.M.Tovmassian, R.Kh.Hovhannessian, R.A.Epremian, M.A.Mkrtchian, Yu.M.Khodjayants, M.N.Krmoyan, A.L.Kashin, D.Huguenin, Yu.V.Romanenko, A.P.Alexandrov, B.G.Titov, M.Kh.Manarov, A.A.Volkov, S.K.Krikalev*, Astrofizika, 32,197,1990.
4. *H.M.Tovmassian, R.Kh.Hovhannessian, R.A.Epremian, D.Huguenin, A.S.Viktorenko, A.A.Serebrov,* Russian Astron.J., 68, 942, 1991.
5. *H.M.Tovmassian, R.Kh.Hovhannessian, R.A.Epremian, D.Huguenin, A.A.Volkov, S.K.Krikalev*, Astrofizika, 35, 167,1991.
6. *H.M.Tovmassian, R.Kh.Hovhannessian, R.A.Epremian,D.Huguenin, Yu.M.Khodjayants, M.N.Krmoyan, A.L.Kashin, Yu.V.Romanenko, A.P.Alexandrov*, Astrophys. Space Sci., 188, 217,1992.
7. *H.M.Tovmassian, R.Kh.Hovhannessian, R.A.Epremian, D.Huguenin*, Astron. Astrophys. Suppl.Ser., 100, 501, 1993.
8. *H.M.Tovmassian, R.Kh.Hovhannessian, R.A.Epremian, D.Huguenin*, Russian Astron.J.,70, 451,1993.
9. *H.M.Tovmassian, R.Kh.Hovhannessian, R.A.Epremian, D.Huguenin*, Mon.Not.Roy.Astron.Soc., 266,337, 1994.
10. *H.M.Tovmassian, R.Kh.Hovhannessian, R.A.Epremian, D.Huguenin,* Astrofisika,

33, 329, 1990; 34, 301, 1991; 36, 35, 36, 165, 1993.

11. G.Neugebauer et al, Infrared Astron. Satellite(IRAS) Catalogues and Atlas, V.2-6, 1988.
12. *R.Kh.Hovhannessian, R.A.Epremian, A.A.Karapetian*, Astrofisika 98, 1995 (submitted).
13 *A.T.Garibjanian*, Astrofizika, 20, 437,1984.
14 *A.T.Garibjanian, K.G.Gasparian, R.Kh.Hovhannessian*, Astrofizika, 20, 245, 1984.
15. *I.M.Kopilov*, The Problems of Cosmogony (VII), Ed. Acad.Sci SSSR, M.p.258, 1960.
16. *L.V.Mirzoyan*, Comm. of Byurakan Obs., 35, 75, 1964.
17. *D.L.Crawford, J.W.Glaspey, C.L.Perry*, Astron.J., 75, 822,1970.
18. *P.N.Kholopov*, Russian Astron.J., 57, 12, 1980.
19. *L.G.Balazs, A.T.Garibjanyan*, Astrofizika, 27, 245, 1987.
20. *L.V.Mirzoyan, V.V.Hambarian, A.T.Garibjanyan*, Astrofizika, 34, 357, 1991.

АСТРОФИЗИКА

ТОМ 38 НОЯБРЬ, 1995 ВЫПУСК 4

ABUNDANCE STRATIFICATION IN THE OUTER LAYERS OF MAIN-SEQUENCE STARS

G.ALECIAN

Laboratoire d'Astrophysique Extragalactique et de Cosmologie
CNRS-URA173- Observatoire de Paris
DAEC, Observatoire de Meudon
F-92195 Meudon Cedex, France

A short review on diffusion processes in atmospheres of stars is given. The diffusion model and its application for interpretation of spectral features of Am and Ap stars are described schematically. The building of abundance stratification and the case of calcium in Am stars are described briefly.

1. Abundance anomalies observed in Main Sequence stars. Strong abundances anomalies (more than ten times solar values) may be found among the Main Sequence A and F stars. These stars are the so called Chemically Peculiar stars (CP). Although the existence of anomalies is known for many decades, their origin is understood only since the pioneering work of Michaud (1970).

There are mainly 5 groups of CP stars on the Main-Sequence (the detected over and underabundances are written respective to the sun):

FmAm

$T_{eff} \approx 7500 - 9500$

Overabundances: iron peak elements (about a factor of 10)

Underabundances: Sc, Ca (about x0.1)

peculiarities: all are binaries, slow rotation (v.sin i < 100 km/s)

Ap (Sr-Cr-Eu)

$T_{eff} \approx 8000 - 12000$

Overabundances: iron peak elements (about x102), rare earths (up to x105)

Underabundances: Ti (about x0.01)

Peculiarities: slow rotation, magnetic field, spectroscopic variability

Ap (Si)

$T_{eff} \approx 9500 - 16000$

Overabundances: iron peak elements (about $x10^2$), rare earths (up to $x10^2$)

Underabundances: He, Ti (about x0.01)

Peculiarities: slow rotation, strong magnetic field, spectroscopic variability.

Ap (HgMn)

$T_{eff} \approx 9500 - 16000$

Overabundances: iron peak elements (about $x10^2$), Mn, Hg, Xe (up to $x10^5$)

Underabundances: He

Peculiarities: slow rotation, binarity frequency higher than normal, no detection of magnetic field.

He

$T_{eff} \approx 14000 - 30000$

Overabundances: He3 (Teff (15000-21000), He (x10, Teff (21000-30000)

Underabundances: He (x0.01, Teff (15000-21000)

Peculiarities: magnetic field, spectroscopic variability.

For more details the reader may refer to, for instance, review papers by Boyarchuk & Savanov (1986), Cayrel et al (1991), and Takada-Hidai (1990).

2. The diffusion model. Various theories have been proposed during the sixties to explain the CP phenomenon. They were unsuccessful except diffusion theory.

Very schematically, a star may be considered as composed by successive layers where different processes occur according to the local physical conditions. Matter is generally mixed by macroscopic motions as convection, turbulence, large scale circulations. However, some layers may be quiet. In these layers, chemical separation (or microscopic diffusion) can occur efficiently, providing that diffusion time-scales are shorter than mixing time-scales (the first ones lay approximately from some years to 106 years according the CP group). Diffusion is mainly due to the competition of two forces: one due to gravity, the other one due to absorption of photons.

Microscopic diffusion is a physical process always active in stars, the problem being to know when it produces detectable effects. It is clearly inefficient in the majority of Main Sequence stars where convective motions are important and which show abundances close to solar ones.

For CP stars, diffusion model was first proposed by G. Michaud (1970), it is supported by several basic constatations:

The abundance anomalies are related to atmospheric parameters (effective temperature, magnetic field).

There is a clear correlation between the superficial abundance anomalies and the radiative accelerations in the quiet zone.

The CP's are stars where mixing motions may be slower than in any other Main Sequence stars: slow rotation (v sin i < 100 km/s), shallow superficial convection zone, undetectable mass-loss rate, and/or strong magnetic field (which may help to stabilize turbulent motions), see Vauclair & Vauclair (1979).

There is not evolved stars (outside the Main Sequence) with the same anomalies. This proves that anomalies are located in the outer layers during the Main Sequence life-time, and then, these layers are mixed with deep " normal " ones when convection develops as the stars evolve.

We shall now detail the model for Am and Ap stars (for the sake of conciseness, we do not consider here the case of He stars). Note that diffusion process may be effective in some evolved stars (Horizontal Branch stars, White Dwarfs) but this is out the scope of the present review.

2.1 Am stars. The classical scenario for FmAm stars is the following (see Michaud, 1986). Normal F and A stars have two superficial convection zones due to hydrogen and helium ionization. These two zones are generally very close to each other and may be considered as to form one unique thick zone. If the star has low rotational velocity (due for instance to tidal effects in binary systems), large scale circulations below the convection zone is weak enough for helium to settle down by diffusion (the balance between gravity and radiative acceleration is in favour of gravity for this element). The time needed for helium settling is smaller than the life-time on the main sequence (Charbonneau & Michaud, 1988). Helium leaves the external layers and the convection zone due to helium progressively disappears as the He abundance decreases in the envelope. The star remains with a shallow superficial convection zone due to hydrogen ionization and then microscopic diffusion may act for metals, just below (in the radiative zone), with short time scales (the time scales are decreasing with decreasing mass-density). Detectable effects are produced at the stellar surface: due to mixing in this shallow convective zone, the superficial abundances reflect the abundances at the upper boundary of the stable radiative zone where stratifications take place.

2.2 Ap stars. For Ap stars, the classical scenario is the same as for FmAm stars except that due to their higher effective temperature, the remaining superficial hydrogen convection zone is very thin or non-existent. Therefore, diffusion processes occur in the atmosphere where time-scales are much shorter and diffusion much more efficient. The abundance anomalies of metals are much stronger than in FmAm stars and appear faster.

In case of strong horizontal component of magnetic field, the vertical motions of ions are strongly smoothed down and then diffusion can produce horizontal inhomogeneities. This explains the spectroscopic variability's of magnetic Ap stars and their correlation with the rotational period.

3. The radiative acceleration. The radiative acceleration (which acts against gravity) is due to photoabsorption of ions. Momentum is transferred from the radiation field to ions, according to their atomic properties. Since these properties are different from one ion to the other, the radiative acceleration (and then diffusion velocity) is also different from one ion to the other, this is why diffusion produces abundance stratifications.

A general expression of the radiative acceleration due to an atomic radiative bound-bound transition l (from level k to level m) is:

$$g_{il} = \frac{1}{A_i m_p n_i} \int_0^{\infty} n_{ik}\, \sigma_{i,lkm}(\nu) \frac{\phi(\nu)}{c} d\nu, \qquad (1)$$

where

$\phi(\nu)d\nu$ is the net energy flux (erg cm^{-2}s^{-1}) transported by photons with frequency between ν and ν+dν.

$\sigma_{i,lkm}$ absorption cross-section of ion A^{+i}, for transition from energy level k to m,

$A_i m_p$, the mass of the ion (in g)

n_{ik}, the number of ions A^{+i} per cm^3, in level k.

There is slightly different expression for bound-free absorption (see Alecian, 1994), but the acceleration due to the continuum of ions is often negligible and here, it will be neglected.

Eq. (1) gives the contribution of one individual transition, and then, the total acceleration for A+i is the sum over all the bound-bound transitions l:

$$g_i^{rad} = \sum_l g_{il}. \qquad (2)$$

The total number of transitions may be very huge (more than several tenths of thousands per ion are available in some atomic data bases), however, the computations are generally restricted to the most efficient transitions.

One important property of eq. (1) is that the flux $\phi(\nu)$ depends on the concentration of A^{+i} through monochromatic opacity. At the beginning of the diffusion process, one considers that the concentration is homogeneous and solar. After stratification, the local concentration of A^{+i} is changed and then the local monochromatic opacity too. There is not a simple analytic expression giving the radiative acceleration as a function of the number of A^{+i} particles (n_i). This makes the detailed computation of the abundance stratification (which depends on the time) very difficult to carry out. However, for saturated lines with lorentzian profile, it is known that the radiative acceleration varies as $n_i^{-1/2}$.

3.1 Some results for Ap stars. For Ap stars (where diffusion occurs in the atmosphere), expression (1) must be computed in the optically thin case. This means that the flux $\phi(\nu)$ is obtained through a detailed transfer computation for each line of A^{+i}, which is very heavy to carry out (due the great number of lines to consider) even if NLTE effects are neglected. The situation is still more difficult if one wants to compute time-dependent diffusion, since in that case the radiative acceleration has to be computed at each time step.Although accurate calculation cannot be done presently for time-dependent stratification in the atmosphere, it is possible, considering accelerations alone at initial time (homogeneous normal concentration), to have a first guess of what kind of abundance anomalies can be produced by diffusion. This is often called the zero order approximation. In that context, encouraging results have been obtained for Ap stars concerning some iron peak elements. For manganese, Alecian and Michaud (1981) have found the maximum overabundance that can be produced by diffusion in the atmosphere of HgMn stars and their prediction was confirmed by observations (Smith, 1993). For silicon in magnetic Ap stars, Vauclair et al (1979) and Alecian and Vauclair (1981) have explained the complex behavior of that element. A same kind of work has been done about gallium by Alecian and Artru (1987).

3.2 The case of Am stars. The situation is strongly different in Am stars where diffusion occurs in the envelope (optically thick). The Milne's approximation makes the radiation transfer computation easier, however, one must here consider (for a given element) many stages of ionization with high charge. The data were often lacking, but this is no more the case for elements with atomic number less than 15, plus argon, calcium and iron, since OPACITY project has produced a large set of atomic data (Seaton 1987, The OP team, 1995).

In optically thick case, the radiative acceleration may be written as:

$$g_{ij} = 4.377 \cdot 10^{7}\, T_{eff}^{4}\, \kappa_R \left(\frac{R}{r}\right)^{2} \frac{1}{A_i n_i} \int_0^{\infty} \frac{\kappa_{ij}}{\kappa_b + \kappa_{ij}} P(u)\, du, \qquad (3)$$

where R and r are the total and local radius, T_{eff} the effective temperature of the star, κ_b and κ_{ij} the monochromatic opacities of respectively the background and the one due to the considered transition (Michaud et al, 1976). The other quantities are defined as:

$$u = \frac{h\nu}{kT}. \tag{4}$$

$$P(u) = \frac{u^4 e^u}{\left(e^u - 1\right)^2}. \tag{5}$$

For rapid computation in time-dependent diffusion studies involving large quantities of atomic data, an approximation has been proposed by Alecian (1985), and Alecian & Artru (1990):

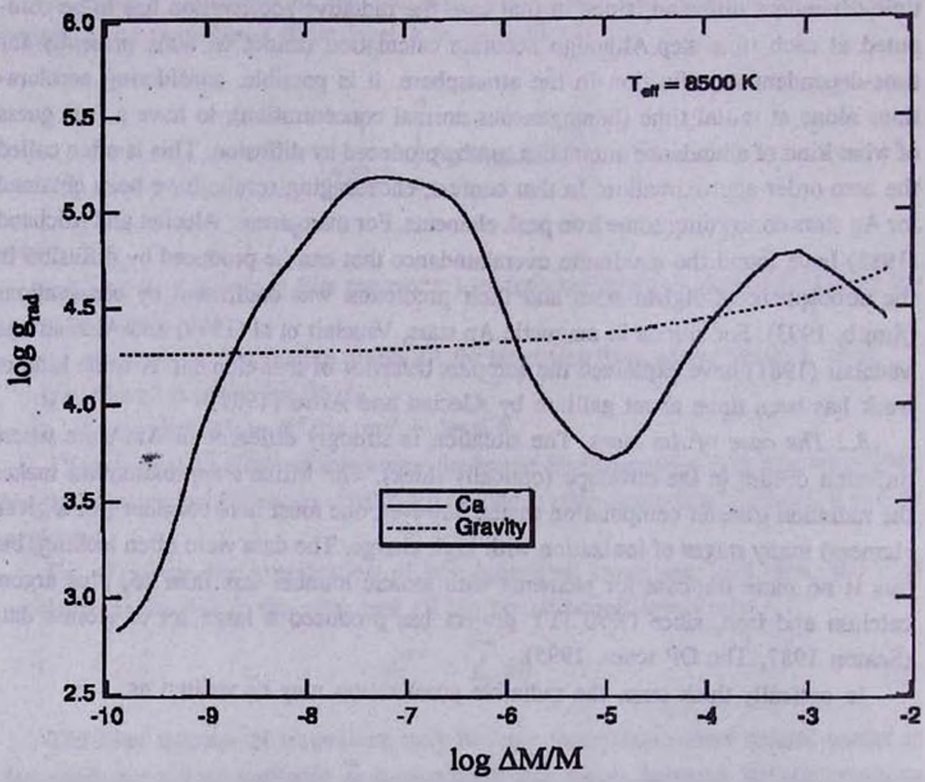

Fig. 1. Radiative accelerations on calcium in the envelope of an A star. Logarithm of acceleration (in cgs) is plotted versus the logarithm of the mass fraction above the point of interest. Calcium is pushed toward the stellar surface in the layers where the radiative acceleration is greater than local gravity (the dashed line). The left boundary corresponds roughly to the bottom of the superficial convection zone (T≈24000K), the right boundary is the deepest point of the envelope model (T≈2.7 10^6K). A mass-loss rate of 10^{-14} solar mass per year has been considered in this simulation.

$$g_i^{rad} \approx g_{i,0}^{rad}\left(1+\frac{C_i}{C_{i,s}}\right)^{-1/2}. \tag{6}$$

where C_i is the concentration at radius r of ion A^{+i}, C_{is} a function independent of time, and $g_{i,0}^{rad}$ the radiative acceleration at the limit of zero concentration of the considered element.The approximation (6) using the OPACITY-project data has been checked successfully in the case of iron in F and A stars (Alecian et al, 1994). Calcium has been also investigated recently by Alecian (1995), see Fig. 1.

4. Time-dependent diffusion. As we have already mentioned, the knowledge of the radiative acceleration is not enough to predict accurately the abundance anomalies that can be observed at the stellar surface. For that, one needs to compute the stratification process which requires solving the following continuity equation (valid for test particles only, not for helium):

$$\partial_t n + \nabla_r\left(V_D + nV_M\right) = 0, \tag{7}$$

where n is the number density of the considered element, V_M is a bulk velocity (stellar wind for instance) and V_D the diffusion velocity with respect to protons. The diffusion velocity of ions V_{ip} with respect to protons is derived from the Boltzmann equation (see for instance Chapman and Cowling, 1960, Burgers, 1969; Aller and Chapman 1969):

$$V_{ip} \approx D_{ip}\left[-\partial_r \ln\frac{n_i}{n_p} - \left(A_i - \frac{Z_i - 1}{2}\right)\frac{m_p}{kT}g + A_i\frac{m_p}{kT}g_i^{rad} + \ldots\right] \tag{8}$$

D_{ip} is the diffusion coefficient, and n_p the number density of protons. We have neglected the additional term due to thermal diffusion.Eq. (8) is for one kind of independent charged test particle. The element is simultaneously in several ionization stages linked by the Saha equations, and then, the total diffusion velocity is approximated by the following sum (for more details, see Montmerle and Michaud, 1976):

$$V_D = \frac{1}{n}\sum_i n_i V_{ip}. \tag{9}$$

4.1 The building of abundance stratifications and the case of Calcium in Am stars. The continuity equation (7) must be solved numerically because it is strongly non-

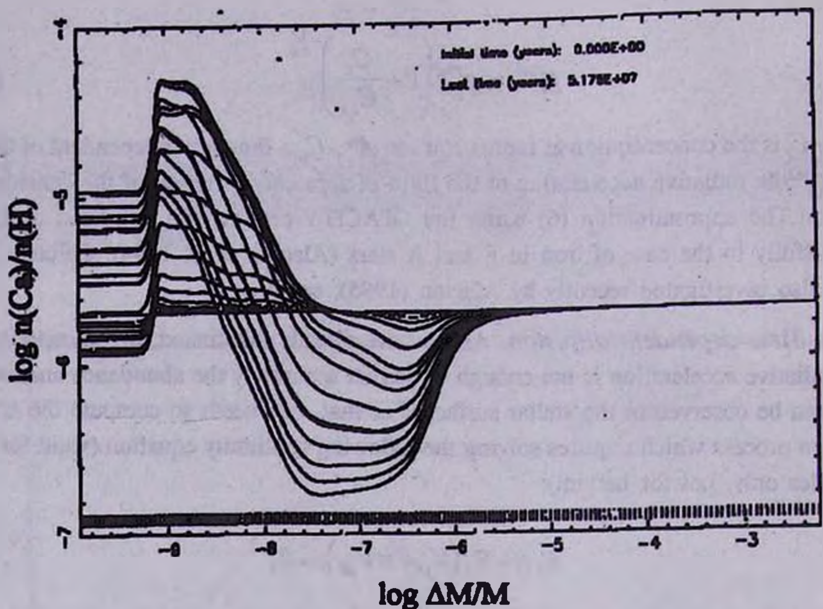

Fig. 2. Evolution of the calcium concentration in the same star as in Fig. 1. The logarithm of calcium abundance is plotted versus the logarithm of the mass fraction above the point of interest. At time t = 0, calcium is homogeneous and solar, the curves represent the abundance at successive time steps. The final time step corresponds to t = 5.175 10^7 years.

linear (Alecian and Grappin, 1984, Alecian, 1986). This is difficult to do for several reasons. One of them is that the diffusion time scale at the bottom (downward boundary) is very different from the one at the top. On another hand, the characteristic time of the stratification process is often of the same order of magnitude than the time needed to the stars' structure to evolve significantly and then, a detailed computation should take into account the changes of the internal structure (Richer and Michaud, 1993).

Although these difficulties, some results have been obtained recently on the time dependent diffusion of calcium in Am stars. This element is important because its deficiency is one of the main peculiarities of Am stars. Alecian (1995) has shown that the abundance of this element may present different phases according the importance of the mass-loss rate (bulk velocity) and the extension of the superficial mixing zone (Fig. 2). Calcium may show a " short " phase of overabundance in Am stars before to become underabundant. This phase should be detectable in very young galactic clusters (less than 5.10^7 years old). Therefore, comparison between computations and observations of F and A stars in very young open clusters may give interesting insight into the stellar structure. Am stars may be considered as a new tool for stellar physics.

5. Conclusion. Diffusion process in stars is known, for about twenty years, to be a powerful mechanism in explaining the CP phenomenon. But the accurate computation of the radiative accelerations, the detailed modelling of the stratification process are difficult to carry out, and then, quantitative predictions were often very inaccurate. The recent availability of large atomic data base and the increase of computing power have strongly changed the situation.

We have tried to give, in this short review, a glance on diffusion processes in stars. Of course, many aspects have not been discussed or have been omitted in this presentation. This concerns mainly what happens in stellar atmospheres. Indeed, there are several important effects which are neglected in envelope's layers but, they must be considered in the atmosphere: effect of magnetic field, momentum redistribution between neutral and ionized stages, light induced drift, etc. On another hand, we have not discuss on the consequences of microscopic diffusion in normal stars, like the effects on lithium abundances in solar type stars. The recent progresses in stellar modelling impose more and more to take into account this kind of transport processes.

СТРАТИФИКАЦИЯ ОБИЛИЯ ЭЛЕМЕНТОВ ВО ВНЕШНИХ СЛОЯХ ЗВЕЗД ГЛАВНОЙ ПОСЛЕДОВАТЕЛЬНОСТИ

Ж.АЛЕСЯН

Дан краткий обзор диффузионных процессов в атмосферах звезд. Схематически описаны диффузионная модель и ее применение для объяснения спектральных особенностей звезд типов Am и Ap. Кратко описаны образование стратификации обилия элементов, а также случай кальция в Am звездах.

REFERENCES

G.Alecian, 1985, Astron. Astrophys. (RN), Vol.145, p.275.

G.Alecian, 1986, A&A, Vol.168, p.204.

G.Alecian, 1994, A&A, Vol.289, p.885.

G.Alecian, 1995, A&A, to be published.

G.Alecian, M.-C.Artru: 1987, A&A, Vol.186, p.223.

G.Alecian, M.-C.Artru: 1990, A&A, Vol.234, p.323.

G.Alecian, R.Grappin: 1984, A&A, Vol. 140, p.159.

G.Alecian, G.Michaud: 1981, Astrophys.J., Vol. 245, p.226.

G.Alecian, G.Michaud, J.Tully: 1993, ApJ, Vol.411, p.882.

G.Alecian, S.Vauclair: 1981, A&A, Vol. 101, p.16.

L.H.Aller, S.Chapman: 1960, ApJ, Vol. 132, p.461.

A.A.Boyarchuk, I.S.Savanov: 1986, Upper Main Sequence Stars with Anomalous Abundances, IAU col. 90, held in Crimea (USSR), p.433.

J.M.Burgers: 1969, Flow Equation For Composit Gases, Academic Press.

R.Cayrel, C.Burkhart, C.Van't Veer: 1991, IAU Symposium N¡145, Evolution of stars: the photospheric abundance connetion, Bulgaria, G. Michaud and A. Tutukov, p.99.

S.Chapman, T.G.Cowling: 1970, The Mathematical Theory of Non-uniform Gases, Cambridge University Press, 3rd ed.

P.Charbonneau, G.Michaud: 1988, ApJ, Vol.327, p.809.

G.Michaud: 1970, ApJ, Vol. 160, p.641.

G.Michaud: 1986, Upper Main Sequence Stars with Anomalous Abundances, IAU col. 90, held in Crimea (USSR), p.459.

G.Michaud, Y.Charland, S.Vauclair, G.Vauclair: 1976, ApJ, Vol.210, p.447.

T.Montmerle, G.Michaud: 1976, Astrophys. J. Suppl., Vol. 31, p.489.

J.Richer, G.Michaud: 1993, ApJ, Vol.416, p.312.

M.J.Seaton: 1987, J. Phys. B: Atom. Molec. Phys., Vol.20, p.6363.

M.Takada-Hidai: 1990, "Evolution of stars: the photospheric abundance connection", IAU Symposium N¡145, Golden Sands, Bulgaria.

The Opacity Project (Op) Team: 1995, The Opacity Project, Vol.1.

S.Vauclair, J.Hardorp, D.M.Peterson: 1979, ApJ, Vol. 227, p.526.

S.Vauclair, G.Vauclair: 1979, Les elements et leurs isotopes dans l'Univers , 22nd Liege Int. Astrophys. Symp., ed. G. Grevesse, Universite de Liege, p.389.

АСТРОФИЗИКА

ТОМ 38 НОЯБРЬ, 1995 ВЫПУСК 4

THE FIRST BYURAKAN SPECTRAL SKY SURVEY. INVESTIGATIONS OF STARS OF LATE M AND C SPECTRAL CLASSES

K.S.GIGOYAN, V.V.HAMBARIAN, H.V.ABRAHAMIAN

Byurakan Astrophysical Observatory

The results of investigations of new faint M and C type stars discovered on the plates of the First Byurakan Spectral Sky Survey are reported. Among 161 newly discovered stars, 98 are identified with unknown IRAS point sources. It is probable, that the majority of new M stars are Mirids according to their distributions on the IRAS color - color diagram. For J - stars, a correlation between EW(C_2+CN) and EW(C_2(0,1)) is found.

1. *Introduction.* In the course of 15 years(1965 - 80) in Byurakan Astrophysical Observatory by Markarian and his colleagues the First Byurakan Spectral Sky Survey (FBS) was carried out [1].

The main aim of the FBS was the search of galaxies with strong UV - excess at high galactic latitudes ($|b| > 30°$, $\delta > -15°$). The observations have been done using 1 m Schmidt telescope of the Byurakan Observatory with the combination of 1°.5 objective prism(low - dispersion spectra in the range 3400-6900A, inverse dispersion 1800A/mm at H_γ) [1,2]. Since 1987 the second part of the FBS is carried out in order to search and select star - like objects with strong UV - excess [3].

The search, selection of faint late M and C type stars are carried out on the plates of the FBS, including investigation of these objects at high galactic latitudes. The necessity of doing this work is connected with the fact, that systematic investigations of faint C and M stars at high galactic latitudes have not been done. Very faint C and M stars are of special interest, because they are relatively distant objects and probably a part of them are objects of Galactic halo population. Investigations of such faint "peculiar" stars at high latitudes, undoubtedly, is very important for the investigation of the structure, kinematics and the chemical composition of the Galactic halo.

The list of 583 faint M type stars at high galactic latitudes was published by Stephenson [4]. The data of 132 faint M and C type stars, discovered on the plates of the Case - survey, are presented by Sanduleak and Pesch [5].

Recently Green et al.[6] have started a wide - area CCD survey of very faint high - latitude carbon stars with the KPNO 0.9 m telescope.

In [7,8] is presented a survey of faint C stars at high galactic latitudes, however the results of spectroscopic investigations and IR - photometric data are presented for a small number of C stars, towards the north and south Galactic poles.

In this work we present some results of investigation of faint M and C stars, discovered on the plates of the FBS [9].

2. *Selection of C and M stars.* As it was mentioned above, low - resolution spectral observations in the range 3400 - 6900A of FBS - survey permit distinguish star - like objects with strong UV - excess and red stars late spectral classes. Carbon stars can be recognized by the presence of absorption bands at 4737, 5165 and 5636A of C_2 molecule. Early - type carbon stars (R - stars) show also 4382A band of C_2. The spectra of M stars show bands at 4584, 4762, 4950 and 5165A of TiO. M stars of late - subclasses show mainly bands at 5445, 5850 and 6162A of TiO.

The limiting magnitude of FBS - survey for stars of late spectral classes is estimated to be 15 - $15^m.5$ in V - band, accepting, that the limiting photographic magnitude of the survey is 17 - $17^m.5$ [2]. The bright limit for selection of M and C type stars depends, indeed, on the limit of each plate, which changes insignificantly from plate to plate. On the plates of the FBS this limit for C stars on average (for the bright nonvariable stars of R - classes, for which all the absorption bands of C_2 become invisible due to photographic effects) is estimated as $m_V = 10^m$, on the basis of examination on the plates of several known bright R stars, having V - magnitudes in the Stephensons carbon star catalogue [10].

This bright limit for M stars is estimated to be 11 - $11^m.5$. On the low - resolution spectra absorption bands of TiO of M stars brighter than 11^m become invisible.

3. *Spectroscopic investigation of M and C stars.* For selected faint and M stars spectroscopic observations have been carried out with the spectrograph UAGS with YMK - 91B image - tube, placed in the Cassegrain focus of the 2.6 m telescope of the Byurakan Observatory. The slit spectra are obtained mainly in the wavelength range 4700 - 6800A [11,12].

At the 2.6 m telescope we obtained about 300 slit spectra for 50 M and 45 C stars.

M stars. Spectral subclasses (pseudo - MK classes) for the first 15 faint M stars are determined by means of spectral indices, taken from Pritchet and van den Berg work [13]. The results of two - dimensional classification are given in [11]. Two new faint stars (FBS 0748 + 410 and FBS 2221 + 375) are classified as M dwarfs and their absolute visual magnitudes are estimated [11].

C stars. 22 faint carbon stars (6 of them are ascribed to the group of carbon Mirids [14]) are studied spectroscopically. The one - dimensional classification (R and N) is carried out [15]. Spectroscopic characteristics such as color temperature, equivalent widths of most known absorption bands are determined.

An attentive examination of the spectra of faint carbon stars and the spectra of some of bright carbon stars show, that in the spectra of most of them a depression in the range of 5700 - 6200A is observed, but in the spectra of some of them this depression is stretched up to 6700A. For 44 C stars (22 faint and 22 bright) we have determined equivalent widths of the total absorption in the range 5720 - 6765A assuming, that these points are the points of quasi - continuum, and in this wavelength range are situated the absorption bands of C_2 and CN mainly. When we compared the equivalent width of C_2 (0, 1) Swan band and the equivalent width of a total absorption in the range 5720 - 6765A the following picture is observed. As shown in Fig. 1, there are concentration in the region 100A < EW (C_2+CN) < 225A, and 100A < EW(C_2(0, 1)) < 200A, but J - stars - stars with strong isotopic bands in the spectrum(the

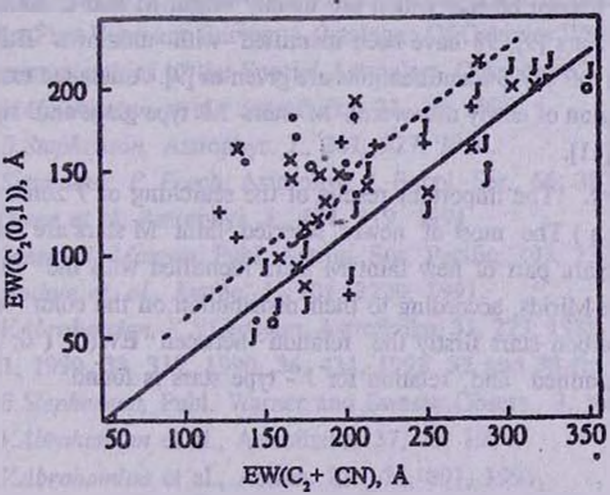

Fig. 1. The relation between the equivalent width of Swan (0,1) band and equivalent width of a total absorption in a range 5720 - 6765A. The straight line is drawn only for J - type stars by the least square method. Dotted line separates the J - stars from others. Symbols: N stars are plotted as dots, R - N stars as plus sign, R stars as open circles, crosses - bright N stars, closed circles - bright R stars [12,15].

isotope of carbon and cianogen molecules) are situated along a straight line, drawn by the least square method (the dotted curve separates the J - stars from others).

The relation between equivalent widths of two bands for J - type stars has the following form:

$$EW(C_2\ (0,\ 1)) = 0.7\ EW(C_2 + CN) - 30.72 \quad (n = 17,\ \ r = 0.95)$$

This relation was given firstly in our previous work [12]. Additional observations of large number of J - stars will allow to examinate this correlation in more details. The next important question is whether the isotopic bands are observed in the spectra of stars having strong depression in the 5700 - 6700A range, i.e. whether these stars are J - type stars.

4. *IR - photometry.* Near - infrared photometry was carried out for 13 faint carbon stars at J, H and K bands [16].

The photometric data in J and K bands [16] are used to estimate the effective temperatures and the bolometric magnitudes of investigated stars.Using the data in K band for 4 carbon stars (they have indices J - K > $1^m.7$) distances, therefore absolute bolometric magnitudes were estimated [16].

5. *IRAS identification.* The selected M and C stars have been identified with the IRAS point sources [17, 19]. 124 stars of 285 found in 7 FBS -survey zones have been identified with known objects which are mainly bright M and C stars. Among 161 new discovered stars [9], 98 have been identified with unknown IRAS point sources. The results of IRAS identifications are given in [9]. A detailed examination shows, that in the region of newly discovered M stars M type giant and supergiants (Mirids)are located [11].

6. *Conclusions.* The important results of the searching of 7 zones of FBS - are the followings: a) The most of newly selected faint M stars are stars of late subclasses, b) the main part of new faint M stars identified with the IRAS point sources, probably are Mirids, according to their distribution on the color - color diagram and, c) for carbon stars firstly the relation between $EW(C_2\ (0,\ 1))$ and $EW(C_2 + CN)$ is examined and relation for J - type stars is found.

ПЕРВЫЙ БЮРАКАНСКИЙ СПЕКТРАЛЬНЫЙ ОБЗОР НЕБА. ИССЛЕДОВАНИЕ ЗВЕЗД ПОЗДНИХ М И С СПЕКТРАЛЬНЫХ КЛАССОВ

К.С.ГИГОЯН, В.В.АМБАРЯН, Г.В.АБРАМЯН

Приведены результаты исследоввния новых слабых звезд М и С спектральных классов, выявленных на пластинках Первого Бюраканского спектрального Обзора Неба. 98 звезд из 161 идентифицированы с IRAS источниками. Согласно расположению на IRAS цвет - цвет диаграмме, большая часть новых М звезд, вероятно, являются Миридами. Для J - звезд обнаружена корелляция между эквивалентными ширинами суммарного поглощения в области 5700 - 6700A.

REFERENCES

1. *B.E.Markarian* et al., Astrofizika, 17, 619, 1981.
2. *B.E.Markarian, V.A.Lipovetsky, J.A.Stepanian, L.K.Erastova, A. I. Shapovalova*, "The First Byurakan Survey. A Catalogue Of Galaxies With UV - Continuum", Communications of the Special Astrophys. Obs., No 62, 1989.
3. *H.V.Abrahamian* et al., Astrofizika, 32, 29, 1990.
4. *C.B.Stephenson*, Astrophys. J., 301, 927, 1986.
5. *N.Sanduleak, P. Pesch*, Astrophys. J. Suppl. Ser., 66, 387, 1988.
6. *P.Green et al*, Astrophys. J., 434, 319, 1994.
7. *P.Green, B. Margon*, Publ. Astron. Soc. Pacific, 102, 1372, 1990.
8. *G.Bothun et. al.*, Astron. J., 101, 2220, 1991.
9. *H.V.Abrahamian, K.S.Gigoyan*, Astrofizika, 31, 223, 1989, 31, 601, 1989, 32, 501, 1990, 33, 317, 1990, 36, 431, 1993. 37 and 38 (in press).
10. *C.B.Stephenson*, Publ. Warner and Swasey Observ., 3, No 2, 1989.
11. *H.V.Abrahamian* et al., Astrofizika, 37, 73, 1994.
12. *H.V.Abrahamian* et al., Astron. Zh., 71, 891, 1994.
13. *C.Pritchet, van den Bergh*, Astron. J. Suppl. Ser., 34, 101, 1977.
14. *H.V.Abrahamian, K.S.Gigoyan*, Astron. Zh., 70, 116, 1993.
15. *H.V.Abrahamian, K.S.Gigoyan*, Astrofizika, 36, 181, 1993.
16. *K.S.Gigoyan, et al.*, Astron. Zh., 71, 897, 1994.

17. IRAS Point Catalog. On The Optical Disk. "Sel. Astron. Catalogs." Supplied By NASA, V. 2, 1989.
18. IRAS Faint Source Catalog. b > 10° Degrees. On The Optical Disk. " Sel. Astr. Catalogs." Supplied By NASA, V. 2, 1989.
19. IRAS Serendipitious Survey Catalog. On The Optical Disk. " Sel. Astr. Catalogs. " Supplied By NASA, V. 2, 1989.

АСТРОФИЗИКА

ТОМ 38 НОЯБРЬ, 1995 ВЫПУСК 4

ON THE DUPLICITY OF COOL GIANT AND SUPERGIANT VARIABLE STARS

R.A.VARDANIAN

Byurakan Astrophysical Observatory

From the analysis of photometric, colorimetric and polarimetric data it follows that high luminosity red variable stars are divided into two groups: group I - double stars with brightness variation periods more than 480 days, group II - single stars with period less than 480 days. Moreover, double stars possess: a) high coefficients of correlation between brightness *V* and *U-B; B-V* colours. b) relatively low values of *U-B* (< 1^m5) and high infrared excess. c) strong variations of parameters of polarization ($\overline{S}_{p,\theta}$> 1.5) and often those are associated with maser sources.

1. *Introduction.* The variations of stellar polarization with time were first discovered in 1958 in Byurakan by Grigorian [1] for the red supergiant star μ Cep. The intrinsic polarization was discovered during observations of T Tau, RY Tau in 1964 by Vardanian [2]. A variable intrinsic polarization of T Tau type stars [2] and a dozen of red giants and supergiants was discovered in 1965 - 1985 by Vardanian [3-4] and Abrahamian [5-6].

For the stars with intrinsic polarization we have found a dependence of the degree of polarization on the variability of brightness and the spectral range [3,4].

These polarimetric, photometric and statistical investigations allowed us to find a criterrium of duplicity of cool giant and supergiant variable stars.

2. *Some polarimetric and photometric peculiarities of high luminosity red variable stars.* The analysis of observational data of red variables shows that:

a) About 10% of them possess of high degree of intrinsic light polarization (P>1.5%) and many of them exhibit variations of polarization parameters (p,θ).

b) With the decreasing of the brightness and wavelength the percentage of the intrinsic polarization increases.

c) The percentage of stars which are associated with maser sources and exhibit intrinsic light polarization increases when the period of light variations are larger or the spectral class of stars is later.

d) Most of them shows infrared excess: $I\text{-}K>0.65K+4.0$; $V\text{-}K>5.^m0$, when $I\text{-}K$ increases the polarization degree increases as well up to 5-6%.

e) For most of the stars, with periods greater than 400 days and exibiting a high polarization, the period is a decreasing function of time.

f) The intrinsic polarization of cool variable stars is caused by the scattering of light by solid particles in the atmospheres or in the envelopes of these stars.

Now we shall consider the relations between the degree of variability of polarization, position angle, brightness and colours of high luminosity red variable stars and parameters of duplicity.

3. *The identification of high luminosity double red variable stars from the character of brightness, colours and variations of parameters of polarization.* In Abrahamian's paper [6] the polarimetric and photometric data for 79 red variable supergiant stars are given, namely, the values of variations of polarization parameters (S_p, S_θ), their dispersions (σ_p, σ_θ), coefficients of correlation between V magnitude and $(B\text{-}V)$ and $(U\text{-}B)$ colours [$r_v(B\text{-}V)$; $r_v(U\text{-}B)$], the errors of correlation coefficient are presented ($r_{0.05}$-for the absence of correlations [6]).

Using these data the mean values of $(U\text{-}B)$, relative coefficients of correlation $K=\left|r_v(B-V)\,/\,r_{0.05}\right|$; the dates S_p/σ_p, S_θ/σ_θ and their mean values $S_{p\theta}=1/2(S_p/\sigma_p+S_\theta/\sigma_\theta)$ were calculated. These data are presented in Table 1.

We obtained the dependences of K parameter on $(U\text{-}B)$ colours as well as on the mean value $S_{p\theta}$. One can see from Fig . 1, that the double stars are separated from single ones. Moreover the obtained results show that for the double stars $(U\text{-}B)<1^m.5$ and the value of the coefficient of relative correlation $K>1^m.5$ [7]. It means that for double stars a tight correlation between the variation of brightness (V) and colours $(U\text{-}B)$; $(B\text{-}V)$ exists.

The obtained small values of colours $(U\text{-}B)<1^m.5$ are due to a hot component of these binaries. The relation presented in Fig.1 shows that for double stars the mean value of variations of polarization parameters ($\overline{S}_{p,\theta}$) exceeds 1.5 and their periods are larger than 450 days. The last result allows to propose that the periods of light variations for double stars are longer than for single stars.

We see that most of high luminosity red variable stars, with periods more than 500 days, are double stars [8]. And on the other hand almost all stars with periods smaller than 400 days are single stars.

Table 1

SOME PHOTOMETRIC AND POLARIMETRIC PARAMETERS OF COOL SUPERGIANT VARIABLE STARS

Name of stars	$K = \left| r_v(B-V) / r_{0.05} \right|$	U-B	$\overline{S}_{P,0}$	Periods	Sp
KN Cas	1.69	0.50	1.29	-	M1EPIB+B2.6V
V466 Cas	1.95	2.29	1.41	-	M1.5IB
AZ Cas	2.23	0.56	2.50	3402	MOEIB+BO-B1V
EZ Per	1.13	2.44	0.83	184	M0.5IAB-M2OIAB
XX Per	2.10	1.31	2.33	415	M4IAB+B
KK Per	0.49	2.39	1.00	-	M1.0IAB-M3.5IAB
BU Per	1.62	2.57	1.33	367	M3.5IB
PR Per	0.66	2.6	1.33	-	M1IAB-IB
SU Per	0.21	2.08	0.83	533	M3.5IAB
RS Per	1.56	2.08	1.16	244.5	M4IAB
T Per	1.25	2.41	1.50	379	M2IAB
BD+58°445	1.10	2.57	1.00	-	K5.7IAB
BD+56°609	0.40	2.24	1.00	-	M3.1IAB
BD+29°897	0.44	2.45	0.84	-	M1.7IAB
NO Aur	1.50	2.18	1.00	-	M2.5IAB
TV Gem	1.71	1.70	1.00	-	K5.5-M1.3IAB
WY Gem	1.64	0.19	1.25	-	M2EPIAB+B2V-B3V
ψ Aur	1.18	2.26	1.40	-	K5-M0IAB-IB
Y Lyn	0.92	0.89	0.85	110	M6.5IAB-II
RS Cnc	0.46	1.03	-	120:	M6EIB-II(S)
YY Lyr	1.61	1.34	0.94	- .	M4-5IAB-II
AZ Cyg	1.86	2.73	2.00	459	M2-4IAB
μ Cep	2.07	2.57	8.00	730	M2EIA
VV Cep	2.21	0.56	1.41	7430	M2EPIA-IAB+B8:EV
ST Cep	1.61	2.43	1.35	-	M2IA-IAB
U Lac	2.85	1.29	2.12	550-690	M4EPIAB+B
PZ Cas	2.70	0.91	2.50	925	M2-4IA

This evidence gives us a basis to conclude that luminous red variables are dievided into two groups:

I - the group of double stars with greater periods and II - the group of single stars with smaller periods.

To confirm this conclusion, we have analyzed the IRAS [9] data of objects belonging to the bulge of the Galaxy. Using the data given in [9] we worked out a histogram exhibiting the distribution of *H-K* colours of stars (mainely Mira stars). There are two maxima in this distribution: at *H-K* = $0^m.75$, and the other at *H-K* = $1^m.45$.

Minimum value is observed between the maxima at *H-K* = $1^m.25$. (It is of interest to mention, that a similar maximum is observed also for red variable stars of the LMC at *H-K* = $0^m.75$.)

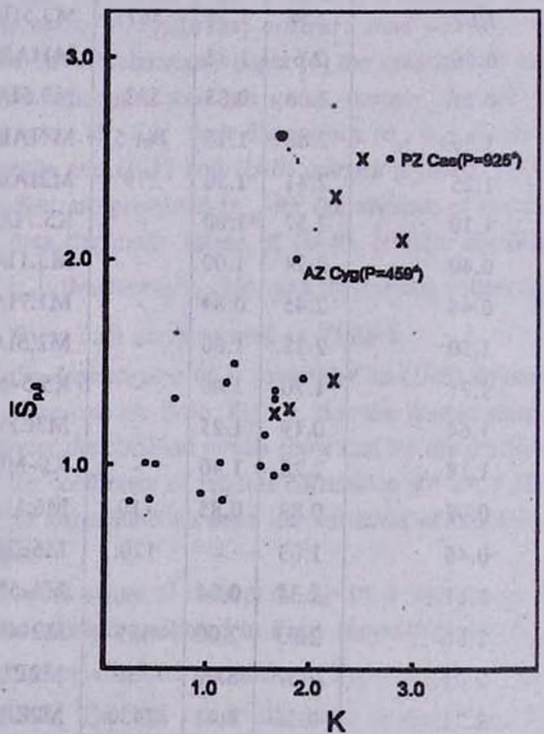

Fig. 1. Dependence of variation of polarization parameters from the K parameter x - double stars, • - single stars.

To determine the periods which have the red stars with $H\text{-}K = 1^m.25$ we considered another relation, namely, the relation between $H\text{-}K$ colours and amplitudes of brightenss variations of (ΔK) in the K spectral range [9]. For this analysis the stars with $K<5^m.0$ and with doubtful periods were not considered. The mentioned relation between K and $H\text{-}K$ shows that red variable stars with $H\text{-}K>1^m.2$ (≈80%) have periods larger than 480 days, and the overwhelming majority of stars (93%) with $H\text{-}K \leq 1.2^m$ have periods smaller than 480 days [7].

4. *Conclusion.* From the analysis of photometric, polarimetric and colorimetric data of high luminosity red variable stars follows that these stars are divided into two groups:

I group - stars with periods $P > 480^d$, colours $H\text{-}K>1^m.2$, variations of polarization parameters $S_{p,\theta} > 1.5$, and high coefficient of relative correlation $K>1^m.5$ are double, II group- stars with smaller periods $P < 480^d$, colours $H\text{-}K < 1^m.2$, and parameters $S_{p,\theta} < 1.5$, $K<1^m.5$ are single ones.

О ДВОЙСТВЕННОСТИ КРАСНЫХ ПЕРЕМЕННЫХ ЗВЕЗД ГИГАНТОВ И СВЕРХГИГАНТОВ

Р.А.ВАРДАНЯН

Из анализа фотометрических, колориметрических и поляриметрических данных получено, что красные переменные звезды высокой светимости делятся на две группы: группа I-двойные звезды с периодами изменения блеска больше 480 дней: группа II-одиночные звезды с периодами меньше 480 дней. Более того, двойные звезды характеризуются: а) большими коэффициентами корреляции между изменениями блеска V и цветами $U\text{-}B$, $B\text{-}V$: б) относительно меньшими значениями цвета $U\text{-}B$ ($<1^m.5$): и большими инфракрасными избытками. в) сильными изменениями параметров поляризации ($\bar{S}_{p,\theta}>1.5$), притом они часто ассоциированы с мазерными источниками.

REFERENCES

1. *K.A.Grigoryan*, Soob. Byurakan Obs., No 25, 45, 1958.
2. *R.A.Vardanian*, Soob. Byurakan Obs., No 35, 3, 1964.
3. *R.A.Vardanian*, Astrofizika, No 6, 77, 1970.
4. *R.A.Vardanian*, Soob. Byurakan Obs., No 46, 33, 1975.
5. *H.V.Abrahamian*, Soob. Byurakan Obs., No 52, 24, 1980.
6. *H.V.Abrahamian*, preprint 8 and 9 Byurakan obs., Yerevan, 1981.
7. *R.A.Vardanian*, Astrofizika, 37, 235, 1994.
8. *P.N.Kholopov, et. al.*, General Catalogue of Variable Stars, Moscow, 1985.
9. *P.Whitelock, M.Feast, R.Catchpole*, Mon. Not. Roy. Astron. Soc., 248, 276, 1991.
10. *R.Neid, I.S.Glass, R. M. Catehpole*, Mon. Not. Roy. Astron. Soc. 232, 53, 1988.

АСТРОФИЗИКА

ТОМ 38 НОЯБРЬ, 1995 ВЫПУСК 4

APPEARANCE OF A NEBULA NEAR Y ORI

N.D.MELIKIAN

Byurakan Astrophysical Observatory

The results of photographio and photoelectric observations for the star Y Ori are presented. During these observations a red nebulosity was appeared around the star Y Ori near the maximum of brightness. The optical sizes of the nebulosity are comparable with the OH sizes of long period variables and OH/IR stars. A real brightness increase on the decreasing branch of light curve was detected in U band of spectrum.

1. *Introduction.* Mira Ceti type long-period variables show variations in the optical range of the spectrum with amplitudes more than 2^m and periods from 200 to 500 days. These stars are red giants of late spectral classes, characterized by the presence of emission lines in their spectra. The variable stars catalogue [1] contains about 5800 Mira variables.

The star Y Ori is known as a long period variable and has a spectrum M3-M5 [1]. During the photographic UBV observations of flare stars in the Orion region in 1980 brightness variations of Y Ori were detected accidentally, near the maximum of the light curve [2].

On the base of our photographic observations the light curve of Y Ori is constructed, using the photographic material obtained during more than 20 years in Byurakan and Abastumani Observatories. The star Y Ori has a period P=271.3 days [1]. On the base of our observations the period (P), rise time (T_r) and dacay time (T_d) of light variations have been determined with a sufficiently high accuracy [2], using the method suggested by Lafler and Kinman [3].

$$P=270.5, \quad T_r=83.9, \quad T_d=186.6.$$

Photoelectric observations have been done in 1989, during more than 3 months [4]. These observations show that the brightness of Y Ori in BVR colours monotonically decreases after the maximum, while in the U band the brightness increase with an amplitude ΔU=0.7 is detected in 48 days after the maximum.

It is known from the results of multicolour photoelectric observations of Mira Ceti type stars, that the colour U-B has a minimum value near the minimum of brightness [5,6]. Our photographic and photoelectric observations show the same results [2,4].

In this report the results of our observations of Y Ori are presented.

2. *Observations.* The photographic observations were carried out in Byurakan and Abastumani Observatories, while the photoelectric observations - at high mountain Maydanak station of Tashkent Astronomical Institute. For the photographic observations the 40" (Byurakan) and 70cm (Abastumani) telescopes were used. The photoelectric observations were carried out with the 60cm telescope of the Maydanak station. The photoelectric observations have been obtained in *UBVR* bands, the photographic observations - in UBVRI.

More detailed information on these observations was already published [2,4].

3. *Nebulosity around the star Y ORI.* During the photographic observations a red nebulosity was detected around Y Ori on the photographic plates near the maximum of brightness obtained from 2 to 11 of February in 1983 [2]. The plates obtained in ultraviolet (U) and red (R) bands 50 days before show the absence of this nebulosity.

Thus, one can see the nebulosity only near the maximum.

The nebulosity has an elliptical form. The rough estimation gives for angular sizes of this ellipse a value of the order of 23"×16". At Orion assosiation distance (~450pc) it corresponds to linear dimensions about 0.05×0.035pc. So the nebulosity originated during less than 50 days.

It is already known that around Mira Ceti type stars gas shells exist, which extend with velocities of the order of 10-40 km/s. Usually the sizes of these shells are unknown. Deutsch [7] was the first who has measured the external radius of gas shell around α Her to be at least 200000 times larger than the radius of the Sun.

The results of radio observations show, that a high percentage (>30%) of Mira Ceti type stars have H_2O maser emission [8]. 1667MHz OH- emission is observed for 34% of these stars [9]. The typical values are of the order of 8×10^{15} cm for the radii of Mira Ceti variables, and 5×10^{16} cm for the OH/IR stars [10]. These results are in a good accordance with our estimation of the sizes of nebulosity around the Y Ori.

4. *Conclusion.* It is necessary to point out that Orion region was observed systematically in Byurakan and Abastumani observatories in the period 1974-1985. The analysis of these photographic observations did not show any trace of nebulosity

around Y Ori, in spite of the fact, that this star was registered repeatedly near the maximum of brightness.

The mean absolute magnitude of a normal red giant of a spectral class M4 is $M_v = -0.8$. The visual magnitude of Y Ori is $M_v=14.7$. If one assumes that this star is at Orion assosiation distance we obtain for the interstellar absorption $A_v=7.24$, while according to spectral observations, carried out for more than 100 stars in Orion region by Cohen and Kuhi [11], the highest value of interstellar absorption is $A_v=3.68$ for the star Haro 4-255.

On the other hand, using the spectral slopes (a12, a25) Weintraub [12] has classified more than 300 stars. Particularly he comes to a conclusion, that if both spectral slopes accept negative values simultaneously, it means that the star is surrounded by a very cold absorptive matter. We have for the star Y Ori a12= −3.64, and a25= −0.88. Thus, in all probability the star Y Ori is surrounded by a cold absorption material.

The main results for the star Y Ori on the base of our observations can be summarized as follows:

1. Near the maximum of brightness in red light a nebulosity was discovered around the star. The optical sizes of this nebulosity are comparable with OH sizes of long period variables. Such a formation has been observed for the first time not only for the star Y Ori, but for long period variables in general.

2. It should be noticed, that in 48 days after the maximum on the decreasing branch of light curve an increase of brightness has been detected which was registered in U band only.

3. Near the maximum brightness U-B=1.4, and two months later U-B = +0.3 − +0.7 [2,3].

ПОЯВЛЕНИЕ ТУМАННОСТИ ВОКРУГ ЗВЕЗДЫ Y ORI

Н.Д.МЕЛИКЯН

Приводятся результаты фотографических и фотоэлектрических наблюдений звезды Y Ori . Во время наблюдений вблизи максимума блеска зарегистрирована туманность в красных лучах. Такое образование вокруг звезд типа Миры Кита зарегистрирована впервые. Оптические размеры туманности сравнимы с OH размерами долгопериодических переменных звезд типа Миры Кита и OH/IR звезд. В период фотоэлектрических наблюдений на нисходящей ветви кривой блеска зарегистрировано

повышение блеска через 48 дней после максимума только в ультрафиолетовых лучах с амплитудой ΔU=0.7.

REFERENCES

1. *P.N.Kholopov, N.N.Samus, M.S.Frolov, V.P.Goranskij, N.A.Gorynya, E.V.Kazarovets, N.N.Kirieeva, N.P.Kukarkina, N.E.Kurochkin, G.I.Medvedeva, N.B.Perova, A.S.Rastorguev, S.Yu.Shugarov*, General Catalogue of Variable Stars, II, "Nauka", Moscow 1985.
2. *N.D.Melikian, R.Sh.Natsvlishvili, M.Della Valle*, Astrofizika, 28, 329, 1988.
3. *J.Lafler, T.D.Kinman*, Astrophys.J., Suppl.Ser.,11, 216, 1965.
4. *N.D.Melikian, S.D.Jakubov*, Astrofizika, 1995, in press.
5. *V.Mendoza*, Bol.Obs.Tonantzintla, 4, 28, 1967.
6. *L.Celis S.*, Astron.J., 87, 1791, 1982.
7. *A.J.Deutsch*, Astrophys.J., 123, 210, 1956.
8 *P.F.Bowers, W.Hagen*, Astrophys.J., 285, 637, 1984.
9. *Nguyen-Q-Rieu, C.Laury-Micoulaut, A.Winnberg, G.V.Schultz*, Astron. Astrophys., 75, 351, 1979.
10. *J.Herman, H.J.Habing*, Astron.Astrophys.Suppl.Ser., 59, 523, 1985.
11. *M.Cohen, L.V.Kuhi*, Astrophys.J., Suppl.Ser., .41, 743, 1979.
12. *D.A.Weintraub*, Astrophys.J., Suppl.Ser., 74, 575, 1990.

АСТРОФИЗИКА

ТОМ 38 НОЯБРЬ, 1995 ВЫПУСК 4

FRENCH - ARMENIAN SCIENTIFIC COOPERATION ON STUDY OF SOME HII-REGIONS WITH CIGALE

L.V.MIRZOYAN[1], M.MARSELIN[2], A.T.GARIBJANIAN[1], J.BOULESTEIX[2], Y.M.GEORGELIN[2], V.V.HAMBARIAN[1], A.L.MIRZOYAN[1], E.LE COARER[2], A.LAVAL[2]

1. Byurakan Astrophysical Observatory (Armenia)
2. Marseille Observatory (France)

The results of the scientific cooperation between astronomers of the Byurakan and Marseille observatories on the study of diffuse matter in the Galaxy are presented. The H_α-emission is discovered in the direction of h and χ Per. The Fabry-Perot observations of three HII-regions: Sh2-152-153 and 106 show the expansion of the diffuse matter relative to the exciting stars. In the Sh2-106 region a probably jet is found. It is shown that in star forming regions the diffuse matter is taking part in expansion motions together with stars.

1. *Introduction.* In autumn 1985 the improved scanning Fabry-Perot interferometer (equipment "CIGALE" [1,2]) has been mounted on prime focus of 2.6-m telescope of the Byurakan Astrophysical Observatory (Armenia) for observations of diffuse matter. This interferometer created in the Marseille Observatory (France) has very perfect construction and gives possibility to measure radial velocities of diffuse matter in numerous points in some HII-regions for study of their velocity field. The search of H_α -emission in the direction of the h and χ Persei (Per OB1 association) was another separate problem, which was significant since up to these observations it was not known the existence of such emission. Thus the spontaneous scientific cooperation began between two mentioned observatories.

However, the strong earthquake in Armenia and very difficult consequences after it forced to forget these observations for long time. And only persistence of Armenian astronomers allowed to obtain the results which seem to be important.

All the work connected with processing of the obtained observational material was done after many years with computer "VAX" in the Marseille Observatory by French and Armenian astronomers.

In this paper some essential results of this scientific cooperation are presented.

2. *H_α-emission in the direction of h and χ Persei system.* Per OB1 association is the only one which is not connected with any diffuse nebulae. This association of blue and red giant and supergiant stars is in fact a superposition of two OB-associations (designed by us Per OB1 and OB2 [3]) projected on each other. They are on the distances about 1150pc and 2300pc respectively [4,5]. The study of space distribution of absorbing matter in the direction of h and χ Per showed that the absorption is concentrated completely inside of these two associations [4]. The presence of absorbing matter (dust) in this direction gives us some grounds to expect the existence of gaseous matter also in them.

After some attempts the H_α-emission was found in the direction of h and χ Persei (R.A.(1985)=$2^h19^m08^s$ and Dec.(1985)= 57°06'10"). The exposure time of these H_α-observations was 6000 seconds. The observed field was equal to 9'×9' (every pixel was equal to 2".13×2".13). The intensity of the observed H_α-emission is about 2×10^{-6}erg $cm^{-2}s^{-1}sr^{-1}$ [6].

It is possible that this H_α-emission comes mainly from the nearest OB-association (Per OB1), since the emission from farthest one must be too faint [5]. The detection of the H_α-emission in the direction of Per OB1 and Per OB2 associations means that the gas and dust are mixed in them.

3. *Fabry - Perot interferometric observations of HII-regions.* Soon after the discovery of stellar associations in the Galaxy [7] it has been established that they are non-stable stellar systems. The new formed stars are moving off from the volumes of their formation. These motions bring to the expansion and decay of associations. The final result is disintegration and dissipation of matter from the regions of star formation (see, for example, [7]).

From this point of view it was significant to study the motions of diffuse matter, in particular of the hydrogen.

At present the study of velocity fields for three HII-regions is finished and here the obtained results are presented.

Sh2-152 and Sh2-153. In the first H_α -interferometric study Pismis and Hasse [8] have determined the general distribution of the ionized hydrogen in Sh2-152. It is not symmetrical relative to its exciting star. HII-region Sh2-152 consists of two components: the very bright component of the "triangular" form and a fainter curling component which seems to be the continuation of the main component.

The new H_α -interferometric observations of Sh2-152 confirm this general structure. New observations obtained with a higher resolution showed additional condensations around the exciting star. Besides the condensation situated just around the exciting star two other condensations are observed to the west of it. One of them seems to be even denser than the condensation around the exciting star. The Fabry - Perot observations of two HII-regions: Sh2-152 and Sh2-153 connected with each other and representing a part of more extended region containing other HII-regions too (see, for example, [9]) showed an expansion of hydrogen matter in these regions.

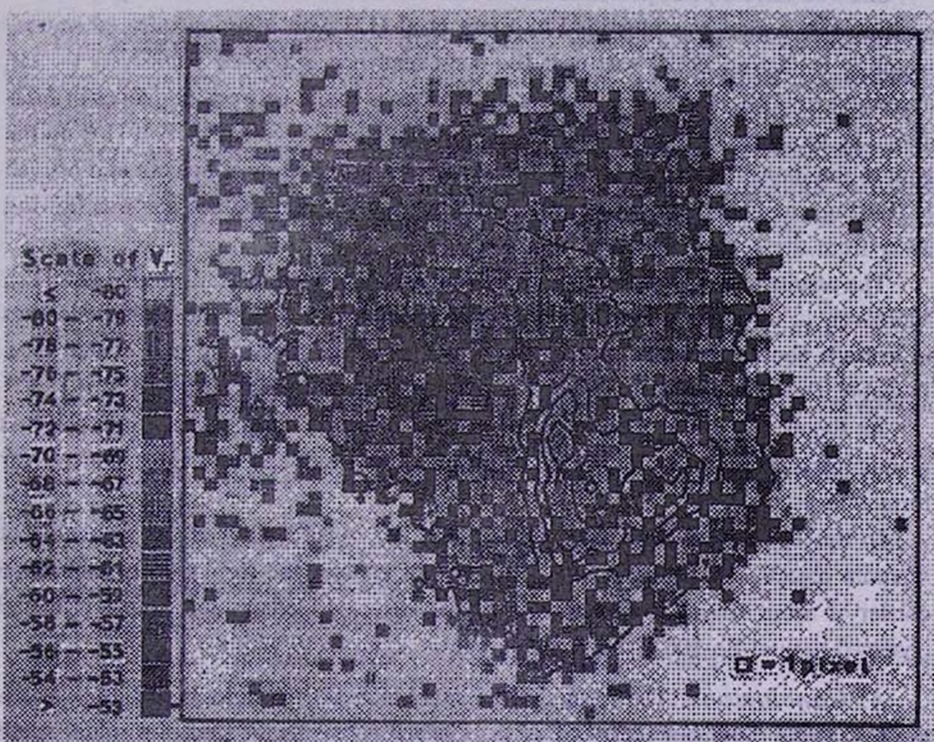

Fig. 1. An example of the distribution of radial velocities in HII Region of Sh2 - 152 [10].

The radial velocities of hydrogen atoms reach considerable magnitudes: about -70km/s near to exciting stars in both HII- regions. Their dispersion is enough large (from about 5-10km/s up to 30-40km/s) especially at large distances from the exciting star.

Namely, the dispersion of individual radial velocities in Sh2-153-region increases almost regularly and reaches to about 20km/s on the distance of 100 arcsec (in projection on the sky) from the exciting star. This dispersion is much larger, in general, in Sh2-152-region on the distance about 40 arcsec from the exciting star and remains practically unchanged up to distance 100 arcsec.

Sh2-106. One of the most peculiar objects among observed HII-regions is Sh2-106. Owing to its unusual shape this region has been oftenly studied in details in optics, infrared and radio. The main results of the studies of Sh2-106, are presented by Staude and Elsasser [11] recently.

Sh2-106 have bipolar structure and is situated on the distance 500-600pc.The star exciting this region was identified by Eiora et al [12] with a strong infrared source, which is in fact an O-BO star near the main-sequence, supposed intensively (~ 21^m according to [12]) absorbed. The absorbing matter is found between two lobes of Sh2-106. The motions of diffuse matter in Sh2-106 have been revealed by Solf [13] on the base of the longslit spectroscopy and by Maucherat [14] and by Hippelein and Munch [15] using the Fabry - Perot observations. They showed that ionized gas was flowing away from the central region of Sh2-106.

The results of our Fabry - Perot interferometric observations confirm this fact [16]. Moreover, in the southern lobe there is a compact region where the radial velocities in average about two times exceeds the velocities of the remaining part of that lobe. Probably, this fact can be considered as an evidence of jet-like structure in it.

As Evans [17] noted the process of outflow of matter from all peculiar objects is ubiquitous and definitely show the direction of the motions of matter during star formation process.

In this connection it should be noted that the consideration of the formation of separate objects, for example Sh2-106, can not explain the formation of embedded cluster of about 160 stars of moderate masses detected Hodapp and Reiner [18] and observed around Sh-106 (the probable age is about 2×10^6yr [18]).

4. *Conclusions*. The results of the study of stellar motions in OB-associations are the strong argument in favour of the dissipation of matter from the initial small volumes as the paramount feature of cosmic evolution [19]. They always indicate the moving off young stars from the regions where they are formed. It means that the dissipation of the matter is inevitable in the regions of star formation [7].

The presented results concerning the motions of hydrogen matter in the HII-regions obtained on the base of Fabri-Perot interferometric observations are in complete agreement with this idea. They confirm Ambartsumian's [19] fundamental conclusion that "the decay and dissipation... characterize general trend of cosmogonic processes". New Fabry - Perot observations showed that not only stars, but also diffuse matter takes part in this dissipation processes connected with the formation of stars and stellar systems-centres of star formation in stellar associations.

ФРАНКО-АРМЯНСКОЕ НАУЧНОЕ СОТРУДНИЧЕСТВО В ИЗУЧЕНИИ НЕКОТОРЫХ НII-ОБЛАСТЕЙ С CIGALE

Л.В.МИРЗОЯН, М.МАРСЕЛИН, А.Т.ГАРИБДЖАНЯН,
Ж.БУЛЕСТЕКС, У.М.ЖОРЖЕЛИН, В.В.АМБАРЯН,
А.Л.МИРЗОЯН, Е.ЛЕ КОАРЕР, А.ЛАВАЛ

Представлены результаты Фабри-Перо наблюдений 4 полей, полученных в первычном фокусе 2.6 м телескопа в Бюракане (Армения), прибором "CIGALE" Марсельской обсерватории. Обнаружено H_α-излучение в направлении ассоциации Персея. Показано, что межзвездный водород в ассоциациях участвует в расширительных движениях материи приводя к рассеянию и дезинтеграции материи в Галактике.

REFERENCES

1. *J.Boulesteix, Y.P.Georgelin, M.Marselin, G.Monnet*, SPIE Conf.Instrum. Astron., V, 445, 37, 1983.
2. *A.Laval, J.Bouleesteix, Y.P.Georgelin, M.Marcelin*, Astron.Astrophys., 175, 199, 1987.
3. *L.V.Mirzoyan, V.V.Hambarian, A.T.Garibjanian*, Astrofizika, 34, 357, 1991.
4. *A.T.Garibjanian*, Astrofizika, 20, 437, 1984.
5. *L.G.Balazs, A.T.Garibjanian*, Astrofizika, 27, 245, 1987.
6. *L.V.Mirzoyan, M.Marselin, A.T.Garibjanian, J.Boulesteix, A.L.Mirzoyan, Y.M.Georgelin*, Astrofizika, 34, 67, 1991.
7. *V.A.Ambartsumian*, Stellar Evolution and Astrophysics, Acad. Sciences of Armenia, Yerevan, 1947.
8. *P.Pismis, I.Hasse*, Rev.Mexicana, Astron.Astrofiz., 5, 39, 1980.
9. *C.Kahane, S. Guilloteau, R.Lucas*, Astron.Astrophys., 146, 325, 1985.
10. *L.V.Mirzoyan, J.Boulesteix, V.V.Hambarian, M. Marcelin, A.L.Mirzoyan, Y.M.Georgelin, E. Le Coarer, A. Laval*, Astrofizika, 37, 175, 1994.
11. *H.J.Staude, H.Elsasser*, Astron.Astrophys.Rev. 5, 165, 1993.
12. *C.Eiora, H.Elsasser, J.F. Lahulla*, Astron.Astrophys., 74, 89, 1979.
13. *J.Solf*, Astron. Astrophys., 92, 51, 1980.
14. *A.J.Maucherat*, Astron.Astrophys., 45, 193, 1975.
15. *H.H.Hippelein, G.Munch*, Astron.Astrophys., 99, 248, 1981.

16. *L.V.Mirzoyan, J.Boulesteix, V.V.Hambarian, M. Marcelin, A.L.Mirzoyan, Y.M.Georgelin, E. Le Coarer, A. Laval*, Astrofizika, 38, 1995.
17. *N.J.Evans II*, Protostars and Planets II, Tucson, Arizona, eds. David C.Black and Mildred Shapley Matthews, 1985, p.175.
18. *K.W.Hodapp, J.Reiner*, Astron.J., 102, 1108, 1991.
19. *V.A.Ambartsumian*, Probleme der Modernen Kosmogonie, Academie Verlag, Berlin, 1980, p.4.

АСТРОФИЗИКА

ТОМ 38 НОЯБРЬ, 1995 ВЫПУСК 4

FORMATION OF SPECTRAL LINES IN STELLAR ATMOSPHERES. LINEAR AND NONLINEAR THEORY

N.B.YENGIBARIAN, A.Kh.KHACHATRIAN

Byurakan Astrophysical Observatory

The present paper represents a short review of some directions of Radiative Transfer Theory in spectral lines (RTSL) concerning investigations of authors in this field.

1. *Nonlinear transfer theory of coherent or completly non coherent scattering*. It is well known, that due to an interaction of the strong radiation field with medium the local optical properties of the medium depend on the state of radiation field. At RTSL strong radiation field reduces to the high excitation of atoms and as a result of it the absorption capacity of the medium decreases (in a series of the ground state) and the effects of stimulated absorption begin to play role (negative absorption). Then the Transfer equation becomes nonlinear. Nonlinear Transfer Problems (NLTP) are of a great importance not only in astrophysics, but also in the theory of quantum optical generators.

Up to the 60 - s. the analytical theory of NLTP was absent. Although in that period the physics of local act of interaction of the strong radiation field was well known.

In 1963 the creation of the nonlinear theory of RTSL was undertaken by academician V.Ambartsumian and his followers.The investigations have been carried out by two basic directions.

a) Application of the principle of invariance (PI) of Ambartsumian to NLTP.

b) Development and creation of the method of self-consistent optical depths (SCOD).

The basic results due to the method of SCOD were obtained. The idea of this method which was suggested by V.Ambartsumian in 1964, was based on the possibility of exact linearization of NLTP in homogeneous plane layer by means of transition from limiting optical depth to real optical depth (which depends on radiation field) (see [1]).

The method of SCOD was realized by N.B.Yengibarian [2] where for the first time NLTP in three dimensional medium was exactly solved. The electron collision of the second kind was taken into account. It was also assumed, that in spectral line coherent scattering took place. This assumption means that the profile of absorption coefficient is directangle.

One of the most basic questions connected with application of SCOD (within linearization of the transfer equation) is determination of the real optical thickness of medium in spectral lines.

In [2] the following formula connected with limiting (y_0) and real (τ_0) optical thickness in case of two level atoms was found

$$y_0 = \tau_0 + \gamma \cdot \int_0^{\tau_0} S(\tau, \tau_0)\, d\tau \tag{1}$$

where S- is the source function for linear transfer problem in slab of thickness τ_0 and γ=const.

In [2] NLTP in the medium, consisting of three level atoms, when the transition $1 \leftrightarrow 2$ are forbidden, was also solved.

In the work [3] by Therebij the method and results of the [2] were propagated for the case, when in spectral lines takes place complete redistribution in frequencies with an assumption coincidence of the profiles of absorption, stimulated and spontaneous emissions.

A number of monochromatic and polychromatic scattering problems representing essential astrophysical interest, were solved in the papers of Yengibarian, Vardanian, Therebij, Abramov, Dikhne, Napartovich and others (see [3-6]) by using methods of [2]; NLTP in presence of scattering and absorbing atoms, internal energy sources, taking into account electron collisions of the first and second kinds and so on among them were also solved.

The paper [7] of Khachatrian is devoted to the mathematical substantiation of the SCOD's method. In Yengibarian's work [8] nonlinear Miln's problem has been studied by using the method of [2]. In particular it was shown, that in the case of coherent scattering even for $\lambda < 1$, the solution of the problem lineary decreases with the geometrical depth.

The application of the results of the above mentioned works to the concrete astrophysical problems is not enough advanced yet.

In the 60-s some NLTP in a one dimensional medium and nonlinear nonstationary transfer problems were solved by means of application of PI and direct methods (see [9-11]). Some NLTP connected with an application in the theory of quantum optical generators have been studied too.

2. *Transfer in spectral lines with partial redistribution in frequencies (PRF).* The redistribution of radiation by frequencies at an elementary act of scattering (noncoherent scattering) plays an important role. It is described by redistribution function (RF)

$$r(x,x') = g(x,x')\alpha(x') \tag{2}$$

where $g(x,x')$ is the probability that an incident photon with a dimensionless frequency x' before scattering will acquire a frequency in the range from x to $x+dx$; and $\alpha(x)$ is the profile of absorption.

In general r depends also on the angle of scattering γ

$$r = r(x,x',\gamma).$$

The basic physical processes reducing to the noncoherent scattering are the following: natural width of spectral lines, Doppler broadening due to thermal or other kind of motions moving of atoms, pressure effects and etc.

In the middle of the 60-th the expressions of the function r corresponding to the basic mechanism of redistribution already were well known. Although up to the 70-th Transfer problems in spectral lines with simplest assumption on complete redistribution by frequency (CRF), as a rule, were considered (see [12]). Then $r = A\,\alpha(x)\alpha(x')$. In those cases, when the Doppler effect plays an essential role in process of redistribution, the assumption CRF become inadequated.

In 1971 in [13] the creation of analytical theory of RTSL at real physical laws of noncoherent scattering was begun byYengibarian.Here we shall use the therm "partial redistribution by frequencies" (PRF) adopted in astrophysical literature.Further a number of papers of Yengibarian, Nikoghossian, Gevorkian, Harutyunian, Pikichian, Khachatrian and others appeared, devoted to the development of PRF theory (see [14-20]).

In these works a number of problems of spectral lines formation in stellar atmosphere and other cosmic objects have been effectively solved. In [21-25,12] a rich arsenal of classical and new methods of the transfer theory and the theory of integral equations have been applicated; PI method, Probability method of Sobolev [12], Yengibarian's nonlinear factorization equation method [21,22], matrix method [19,20], the special method which reduced transfer problem in the plane layer of finite thickness to the corresponding transfer problem in half space [23,24], modification of

Chandrasekhar's discrete ordinate method [25], methods of analytical semigroups [23] and so on among them.

In [14] and in the next works the following bilinear expansion of RF plays a principle role

$$r(x,x') = \sum_{k=1}^{\infty} A_k \, \alpha_k(x)\alpha_k(x'). \tag{3}$$

It was shown the importancy of the expansion (3) in the case,when the $\{\alpha_k(x)\}$ are orthogonal with the weighting factor $1/\alpha$

$$\int_{-\infty}^{\infty} \frac{\alpha_k(x)\alpha_m(x)\,dx}{\alpha(x)} = \delta_{km} \,. \tag{4}$$

The works of Hummer and Avrett and other astrophysists (see [26-32]) for studing RF and creation of the expansion of type (3) a very important role have played.

In the case, when r depends on γ, the following decomposition is used

$$r(x,x',\gamma) = \sum_{l} P_l(\cos\gamma) \sum_{k} A_{lk} \, \alpha_{lk}(x)\alpha_{lk}(x') \tag{5}$$

where P_l - are Leghandre polynomials.

During the numerical solution of transfer problems with PRF in many cases various approximation methods were parallelly used.Comparison of the results shows neglected divergence of results. Matrix method is simpler from the point of view of calculation.

For the last years in astrophysical literature a number of investigations for the problems RTSL with PRF appeared,where different methods of discretization by frequencies were used (see [26-32]).

One of the most interesting case of the theory of RTSL with PRF is the problem, when

$$r(x,x') = a\alpha(x)\alpha(x') + b\alpha(x)\delta(x-x'). \tag{6}$$

This problem in work [33] of authors of the present paper, in context with application to the problems of the γ-quantum scattering on Mossbauer nuclei was solved.

3. *Nonlinear problems RTSL at PRF.* Consideration of the real laws of redistribution by frequencies is the actual problems of nonlinear theory of RTSL. In 70-s in astrophysical literature a number of s.c. works concerning above mentioned problems appeared, some results of which are published in monograph by D.Mihalas [29].

In these works "Full linearization method" (FLM) of Milkey and Mihalas takes the main place. FLM based on special iteration processes.Although (by admition of authors) this iteration processes are very laborious.

In the works [34,35] an analytical approach to the solution of NLTP with PRF is developed.This approach is based on the method of SCOD and the methods of linear theory of noncoherent scattering with PRF.

An assumption is made on the coincidence of the absorption coefficient profile $\alpha(x)$ with that of stimulated coefficient profile $\psi^*(x)$. It allows us exact linearize NLTP and reduce it to the analytical solution of the problem,by means of Ambartsumian's generalizing functions or matrix analogy.

Functions $\alpha(x)$, $\psi^*(x)$ and $\psi(x)$ (profile of spontaneous radiation) theoretically are different,connected with it, that on different levels, particularly in the excited states, the deviation of velocity distribution from Maxwell velocity distribution is appreciable, that is conditioned by the selective character of atom excitation by quanta of this or that frequency (see [36-38]). The numerical results show (see [37]) , that the relative deviation $\dfrac{\psi^* - \alpha}{\alpha}$ is of the order of 5 per cent in the center,which is well agreed with the results of [38]. That's why the assumption of coincidence α and ψ^* is a good first approximation to the solution of the problem. In [39] the second approximation, taking into account differences between α and ψ^* is given.

4. *Radiative transfer in the random nonhomogeneous medium (RNHM).* For the first time in astrophysics the transfer problem in RNHM with random local optical properties was considered and solved by Yengibarian and Nikoghossian [40]. Solution of such problems contains valuable information about local optical properties of the medium and presents essential astrophysical interest.

The problem of diffuse reflection from random inhomogeneous plane layer is solved by means of application of PI. It was assumed that albedo of scattering $\lambda = \lambda(\tau)$ is a random function of optcal depth, which is described by Gauss-Markov random process.

Solution and studying of the transfer problems (for different models) in RNHM were continued by Yengibarian, Vardanian and others (see [41]).

In the 70-s in astrophysical literature a number investigations devoted to the radiative transfer in RNHM appeared.

ОБРАЗОВАНИЕ СПЕКТРАЛЬНЫХ ЛИНИЙ В ЗВЕЗДНЫХ АТМОСФЕРАХ. ЛИНЕЙНАЯ И НЕЛИНЕЙНАЯ ТЕОРИИ

Н.Б.ЕНГИБАРЯН, А.Х.ХАЧАТРЯН

Статья представлят собой краткий обзор некоторых направлений теории переноса излучения в спектральных линиях, развитых авторами.

REFERENCES

1. *V.A.Ambartsumian*, Sb."Theoria zvezdnikh spectrov".Nauka, M, 1966.
2. *N.B.Yengibarian*, Astrofisica, 1, 297, 1965.
3. *V.U.Therebij*, Astrofisica, 3, 282, 1967.
4. *N.B.Yengibarian*, Astrofisica, 2, 31, 1966.
5. *U.U.Abramov, A.M.Dikhne, A.P.Napartovich*, GETF, 52,536, 1967.
6. *R.S.Vardanian, N.B.Yengibarian*, DAN Arm.SSR, 3,135, 1967.
7. *S.A.Khachatrian*, Sb."Math. analyse i ego prilogenia".Yerevan, 1980.
8. *N.B.Yengibarian*, Astrofisica, 16, 595, 1980.
9. *A.G.Nikoghossian*, Astrofisica, 1, 285, 1965.
10. *N.B.Yengibarian*, Astrofisica, 3, 325, 1967.
11. *N.B.Yengibarian*, R.S.Vardanian, Astrofisica, 5, 203,1969.
12. *V.V.Sobolev*, Perenos Luchistoi energi, M, 1956.
13. *N.B.Yengibarian*, Astrofisica, 7, 573, 1971.
14. *N.B.Yengibarian, A.G.Nikoghossian*, Astrofisica, a). 8,71,1972; b) 8,215,1972; c) 9,79,1973.
15. *N.B.Yengibarian, A.G.Nikoghossian*, J.Q.S.R.T. 13,787,1973.
16. *M.S.Gevorkian, N.B.Yengibarian, A.G.Nikoghossian*, Astrofisica, 22, 599, 1985.
17. *H.A.Harutyunian, A.G.Nikoghossian*, DAN SSSR, 242,66,1978.
18. *O.V.Pikichian*, Astrofisica, 14, 169,1978.
19. *M.S.Gevorkian, A.Kh.Khachatrian*, Astrofisica, 22,599,1985.
20. *A.Kh.Khachatrian, A.A.Akopian, E.A.Melkonian*, J.Q.S.R.T. 45,367,1991.
21. *N.B.Yengibarian, A.A.Arutunian*, Math.Sbornik, 97,35,1975.
22. *N.B.Yengibarian, L.G.Arabadjian*, Itogi Nauki i Teckniki M. 22,175,1984.

23. *N.B.Yengibarian, M.A.Mnatsakanian,* DAN SSSR, 217,533,1974.
24. *N.B.Yengibarian, M.A.Mnatsakanian,* Math.Zametki,19,927. 1976.
25. *N.B.Yengibarian, E.A.Melkonian,* DAN SSSR,292,322, 1987.
26. *D.G.Hummer,* M.N.RAS 128,21,1962.
27. *E.H.Avrett, D.G.Hummer,* M.N.RAS 13O,295,1965.
28. *D.G.Hummer,* M.N.RAS 145,95,1969.
29. *D.Mihalas,* Stellar Atmospheres v.1,2. 1982 (in Russian).
30. *R.Milkey, D.Mihalas,* Ap. J. 185, 709, 1973.
31. *R.Heasley, F.Kneer,* Ap.J. 203, 660, 1970.
32. *J.Hubeny,* Bull. Astron. Inst. Czech. 32, 271, 1981.
33. *N.B.Yengibarian, A.Kh.Khachatrian,* J.Q.S.R.T. 46, 565, 1991.
34. *N.B.Yengibarian, A.Kh.Khachatrian,* Astrofisica, 23, 145, 1985.
35. *A.Kh.Khachatrian,* Astr.and Space Science, 172. 167, 1990.
36. *J.Oxenius,* J.Q.S.R.T. 5, 771, 1965.
37. *A.Kh.Khachatrian, A.A.Akopian,* Astrofisica, 25, 189, 1986.
38. *R.Steinitz, R.Shine,* M.N.RAS 162, 197, 1973.
39. *A.Kh.Khachatrian,* Candidate Dissertation, Tartu, 1987.
40. *N.B.Yengibarian, A.G.Nikoghossian,* Sb. Zvezdi,Tumannosti, Galaktiki, Yerevan, 1969.
41. *N.B.Yengibarian, R.S.Vardanian,* Astrofisica, 31, 162, 1989.

АСТРОФИЗИКА

ТОМ 38 НОЯБРЬ, 1995 ВЫПУСК 4

RELATIVISTIC ROTATION AND PULSAR ELECTRODYNAMICS

R.A.KRIKORIAN

College de France
Institut d'Astrophysique

Two illustrative examples are presented as an application of the relativistic rotation transformation and the nonlinear speed-distance relation.

1. Introduction. The hypothesis that the magnetosphere of a pulsar is a plasma in rotation, the rotation velocity approaching the light velocity for regions located close to the light cylinder, permit to describe certain characteristics of the pulsar phenomenon. The phenomenological models [1-4], describing the properties of pulsar emission, as well as the theoretical investigations [5-8] treating of the electrodynamics of pulsar are all based on the hypothesis that the rotation velocity v, at a distance r from the axis of rotation, is given by the well known linear law

$$v = r \cdot \omega \tag{1}$$

Although this law is rendered compatible with special relativity by limiting the rotation to regions interior to the light cylinder $r_L = c/\omega$, it is not satisfactory from the relativistic standpoint for the following reasons:

a) It implies the absolute character of simultaneity at a distance;

b) It does not satisfy the relativistic composition law of velocities;

In the 1950's, Takeno [9] and Trocheris [10] proposed to describe uniform rotation in special relativity by the following transformation

$$\begin{aligned} r'\varphi' &= r\varphi \,\mathrm{ch}\lambda - ct\,\mathrm{sh}\lambda \qquad r' = r \\ ct' &= ct\,\mathrm{ch}\lambda - r\varphi\,\mathrm{sh}\lambda \qquad z' = z \end{aligned} \qquad \lambda = \frac{\omega r}{c} \tag{2}$$

This transformations, which respects the relativity of simultaneity at a distance, the relativistic composition law of velocities and the addition law for angular velocities, leads to the non linear speed - distance relation

$$v = c\,\mathrm{th}\lambda \tag{3}$$

As we see the rotation velocity v is never larger than c and reduces to its galilean value when $\lambda \ll 1$. The light-cylinder is then no more meaningful as it goes to infinity. It therefore appears necessary to investigate how the overall picture of the pulsar phenomenon is modified when one uses the relativistic rotation transformation (2) and the non linear speed - distance relation (3). We briefly present two illustrative examples of such modifications. For further details and applications see ref. [11-13].

2. The co-rotating source model. According to this model [1-4] the radiation source is located close to the light cylinder and the main characteristics of the pulsar radiation appear as relativistic effects of a very rapidly rotating source ($v \sim c$). The use of transformation (2) and formula (3) modifies slightly the characteristic parameters of pulsars. Assuming that the energy flux $f'(\nu')d\nu'$ in the instantaneous rest frame K' of the radiation source is given by a power law spectrum

$$f'(\nu') = E\nu'^{-\varepsilon} \qquad (E, \varepsilon = \mathrm{const}) \tag{4}$$

we obtain from (2) the following expression for the observed spectral distribution [11]

$$f(\nu,\varphi) = E[\gamma(1-\mathrm{th}\lambda\cdot\cos\varphi)]^{-(3+\varepsilon)}\cdot\nu^{-\varepsilon}$$
$$\gamma = \mathrm{ch}\lambda. \tag{5a}$$

Equation (5a) permits the determination of the beam width $\Delta\varphi = 2\varphi_{1/2}$ corresponding to the halfpower level, we have

$$\left(\frac{1-\mathrm{th}\lambda\cdot\cos\varphi_{1/2}}{1-\mathrm{th}\lambda}\right)^{3+\varepsilon} = 2.$$

which for $\mathrm{th}\lambda \cong 1$ leads to

$$\Delta\varphi = 2\varphi_{1/2} \cong 2a\gamma^{-1}, \quad a = (2^{\frac{1}{3+\varepsilon}} - 1)^{1/2} \tag{5b}$$

the duration of the pulse is given by the difference between the time during which the radiation pattern of width $\Delta\varphi$ is directed to the earth and the time for radiation to cover the shift of source, we have [2]

$$\Delta P = r\frac{\Delta\varphi}{v} = \frac{2r}{c}\sin\Delta\varphi/2$$

using $\mathrm{th}^{-1}\beta = \lambda$ and $P = 2\pi/\omega$ period of the pulsar relative to the observer we obtain

$$\Delta P = \frac{P}{2\pi}\frac{\mathrm{th}^{-1}\beta}{\beta}(\varphi_{1/2} - \beta\sin\varphi_{1/2}) \tag{5c}$$

which for ultrarelativistic motion, i.e. $\beta \approx 1$, reduces to

$$\Delta P \cong \frac{aP}{2\pi}\gamma^{-3/2}\log 2\gamma .$$

Table 1 illustrates the modifications brought by the non linear laws in the values of the characteristic parameters for the pulsar PSR 0833 [2], period $P = 9\cdot 10^{-2}$s, pulse duration $\Delta P = 2\cdot 10^{-3}$s, index of frequency spectrum $\varepsilon = 1$.

Table 1

Parameter	linear law	nonlinear law
β	0.79	0.83
$\Delta\varphi$	0.64 rad	0.56 rad
r	$3.4\cdot 10^8$ cm	$5.1\cdot 10^8$ cm
$f(\nu,0)/f_0$ $f_0=E\nu^{-\varepsilon}$	73	116

We see that

1) the source is located at a distance close to the light cylinder $r_L = 4.3\cdot 10^8$cm for the linear law and larger than r for the non linear law;
2) is less than unity in both cases;
3) the beamwidth is smaller for the non linear law while the increase in the energy flux is more important.

3. *The quasi-static condition.* In pulsar electrodynamics one often uses the so-called quasi-static condition [5-7]

$$\frac{\partial}{\partial t} = -\omega\frac{\partial}{\partial\varphi}, \tag{6}$$

where the time t and the azimuthal angle φ refer to the laboratory frame K. Condition (6) may be stated in a coordinate independent manner with the help of the Lie derivative. When applied to a 4-vector A^i it takes the form:

$$L(X)A_i = X^k\,\partial_k A_i + A_k\,\partial_i X^k = 0, \quad \partial_k = \frac{\partial}{\partial r^k} \tag{7}$$

where $X_i^i = (1, 0, \omega/c, 0)$ in coordinates $(x^0 = ct, r, \varphi, z)$. We have $X^i X_i = -1 + \omega^2 r^2/c^2$; hence X^i is timelike inside the light cylinder and spacelike outside. This leads Ardavan [7] to claim that under condition (6) the wave equation, for the 4 potential A, changes type (elliptic $\rightarrow$ hyperbolic) when crosses the light cylinder. From transformation (2) and the non linear law (3) the quasi static requirement can be generalized in an invariant form to:

$$L(u)A_i = 0, \quad u^i = (\mathrm{ch}\lambda, 0, \mathrm{sh}\lambda/r, 0). \tag{8}$$

In the case of the 4 potential A_i equation (8) gives

$$L(u)A_i = (\mathrm{ch}\lambda\partial_0 + \mathrm{sh}\lambda/r\,\partial_\varphi)A_i = 0 \tag{9}$$

The generalized quasi static condition (9) clearly gives the classical condition (6) when $\lambda \ll 1$.

Now, in the Lorentz gauge, the 4 potential A_i satisfies the wave equation

$$\Box A_i = g^{hk}\,\nabla_h\nabla_k A_i = -J_i \tag{10}$$

where J_i is the 4 current. It reads for instance in the case of A_0, when $\partial_{00} A_0 = \frac{1}{r^2}\mathrm{th}^2\lambda\frac{\partial^2 A_0}{\partial\varphi^2}$ is substituted from equation (9)

$$r^{-1}\frac{\partial}{\partial r}(rA_0) + r^{-2}(1-\mathrm{th}^2\lambda)\frac{\partial^2 A_0}{\partial\varphi^2} + \frac{\partial^2 A_0}{\partial z^2} = -J_0. \tag{11}$$

Unlike with condition (6), the coefficient of $\partial^2 A_0/\partial\varphi^2$ has its sign constant with the generalized condition (9) and the wave equation does not change type.

4. Conclusion. The use of transformation (2) and of the non linear speed-distance relation (3) by sending the light cylinder at infinity modifies the characteristic parameters of pulsars in the co-rotating source model circumvents the change of type of the 4 potential equation when a quasi-static type constraint is assumed. In brief, the light cylinder concept is a byproduct improper use of the linear speed-distance relation at relativistic velocities.

РЕЛЯТИВИСТСКОЕ ВРАЩЕНИЕ И ЭЛЕКТРОДИНАМИКА ПУЛЬСАРОВ

Р.А.КРИКОРЯН

В качестве применения преобразования релятивистского вращения и нелинейного соотношения скорость - расстояние приведены два иллюстративных примера.

REFERENCES

1. *F.G Smith*, Mont. Not. Roy. Ast. Soc., 149, 1, 1970; ibid, 154, 5p, 1971.
2. *V.V. Zheleznyakov*, Astrophys. Sp. Sci., 13, 87, 1971.
   V.V. Zheleznyakov, V.E. Shaposhnikov, ibid, 18, 166, 1972.
3. *W.H.McCrea*, Mont. Not. Roy. Ast. Soc., 157, 359, 1972.
4. *D.C.Ferguson*, Nature, 234, 86, 1971.
5. *V.S.Beskin, A.V.Gurevich, Ya.Istomin*, Soviet Phys. JETP Lett., 58, 235, 1983.
6. *L.Mestel*, Nature, 233, 149, 1971; Astrophys, Sp. Sci., 24, 289, 1973.
7. *H.Ardvan*, Astrophys. J., 251, 674, 1981.
8. *W.H.Fawley, J.Arons, E.T.Scharlemann*, Astrophys. J., 217, 227, 1977.
9. *H.Takeno*, Progr. Theor. Phys., 7, 367, 1952.
10. *M.G.Trocheris*, Phil. Mag., 40, 1143, 1949.
11. *S.Kichenassamy, R.A.Krikorian*, Astrophys. J., 371, 279, 1991.
12. *S.Kichenassamy, R.A.Krikorian*, Astrophys. J., 431, 715, 1994.
13. *S.Kichenassamy, R.A.Krikorian*, J. Math. Phys., 35, 5726, 1994.

АСТРОФИЗИКА

ТОМ 38 НОЯБРЬ, 1995 ВЫПУСК 4

SOME NEW NONLINEAR RELATIONS OF THE RADIATIVE TRANSFER THEORY

A.G.NIKOGHOSSIAN

Byurakan Astrophysical Observatory,
378433, Armenia

The paper presents a part of new results concerning the generalization and physical interpretation of Rybicki's quadratic and bilinear relations. The fundamental equations obtained on the base of Ambartsumian's invariance principle and regarded as its extension to all depths in the atmosphere, imply the Q- and R- relations with more general structure than those known up to the present. These equations admit a simple probabilistic interpretation. Some bilinear relations are derived to connect the transfer problems of different sorts. For the sources distributed in the semi-infinite atmosphere by exponential law, the separate Q-and R-relations are obtained.

1. *Introduction.* As it was shown in the G.B. Rybicki's paper [1], for some cases the transfer equation admits integrals that involve quadratic moments of the radiation field. They permit one to generalize to all depths in the atmosphere some surface results as the Hopf-Bronstein equation or the $\sqrt{1-\lambda}$ -law. The cases treated encompass the exponential and power laws for distribution of internal sources of energy. The more general conception of "bilinear integrals" were introduced for quadratic integrals that connect the radiation fields of two separate transfer problems. Although the bilinear integrals were not derived in [1], they obviously were known to the author by that time. Later we shall see that the quadratic and bilinear integrals follow from the simple relations between well-defined physical quantities, in deriving of which no integration is required so that in further discussion we shall prefer the term "relations" to "integrals".

Some generalization of G.B. Rybicki's results for the plane-parallel medium was given by V.V. Ivanov [2]. The so-called "two-point" relations were found that couple the intensities of equally directed radiation at two different depths in the atmosphere. While the author calls them also "bilinear relations", by its sense they are out of keeping the definition given in [1]. Similar results were obtained in [3].

Regardless of the new results, thc main question on the physical nature of the such kind quadratic relations remains still abstruse. This point is of particular concern also for the second-order escape probability methods recently developed for computational radiative transfer [4].

It is the purpose of this paper to demonstrate the profound connection of the quadratic and bilinear relations with the invariance principle, what suggests a statistical interpretation for these relations. For the first time, there derived two fundamental equations that enable to generalize the major part of hitherto known results for the semi-infinite atmosphere. Bilinear relations for some important transfer problems are given.

2. *The invariance principle and basic equations.* We start with treating the case of monochromatic, isotropic scattering in a semi-infinite, plane-parallel atmosphere. Assume also that the atmosphere is homogeneous and does not contain energy sources. One of the most important characteristics of an atmosphere is its reflectivity that involves also an information on the internal field of radiation established in the presence of initial energy sources.

It is well known [5-7] that the function ρ referred to as «reflection coefficient» or "reflection function" can be found from the separate functional equation obtained on the basis of the Ambartsumian's invariance principle (hereafter we are concerned with the azimuth-averaged quantities)

$$(\eta+\xi)\rho(\eta,\xi)=(\lambda/2)\varphi(\eta)\varphi(\xi) \tag{1}$$

where

$$\varphi(\eta)=1+\eta\int_0^1\rho(\eta,\eta')\,d\eta' \tag{2}$$

is known as Ambartsumian's φ-function. The incidence and reflection angles $\cos^{-1}\xi$ and $\cos^{-1}\eta$ are referenced correspondingly from inward and outward normal directions. The reflection coefficient possesses a symmetry property $\rho(\eta,\xi)=\rho(\xi,\eta)$, resulting from the reciprocity principle of the optical phenomena. Taking together, equations (1) and (2) lead to the separate equation for the function $\varphi(\eta)$

$$\varphi(\eta)=1+(\lambda/2)\eta\int_0^1\varphi(\eta)\varphi(\eta')\,d\eta'/(\eta+\eta') \tag{3}$$

which implies the zero-moment of $\varphi(\eta)$:

$$\alpha_0 = \int_0^1 \varphi(\eta)\, d\eta = 2[1-\sqrt{1-\lambda}]/\lambda. \tag{4}$$

Making use (4), equations (2) and (1) can be rewritten as follows

$$\sqrt{1-\lambda}\varphi(\eta) = 1 - \int_0^1 \rho(\eta,\eta')\eta'\, d\eta' \tag{5}$$

and

$$(1-\lambda)\rho(\eta,\xi) = (\lambda/2)[1-\int_0^1 \rho(\eta,\eta')\eta'\, d\eta'][1-\int_0^1 \rho(\xi,\eta')\eta'\, d\eta']. \tag{6}$$

Now let us introduce into consideration the function $P(\tau,\eta,\mu)$ to denote the surface value of the Green function (i.e. one of its depth arguments is taken to be zero); [8]. In the probabilistic language $P(\tau,\eta,\mu)$ characterizes the probability of the photon exit from the atmosphere in direction μ, if originally it was moving at depth τ with directional cosine η. All the angles are referenced from outward directed normal to the surface of a medium. The symmetry property of the P-function ensues from the reciprocity principle and can be written in the form:

$$|\eta|\, P(\tau,\eta,\mu) = |\mu|\, P(\tau,-\mu,-\eta) = |\mu|\, \widetilde{P}(\tau,\mu,\eta). \tag{7}$$

Here we introduced for brevity the function P with angular arguments referenced from the inward normal direction. This function also admits a probabilistic interpretation such that $\widetilde{P}(\tau,\mu,\eta)\, d\eta$ is the probability that a photon incident on the atmosphere with the directional cosine μ will move (in general, as a result of multiple scatterings) at depth τ within the directional interval $(\eta, \eta + d\eta)$. Keeping in mind the probabilistic meaning of the reflection coeefficient $\eta\rho(\eta,\xi)d\eta$ gives the reflection probability for the photon with the angle of incidence $\cos^{-1}\xi$), we see that $\widetilde{P}(0,\mu,\eta) = \eta\rho(\eta,\mu)$

It is obvious that [6]

$$P(\tau,-\eta,\mu) = \int_0^1 P(\tau,\eta',\mu)\rho(\eta',\eta)\eta'\, d\eta' \tag{8}$$

$$\widetilde{P}(\tau,\mu,-\eta) = \eta\int_0^1 \widetilde{P}(\tau,\mu,\eta')\rho(\eta,\eta')\, d\eta' \tag{9}$$

Multiplying equation (1) by $P(\tau,\xi,\mu)P(\tau',\eta,\mu')$ and integrating over ξ and η from 0 to 1, we arrive at the first fundamental result

$$\int_{-1}^{+1} P(\tau,\varsigma,\mu)\,P(\tau',-\varsigma,\mu')\,d\varsigma = (\lambda/2)\left(\int_{-1}^{+1} P(\tau,\varsigma,\mu)\,d\varsigma\right)\left(\int_{-1}^{+1} P(\tau',\varsigma,\mu')\,d\varsigma\right) \quad (10)$$

in which the relations (8) and symmetry property of the reflection coefficient ρ were used. We shall see later that this formula implies, in particular, all the Q-quadratic and bilinear relations given in [1,2]. To make clear the probabilistic meaning of this equation, we rewrite it in the form

$$\chi(\tau,\mu;\tau',\mu') = \lambda/2 \quad (11)$$

where

$$\chi(\tau,\mu;\tau',\mu') = \int_{-1}^{+1} P(\tau,\varsigma,\mu)\,P(\tau',-\varsigma,\mu')\,d\varsigma \Big/ \left(\int_{-1}^{+1} P(\tau,\varsigma,\mu)\,d\varsigma\right)\left(\int_{-1}^{+1} P(\tau',\varsigma,\mu')\,d\varsigma\right)$$

It is seen that χ can be regarded as the correlation coefficient of two random events so that this result can be stated in the following probabilistic language.

Two random events consisting in two photons exit from the semi-infinite atmosphere in certain fixed (diverse, in general) directions, if originally they were moving at some different optical depths in opposite directions, are correlated with the correlation coefficient equaled to $\lambda/2$.

The second fundamental result, generating all the R-quadratic and bilinear relations, can be found by similar manner from equation (6). Multiplying (6) by $\widetilde{P}(\tau,\mu,\eta)\,\widetilde{P}(\tau',\mu',\xi)$ and integrating over η and ξ in the range (0,1), we use equation (9) to obtain

$$(1-\lambda)\int_{-1}^{+1} \widetilde{P}(\tau,\mu,\varsigma)\,\widetilde{P}(\tau',\mu',-\varsigma)\,d\varsigma =$$
$$= (\lambda/2)\left(\int_{-1}^{+1} \widetilde{P}(\tau,\mu,\varsigma)\varsigma\,d\varsigma/|\varsigma|\right)\left(\int_{-1}^{+1} \widetilde{P}(\tau',\mu',\varsigma)\varsigma\,d\varsigma/|\varsigma|\right) \quad (12)$$

To assign a probabilistic sense to this result, we rewrite (12) in the form

$$\chi(\tau,\mu;\tau','\mu') = \lambda\kappa(\tau,\mu)\kappa(\tau',\mu')/(1-\lambda) \quad (13)$$

where

$$\kappa(\tau,\mu) = \left(\int_{-1}^{+1} \tilde{P}(\tau,\mu,\varsigma)\varsigma\, d\varsigma / |\varsigma|\right) \Big/ \left(\int_{-1}^{+1} \tilde{P}(\tau,\mu,\varsigma)\, d\varsigma\right).$$

Thus, it is seen that c also can be regarded as the correlation coefficient for the ingoing radiation, and now it is not constant as for upward directed radiation, but is given by much more complex expression. As should be expected, the upward and inward di-rections are not tantamount. So, this result also can be formulated in probabilistic language.

Two random events, consisting in that two photons incident on the semi-infinite atmosphere in certain fixed (diverse, in general) directions, will move at some (different) depths in opposite directions, are correlated with the correlation coefficient given by (13).

Utilizing the reciprocity principle (7) in (10) and (12), one can write another pair of equations for the functions $\tilde{P}$ and P:

$$\int_{-1}^{+1} \tilde{P}(\tau,\mu,\varsigma)\, \tilde{P}(\tau',\mu',-\varsigma)\, d\varsigma / \varsigma^2 = \\ = (\lambda/2)\left(\int_{-1}^{+1} \tilde{P}(\tau,\mu,\varsigma)\, d\varsigma / |\varsigma|\right)\left(\int_{-1}^{+1} \tilde{P}(\tau',\mu',\varsigma)\, d\varsigma / |\varsigma|\right) \tag{14}$$

and

$$(1-\lambda)\int_{-1}^{+1} P(\tau,\varsigma,\mu)\, P(\tau',-\varsigma,\mu')\varsigma^2\, d\varsigma = \\ = (\lambda/2)\left(\int_{-1}^{+1} P(\tau,\varsigma,\mu)\varsigma\, d\varsigma\right)\left(\int_{-1}^{+1} P(\tau',\varsigma,\mu')\varsigma\, d\varsigma\right) \tag{15}$$

Equations (10), (12) (alongside with (14) and (15)) involve four free parameters, so that they are pithy and have many consequences. In particular, letting in these equations $\tau = \tau'$ and $\mu = \mu'$, we obtain quadratic relations that are the prototypes of those obtained in [1].

3. *Some consequences and applications*. This section demonstrates how can be found and generalized the existing results and presents some new results.

i. *Ambartsumian's invariance equation*. Setting in (10) $\tau = \tau'$ and taking into account the condition $P(0,\xi,\mu)=\delta(\xi-\mu)$ (δ is the Dirac δ-function), we arrive at the well-known invariance functional equation (1) for the reflection coefficient ρ. To elucidate the similarity of equations (1) and (10), it is expedient to rewrite them as follows:

$$(\eta+\xi)\rho(\eta,\xi) = (2/\lambda)p(0,\eta)p(0,\xi), \tag{16}$$

$$\int_{-1}^{+1} P(\tau,\varsigma,\eta)\,P(\tau',-\varsigma,\xi)\,d\varsigma = (2/\lambda)\,p(\tau,\eta)\,p(\tau',\xi) \tag{17}$$

where $p(\tau,\eta)$ is the photon exit probability [7] designed for the photon *absorbed* at optical depth τ. It is seen that these two relations are constructed by similar fashion with the latter having more general meaning, so that relation (17) (i.e. (10)) can be regarded as the extension of the Ambartsumian's invariance equation to the all depths in the atmospheres concerned with two separate transfer problems.

ii. *The problem of diffuse reflection.* Suppose that the atmosphere is illuminated from outside by parallel beam of radiation of unit intensity (what does not impose any restriction) with directional cosine μ. Using the superscripts + and - to denote the intensity with angular argument $+\eta$ and $-\eta$, respectively, and taking into account the probabilistic interpretation of the function $\tilde{P}$, one can write

$$I^+(\tau,\eta,\mu) = \tilde{P}(\tau,\mu,-\eta)/\eta, \quad I^-(\tau,\eta,\mu) = \tilde{P}(\tau,,\mu,\eta)/\eta. \tag{18}$$

Then equations (14) and (12) correspondingly yield:

$$Q(\tau,\mu;\tau',\mu') = \lambda\,J(\tau,\mu)\,J(\tau',\mu') \tag{19}$$

and

$$(1-\lambda)\,R(\tau,\mu;\tau',\mu') = \lambda\,H(\tau,\mu)\,H(\tau',\mu') \tag{20}$$

in which the notations of [1] are used:

$$J(\tau,\mu) = (1/2)\int_0^1 [I^+(\tau,\eta,\mu) + I^-(\tau,\eta,\mu)]\,d\eta, \tag{21}$$

$$H(\tau,\mu) = (1/2)\int_0^1 [I^+(\tau,\eta,\mu) - I^-(\tau,\eta,\mu)]\,d\eta, \tag{22}$$

$$Q(\tau,\mu;\tau',\mu') =$$

$$= (1/2)\int_0^1 [I^+(\tau,\eta,\mu)I^-(\tau',\eta,\mu') + I^+(\tau',\eta,\mu')I^-(\tau,\eta,\mu)]\,d\eta \tag{23}$$

$$R(\tau,\mu;\tau',\mu') =$$

$$= (1/2)\int_0^1 [I^+(\tau,\eta,\mu)\,I^-(\tau',\eta,\mu') + I^+(\tau',\eta,\mu')\,I^-(\tau,\eta,\mu)]\eta^2\, d\eta \tag{24}$$

The derivation of the corresponding quadratic relations is straightforward. The angular arguments m and m', which specify the directions of incident radiation in two diverse problems, enter into (19) and (20) as parameters, so that the relations of this type can be written for arbitrary angular distribution of illuminating radiation. Note also that equations (19) and (20) are the further generalization of proper equations of [2] and those given in [9]. They connect the radiation fields at diverse depths pertaining two separate problems of diffuse reflection. Letting $\mu=\mu^1$, we obtain the Ivanov's results; Rybicki's results assume $\tau=\tau'$.

iii. *Uniformly distributed sources.* As in [1,2], the initial sources of energy are assumed to be due to thermal emission, therefore the source function has a form

$$S(\tau) = \lambda J(\tau) + (1-\lambda)\, B \tag{25}$$

where $B=\text{const}$ is related to the Planck function. This problem, as it was shown in [10], is closely connected with that of diffuse reflection treated in the previous subsection. Especially simple relationship exists between radiation fields in the atmosphere with uniformly distributed sources such that (25) holds, and the atmosphere illuminated by isotropic radiation. The plain probabilistic considerations, based on the fact that the photon, moving somewhere in the semi-infinite atmosphere, will either be destroyed or escape it, enable one to write

$$I_*^\pm(\tau,\eta) = \int_0^1 I_*^\pm(\tau,\eta,\mu)\, d\mu = 1 - I_*^\pm(\tau,\eta,B)/B \tag{26}$$

where the intensities relevant to the problem of diffuse reflection are supplied by asterisk. It is also convenient to mark explicitly the internal source in arguments of the proper intensities.

Integrating equations (19) and (20) over μ and μ' from 0 to 1, and incorporating the formulas (26) applied to the two separate problem with different values of sources B and B', after some algebra one can obtain

$$\begin{aligned} Q(\tau,B;\tau',B') &= \lambda J(\tau,B)J(\tau',B') + \\ &+ (1-\lambda)[BJ(\tau',B') + B'J(\tau,B)] - (1-\lambda)\,BB', \end{aligned} \tag{27}$$

$$(1-\lambda) R(\tau,B;\tau',B') = \lambda H(\tau,B) H(\tau',B') + \\ +(1-\lambda)[BK(\tau',B') + B' K(\tau,B)] - 1/3(1-\lambda) BB' \tag{28}$$

where

$$K(\tau,B) = 1/2\int_0^1 [I^+(\tau,\eta,B) + I^-(\tau,\eta,B)]\eta^2 \, d\eta, \tag{29}$$

and other quantities are given by (21)-(24) with μ and μ' replaced by B and B', respectively. In terms of the source function equation (27) takes a form:

$$\lambda Q(\tau,B;\tau',B') = S(\tau,B) S(\tau',B') - (1-\lambda) BB' \tag{30}$$

Again, as in the previous subsection, the bilinear relations are obtained that connect the radiation fields at different depths in two separate problems, what also generalize the existing results. Inasmuch as at the surface ($\tau = \tau' = 0$) Q and R vanish, equation (30) yields $S(0) = B\sqrt{1-\lambda}$, where as equation (28) leads to the simple relation between the first- and second-order moments of the φ-function.

It is evident that we could integrate equations (19) and (20) merely over one of two angular variables to obtain relations, connecting radiation fields pertaining two diverse problems, namely, the problem of diffuse reflection and that for an atmosphere with uniformly distributed sources. For instance, integrating (19) and (20) over μ' from 0 to 1 and utilizing (26), one can write

$$Q(\tau,\mu;\tau',B) = J(\tau,\mu) S(\tau',B), \tag{31}$$

$$(1-\lambda) R(\tau,\mu;\tau',B) = \lambda H(\tau,\mu) H(\tau',B) + (1-\lambda) BK(\tau,B), \tag{32}$$

where Q and R are given by (23) and (24), respectively, with μ' replaced by B.

iv. *Exponential source distribution.* Having bilinear relations for the problem of diffuse reflection, one can readily derive appropriate relations in the case of an atmosphere that contains energy sources with exponential variation over depth. As in [1], the sources of the form $b(\tau,m) = B(1-\lambda)\exp(-m\tau)$ will be treated. However, we start with considering the case in which the initial sources distributed according to the formula $(\lambda/2)\exp[-(\tau/\mu)]$. It is clear physically that the radiation field in such atmosphere differs from that in the atmosphere illuminated by parallel beam of radiation merely by the contribution of non-scattered quanta into downward directed flux. Therefore, one can write

$$I^+(\tau,\eta,\mu) = I_i^+(\tau,\eta,\mu); I^-(\tau,\eta,\mu) = I_i^-(\tau,\eta,\mu) + \delta(\eta-\mu)\exp(-\tau/\mu) \tag{33}$$

where I^+ correspond to the case of internal sources. Insertion (33) into (19) leads to the following Q-relation

$$\lambda Q_i(\tau,\mu;\tau',\mu') = S_i(\tau,\mu)S_i(\tau,\mu') + \\ + \lambda/2\{I_i^+(\tau,\mu,\mu')\exp(-\tau'/\mu') + I_i^+(\tau',\mu,\mu')\exp(-\tau/\mu)\} \tag{34}$$

where $Q_i(\tau,\mu;\tau',\mu')$ is given by (23) with I_i^+ taken in place of I^+, and $S_i(\tau,\mu) = \lambda J_i(\tau,\mu) + \lambda/2\exp(-\tau/\mu)$. The final result for the sources distributed as $b(\tau,m)$ can be found formally by replacing the second arguments of I_i^+ in (48) as follows $\mu \to 1/m$, $\mu' \to 1/m'$, and multiplying both sides of this relation by $(2/\lambda)^2(1-\lambda)^2\, BB'$. It is apparent that such replacement is justified physically only for $m, m' \geq 1$. Remind also that μ and μ' as the third arguments of I_i^+ (and as the second ones of S_i or J_i) specify the problem at hand so that must be replaced by m and m', respectively. As a result the following Q-relation is obtained:

$$\lambda Q(\tau,m;\tau',m') = S(\tau,m)S(\tau',m') - \\ -[B(\tau,m)I^+(\tau',1/m,m') + B(\tau',m')I^+(\tau,1/m',m) \tag{35}$$

where $b(\tau',m') = -B'(1-\lambda)\exp(-m'\tau') - \tau/\mu, S(\tau,m) = \lambda J(\tau,m) + b(\tau,m)$; and $Q(\tau,m;\tau',m')$ is given according to the formula (23) with m and m' substituted for μ and μ', respectively. By analogous manner one can derive R-relation for the same sources, viz.

$$\lambda(1-\lambda)R(\tau,m;\tau',m') = [\lambda H(\tau,m) - b(\tau,m)][\lambda H(\tau',m') - b(\tau',m')] - \\ -(1-\lambda)[(1/m'^2)b(\tau',m')I^+(\tau',1/m',m) + (1/m^2)b(\tau,m)I^+(\tau',1/m,m') \tag{36}$$

where the notation R is adopted for that of (24) with μ, μ' replaced by m, m'.

The derivation of appropriate "two-point" and quadratic relations on the base of (35) and (36) is straightforward. Note that in the specific case of $m = m'$ and $\tau = \tau'$, these equations enable one to exclude $I^+(\tau,1/m,m)$, yielding the combined quadratic relation obtained in [1]. The latter is obviously valid for any value of m. The procedure alluded to above can be carried out with respect to only one triad of variables to give the Q- and R-relations, connecting the problem at issue with that of diffuse reflection.

Thus, it is seen that there exists a class of transfer problems pertaining to the semi-infinite atmosphere, which are related by means of bilinear equations. It can be shown that this class can be extended to include the sources with the power-law distribution in the atmosphere.

НЕКОТОРЫЕ НОВЫЕ НЕЛИНЕЙНЫЕ СООТНОШЕНИЯ ТЕОРИИ ПЕРЕНОСА ИЗЛУЧЕНИЯ

А.Г.НИКОГОСЯН

В статье представлена часть новых результатов, касающихся обобщения и физической интерпретации квадратичных и билинейных интегралов Райбики. Полученные на основе принципа инвариантности Амбарцумяна фундаментальные уравнения могут рассматриваться как распространение этого принципа на все глубины среды. Они позволяют вывести *Q*- и *R*-соотношения более общей структуры, чем те, которые извесны в настоящее время, и допускают простое вероятностное истолкование. Получено несколько соотношений, связывающее между собой задачи переноса излучения различного типа. Дается вывод отдельных *Q*- и *R*- уравнений для случая, когда источники распределены в полубесконечной среде по экспоненциальному закону.

REFERENCES

1. *G.B.Rybicki*, 1977, Astrophys. J., 213, 165.
2. *V.V.Ivanov*, 1978, Sov. Astron., 22, 612.
3. *E.G.Yanovitskii*, 1981, Sov. Astron., 25, 66.
4. *G.B.Rybicki*, 1984, in: Methods in Radiative Transfer, ed. W. Kalkofen, CambridgeUniversity Press, Cambridge, p. 173.
5. *V.A.Ambartsumian*, 1960, Scientific Works, vol. 1 (Yerevan: Izd. Acad. Nauk Arm. SSR, [in Russian]).
6. *S.Chandrasekhar*, 1960, Radiative Transfer (New York: Dever).
7. *V.V.Sobolev*, 1963, A Treatise on Radiative Transfer (Princeton: van Nostrand).
8. *K.M.Case, P.F.Zweifel*, 1967, Linear Transport Theory (Reading, Mass,: Addison-
9. *R.A.Krikorian, A.G.Nikoghossian*, 1995, J.Quant. Spectrosc. Rad. Trans. (in press).
10. *A.G.Nikoghossian, H.A.Haruthyunian*, 1979, Astrophys. Sp. Sci., 64, 285.

АСТРОФИЗИКА

ТОМ 38 НОЯБРЬ, 1995 ВЫПУСК 4

THE RADIO LUMINOSITY OF PULSARS AND THE DISTRIBUTION OF ELECTRON DENSITY IN THE GALAXY

R.R.ANDREASYAN, T.G.ARSHAKIAN
Byurakan Astrophysical Observatory, Armenia 378433
E-mail address: byur@mav.yerphi.am

Radio luminosities of pulsars are depended on their periods and periods derivatives. The parameters of that dependences and the independent distances for 288 pulsars are determined. The known dispersion measures are used for determination of the mean electron densities in the direction of pulsars. The obtained results are used for investigation of the large-scale distribution of electron concentration in the Galaxy. The maximum value of that distribution is found at the distance of 9 kpc from the galactic centre in the Sagittarius arm. In the inter arm regions electron density decreases roughly exponentially.

1. *Introduction.* The general observational parameters such as period, period derivative, etc. have been determined for most of pulsars (PSRs). This makes possible to use them in statistics.

For most PSR distances are determined by means of both the dispersion measure value (DM) and the mean electron concentration (n_e) on the line of sight.

$$DM = \int_0^R n_e dr = \overline{n}_e R. \qquad (1)$$

The first parameter is defined from observations. For the second one a value of the electron concentration in solar vicinity is adopted, which is equal to $\sim 0.03 cm^{-3}$.

The distances determined in such a way could contain large sistematic errors, because of an insufficient knowledge of the electron density distribution in the Galaxy. In present paper we examine the possibility to determine the luminosities of PSRs without knowing the distances to them beforehand. It allows us to calculate the PSR distances without values DM and n_e . Having the pulsars distances, found by independent method we can calculate the mean value of electron density in the direction of each pulsar from (1) and then reconstruct its distribution in the Galaxy.

2. *The Radioluminosities of Pulsars.* It is generally accepted that pulsars emit at the expence of the rotation energy loss. Apparently the bolometric luminosity of PSRs depends on the total rotation energy and on the rate of spin up down[1], which is determined by period P and period derivative $dP/dt = \dot{P}$ of PSRs. On the other hand, if we accept, that the rotation energy of PSR spin up down due to the magnetodipol emmision, then the magnetic field of PSR be equal $B_0 \sim P\dot{P}$ and the energy loss rate is $W \sim B_0^2$ [2]. So one may write that the bolometric luminosity depends on P and $\dot{P}$ as

$$L = \gamma\, P^{\alpha}\, \dot{P}^{\beta} \tag{2}$$

where α, β and γ are unknown parameters.

A more complete information about PSRs is obtained at the frequency 400 MHz, therefore we shall use the radio luminosity at the same frequency determined as in [2]

$$L_{400} \sim \frac{W_e}{P} S_{400} R^2 ,$$

where R is the distance of PSR from the Sun, S_{400} is the emission flux density and W_e is the pulse equivalent width. So we have

$$\frac{W_e}{P} S_{400} R^2 = \gamma\, P^{\alpha} \dot{P}^{\beta}. \tag{3}$$

Taking logarithm of (3) we can obtain a linear equation concerning α, β and logγ . Such an equation one may write for each pulsar separately in the form of

$$\log\left(\frac{W_e}{P} S_{400} R^2\right) = \log\gamma + \alpha\log P_i + \beta\log \dot{P}_i \tag{4}$$

where i=1,...,N (N is the PSRs number). The solution of the system (4) by the least square fit gives the values of parameters a, b and logg . It should be noted, that in the papers [3,4] the following values of parameters respectively were obtaind: a =-1.04±0.15, β=0.35±0.06 and a=-0.86±0.2, β=0.38±0.08.

In this paper we used a greater number of PSRs than in [3,4] and the obtained results are used for the study of distribution of free electrons concentration in the Galaxy. The needed parameters (W_e, P, $\dot{P}$, S_{400}, R) are known for 288 PSRs [2]. Using these data, the α, β, γ, its dispersions and the correlation coeficient (ρ) were defined from the system of linear equations (4). The obtained results are shown in Table 1.

Table 1

P(sec)	N	logγ	α	β	ρ
All	288	8.26 (0.0008)	-1.42 (0.19)	0.33 (0.013)	0.43
<0.7s	148	10.03 (0.0012)	-0.61 (0.41)	0.43 (0.037)	0.34
>0.7s	140	6.86 (0.0010)	-2.11 (0.49)	0.23 (0.018)	0.34

The pulsars with periods P>0.7s and P<0.7s are distinguished by the distribution of duty cycle (W_e/P)[5]. Since the value W_e/P figures in the equation (4), we have solved the system (4) for two groups separately. The calculations are shown in Table 1. Hence it is seen that the values α and β, obtained for all pulsars, are close to the results of other authors.These parameters are strongly differ from each other for isolated groups. It speaks in favour of independence both short-period and long-period pulsars and differences between them by various features. So let us write the relation (3) in the form:

$$R_t = \sqrt{\gamma \frac{P^{\alpha+1}\dot{P}^{\beta}}{S_{400}W_e}} \tag{5}$$

Using the calculated parameters α, β and γ, obtained for two groups separately and observed values S_{400}, W_e we have defined the new distances of pulsars. How far the obtained distances are true? It will be discussed in the next section.

3. The Distribution of The Galaxy Free Electrons. The study of the large-scale distribution of free electrons in the Galaxy is of great theoretical and

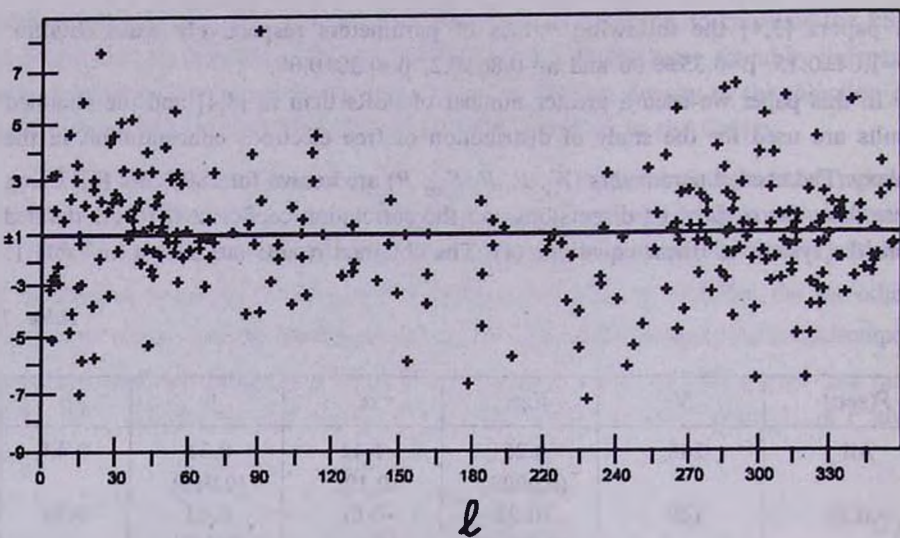

Fig. 1. The mean relative electron density as a function of Galactic longitude. In the cases when n_e>0.03 and n_e<0.03 we have taken the values n_e/0.03 and -0.03/n_e respectively.

practical importance. The values of dispersion measure and the pulsar's distances, determined by independent method are used for determination of the mean electron density in the direction of pulsars (see for example[6]). The relation between the electron density and the height of pulsars over the Galactic plane in the solar vicinity has been obtained

$$n_e(z) = n_0 e^{-z/h},$$

where n_0 =0.03 cm^{-3}, h - 1000 pc.

Now we shall use the distances obtained in preceding section for the study of the large-scale distribution of free electrons.Using the relation (1) and obtained distances R_t (5) the mean electron density has been found in the direction of 288 pulsars

$$\bar{n}_e = \frac{DM}{R_t}.$$

In Fig. 1 we plot the relative electron density as a function of Galactic longitude. We can see that the values n_e are higher, regardless of a large dispersion, than the mean electron density (~ 0.03) in directions to the Galactic centre and are well below of the value 0.03 in opposite directions(120°<l<240°).

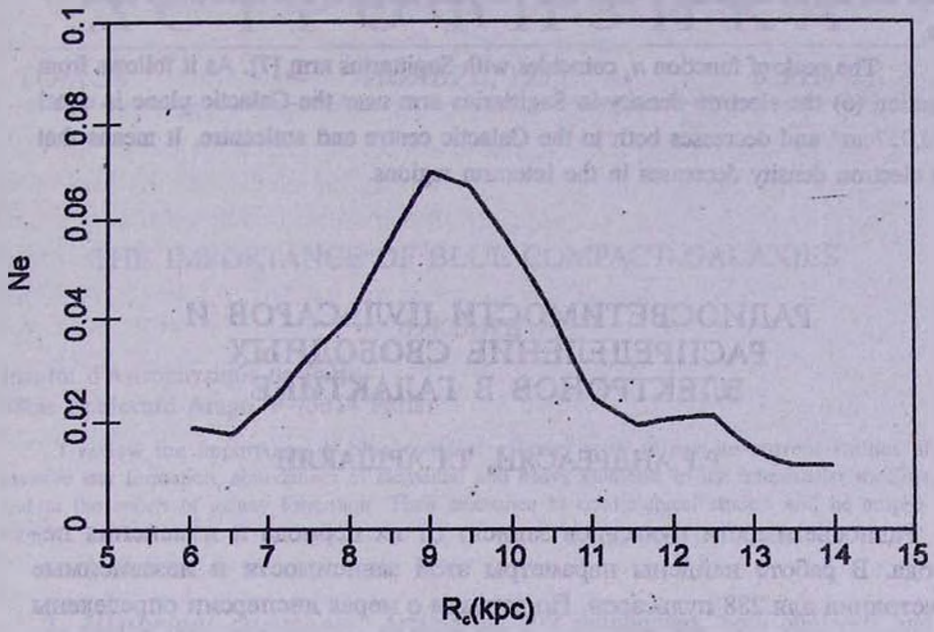

Fig. 2. The mean electron density versus Galactocentric distances. The PSRs with R_1<1kpc were excepted because the neighbouring dense HII regions can essentially increase the mean electron density in the given direction.

Since distribution of the free electrons coincides with the space distribution of HII regions surrounding O-B stars, associations and young star clusters and they are sources of free electrons, then one may suggest that obtained distances R_1 are well defined. For this purpose we plot the mean electron density versus Galactocentric radius (Fig.2). It is seen that there is a dependence between the values n_e and r_c. This relation could be aproximated by the function in the range of 6 kpc to 12 kpc (β =2)

$$n_e(r_c, z) = n_1 + n_0 e^{-z/h_e[(r_c - r_0)/\sigma]^{\beta}}, \tag{6}$$

where the terms $e^{-z/h}$ and $e^{[(r_c - r_0)/\sigma]^{\beta}}$ describe the variation of electron density by z and by Galactocentric radius respectively.

Varying the values n_1 and r gives most probable values for n_0, h, and σ :

n_0 =0.052cm^{-3}, r_0 =9 kpc, σ=2.88 kpc,

n_1 =0.005cm^{-3}, h =0.7 kpc.

We obtained a symmetric function, which reaches to its maximum at the distance

9 kpc and has an halfwidth σ=2.88 kpc. The scale height of free electrons is equal 0.7 kpc.

The peak of function n_{e} coincides with Sagittarius arm [7]. As it follows from equation (6) the electron density in Sagittarius arm near the Galactic plane is equal to 0.057cm^{-3} and decreases both to the Galactic centre and anticentre. It means that the electron density decreases in the interarm regions.

РАДИОСВЕТИМОСТИ ПУЛЬСАРОВ И РАСПРЕДЕЛЕНИЕ СВОБОДНЫХ ЭЛЕКТРОНОВ В ГАЛАКТИКЕ

Р.Р.АНДРЕАСЯН, Т.Г.АРШАКЯН

Радиосветимости пульсаров зависят от их периода и изменения периода. В работе найдены параметры этой зависимости и независимые расстояния для 288 пульсаров. По данным о мерах дисперсии определены средние плотности в направлениях пульсаров и крупномасштабное распределение электронной концентрации в Галактике. На расстоянии 9 кпк от центра (в рукаве Стрельца) наблюдается максимум распределения. В межрукавных областях электронная концентрация убывает экспоненциально.

REFERENCES

1. *J.E.Gunn, J. P. Ostriker,* Astrophys. J., 160, 979, 1970.
2. *R.N.Manchester, J. H. Taylor,* Astron. J., 86, 1953, 1981.
3. *M.Proszinski, D. Przybycien,* In Proccedings od the Workshop on "Millisecond Pulsars", held at NRAO, Greenbank, W. Virg., June, 1984.
4. *M.Vivekanand, R. J. Narayan,* Astron. Astrophys., 2, 315, 1981.
5. *T.G.Arshakian,* Astronomy Reports, 38, 239, 1994.
6. *J.H.Taylor, R. N. Manchester,* Astrophys. J., 215, 885, 1997.
7. *Y.M.Georgelin, Y. P. Georgelin,* Astron. Astrophys., 49, 57, 1976.

АСТРОФИЗИКА

ТОМ 38 НОЯБРЬ, 1995 ВЫПУСК 4

THE IMPORTANCE OF BLUE COMPACT GALAXIES

D.KUNTH

Institut d'Astrophysique de Paris,
98bis Boulevard Arago, F-75014 Paris

I review the importance of blue compact galaxies with respect to current studies of massive star formation, abundances of elemental and heavy elements in the interestellar medium and to the epoch of galaxy formation. Their relevance to cosmological studies will be emphasized.

1. *Historical comments.* Around the 60's astronomers, both observers and theoreticians were discussing the problem of galaxy formation with sometimes quite drastic opposite points of view. In Armenia, Professor V.A.Ambartsumian had envisioned the view that galaxy nuclei generate from explosive events while in the US a picture involving gravitational collapse from primordial HI clouds was prefered. F.Zwicky following a distinct line of thinking and unlike E.Hubble soon argued that dwarf galaxies would be the dominant population in the Universe. He furthermore speculated that at their ultimate stage cosmological entities would evolve into highly concentrated densities as it was indeed found with neutron stars. At larger scale, he envisioned that galaxies with high stellar densities, that he named "compact galaxies" should also be found.

It is interesting to note what regardless their predictive pertinence, these leading views have been quite fruitful for the development of science and led to numerous studies of a large variety of new class of galaxies hence opening new areas of research. This appears to be true for AGN studies, and as well for the discovery and follow up studies of blue compact galaxies. In particular numerous surveys were carried out at that time, starting with the search for ultraviolet excess galaxies by Markarian (1967) at Buyrakan while Zwicky (1971) was completing his first lists of blue and red "compact" galaxies. Since then other surveys have been carried out, either with different complementary techniques, or other much larger areas of the sky. A series of follow up studies involving spectroscopic and morphological material were pioneered by Petrosian, Sahakian and Khachikian (1978), showing the increasing importance of multiple nuclei in galaxies that undergo large episodes of star formation. Other studies by Huchra and Sargent (1973), the armenian astronomers (see Khachikian, 1978 for a review) and many others, were decisive to identify the main properties of new type of galaxies. The markland was made in the 70's with the seminal paper of Searle and Sargent (1972) recognizing the importance of blue compact *dwarf* galaxies as a new class of objects from their spectroscopical study of IZw18 and IIZw40. They were also named "extragalactic HII regions" and sometimes "HII galaxies" as their properties are almost undistinguishable spectroscopically from those of giant HII regions. Their properties make them suitable for studies abundances of their ISM abundances, star formation, galaxy formation and evolution and cosmology. I will review the most recent developments along these topics after a short summary of the main observational properties of blue compact dwarfs.

2. *Main general observational properties*. These galaxies have bluer colors (U-B=−0.6; B-V=0.0 to 0.3 on average) than ordinary irregular galaxies and their surface brightness is much higher. Their absolute blue magnitude, dominated by their stellar contribution, ranges from -17 down to -13. Spectroscopically they exhibit a high excitation spectrum with the forbidden line 5006Å to H_β ratio ≥ 5. Such colors and ionization of the gas is due to OB stars complexes indicating a burst of star formation. A straightforward analysis of the ionized gaz spectrum leads to underabundances with respect to solar values. On the other hand their neutral gas contents is relativily high, amounting a few 10^7 solar masses on average, or 0.3 to 0.5 times the luminous mass (on the other hand there are strong indications that the dynamical mass is much larger, in this case the HI mass would only represent around 0.1 of the total). All these properties show that these galaxies are the most chemicallyy unevolved galactic systems known, which undergo a strong burst of massive star formtaion. Their metal distribution peaks at 1/10th the solar value while the most deficient galaxy is IZw18 at about $Z_\odot/40$. Their present-day star formation rates range from 0.1 to 1 $M_\odot$/yr, involving thousands of massive stars. These figures indicate that such a rate, compared with the available HI reservoir would not be sustained over more than 10^8 years. These galaxies hence, are potentially interesting for theories of star formation and galaxy formation. Some of them may be forming stars today although many of these dwarfs are obviously older systems that have undergone one or several bursts in the past. The study of their underlying older population using the HST may reveal time sequence among bursts (Hunter et al. 1995, but see Smecke-Hanes et al., 1994 and Tosi, 1993 who have performed similar study on spheroidal and nearby

dwarf irregular galaxies using modest-sized ground-based telescopes) and possibly an evolutionary sequence among diffrent type of dwarfs.

3. *Abundances*. Abundances most currently measured in blue compact galaxies are obtained from emission line studies of the nebular gas. In the optical, data have been extensively gathered for O, N, S, Ne, He and Ar while more recently Fe has been discussed from more accurate measurements (Thuan et al., 1995). With the launch of the HST other key elements such as C and Si have been measured. Until now, the ISM is found to be metal deficient with no exception. Four points are worth to outline:

1) recent studies from Thuan et al. (1995) of a set of 14 BCDGs selected from the First (FBS) and Second (SBS) Byurakan Surveys re-enforces previous claims that at low metallicity N is essentially primary. It remains surprising that the dispersion of the N/O ratio is found to be so small considering the weakness of the N lines at low metallicity and the fact that most of the N is in N^+ form forcing to adopt large correction factors for unseen stages. This study also shows that BCDGs show similar O/Fe overabundance with respect to the sun (around 0.34 in the log) as galactic halo by a Population III stars.
2) Dwarf emission-line galaxies are useful objects for studying the primordial helium abundance Yp, as it was pointed out by Searle and Sargent (1972) who found that IZw18 and IIZw40 were metal poor but have roughly solar helium, consistent with a primordial origin. For a long time a gap has been present in between IZw18 and most galaxies with metallicities peaking at around 1/5 to 1/10th. Objects from the Second Byurakan Survey now fill in this gap. One of the problems associated with the Yp derivation is the need to extrapolate the (Y, Z) relationship to the zero intercept. Detailed reviews of the potential problems related with this derivation are discussed in Olive (1995) and Kunth (1995) for both statistical and observatioanl uncertainties.
3) On the other hand, the lack of known dwarf galaxies with abundances much smaller than in IZw18 is a long lasting puzzle. This led Kunth and Sargent (1986) to postulate that most metal poor galaxies such as IZw18 could be primordial objects in which the observed HII regions were too much self-polluted with supernovae ejectae (α-elements) to exhibit their true abundance. They predicted that their neutral gas should be pristine. The Kunth et al. (1994)' HST-GHRS estimation of O/H in the cold HI of IZw18 indicates 1/1000 of the solar value in agreement with the self-pollution hypothesis. However their derivation suffers from large uncertainties (Pettini and Lipman, 1995) hence awaiting for confirmation.
4) The Hubble space telescope offers the possibility to observe a series of collisionally-

excited inter-combination transitions in the 1600-2000Å range. In particular it offers the possibility to derive C and Si abundances. The way C and O evolve with time is constraining for chemical evolution models since C is ejected with some delay with respect to the O elements. Garnett et al. (1994)' results appear to indicate that C, O,.Ne and S are mostly manufactured in massive stars rather than in intermediate mass stars. Si/O is found constant, very close to values in the solar vicinity. All pointing to the fact that Si is little depleted onto dust grains in giant HII regions.

4. *Star-formation studies.* Processes of massive star formation have been studied from the UV to the optical and the near IR. The concensus clearly states that star formation in Irrs and BCDGs processes in a discontinuous manner. Most synthetic stellar evolutionary studies hardly distinguish between a continuous burst lasting over less or equal to about 10^7 years or an instantaneous burst in which all the stars are formed at once and evolve over time scales of few 10^6 years. This distinction between both scenari appear less semantic that it looks *a priori* and is dicussed at large in Mas-Hesse and Kunth (1996). Their study also finds no evidence for large variations in the IMF (very close to Salpeter's value or slightly flatter), and no obvious trend with metallicity.

The importance of WR stars in HII galaxies has been considered many times (Vacca and Conti, 1992) and it can be seen that they are certainly one of the best

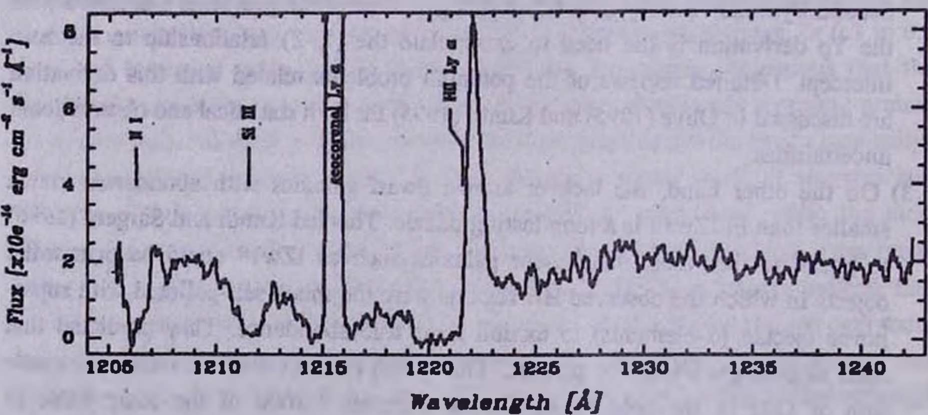

Fig. 1. Lyman α spectral region with the identification of some lines. The mark at 1221.6Å indicates the position of the Lyman α emission line according to the redshift derived from the optical emission lines. Note the asymmetry of the profile and the deep Lyman α absorption blueshifted with respect to the emission line.

constraining indicators for the nature of the star-formation machanism in BCDGs (Cervino and Mas-Hesse, 1994) in the sense that only instantaneous bursts can lead to large numbers of WR stars at a given time in HII galaxy as currently observed.

The impact of a starburst onto the interstellar medium has received observational new supports recently. It becomes clear that massive stars input large amounts of energy from supernovae and stellar winds (WRs). HST spectra of the BCDG Haro2 (Fig. 1) provide evidence for a gas outflow from the galaxy (more precisely the massive stellar cluster) at mean velocity of 200 km s^{-1} (Lequeux et al. 1995). This is the probable detection of a *galactic wind* since it is very likely that the material will leave the galaxy. The mass of this shell is estimated to be of the order of 10^7 solar masses hence the kinetic energy of such a shell expanding at 200 km s^{-1} is $4{\cdot}10^{54}$ ergs comparable to that of the super-bubble discovered by Kamphuis et al. (1991) in M is $2.5{\cdot}10^{53}$ ergs, and the total energy of the expanding gas around the galaxy NGC 6946 is about 10^{55} ergs (Kamphuis & Sancisi 1993). The present kinetic energy of the Haro2 bubble is equivalent to the total energy of several thousand supernovae: this is a major phenomenon. Mas-Hesse & Kunth (1996) estimate a rate of supernova explosions of 1 per century in the HII region, producing a few 10^{54} ergs of total energy in say 1 million years. Other cases of outflows from blue compact galaxies have recently been presented. Papaderos et al. (1994) report X-ray emission in VIIZw403 as a result of a hot gas outflow from the core of this galaxy. Marlowe et al. (1995) bring convincing evidence for large scale expansion of the ionized interstellar media of dwarf galaxies.

If such ejected material can leave a galaxy, a likely possibility, this will strongly influence its chemical evolution. Metal-enriched galactic winds have been introduced (Marconi et al. 1994) to explain the chemical discontinuity observed between the HI and HII phases of IZw18 discussed above. Roy and Kunth (1995) pointed out that the mixing of elements in low-mass galaxies might be poorly efficient. Indeed stimulated star formation is much less effective than in large spirals, and the most powerful mixing mechanisms are absent; the escape of newly enriched material due to galactic winds powered by the starburst events, the lack of large-scale stirring, and the long dormant phase between successive star forming episodes make possible the survival of large abundance discontinuities. In order to reproduce the observed O/H value of the cold gas in IZw18 a chemical evolution model was presented by Kunth et al. (1995) showing that this galaxy must have experienced in the past one or at most two major events of star formation separated by a temporal gap of at least 1Gyr. However it is a curious observational fact that the N/O ratio in this galaxy is nearly solar making difficult to envisage a very short age for the ongoing burst if N were to be manufactured by the same star-formation episode than the O elements. Hence the N abundance argues in favor of a differential wind scenario *together* with primary production of N in massive stars. In such a picture type II SNe elements, such as oxygen, can be lost while elements such as N and He remain bound to the stellar region. Moreover regardless the exact adopted scheme (one or several burst/s) the production of stellar helium remains negligible. This reenforces the importance of extreme metal-poor galaxies for the primordial helium determination.

5. *What triggers star formation?* Starbursts and in particular BCDGs open the question of the origin for bursts. External events such as merging (IIZw40 is such a typical case), interacting systems (IIZw70-71 is a pair in which IIZw70 is undergoing a strong burst) can induce such large scale phenomenon. Cloud-cloud collisions is another appealling scenario. Constraints are given by the lack of pure HI clouds that sit in the sky with no optical counterpart. It is also possible to assume that after long time scales spontaneous star formation takes place followed by SN induced stochastic star formation. Recent developments along these ideas can be found in Vacca (1994, UV imaging), Taylor, Brinks and Skillman (1993a, b HI counterparts of HII galaxies) and Telles and Terlevich (1995, environments of HII galaxies). Some tantalizing questions are however pending:

i) why some extreme gas-rich galaxies spend long time (over 10^9 years) in quiescent phase although their N(HI) exceeds 10^{20} atom cm^{-2}?

ii) what are the progenitors of BCDGs?

iii) what are the post-phases?

In a review paper entitled "The Dwarf Galaxy Star-Formation Crisis", Skillman and Bender (1995) review the ideas concerning the process of gas removal from dwarf galaxies at the onset of massive star formation, hence their relationship with formation and evolution of dwarfs. They suggest that neither the stripping scenario by which, in clusters one removes gas from dIs to make dEs, nor the one that pictures the evolution as a result of gas outflow by energetic events associated with star formation (SN and stellar winds) are globally satisfactory. Instead they argue for a more unified scheme making both type of dwarfs originate from a common ancestor that would have evolved via different star formation history.

6. *Cosmology.* The last topic i'll like to mention is cosmology. Here again, dwarfs are palying quite a role. One still imagine that they are the first entity to appear in the early Universe and that larger structures subsequently turn on from merging of these building blocks. Dekel and Silk (1986) suggested that cold dark matter cosmology with biasing would identify the formation of dwarf (all types) with density fluctuations of lower initial amplitudes than normal E and S galaxies. This scenario is no

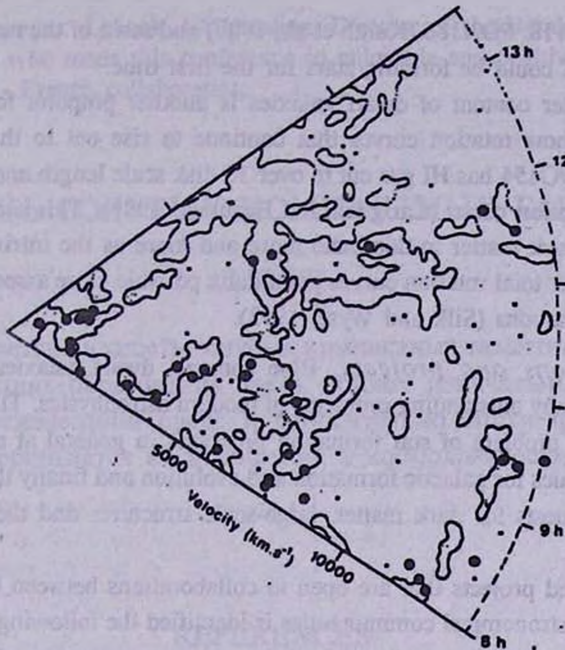

Fig. 2. Cone diagram from Comte et al. 1994, showing a portion of the Center for Astrophysics "slices" of the northern sky. It shows that the observed distribution of the Kiso Ultraviolet Galaxies (black dots) coincides with that of the areas populated by the CfA galaxies (Light shade).

longer valid partly because contrary to expectations it has been shown that dwarfs and emission-line galaxies are not found preferentially in the voids (Iovino et al., 1988; Salzer et al., 1988, 1989 a, b; Thuan, 1988; Comte et al., 1994, see Fig. 2).

Dwarfs may be parent populations of E and S galaxies. HST images do not provide complete answer to this problem and will possibly never do since imaging capability of the HST for the primordial galaxies search is limited by the image scale of the instrument. Further quasar absorption lines of the Lyman α forest may settle whether dwarfs are responsible for most of the observed lines. In this case the Lyman α lines would indicate that gas-rich dwarfs were more numerous in the past and have evolved in some ways. Finally the question remains to know whether some initial fluctuations still condense at present and form galaxies for the first time. Among BCDGs form a morphologically diverse sample (Loose and Thuan, 1985; Kunth et al., 1988), with some extreme examples being very compact with sizes typically below 1 kpc in diameter. No obvious triggering mechanism such as galaxy-galaxy interaction is visible.

Objects such as IZw18, POX186 (Kunth et al., 1988) and some of the new BCDGs that pertain to the SBS could be forming stars for the first time.

The dark matter content of dwarf galaxies is another pinpoint for cosmologist. Gas-rich dwarfs show rotation curves that continue to rise out to the most remote observed point. DDO154 has HI gas out to over 15 disk scale length and shows a clear turnover in its rotation curve (Carignan and Beaulieu, 1989). This seems to confirm the tendancy for dark matter to dominate more and more as the intrinsic luminosity decreases. Moreover total rotation curves point out a possible close association between dark matter and baryons (Silk and Wyse, 1993).

7. *Conclusions and projects.* Blue compact dwarf galaxies are obviously ideal targets for many outstanding problems of modern astrophysics. Their study sheds some light on the problem of star formation processes in general at any scale. They provide possible clues for galactic formation and evolution and finally they are relevant to cosmological quests for dark matter, large-scale structures and the first epoch of gaalxy formation.

Among selected projects that are open to collaborations between both the Armenian and French astronomical communauties is identified the following (that are hopefully not exhaustive since international facilities give many ways to submit interesting proposals as well):

i) deep surveys: the SBS and follow up spectroscopy and imaging will allow to increase the small known sample of potentially "young galaxies". Such a program permits to constrain the luminosity function of BCDGs at the very low-luminosity end. It will give further constraints on galaxy clustering.

ii) IR imaging: IR imaging will provide interesting clues on the presence of older population that underline the actual ionizing blue clusters. This can be achieved with modern large 2D IR receivers. IR spectroscopy will also be at reach for studying merging systems and the physics of the gas in dusty regions.

iii) The use of the HST gives the unique possibility to study the Lyman α emission that escaped from the HII regions in starburst galaxies, offering the opportunity to probe the HI gas and study C and Si abundances.

iv) Potentially spectro-imaging studies using multi-pupil spectrograph, long slit or multi-slit spectra will allow to understand the interplay between dust, ionized gaz and the properties of the star clusters (WR stars, O stars etc...).

v) the advent of large millimeter receivers (IRAM, ESO-SIST) leaves optimistic possibility in the future to reach enough sensitivity so as to be able to probe molecular gas in such metal-poor galaxies.

Acknowlegments. I thank A. Petrosian, Director of the Byrakan Observatory and his collegues who made this conference so enjoyable and positive for the future of the Armenian - French collaboration.

ВАЖНОСТЬ ГОЛУБЫХ КОМПАКТНЫХ ГАЛАКТИК

Д.КУНТ

Рассматривается важность голубых компактных галактик в современных исследованиях образования звезд, обилия изначальных и тяжелых элементов в межзвездной среде и относительно эпохи формирования галактик, подчеркивается их отношение к космологическим исследованиям.

REFERENCES

C.Carignan, S.Beaulieu, 1989, ApJ 347, 760.

G.Comte, R.Augarde, A.Chalabaev, D.Kunth, H.Maehara,1994 A&A, 1, 18.

A.Dekel, J.Silk, 1986, ApJ. 303, 39.

M.Cervino, J.M.Mas-Hesse, 1994, A&A, 284, 749.

D.R.Garnett et al., 1994, ApJ, 443, 64.

J.P.Huchra, W.L.W.Sargent, 1973, ApJ, 186, 433.

D.A.Hunte, H.A.Thronson, 1995, Astrophys. J., 452, 238.

A.Iovino, J.Melnick, P.Shaver, 1988, ApJ Lett. 330, 634.

J.Kamphuis, R.Sancisi, T. van der Hulst, 1991, A&A 244, L29.

J.Kamphuis, R.Sancisi, 1993, A&A 273, L31.

E.Ye.Khachikian, 1978, in Problems of Physics and Evolution of the Universe, Ed. by L. V. Mirzoyan, Erevan, p. 434.

D.Kunth, W.L.W.Sargent, 1986, Ap.J. 300, 496.

D.Kunth, S.Maurogordato, L.Vigroux, 1988 A&A 204, 10.

D.Kunth, J.Lequeux, W.L.W.Sargent, F.Viallefond, 1994, A&A 282, 709.

D.Kunth, F.Matteucci, G.Marconi, 1995, A&A 297, 634.

D.Kunth, 1995, review talk given at the 2nd Rencontres Internationales du Vietnam:to be published in "The Sun and Beyond" Editions Frontieres (ed. J.T.T. Van), 1996.

J.Lequeux, D.Kunth, J.M.Mas-Hesse, W.L.W.Sargent, 1995, A&A 301, 18.
K.Y.Lo, W.L.W.Sargent, K.Young, 1993, A.J. 106, 507.
H.-H.Loose, T.X.Thuan, 1986, ApJ 309, 59.
G.Marconi, F.Matteucci, M.Tosi, 1994, MNRAS 270, 35.
B.E.Markarian, 1967 Astrofizika, 3, 55.
A.T.Marlowe, T.M.Heckman, R.F.G.Wyse, R.Schommer, 1995, ApJ 438, 563.
J.M.Mas-Hesse, D.Kunth, 1996, A&A, in preparation.
K.A.Olive, S.T.Scully, 1995 to be published in International Journal of Modern Physics A.
P.Papanderos, K.J.Fricke, T.X.Thuan, H.-H.Loose, 1994, A&A, 291, L13.
A.R.Petrosian, K.A.Sahakian, E.Ye.Khachikian, 1978, Astrofizika, 14, 69.
M.Pettini, G.Lipman, 1995, Astron. Astrophys., 297, 63.
J.R.Roy, D.Kunth, 1995, A&A, 294, 432.
J.J.Salzer et al., 1988, A.J. 96, 1511.
J.J.Salzer, G.M.Mac Alpine, T.A.Boroson, 1989a, ApJS 70, 447.
J.J.Salzer, G.M.Mac Alpine, T.A.Boroson, 1989b, ApJS 70, 479.
L.Searle, W.L.W.Sargent, 1972, Ap.J., 173, 25.
J.Silk, R.Wyse, 1993 "Galaxy Formation and the Hubble Sequence", in Physics Reports, 231, 293.
E.D.Skillman, R.Bender, 1995, invited talk at the 5th Texas-Mexico Conference on Astrophysics.
T.Smecker-Hane, P.B.Stetson, J.E.Hesser, M.D.Lehnert, 1994, A.J. 108, 507.
C.L.Taylor, E.Brinks, E.D.Skilman, 1993a, A.J., 105, 128.
C.L.Taylor, E.Brinks, E.D.Skillman, 1993b, in the Proceedings of the ESO/OHP Workshop on "Dwarf Galaxies", ed. G.Meylan and P.Prugniel, p. 287.
T.X.Thuan, 1988, in the XXIIIrd Moriond Meetings on "Dark Matter", (ed.) by *J.Audouze and J.Tran Thanh* Van (eds. Frontieres), p. 161.
T.X.Thuan, Y.I.Izotov, V.A.Lipovetsky, 1995, ApJ 445, 108.
M.Tosi, 1993, in the Proceedings of the ESO/OHP Workshop on "Dwarf Galaxies", ed. G.Meylan and P.Prugniel, p. 465.
W.D.Vacca, 1994, Violent Star Formation, ed. Tenorio-Tagle, G., Cambridge University Press, p. 297.
W.D.Vacca, P.S.Conti, 1992 ApJ 401, 543.
F.Zwicky, 1971, Catalog of Selected Compact Galaxies and Post-Eruptive Galaxies.

АСТРОФИЗИКА

ТОМ 38 НОЯБРЬ, 1995 ВЫПУСК 4

HIGH RESOLUTION FABRY-PEROT AND MULTI-PUPIL SPECTRAL OBSERVATIONS OF THE GENUINE BLUE COMPACT DWARF GALAXY IZW18

A.R.PETROSIAN[1], G.COMTE[2], J.BOULESTEIX[2], D.KUNTH[3], T.MOVSESSIAN[1], S.DODONOV[4], E.LE COARER[2], A.BURENKOV[4]

1. Byurakan Astrophysical Observatory, Armenia
2. Marseille Observatory, France
3. Institut d'Astrophysique de Paris, France
4. Special Astrophysical Observatory, Russia

We present the observations of the BCDG IZW18 performed with a Fabry-Perot interferometer at the CFH 3.6m telescope and with a multi-pupil spectrograph at the SAO (Russia) 6m telescope. Morphological structure of the galaxy in emission lines and in continuum, the velocity field of the ionized gas and [OIII]/H_β ratio distribution along the NW component have been investigated. Besides the NW and SE HII components, we find a population of small HII regions. Continuum maps show that the peaks of the stellar light distribution are displaced with respect to the emission lines maxima. The velocity field shows peculiar motions superposed on a approximately regular background implying solid body rotation. Emission line profiles exhibit asymmetric structure, except for the NW compact component. [OIII]/H_β ratio decreases from the centre of the NW component to its edge with the gradient of 1.86 kpc^{-1}.

1. *Introduction.* The dwarf galaxy IZW18 is a well known object belonging to the class of Blue Compact Dwarf Galaxies (BCDGs). After determination that this galaxy has lowest abundance for a Population I object in the Universe (Searle & Sargent 1972; Lequeux et al 1979; French 1980; Kinman & Davidson 1981) the interest on it rapidly has been increased. Last about 15 years more than 50 scientific papers have been addressed to IZw18. Among these articles which contain data on IZw18 as an extended, two component system (Petrosian et al 1978; Mazzarella & Boroson 1993) are very rare. A few imaging studies (e.g Davidson et al 1989; Dufour & Hester 1990) have shown that besides of two NW and SE components the galaxy has more complex structure. Because of its high surface brightness the NW component has been the target of more detail investigation. For it has been found: (i) the existence

of different spatial structure in stellar continuum and emission line lights (Davidson et al 1989); (ii) the lowest oxygen abundance (e.g. Skillman & Kennicutt 1993); (iii) the existence of the underlying, broad (about 3600 km s^{-1}) H_{α} emission (Skillman & Kennicutt 1993).

As part of the program of high spatial and spectral resolution study of genuine BCDGs, in this paper we present results of Fabry-Perot interferometric observations of IZW18 and multi-pupil spectroscopy of its NW component. We shall adopt 10 Mpc as the distance to IZW18, and a Hubble constant H_0=75 km s^{-1} Mpc^{-1}.

2. *Observations and data reduction*

2.1. Fabry-Perot interferometry. Observations have been performed at the Cassegrain focus of the 3.6m Canada-France-Hawaii telescope with the CIGALE instrument (see details in Boulesteix et al 1983).

CIGALE observations enable us to separate monochromatic emission from con-

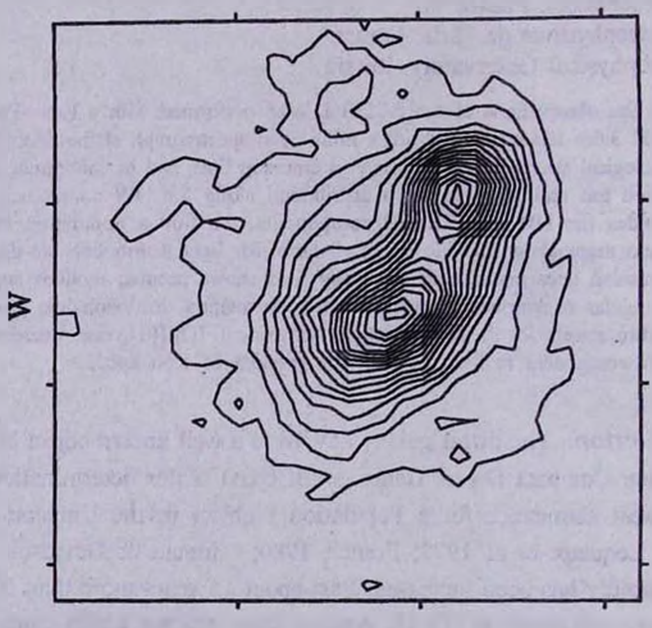

Fig. 1. Integrated 6600A red continuum intensity map of IZW18. The lowest contour corresponds to a flux of a 1.2 10^{-18} ergs cm^{-2} s^{-1} per pixel. Contours are logarithmically spaced with levels separated by a factor 0.1. Condensations observed in red continuum are marked.

tinuum emission (Laval et al 1987). The continuum subtracted H_α line images of IZW18 were calibrated using the absolute flux published by Davidson & Kinman (1985) and Dufour & Hester (1990). In the same way a continuum map in the bandwidth of 10A free from H_α line contribution was built.

2.2. Multi-pupil spectroscopy. The observations have been performed at the Prime focus of the 6m telescope of SAO (Russia) with the multi-pupil spectrophotometer, provided bidimensional spectroscopy of the object. The array 9×11 square microlenses were used. The image scale constructed by one lens was 1.25"×1.25". Two spectral regions have been observed: blue (4600-5200AA) and red (6200-6800AA) with dispersion of about 1A per pixel. 99 spectra were simultaneously registered on the two dimensional photon counting system.

3. *Results.* When the interferometer is scanning the object, the monochromatic emission of this latter is modulated by the interference pattern while the continuum emission remains unaffected. This enables to distinguish line and continuum emission with a much higher contrast than with simple images obtained through interference filters. Figures 1 and 2 show the contour maps of respectively the continuum emission

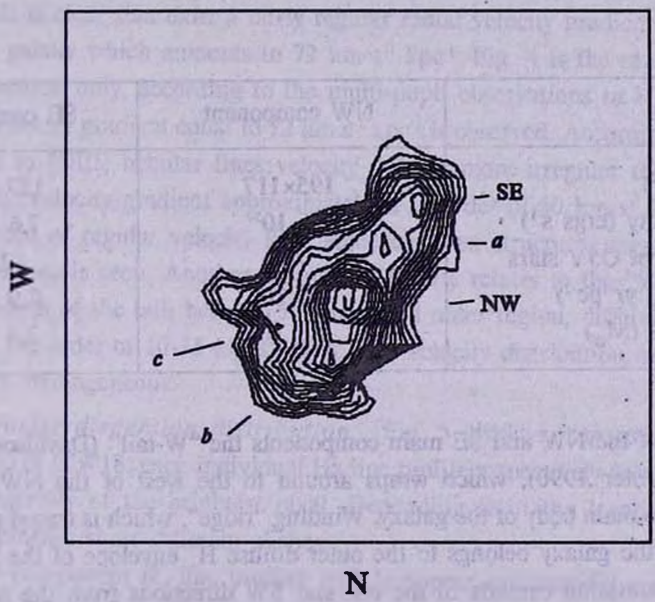

Fig. 2. Integrated H_α line intensity map of IZW18. The lowest contour corresponds to a flux of a 1.0 10^{-17} ergs cm^{-2} s^{-1} per pixel. Contours are spaced with levels separated by a factor 1.58.

and the monochromatic H_α emission in absolute flux units across the main body of IZW18(1.'5×1.'4 field).

3.1 Red continuum morphology. In continuum light besides of two NW and SE components (Davidson et al 1989) a third one (a) is observed half way between them. We identify two other condensations: (b) to the north and (d) to the N-W of the NW compact component. Continuum radiation of IZW18 extends in the NE and SW directions to distances at least 740 pc from the brightest NW component.

3.2. H_α morphology. Our H_α image completely reproduces the structural features which were identified in early H_α observations of IZW18 (Hua et al 1987; Davidson et al 1989; Dufour & Hester 1990).

Both NW and SE condensations are isolated from the main body of the galaxy by an isophote corresponding to 4.5 10^{-15} ergs cm^{-2} s^{-1} $arcsec^{-2}$ of surface brightness. In Table 1 for NW and SE components for this level of surface brightness are presented: linear size; correcting for Galactic reddening the integrated H_α luminosity; assuming Case B conditions, T_e = 18000 K (Dufour et al 1988) and according to Osterbrock (1989) the number of O5V stars; assuming a Salpeter initial mass function, star formation rates of all stars (0.1 to $100M_\odot$); the mass of the ionized gas.

Table 1

	NW component	SE component
Size (pc^2)	195×117	157×117
Luminosity (ergs s^{-1})	1.6 10^{39}	7.6 10^{38}
Number of O5V stars	47	23
SFR ($M_\odot$ $yr^{-1}pc^{-2}$)	4.7 10^{-7}	2.9 10^{-7}
HII mass ($M_\odot$)	7.3 10^5	3.4 10^5

Besides of the NW and SE main components the "W-tail" (Davidson et al 1989; Dufour & Hester 1990), which wraps around to the west of the NW component, belongs to the main body of the galaxy. Winding "ridge", which is traced only by outer isophotes of the galaxy belongs to the outer diffuse H_α envelope of the main body.

The H_α emission extends in the NE and SW directions from the main body of IZW18, to distances at least 1.2 kpc. The extended envelope detected in H_α line is not simply diffuse, it shows numerous condensations. These condensations are thought to be HII regions. A total of 39 HII regions, from which only three show counterparts in red continuum, were identified. They have been detected on the total H_α map and their presence on at least two consecutive channel maps has been checked. The limits of each region are defined at the contour where the intensity of the H_α emission falls to the average local intensity of the diffuse component.

3.3 HII regions size distribution and luminosity function. The size distribution of HII regions is consistent with an exponential $N = N_0 \exp(D/D_0)$ with D_0=24pc. This can be compared to the characteristic D_0 values found for Magellanic Irregular galaxies (Hodge et al 1989; Hodge & Lee 1990).

For IZW18 the small number of HII regions prevents a derivation of an accurate luminosity function, but nevertheless the data are sufficient to get a first approximation. The observed luminosity function of IZW18 shows a turnover with maximum at L = 3.0 10^{36} ergs s^{-1}. This turnover is due to incompleteness of the sample towards fainter luminosities. At luminosities brighter than this turnoff the observed function is reasonably well fitted by a power law $N(L)=AL^{\alpha}dL$ of slope α=-1.6±0.3.This is consistent with the mean value derived for dwarf irregular galaxies (Strobel et al 1991) α=-1.5±0.3.

3.4. H_α velocity field. Fig. 3 is the velocity field superposed on the H_α map of the galaxy. It is clear that exist a fairly regular radial velocity gradient over of main body of the galaxy which amounts to 73 km s^{-1} kpc^{-1}. Fig. 4 is the same cut, on the NW condensation only, according to the multi-pupil observations in H_β line. In this case radial velocity gradient equal to 72 km s^{-1} kpc^{-1} is observed. According to the same observations in [OIII] nebular lines velocity field is more irregular than in Balmer lines, existed velocity gradient approximately is in order of 60 km s^{-1} kpc^{-1}. Against the background of regular velocity field some complex structure, suggesting lots of turbulent motions is seen. Another interesting feature relates to the "W-tail". Along the whole length of the tail, between its inner and outer region, differences in radial velocities of the order of 10-15 km s^{-1} exist, The velocity distribution in the southern ridge is more homogeneous.

3.5. Velocity dispersion distribution. Fig. 5 displays, superposed to the H_α isophotal map of IZW18, each individual Ha line profile respectively normalized to the maximum intensity of the brightest pixel. Depending from the location across the galaxy line profiles show different shapes.

The NW component H_α line profiles mainly appear symmetrical and well represented by a one component Gaussian fit. The same is correct for H_β and [OIII] lines. Averaged over NW component and corrected for the instrumental profile FWHMs of Balmer as well forbidden lines are in the order of 90 km s^{-1}. Because of small free spectral range (375 km s^{-1}) for Fabry-Perot observations and low signal to noise ratio

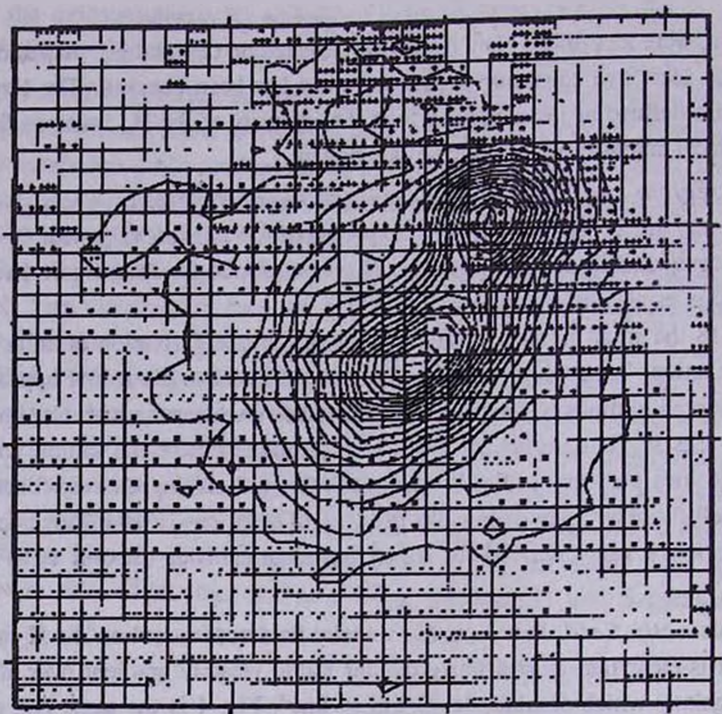

Fig. 3. Velocity field of IZW18 superposed on the H_α map of the galaxy.

(S/N=10 near H_α) for multi-pupil observations we have no chance to detect broad (FWHM about 3600 km s^{-1}) component of H_α line (Skillman & Kennicutt 1993).

All H_α line profiles observed in pixels belonging to the SE component are asymmetric with blue side excesses. Blue component in average is shifted in order of 50 km s^{-1}.

A striking difference is seen between line profiles of the regions corresponding to the "W-tail" and southern ridge of the galaxy. Across the southern ridge, as a whole, profiles with strong blue side asymmetry are typical (two components with about 40 and 80 km s^{-1} shift). In the western tail all regions show red (in order to 50 km s^{-1}) as well blue (in order to 40 km s^{-1}) shifted excesses of velocities. In the outer envelope of the main body, profiles also are asymmetric with red wings in N-NW and the west of the SE component, and blue wings elsewhere.

3.6. [OIII]/H_β ratio distribution along of NW component. Fig. 6 is a position-[OIII]/H_β ratio cut across the optical major axis of the galaxy (PA=143°). Pre-

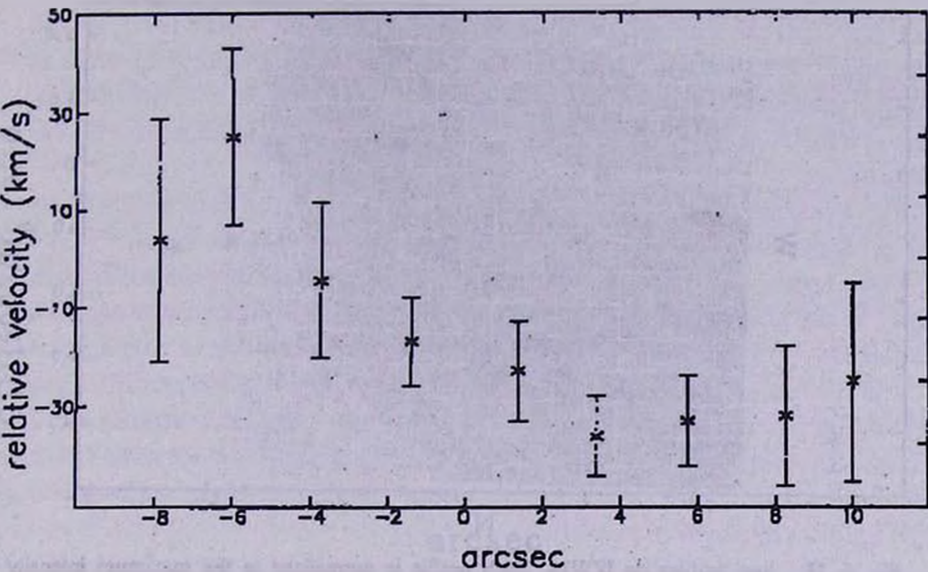

Fig. 4. Position velocity cut across the optical major axis of the galaxy (PA= 143°) in H_β line. Data are averaged within the 30° sector around the PA.

sented data are averaged within the 30° sector around the PA. It is clear from the Fig. 6 that there is a fairly regular, with gradient of 0.0893 $arcsec^{-1}$, decreasing of the $[OIII]/H_\beta$ ratio from the center of the component to its edge.

According to Skillman & Kennicutt (1993) there is tentative indication of a radial gradient in electron temperature ($0.13\ 10^4$ K $arcsec^{-1}$) and no any in electron density for the NW component. We can conclude that ionic abundance of O^{++} which strongly depends from $[OIII]/H_\beta$ ratio and electron temperature as well electron density increase from the centre to the edge of the NW component with the gradient equal to $9.25\ 10^{-7}$ $arcsec^{-1}$. The gradient mainly attributable to the difference in the measured electron temperatures. Unfortunately we have no any information regarding to the distribution of $3727[OII]/H_\beta$ ratio across to the NW component. So it is difficult to do conclusion about oxygen abundance distribution across the component.

4. *Discussion.*

4.1. The structure. Is IZW18 an old system in which some intense episodes of star formation already occurred, or does it form stars for the first time? Loose & Thuan

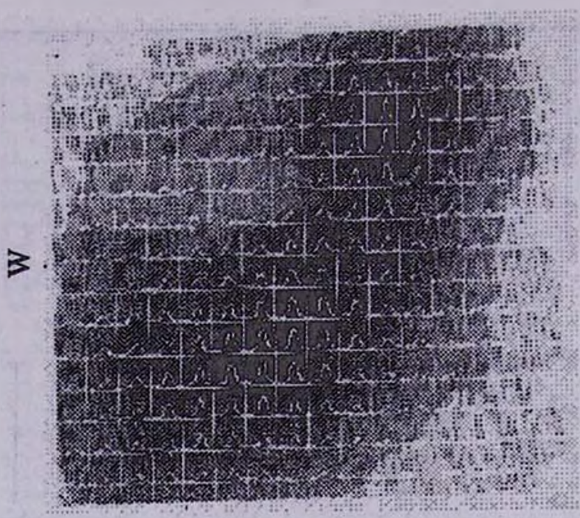

Fig. 5. H_{α} line profiles on IZW18. Each profile is normalized to the maximum intensity of the brightest pixel.

(1986) reported observations of a faint outer component of extended stellar continuum which they attributed to an underlying old population. Thuan (1983) from detected infrared emission, Hua et al (1987), Davidson et al (1989), Dufour & Hester (1990) from red continuum imagery, confirmed the presence of this component.

We have shown that in red continuum light at least three additional brightness concentrations are seen besides the already known compact NW and SE sources. The NW and SE components have an H_{α} peak brightness displaced from the red continuum peak position.

In the following, we make the assumption that H_{α} peaks are related to the current star forming regions and red continuum peaks to the recent or past sites of star formation. The distribution of star forming regions in IZW18 shows a chain like structure. Out of seven identified current and past star forming knots 6 are distributed along a line. The chain of star forming knots is positioned in the direction of elongation of the main body of IZW18 and its position is quite consistent with HI clumps distribution in the vicinity of the galaxy (Lequeux & Viallefond 1980).

In the chain both NW and SE current star forming regions are located between recent or old star forming sites. Is this geometry a random configuration? Does it exemplify the sequential nature of star formation events in the galaxy (Kunth et al. 1988)? Stochastic self propagating star formation simulations of star formation sites

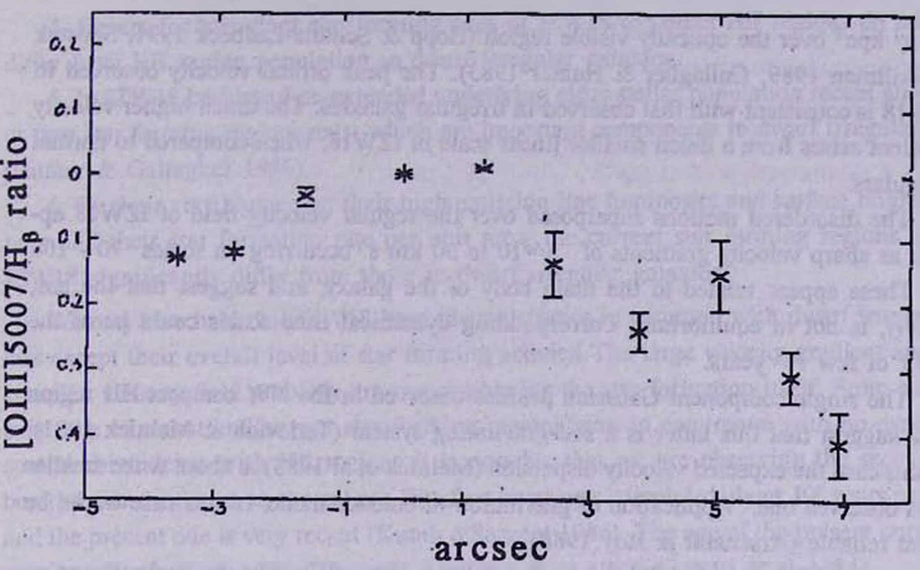

Fig. 6. Position-[OIII]/H$_\beta$ ratio cut across the optical major axis of the galaxy (PA= 143°). Data are averaged within the 30° sector around the PA.

in dwarf galaxies show that the properties of dwarf systems predicted by these models depend on the size ratio of the galaxy to the star formation cells. Small galaxies similar to IZW18 which evolve mainly via a series of disconnected star forming bursts (e.g. Hunter & Gallagher 1986).Therefore, a random origin of the observed "chain" is more plausible .The only evidence is that the main body of IZW18 consists of two séparated star forming areas with associated current and recent or old star forming regions which is confirmed by the differences in velocity between the two main compact components (744±10 km s^{-1} and 782± 6 km s^{-1} respectively for NW and SE components).

4.2. The kinematics and dynamics. What is the mechanism which triggers the subsequent star formation in IZW18? The velocity field may play an important role. The ordered component of the velocity field shows a peak orbital velocity of 45 km s^{-1}. The velocity gradient observed across the offseted HI peak distribution is 50 km s^{-1} kpc^{-1} (Viallefond et al 1987) compared to the about 70 km s^{-1} kpc^{-1} observed along the main star forming regions, both in H$_\alpha$ (our results in Sec. 3.4) and in HI (from the maps of Viallefond et al 1987).

Most irregular galaxies (giant as well as dwarf), exhibit a solid body rotation with peak orbital velocities of 50-70 km s^{-1} but shallow velocity gradients of 5-20 km s^{-1} kpc^{-1} over the optically visible region (Hopp & Schulte-Ladbeck 1991; Shostak & Skillman 1989; Gallagher & Hunter 1983). The peak orbital velocity observed in IZW18 is consistent with that observed in irregular galaxies. The much higher velocity gradient arises from a much smaller linear scale in IZW18, when compared to normal irregulars.

The disordered motions superposed over the regular velocity field of IZW18 appear as sharp velocity gradients of V=10 to 30 km s^{-1} occurring on scales 70 - 100 pc. These appear related to the main body of the galaxy, and suggest that the gas, locally, is not in equilibrium. Corresponding dynamical time scales could be of the order of few 10^6 years.

The single component Gaussian profiles observed in the NW compact HII region may suggest that this latter is a self-gravitating system (Terlevich & Melnick 1981). In this case the expected velocity dispersion (Melnick et al 1988) is about twice smaller than observed one. Application of gravitation-turbulence model in this case would be more reliable (Arsenault & Roy 1988).

In the SE compact HII region the velocity dispersion for the main Gaussian component (about 19 km s^{-1}) is higher than it is expected from self-gravitational model (Terlevich & Melnik1981). The excess velocity dispersion can be caused by the gravity of (a) and SE recent or old star forming regions. The fitted much weaker second Gaussian component can be another isolated HII region in SE area, not distinguishable because of projection effects.

The complex structure of the H_α line profiles observed in the envelope around the main body of the galaxy, with variable asymmetry suggests that we observe gas infall onto the main body of the galaxy, whatever the direction of observation.

4.3. The nature of IZW18. We examine the nature of IZW18 following the hypothesis that in general BCDGs may be considered as the low luminosity end of irregular galaxies (Searle & Sargent 1972, Vigroux et al 1986, Kunth et al 1986, Thuan 1987). The results of comparison of the properties of IZW18 with that of dwarf irregular galaxies may be summarized as follows.

1. IZW18 has an absolute luminosity consistent with that of an "average" dwarf irregular. The small linear size of IZW18 gives a high surface brightness of the optically visible component.

2. HI masses of IZW18 and dwarf irregular galaxies of comparable blue luminosity and the clumpy structure of the HI distribution are similar.

3. A rigid body rotation similar to that observed in dwarf irregular galaxies with quite similar peak orbital velocity is observed in IZW18. The size of IZW18 makes the velocity gradient across it at least 5 times higher than in irregular galaxies.

4. Except for two giant star forming sites of IZW18 the other HII regions do not differ from HII region population in dwarf irregular galaxies.

5. In IZW18 besides of an extended underlying older stellar population recent and/or past star forming regions exist which are important components in dwarf irregulars (Hunter & Gallagher 1986).

6. By their very blue color, their high emission line luminosity and surface brightness and their star formation rate per unit area, the current star forming regions in IZW18 significantly differ from those in dwarf irregular galaxies.

We may conclude that IZW18 have characteristics in common with dwarf irregulars except their overall level of star forming activity. The large velocity gradient and complex velocity field probably are responsible for the star formation itself. From the existence of recent and/or past star forming regions seen in continuum with no exact spatial coincidence with HII regions it is possible that we are observing the second burst of star formation in the galaxy. The first burst was completed about 10^9 years ago and the present one is very recent (Kunth &Sargent 1986). The age of the present burst may be estimated as a few 10^6 years (Lequeux et al 1981; Copetti et al 1984).

ФАБРИ-ПЕРО И МНОГОЗРАЧКОВЫЕ СПЕКТРАЛЬНЫЕ НАБЛЮДЕНИЯ ВЫСОКОГО РАЗРЕШЕНИЯ ИСТИННОЙ ГОЛУБОЙ КОМПАКТНОЙ КАРЛИКОВОЙ ГАЛАКТИКИ IZW18

А.Р.ПЕТРОСЯН, Г.КОНТ, Дж.БУЛЕСТЕКС, Д.КУНТ, Т.МОВСЕСЯН, С.ДОДОНОВ, Е.ЛЕ КОАРЕР, А.БУРЕНКОВ

Представлены результаты наблюдений Голубой Компактной Карликовой Галактики IZW18, выполненных с Фабри-Перо интерферометром на Канадо-Франко-Гавайском 3.6м телескопе и с многозрачковым спектрографом на 6м телескопе САО (Россия). Были исследованы морфологическая структура галактики в эмиссионных линиях и в континууме, поле скоростей эмиссионного газа и распределение отношения [OIII]/H_β вдоль северо-западного (NW) компонента. Кроме северо-западного (NW) и юго-восточного (SE) компонентов отождествлено семейство маленьких HII областей. Показано, что максимумы звездного компонента галактики смещены по сравнению с таковыми для газового

компонента. Поле скоростей показывает пекулярные движения на фоне приблизительно регулярного движения. Профили эмиссионных линий NW компонента симметричны, остальные в основном асимметричны. Отношение [OIII]/H_{β}, с градиентом 1.86 Кпк-1, уменьшается от центра NW компонента к его краю. Обнаружено; что "сгусток" Цвикки - это маленькая HII область с одинаковой как у IZW18 радиальной скоростью.

REFERENCES

R.Arsenault, J.-R.Roy, 1988, A&A, 201, 199.

J.Boulesteix, Y.P.Georgelin, M.Marcelin, G.Monnet, 1983, SPIE Conf. Instr. Astron., 445, 37 opetti M. V. F., Pastoriza M. G., Dottori H.A., 1985, A&A, 152, 427.

K.Davidson, T.D.Kinman, 1985, ApJ, 58, 321.

K.Davidson, T.D.Kinman, S.D.Friedman, 1989, AJ, 97, 1591.

R.J.Dufour, 1986, PASP, 98, 1025.

R.J.Dufour, J.J.Hester, 1990, ApJ, 350, 149.

J.S.Gallagher, D.A.Hunter, 1983, ApJ, 274, 141.

H.B.French, 1980, ApJ, 240, 41.

P.W.Hodge, M.G.Lee, Jr.R.C.Kennicutt, 1989, PASP, 101, 32.

P.W.Hodge, M.G.Lee, 1990, PASP, 102, 26.

U.Hopp, R.E.Schulte-Ladbeck, 1991, A&A, 248, 1.

C.T.Hua, B.Grundseth, T.Nguyen-Trong, 1987, Ap. Letters Comm., 25, 187.

D.A.Hunter, J.S.Gallagher, 1986, PASP, 98, 5.

Jr.R.C.Kennicutt, B.K.Edgar, P.W.Hodge, 1989, ApJ, 337, 761.

D.Kunth, W.L.W.Sargent, 1986, ApJ, 300, 496.

D.Kunth, S.Maurogordato, L.Vigroux, 1988, A&A, 204, 10.

D.Kunth, F.Sevre, 1986, Star Forming Dwarf Galaxies, (eds. D.Kunth, T.X.Thuan, J.T.T.Van), Editions Frontieres, p. 331.

A.Laval, J.Boulesteix, Y.P.Georgelin, Y.M.Georgelin, M.Marselin, 1987, A&A, 175, 199.

J.Lequeux, F.Viallefond, 1980, A&A, 91, 269.

J.Lequeux, M.Peimbert, J.F.Rayo, A.Serrano, S.Torres-Peimbert, 1979, A&A, 80, 155.

J.Lequeux, M.Maucherat-Joubert, J.M.Deharveng, D.Kunth, 1981, A&A, 103, 305.

H.-H.Loose, T.X.Thuan,1986, Star Forming Dwarf Galaxies, (eds. D.Kunth, T.X.Thuan, J.T.T.Van), Editions Frontieres, p. 73.

J.M.Mazzarella, T.A.Boroson, 1993, ApJS, 85, 27.

J.Melnick, R.Terlevich, M.Moles, 1988, MN, 235, 297.

D.E.Osterbrock, 1989,Astrophysics of Gaseous Nebulae and Active Galactic Nuclei (University Science Books: Mill Valley, CA).

A.R.Petrosian, K.A.Saakian, E.E.Khachikian, 1978, Astrophysics, 14, 36.

L.Searle, W.L.W.Sargent, 1972, AJ, 173, 25.

G.S.Shostak, E.D.Skillman, E.Brinks, 1991, BAAS, 23, 920.

E.D.Skillman, Jr.R.Kennicutt, 1993, ApJ, 411, 655.

N.V.Strobel, P.Hodge, Jr.R.C.Kennicutt, 1991, ApJ, 383, 148.

R.Terlevich, J.Melnick, 1981, MN, 195, 839.

T.X.Thuan, 1983, ApJ, 268, 667.

T.X.Thuan, T.B.Williams, E.Malumuth, 1987, Star Bursts and Galaxy Evolution (eds. T.Montmerle, T.X.Thuan, T.T.Van), Editions Frontieres, p. 151.

T.X.Thuan, 1987, Star Bursts and Galaxy Evolution, (eds. T.Montmerle, T.X.Thuan, T.T.Van), Editions Frontieres, p. 129.

F.Viallefond, J.Lequeux, G.Comte, 1987, Star Bursts and Galaxy Evolution, (eds. T. Montmerle, T.X. Thuan, T.-T.Van), Editions Frontieres, p.139.

F.Viallefond, T.X.Thuan, 1983, ApJ, 269, 444.

F.Zwicky, 1966, ApJ, 143, 166.

АСТРОФИЗИКА

ТОМ 38 НОЯБРЬ, 1995 ВЫПУСК 4

HI OBSERVATIONS OF 73 CANDIDATES BLUE COMPACT DWARF GALAXIES

G.A.OHANIAN[1], A.R.PETROSIAN[1], G.COMTE[2]

1 Byurakan Astrophysical Observatory, Armenia
2 Marseille Observatory, Marseille, France

HI observations are reported for a new sample of 73 candidates BCDGs. HI emission have been detected from 53 of them. The distributions of HI parameters are given for detected objects.

1. *Introduction*. Genuine Blue Compact Dwarf Galaxies (BCDGs) are objects with low metal content and high ratios of HI to total mass, forming stars prodigious rates, low luminosity and small size.

In order to enlarge the sample of genuine BCDGs and help to understand their nature we have started a multi-wavelength study of the new sample of the candidates of BCDGs. The new sample was build on the base of Byurakan First (FBS), Second (SBS) and also Case Blue, Kiso's, Wasilewsky's, UM surveys. The selection criteria for our sample of about 200 candidates of BCDGs are:

(I) $M_p > -17^m$, $H_0 = 75$ km s^{-1} Mpc^{-1}.

(II) Compact structure. Clear absence of spiral arms or a obvious irregular morphology, confirmed by high resolution imagery.

(III) The existence of very strong, sharp and narrow emission lines.

Since star formation normally requires the presence of high amount of neutral gas, we have carried out a study of the HI content of a sample in order to determine the amount of neutral gas.

2. *Observations and data reduction*. The observations were carried out at March 1993 and April 1994 at Nancay radio telescope, which has a collecting area equivalent to that of a 94m diameter parabolic dish.

We used a two-channel, dual polarization 21 cm spectrometer as a receiver which was used in the integration mode and was splitted into two banks of 512 channels each with channel width, corresponding to 2.64 km s^{-1}. After boxcar smoothing the final resolution is a typically 10 km s^{-1}. The two polarizations were detected independently and averaged to improve sensitivity. The half-power beam width at 21 cm is 3.6'(EW)×22' (NS) at zero degree declination.

The observations were made in the standard total-power mode, consisting of cycles of 2 min on-source and 2 min off-source integrations. The position of comparison field was approximately 20' eastward from the source. The number of cycles for one transit was between 8 and 15 but usually 12. The calibration of the telescope was obtained by measuring strong radio sources with accurately known fluxes at different declinations.

Data reduction was done using spectral line package DRAWSPEC developed by H.S.Liszt at NRAO. For each final spectra HI profile parameters (the systemic velocity, the line width at the 50% and 20% level of the maximum, the area under the profile) were extracted by fitting of the Gaussian.

3. *Results*. In total on Nancay radio telescope have been observed 73 galaxies. HI emission have been detected from 53 of them. For these 53 galaxies the following parameters are determined: (i) HI heliocentric radial velocity, (ii) HI radial velocity derived from observed HI heliocentric velocity through a spherical Virgo flow model according to the formalism of Bottinelli et al [1], (iii) HI line width measured at 50% and 20% of the maximum intensity, (iv) Area ander the HI profile (v) HI mass in solar units.

In Fig. 1 the radial velocities distribution of the sample is presented. The distribution of HI masses in solar units computed assuming H_0= 75 km s^{-1} Mpc^{-1} is shown in Fig. 2.

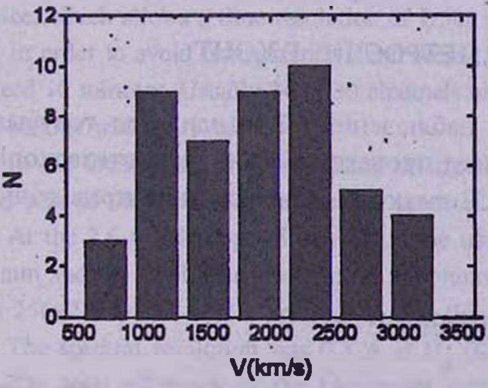

Fig. 1. The heliocentric velocity distribution of 53 detected galaxies.

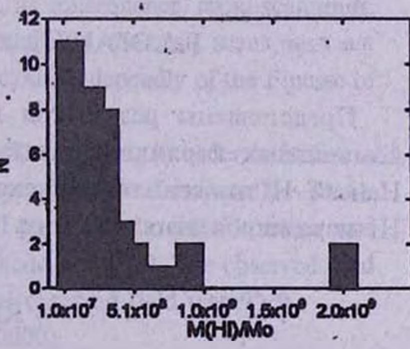

Fig. 2. The distribution of HI masses in solar units for 53 detected galaxies.

In Fig. 3 the distribution of optical magnitudes of detected objects is presented. The median value of the optical magnitudes is equal to 16.0^m. For 20 undetected objects optical magnitudes lie in the range of 15.0^m - 17.0^m with median value equal of 16.5^m.

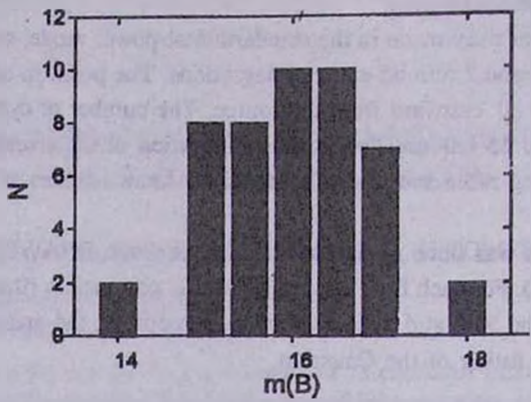

Fig. 3. The optical magnitude distribution of detected objects.

The examination of confusion effect on Nancay radio telescope shows, that only 8 galaxies from 53 detected objects are possibly confused by companions which lie within the beam sizes of Nancay telescope.

A complete analysis of these results with optical data will be presented in forthcoming papers.

HI НАБЛЮДЕНИЯ 73 НОВЫХ КАНДИДАТОВ ГОЛУБЫХ КОМПАКТНЫХ КАРЛИКОВЫХ ГАЛАКТИК

Г.А.ОГАНЯН, А.Р.ПЕТРОСЯН, Г.КОНТ

Представлены результаты HI наблюдений 73 кандидатов голубых компактных карликовых галактик, проведенных на радиотелескопе Нансей. HI эмиссия обнаружена у 53 галактик. Приводится распределение HI параметров этих галактик.

REFERENCE

1. *L.Bottinelli, L.Gouguenheim, P.Teerikorpi*, Astron. and Astrophys., 156, 157, 1986.

АСТРОФИЗИКА

ТОМ 38 НОЯБРЬ, 1995 ВЫПУСК 4

AT THE 2.6 M TELESCOPE OF BYURAKAN PEROT-FABRY OBSERVATIONS OF GAS EMISSION IN NEBULAE WITH CIGALE

J.BOULESTEIX[1], E.LE COARER[1,2],
M.MARCELIN[1], G.MONNET[3,4]

1 Observatoire de Marseille
2 Observatoire de Grenoble,
3 Observatoire de Lyon
4 ESO

During the summer of the year1985, the Perot-Fabry scanning interferometer CIGALE of Marseilles Observatory was installed at the prime focus of the 2 m 60 cm telescope of Byurakan Observatory. The long run (two new moons) was successful and gave matter to numerous publications.

1. *CIGALE instrument.* Cigale instrument is fully described in Boulesteix et al. (1983). It is basically a focal reducer in the parrallel beam of which a scanning Perot-Fabry interferometer is set. The detector is a Thomson photon-counting system device, which allows a time resolution of 1/50s and, as consequence, rapid scannings.

In order to avoid transparencies and seeing fluctuations, the basic scans must not exceed 10 minutes. Usually 24 to 32 channels are scanned, dependly of the Finesse of the etalons which are used.

In the focal plane, a narrow band interference filter is put, in order to isolate a band-pass of the same order of the free spectral range of the interferometer (~10 Å).

At the 2.6 m telescope of Buyrakan, the usefull pupill on the interférometer was 35 mm and the final aperture ratio on the photocathode was f/1.9. The observed field was 256×256 pixels of 2.1 arc sec, so that the total observed field was 9'×9'.

The spectral resolution was 0.3 Å at H_α (R~20000).

The total efficiency of the instrument was estimated to 0.04 and the limit of detection for emission to 10^{-16} erg.s^{-1}.cm^{-1}.arcsec^{-2} for a 2 hours exposure.

The scientific interest of such an instrument is to obtain simultaneously *imagery* and *profiles* on a large field with an important spectral resolution. It is in fact very well adapted to emission of inonized gas in galactic or extragalactic objects. The observer can simultaneously get the narrow-band photometry and the velocity field.

2. *Main published results of the 1985 run.*

- Hydrogen emission in the direction of h and χ Persei (Mirzoyan et al., 1991)

For the first time, this emission, apparently coming from the OB association was detected. Several hypothesis for its origin are described in the paper of L. Mirzoyan

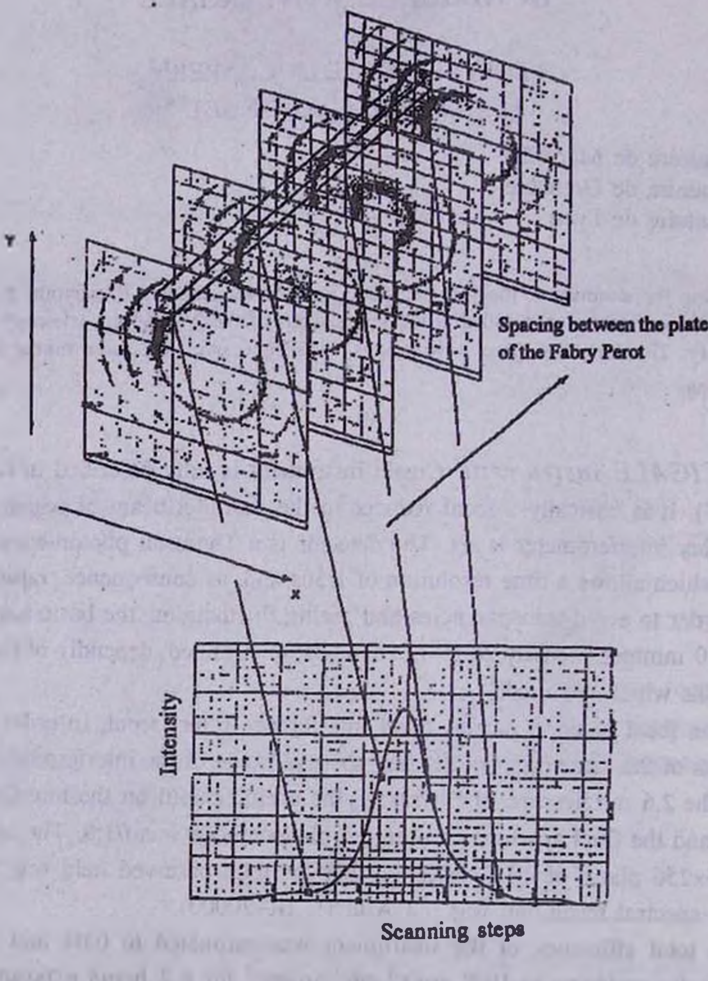

Fig. 1. CIGALE principle of scanning profiles

in these proceedings.

- W 58G: a distant HII region in the HI Cygnus arm (Georgelin et al., 1988) :

Four distinct nebular emissions can be distinguished along the same line of sight. Two are related to the nearby Cygnus complex, one at V_{LSR}=0 km.s^{-1} is associated with the Cygnus Rift at 900 pc and another one at V_{LSR}=60 km.s^{-1} is probably due to stellar winds or supernova remnants. The third emission, at V_{LSR}=-26 km.s^{-1}; is the optical counterpart of the Extented Region South East of W58 in the Perseus arm (8.4 kpc). The fourth emission commes from W58G, an HII region which appears to belong to the HI Cygnus arm, with V_{LSR}=-66 km.s^{-1}, at a distance of 12.4 kpc.

- H_α observations of the HH objects in the NGC 7129 field (Magakian et al., 1994):

H_α emission profiles of HH objects around NGC 7129 were obtained. HH 103 and GGD 35 have broad and double-peaked profiles. One extended arc-shaped HH object was confirmed. The shock velocities and orientation angles were computed.

- Kinematics of the ionized gas in the center of the Andromeda nebula (M31) (Boulesteix et al., 1987):

A very high contrast monochromatic image and a two-dimensional radial velocity field in the 6584 Å line of ionized nitrogen were obtained in the 3'×3' central part. The already known mottled appearance and the presence of 50-100 km.s^{-1} chaotic

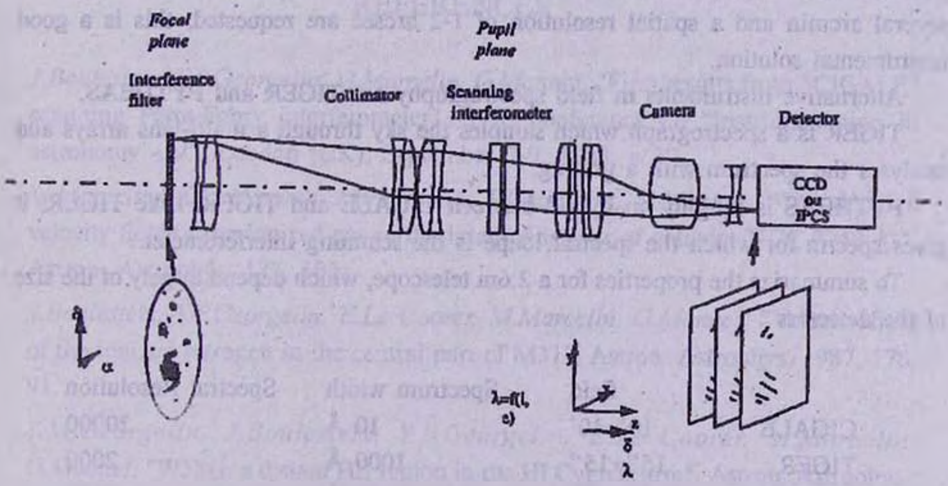

Fig. 2. CIGALE Perot-Fabry spectrometer.

motions were confirmed and connected to injection of kinetic energy in the interstellar medium via supernovae explosions.

- NGC 7752-53 (Marcelin et al., 1987):

More than 1800 velocity points over the whole galaxy and its companion were measured. Both galaxies are warped because of the interaction and the mass of each one was computed. Tidal model was developped.

- The HII regions and the velocity field of NGC 7331 (Marcelin et al., 1994):

47 HII regions of the galaxy were studied and main parameters as diameter, luminosity and velocities were derived. H_α luminosity function was computed. Velocity field reveals non-circular motions, like the classical wiggles of the isovelocity lines when crossing a spiral arm, or the Z shape distortions of the isovelocity lines in the center possibly revealing an unseen bar.

- Some data on IC 5283, a neighbour of NGC 7469 (Petrosyan et al., 1992):

The well-known Seyfert galaxy NGC 7469 was observed in H_α and [NII] 6584. The two arms of the galaxy differs in the star formation rates. The radial distribution of the hydrogen abundance and its mean value are typical of late-type spirals. No azimuthal variation in the nitrogen abundance or variation along a spiral arm could be put in evidence.

3. *Conclusions*. A scanning interferometer attached to a 2.6m telescope is a powerful tool to study the ionized extended gas. For all objects for which a field of several arcmin and a spatial resolution of 1-2 arcsec are requested, this is a good instrumental solution.

Alternative instruments in field spectrography are TIGER and PYTHEAS.

TIGER is a spectrograph which samples the sky through a multi-lens arrays and analyses the spectrum with a grating.

PYTHEAS is roughly an hybrid between CIGALE and TIGER. Like TIGER, it gives spectra for which the spectral loupe is the scanning interferometer.

To summarize the properties for a 2.6m telescope, which depend largely of the size of the detectors :

	field	Spectrum width	Spectral Resolution
CIGALE	10'×10'	10 Å	20000
TIGER	15"×15"	1000 Å	2000
PYTHEAS	15"×15"	1000 Å	2000

Scientific domains which can be studied with these instruments is large: physics of HII regions, planetary nebulae, SNR, super-associations, HH objects, galactic structure, insterstellar medium, kinematics of nearby galaxies, bulges, bars and rings, dark matter, mergers, gas in ellipticals, BGC, AGN, Markarian and Seyfert galaxies, environment effects in clusters, other diffuse emissions.

ПЕРО-ФАБРИ НАБЛЮДЕНИЯ ЭМИССИИ ГАЗА В ТУМАННОСТЯХ НА 2.6М ТЕЛЕСКОПЕ БЮРАКАНА С СИГАЛЕ

Ж.БУЛЕСТЕКС, Е.ЛЕ.КОАРЕР, М.МАРСЕЛЕН, Ж.МОННЭ

В течение лета 1985г. Перо-Фабри сканнирующий интерферометр СИГАЛЕ Марсельской обсерватории был установлен в первичном фокусе 2.6м телескопа Бюраканской обсерватории. Длинный ряд наблюдений (два новолуния) был успешным и предоставил материал для большого числа публикаций.

REFERENCES

J.Boulesteix, Y.P.Georgelin, M.Marcelin, G.Monnet, "First results from "CIGALE" scanning Pérot-Fabry interferometer", SPIE conference on "Instrumentation in astronomy - V", London (UK), September 7-9, 1983, p 37.

M.Marcelin, E.Le Coarer, J.Boulesteix, Y.Georgelin, G.Monnet, "The detailed velocity field of the ionized gas in the interacting pair of galaxies NGC 7752-53", Astron. Astrophys. 179, 101.

J.Boulesteix, Y.P.Georgelin, E.Le Coarer, M.Marcelin, G.Monnet, "Velocity field of the ionized nitrogen in the central part of M31", Astron. Astrophys, 1987, 178, 91.

Y.M.Georgelin, J.Boulesteix, Y.P.Georgelin, E.Le Coarer, M.Marcelin, G.Monnet, "W58G: a distant HII region in the HI Cygnus arm", Astron. Astrophys., 1988, 190, 61.

T.Magakian, J.Boulesteix, M.Marcelin, E.Le Coarer, "H_α observations of the HH objects in the NGC 7129 field", Astron. Astrophys., 1994, 291, 928.

M.Marcelin, A.R.Petrosian, P.Amram, J.Boulesteix, "The HII regions and the velocity field of NGC 7331", Astron. Astrophys., 1994, 282, 363.

A.R.Petrossian, J.Boulesteix, E.Le Coarer, M.Marcelin, A.Zh.Pis'ma, "Some data on the galaxy IC 5283, neighbor of NGC 7469", 1992, 18, 850, Soviet Astron. J. Letters, 1992, 18, 1043, translated into english in Sov. Astron. Lett., 1992, 18(6), 428.

L.V.Mirzoyan, M.Marcelin, A.T.Garibjanian, J.Boulesteix, A.L.Mirzoyan, Y.M.Georgelin, "Hydrogen emission in the direction of h and χ Persei", Astrofizika, 1991, 34, 67.

А С Т Р О Ф И З И К А

ТОМ 38 НОЯБРЬ, 1995 ВЫПУСК 4

OPTICAL IDENTIFICATION OF THE IRAS POINT SOURCES BASED ON THE FIRST BYURAKAN SURVEY

A.M.MICKAELIAN

Byurakan Astrophysical Observatory

Optical identification of infrared sources from the IRAS Point Source Catalogue (PSC) is made by means of low-dispersion spectra of the First Byurakan Survey (FBS) and Palomar Observatory Sky Survey (POSS) red and blue images. The purpose of this work is to examine the composition of the PSC sample of fainter sources at high galactic latitudes and to reveal QSOs, infrared galaxies, red stars (C and M), planetary nebulae, for their further investigation at the optical range. 100 of 108 unknown IRAS sources in the region with $3^h50^m \le \alpha \le 7^h40^m$ and $+69° \le \delta \le +73°$ are optically identified. Optical coordinates, V magnitudes, colour indices and preliminary classes are determined. According to preliminary classification 3 objects turned out to be QSOs, 36 - galaxies with very interesting morphology, 5 - faint planetary nebulae, 9 are carbon stars and 47 - late M-type stars.

1. *Introduction.* During the fulfilment of the second part of the FBS [1] (a search and investigation of the stellar objects on the FBS plates) the author revealed, that the limiting magnitude of the survey in some regions is significantly higher, than it was considered before (17^m-17.5^m) [2]. Some plates have m_{lim} up to 19^m and the mean m is 18^m-18.5^m. These regions are those, where B.E.Markarian started the survey in 1960's with Kodak IIF and Kodak IIAF emulsions. The realization of the Second Byurakan Survey (SBS) [3] in the region of $8^h00^m \le \alpha \le 17^h00^m$ and $+49^0 \le \delta \le +61^0$ also depended on this circumstance. According to our analysis, plates with deep limiting magnitudes are obtained also upon a large surface in three zones ($+61^0 \le \delta \le +73^0$) of the FBS, where the selection of stellar objects is already made.

It is known also, that many Markarian galaxies are infrared sources, as well as some IRAS PSC [4] sources were revealed among the objects of the second part of the FBS. The author examined the correspondence of the IRAS fluxes at 12μm, 25μm, 60μm and 100μm to the optical magnitudes of the FBS low-dispersion spectra for identified objects. The results were rather hopeful: the FBS observational material can serve with success as a base for optical identification of the PSC unknown sources, as the faintest sources in average have m_{pg} near the limit of the FBS good plates. The identificitaion is to be done by means of the FBS low-dispersion spectra, as well as using the images and approximate colours from the POSS charts.

2. *Identification principles.* FBS plates are obtained on Byurakan 1 m Schmidt telescope equipped with 1.5° objective prism. They have 4°x4° sizes and Kodak IIF, IIAF, IIaF and 103aF emulsions. The dispersion of the FBS spectra is 1800 A/mm near H_γ and the scale is 97"/mm. Thus, taking into account, that the spectral range is 3400-6900 A (with a green gap at 5300 A), the prism spectra have 1.7 mm length. The linear resolution of the photographic emulsion is about 25μm. So the magnification of 15^x allows to notice many details of the spectra. The large spectral range allows also to follow and estimate the distribution of the energy in spectrum and separate plane, powered and other types of spectra, as well as to take into account the presence of emission and absorption lines. So it is rather easy to recognize the red stars, and also to separate C and M types among them. Thus the FBS low-dispersion spectra are good indicators of carbon and M stars, planetary nebulae, sometimes - QSOs, and galaxies, objects, which correspond to infrared sources. The mentioned types of objects are not numerous, so it becomes possible to distinguish the optical counterparts in the IRAS coordinates uncertainty boxes, where mostly only one candidate is situated. It is important also, that the accuracy of coordinate determination is high (1ˢ - 2ˢ for α and about 10" for δ) and the fulfilment of the second part of the FBS gave an experience of recognition and classification of the low-dispersion spectra.

3. *Main Results.* The list of 100 IRAS PSC sources, identified by above mentioned way, is beeing prepared to publication and will appear in Astrofizika. Optical coordinates, *V* magnitudes, colours and preliminary types from the low-dispersion spectra are determined for these objects. The objects are situated in the region of the FBS $+69^0 \leq \delta \leq +73^0$, $3^h50^m \leq \alpha \leq 7^h40^m$ and occupy a surface of 75 sq. degree. 3 of the IRAS sources turned out to be QSOs, 36 - IR galaxies, 5- planetary nebulae, 9 - C and 47 - late M stars. Many galaxies have very interesting morphology (with HII regions, various irregulars, Seyfert-like bright nuclei, interacting pairs etc). It must be mentioned, that the region is started with the edge of the FBS survey, i. e. with the edge of the Milky Way, where the galactic *b* is not so large. So with the continuation of the identification to higher galactic latitudes the percentage of the galaxies and quasars will increase. In the

investigated region galactic latitudes are from b=+12° to b=+30°.

The errors of our coordinate determination are 2ˢ for α and 10" for δ. The accuracy of the IRAS coordinates do not differ highly from ours, so not always the selected optical counterpart for the infrared source will be in the uncertainty box. So 15 identified sources come outside the uncertainty ellipses. The m_V magnitudes of the objects are determined by the relation "image diameter-magnitude" according to [5] as 8.2^m -21.3^m . Fig. 1 shows the distribution of the objects with respect to the m_V-s. The colour indices are estimated in a range of 0.0-$+5^m.2$, which can be transformed to B-V colours as follows:

$$B\text{-}V = 0.6\ CI + 0.07$$

As it was mentioned, 61 sources are identified with Galactic and 39 - with extragalactic objects. The types of the 9 carbon stars are also estimated (5 - R-type and 4 - N-type). Galaxies are preliminary classified by means of the POSS images as follows: 14 - ellipticals, 15 - spirals, 2 - irregulars and 5 - Seyferts. The ellipticals may turn out to be other types in the case of detailed classification. The Seyferts are suspected from the bright nuclei and low-dispersion emission spectra. It must be mentioned also, that identified 11 M and C stars are FBS objects and will appear in the next list of late-type stars after Abrahamian and Gigoyan [6].

The sample is investigated also on various IRAS colour-colour diagrams in order to separate various classes of objects. Particularly [12]-[25] / [25]-[60] dia-

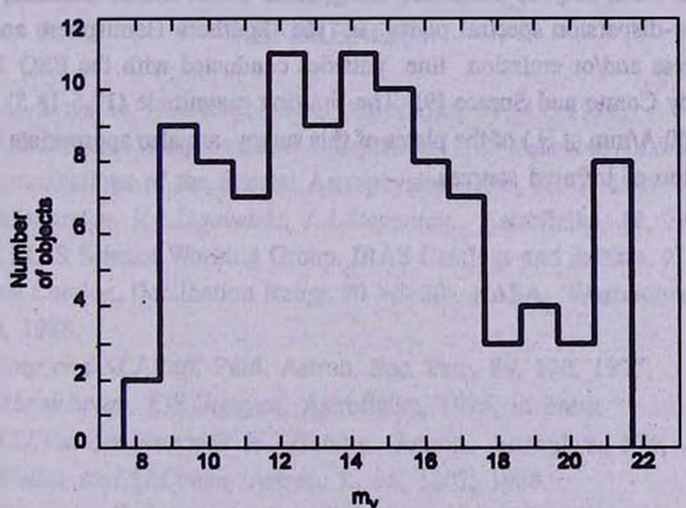

Fig. 1. Distribution of 100 IRAS sources by the optical magnitudes m_V.

gram gives regions for different classes of objects. Late-type stars have large 12μm and 25μm fluxes and smaller 60μm and 100μm fluxes. The stars with dust shells have increased infrared radiation and may deviate from the region of red stars without dust shells. The dust-rich starburst galaxies can be recognized by their IRAS 60μm and 100μm large fluxes in comparison with smaller 12μm and 25μm fluxes, as the ultraviolet flux is partly absorbed by the dust which reradiates in the far infrared (60-100μm). These differences are well seen for example in the papers of Van der Veen and Habing [7] and Walker and Cohen [8]. So the optical characteristics (magnitudes, colours, morphology, low-dispersion spectra) together with the IRAS data on 12μm, 25μm, 60μm and 100μm fluxes, give possibility of immediate classification of the objects and further many-sided research.

4. *Conclusions and perspectives.* As it was seen, low-dispersion spectra are very convenient base for recognition and identification of infrared sources. 100 of 108 IRAS PSC faint sources are identified, 94 of which are confident identifications. The large observational material obtained by means of IRAS needs further investigations, especially at the optical range, in order to discuss the results together with known astronomical objects and phenomena. So such works are necessary and important. For the successful continuation of this work it is desirable to have the digitized POSS. The beginning of the work in Byurakan is made without it and cannot be continued for large amounts of objects. The presence of the POSS and the PSC on CD ROMs together with the FBS plates input by scanner into the computer will give possibility for automatic identification of the IRAS sources.

Similar work may be done also using other observational material, such as the ESO's low-dispersion spectral plates in the Southern Hemisphere and the survey of UV excess and/or emission line galaxies conducted with the ESO 1 m Schmidt telescope by Comte and Surace [9]. The limiting magnitude (17.5-18.5) and the dispersion (450 A/mm at H_γ) of the plates of this survey are also appropriate for optical identification of infrared sources.

ОПТИЧЕСКИЕ ОТОЖДЕСТВЛЕНИЯ ТОЧЕЧНЫХ ИСТОЧНИКОВ IRAS, ОСНОВАННЫЕ НА ПЕРВОМ БЮРАКАНСКОМ ОБЗОРЕ

А.М.МИКАЕЛЯН

Выполнены оптические отождествления инфракрасных источников из Каталога Точечных Источников (PSC) ИРАС, основанные на низкодисперсионных спектрах Первого Бюраканского Обзора (FBS) и красных и голубых изображениях Пломарского Обзора Неба (POSS). Целью настоящей работы является анализ состава выборки относительно слабых источников PSC в высоких галактических широтах и выявление квазаров, инфракрасных галактик, красных звезд (C и M), планетарных туманностей, для их далнейшего изучения в оптическом диапазоне. Из 108 неизвестных источников ИРАС в области с $3^h50^m \leq \alpha \leq 7^h40^m$ и $+69° \leq \delta \leq +73°$ оптически отождествлено 100. Определены оптические координаты, звездные величины *V*, показатели цвета и предварительные классы. Согласно предварительной классификации, 3 объекта оказались квазарами, 36 - галактиками с интересной морфологией, 5 - слабыми планетарными туманностями, 9 - объектов являются углеродными звездами и 47 - звездами M поздних подклассов.

REFERENCES

1. *H.V.Abrahamian, A.M.Mickaelian,* Astrofizika, 37, 43, 1994.
2. *B.E.Markarian, V.A.Lipovetski, J.A.Stepanian, L.K. Erastova, A.I.Shapovalova,* Communications of the Special Astrophysical Obs., 62, 5, 1989.
3. *B.E.Markarian, V.A.Lipovetski, J.A.Stepanian,* Astrofizika, 19, 29, 1983.
4. Joint IRAS Science Working Group. IRAS Catalogs and Atlases. 2. The Point Source Catalog, Declination Range 90 >d>30 . NASA, Washington, DC: US GPO, 1988.
5. *I.R.King and M.J.Raff,* Publ. Astron. Soc. Pac., 89, 120, 1977.
6. *H.V.Abrahamian, K.S.Gigoyan,* Astrofizika, 1995, in press.
7. *W.E.C.J.Van der Veen and H.J.Habing,* Astron. Astrophys., 194, 125, 1988.
8. *H.J.Walker and M.Cohen,* Astron. J., 95, 1801, 1988.
9. *C.Surace and G.Comte,* Astron. Astrophys., 281, 653, 1994.

А С Т Р О Ф И З И К А

ТОМ 38 НОЯБРЬ, 1995 ВЫПУСК 4

BARRED SPIRALS AND DWARF GALAXIES IN THE VIRGO CLUSTER

A.T.KALLOGHLIAN

Byurakan Astrophysical Observatory

Using the extensive Catalog of Binggelli, Sandage and Tammann it is shown that dwarf galaxies in the Virgo cluster are more tightly connected with barred rather than with normal spirals. The number of dwarfs is as higher as greater the number of barreds in the given field. There is no preferential direction in the distribution of dwarfs around barred galaxies.

1. *Introduction.* Dwarf galaxies have been identified in nearby clusters of galaxies as Virgo, Coma and Fornax. It has been shown that there is a close connection of dwarf galaxies with bright galaxies [1,2]. The distribution of dwarf elliptical galaxies of type dE is similar to that of giant E + S0 galaxies . The late type dwarfs show a broader distribution than the giant galaxies.

Giovanardi and Binggeli [3] concluded that more than 95% of all dwarf ellipticals in Virgo cluster must be freely flying around in the cluster potential. Outside the clusters dE galaxies seem all bounded to giant galaxies [4]. Caldwell [5] found that dwarfs in Fornax cluster are less concentrated than the bright galaxies. The ratio of dwarfs to the bright ellipticals is significantly smaller than the ratio found in the Virgo cluster. On the other hand the ratio of dwarf ellipticals to the active star forming galaxies of S and Irr types is similar to that of in Virgo. This result seems to be very important.

In Coma cluster [6] the ratio of numbers of dwarf and bright galaxies is not higher than in the Virgo cluster. It means that this ratio does not rise with the richness of the cluster.

The connection of dwarf galaxies with spiral galaxies has been usually considered together for both barred and normal spirals. However the existence of bright bars gives rise to several inherent features in barred spirals. In particulary the nuclei of barred spirals are more active than that of normal spirals; it is well known that hot spots much more oftenly occur in the nuclear parts of barred spirals; according to [7] the radio emission in barred spirals is essentially more oftenly localized to the centers than that of in normal spirals; as it was shown by Martin and Roy [8] the O/H gradient is flatter in barred rather than in normal spirals which is consistent with recent models of radial flow. It is remarkable that active spectra established by Kinney et al [9] on the base of IUE observations are more oftenly observed in barred spirals.

In 1970 I have shown [10] that dwarf galaxies in Virgo cluster are more tightly connected with barred rather than with normal spirals.But at that time a few dwarf galaxies were known in Virgo cluster.

In this report the problem of connection of dwarf galaxies with barred and normal spirals is considered by using the extensive catalog published by Binggeli, Sandage and Tammann (hereafter catalog BST) [11].

2. *Description of the sample.* The Catalog BST covers 140 sq.degrees in the region of the Virgo cluster and contains 2096 galaxies.Of these galaxies 1277 are certain members of the cluster, 574 objects are possible members and 245 - field galaxies. According to the authors of the Catalog BST, all galaxies with $B_T \leq 18$ have been identified in the survey area. This limiting magnitude corresponds to an absolute magnitude M_{BT}= -13.7 if we take for distance modulus a value m-M=31.7 adopted in the Catalog BST. The Catalog, however, cotains many other objects fainter than this limit till to B_T = 20.0 or to M_{BT}= -11.7. Here we consider only certain members of the Virgo cluster including as all dwarf galaxies fainter than B_T= 16.7 (M_{BT} > -15.0) as well as bright spiral galaxies of both types with B_T < 14.7 (M_{BT} < -17.0). We call the latter galaxies as bright galaxies and the former ones - dwarf galaxies. The number of dwarf galaxies in the Catalog BST is 748. Up to accepted limit in the Catalog BST exist 175 bright spiral galaxies of both types. Of this 52 are barred spirals while 123 - normal spirals, i.e. the barreds are 30% of all spirals in the sample.

Fig. 1 shows the distribution of morphological types of bright spiral galaxies.Two peaks in the distributions of both type of spirals, namely at S0, SB0 and Sc, SBc are strongly pronounced.

Dwarf galaxies were counted in two concentric circles of radii 200 kpc and 100 kpc around every bright spiral galaxy.The obtained results show the same tendency for both radii. In this report we use the data refering to the radius of 200 kpc.

3. *Results.*The comparison of the counted number of dwarfs with the expected value in the case of random distribution is complicated by the fact of overlappings of various fields. For this reason the total number of counted dwarfs is essentially larger than their real number in the Catalog BST. Instead of this we compared the mean number of dwarf galaxies in one field for barred and for normal spirals. Beside of this

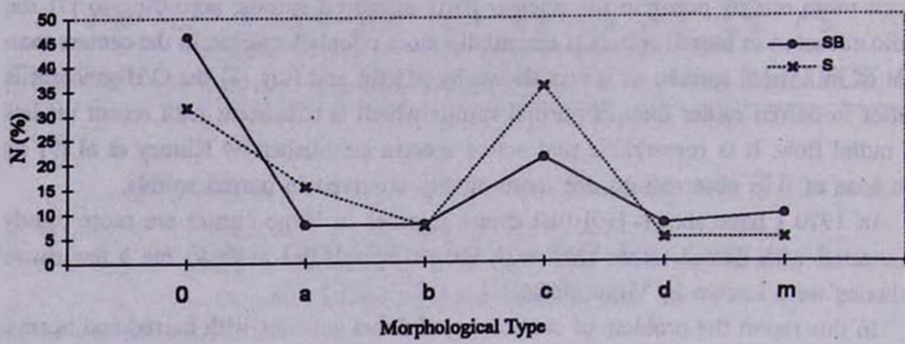

Fig. 1. Distribution of morphological types of bright spiral galaxies.

in the case of normal spirals we distinguish two kind of fields: one kind of fields contains at least one bright barred spiral, the others do not.The distribution of the fields according to this scheme is:

1) Number of fields with central SB-galaxies 52
2) Number of S-fields containing at least one SB-galaxy 60
(hereafter designated as S^{+SB})
3) Number of S-fields without any bright SB-galaxy 63
(hereafter desingnated as S^{-SB}).

Since the number of these three kind of fields is about the same we suggest that the overlapping factor for all of them is about the same. The results of counts of dwarf galaxies refering to one field with R=200 kpc for each of the three samples are presented in Fig. 2. The difference between SB, S^{+SB} fields on one side and S^{-SB} fields - on the other, is quite remarkable. Only at subtype "c" the results of SB and S^{-SB} fields are the same.In all other morphological types the curves for SB and S^{+SB} fields are significantly higher than for S^{-SB} fields.This means that dwarf galaxies appear more oftenly nearby barred spirals or in other words they are more tightly connected with barred galaxies.

Another result from the distributions given in Fig. 2 is that the mean number of dwarfs in one field decreases to the later types of bright central galaxies (from "0" to "d, m"). For "c" subtypes or later this number in the mean is about twice less than in the fields where the central galaxy is of "0" or "a" subtype.

Now we shall look if the number of dwarf galaxies depends on the number of bright SB-galaxies in the field. As well as according to Fig. 2 the SB and S^{+SB} fields show the same features concerning to the connection with dwarf galaxies, we consider

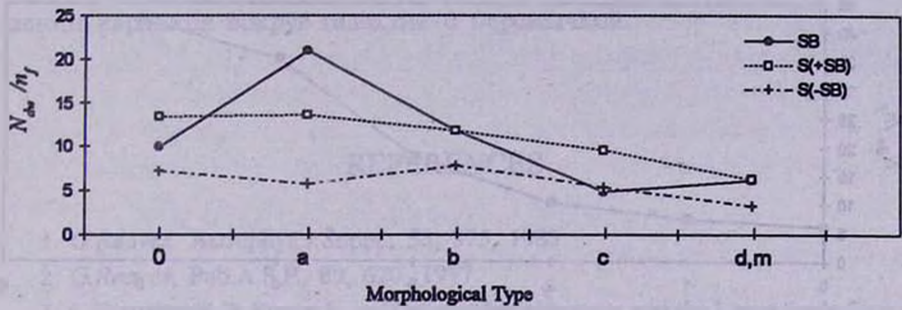

Fig. 2. The number of dwarfs in one field N_{dw}/n_f versus morphological type.Dots are for fields in the center of which are SB-galaxies, squares-for S^{+SB}-fields containing at least one SB-galaxy,crosses-for S^{-SB}-fields without any SB-galaxy.

both kind of fields together. The SB and S^{+SB} fields containing the same number of barred spirals have been combined and the mean number of dwarfs in corresponding fields has been calculated. The results are presented in Fig. 3. On absciss the so called "multiplicity" of barred galaxies in the field is given, on ordinates the number of dwarf galaxies refered to one field is shown. As it is seen the number N_{d}/n_f increases very steeply with increasing of the "multiplicity" of barred galaxies. It is remarkable that the lowest value of N_{d}/n_f is for fields without any SB-galaxy.

We considered also the distribution of dwarf galaxies around barred spirals with respect to the directions of bars. For this the position angles ϑ_p of the directions of bars of all bright SB-galaxies studied in this paper have been roughly estimated on the blue or red charts of Palomar Sky Survey. The dwarf galaxies were counted in slices of 30° wide. Every of four slices symmetricaly located with respect to the direction of the bar were binned together. As a result of these counts we have the following data:

ϑ_p	N_{dw}
0 - 30	143
30 - 60	155
60 - 90	131

We conclude from these results that no preferential direction exists in the distribution of dwarfs connected with barred spirals.

4. *Summary.* The main results of this investigation are:

1) Dwarf galaxies of all types with absolute magnitude M_{BT} >-15.0 more oftenly appear around bright barred spirals rather than around bright normal spirals.

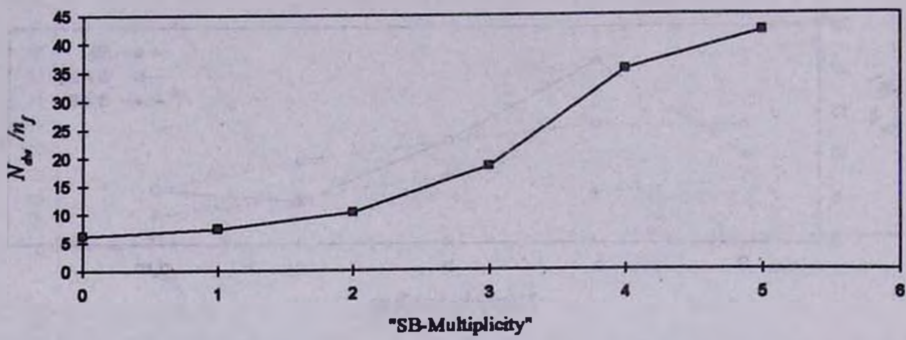

Fig. 3. The dependence of N_{dw}/n_f on the number of SB-galaxies in the field ("SB-multiplicity").

2) The number of dwarf galaxies increases rapidly with increasing of the number of bright barred spirals in the field.

3) The mean number of dwarf galaxies in one field decreases if the central bright spirals of both types are of later morphological types.

4) There is no excess in numbers of dwarf galaxies in the direction of bars.

The first two features apparently are caused by the existence of bar structure in the SB-galaxies. As it was suggested by Ambartsumian [12] the matter of bars may be ejected from the nuclea of galaxies during their activity. In frame of this suggestion it is possible to accept that at least a part of dwarf galaxies observed around SB-spirals,have been originated during nuclear activity of parent galaxies. The uniform distribution of dwarf galaxies around barred spirals does not contradict to this adoption.

ГАЛАКТИКИ С ПЕРЕМЫЧКОЙ И КАРЛИКОВЫЕ ГАЛАКТИКИ В СКОПЛЕНИИ VIRGO

А.Т.КАЛЛОГЛЯН

Используя обширный каталог Бингелли, Сандейджа и Таммана, показано, что карликовые галактики в скоплении Virgo более тесно связаны с галактиками с перемычкой, чем с нормальными спиралями. Число карликовых галактик увеличивается с числом галактик с пере-

мычкой в данной области. Нет примущественного направления в распределении карликов вокруг галактик с перемычкой.

REFERENCES

1. *G.Reaves,* Astrophys.J.Suppl., 53, 375, 1983.
2. *G.Reaves*, Pub.A.S.P., 89, 620, 1977.
3. *C.Giovanardi, B.Binggeli,* in "Galaxy Environments and the Large Scale Structure of the Universe", ed.G.Giuricin, F.Mardirossian, M.Mezzetti, SISSA, Miramare, Trieste-Italy, 22-25 October 1991.
4. *B.Binggeli, M.Tarenghi, A.Sandage,* Astron.Astrophys., 228, 42, 1990.
5. *N.Caldwell,* Astron.J., 94, 1116, 1987.
6. *L.A.Thompson, S.A.Gregory,* Astron.J., 106, 2197, 1993.
7. *A.T.Kalloghlian, R.A.Kandalian,* Astrofisica, 24, 47, 1986.
8. *P.Martin, Jean-Rene Roy,* Astrophys.J., 424, 599, 1994.
9. *A.L.Kinney, R.C.Bohlin, D.Calzetti, N.Panagia, R.F.G.Wyse,* Astrophys.J.Suppl. ser., 86, 5, 1993.
10. *A.T.Kalloghlian*, Astrofisica, 6, 683, 1970.
11. *B.Binggelli, A.Sandage, G.A.Tammann,* Astron. J., 90, 1681, 1985.
12. *V.A.Ambartsumian,* in "The Structure and Evolution of Galaxies", Interscience Publishers, London - New York - Sydney, 1965, p.1.

АСТРОФИЗИКА

ТОМ 38 НОЯБРЬ, 1995 ВЫПУСК 4

GAS CONTENT OF INFRARED LUMINOUS MARKARIAN GALAXIES

R.KANDALIAN[1], J.-M.MARTIN[2], L.BOTTINELLI[2,3], L.GOUGUENHEIM[2,3]

1 Byurakan Astrophysical Observatory,
378433 Byurakan, Armenia
2 Observatoire de Paris, Section d'Astrophysique,
ARPEGES, F- 92195 Meudon Cedex, France
3 Université Paris-Sud, F-91405 Orsay Cedex, France

The atomic and molecular hydrogen gas properties of a complete sample of Markarian galaxies with flux density at 60 μm higher than 1.95 Jy, are presented. We present the improved far-infrared luminosity function of Markarian galaxies, and its comparison with other samples. We find that 40% of the bright IRAS galaxies of far-infrared luminosity higher than $10^{10.5}L_\odot$ are Markarian galaxies.There is an absence of correlation between HI content of Markarian galaxies and current star formation activity, implying that star formation in these systems has complex structure and it is not a simple function of the HI content. On the contrary, the H_2 content of Markarian galaxies is well correlated with star formation activity. It is argued that tight correlation between HI and H_2 contents is a consequence of transformation of atomic hydrogen into molecular.

1. *Introduction.* During the First Byurakan Spectral Sky Survey (FBS) more than 1500 extragalactic objects with strong UV continuum were found ([1] and references therein). The goal of the FBS was to discover active galaxies and it is one of the main sources of optically selected galaxies with enhanced star forming activity (SFA) and active galactic nuclei (AGN). Galaxies display various degree of nuclear activity, from very high (quasars, Seyfert galaxies) to intermediate and low activity (LINERS, starbursts HII region galaxies). Far-infrared luminosity function of Markarian galaxies have been studied by Xu et al.[2] , but due to their sample selection criterion the luminosity function in the high luminosity range was not constructed properly.

The nature of molecular and neutral gas in Markarian galaxies has been less studied. How do neutral and molecular gas properties of Markarian galaxies compare? The CO survey of Markarian objects has been done only for a few dozen galaxies on the basis of neither not complete nor unbiased samples [3-6]. So far neutral hydrogen observations of Markarian galaxies have been performed for about 300 objects. They were included in the HI surveys of the galaxies mainly according to their morphological or by spectroscopical properties [7-14]. In order to investigate far-infrared and gas properties of Markarian galaxies in more detail we have compiled a flux-limited (f(60) > 1.95 Jy) complete sample of these objects from the IRAS survey. Throughout this paper a Hubble constant of 75 km/s Mpc is adopted.

2. *The sample and luminosity function.* The IRAS survey coveres about 96% of the sky. Only 54 of the 1500 Markarian galaxies were not observed by the IRAS satellite. The IRAS Point Source Catalogue (PSC) [15] contains FIR fluxes for 635 Markarian galaxies measured at least in one of four IRAS bands. Both (log*N*-log*S*) relation and V/V_{max} test show that the sample of Markarian galaxies is complete for the objects which have flux density at 60 μm higher than 1.95 Jy. Therefore our working sample contains 155 Markarian galaxies.

Xu et al. [2] have constructed a far-infrared luminosity function of Markarian galaxies using the optical and fractional bivariate (optical, far-IR) lumunosity functions. However, since their sample of Markarian galaxies was selected by the stellar magnitude brighter than 14.5, galaxies which are luminous in the far-IR but exceed this magnitude limit were omitted. As a consequence the far-IR luminosity function of Markarian galaxies was not constructed correctly in the high-luminosity (> $10^{10}L_{\odot}$) range. We have determined far-IR luminosity function of Markarian galaxies using Schmidt's estimator. The derived luminosity function (solid circles) is shown in Fig. 1. For comparison in the same plot are also shown far-IR (open circles) luminosity

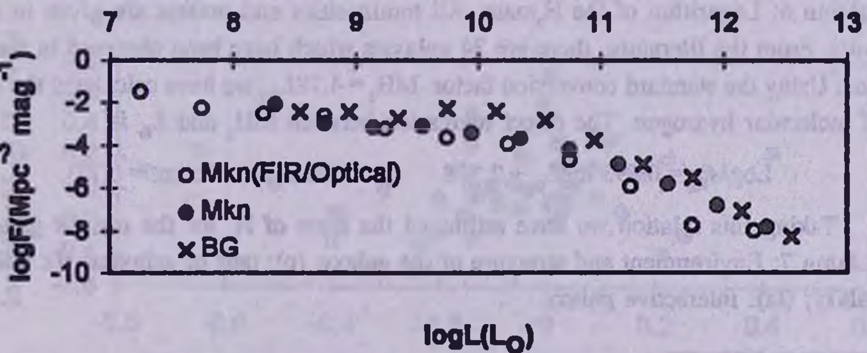

Fig. 1. Far-infrared luminosity function of Markarian galaxies (solid circles). For comparison are also shown, far-IR (open circles) luminosity fuctions of Markarian galaxies derived by Xu et al. [2] and far-IR luminosity function (crosses) of IRAS Bright Galaxy sample, derived by Soifer et al. [16]. Luminosities are defined as vL and are in solar units.

functions of Markarian galaxies derived by Xu et al.[2] and far-IR luminosity function (crosses) of IRAS Bright Galaxy sample (referred to as the BG sample), derived by Soifer et al. [16]. Luminosities are defined as νL and are given in solar units. As shown in Fig. 1, the luminosity functions of Mkn and BG samples are similar up to $\log L$=9.5. The space density of BG is higher in the luminosity range of 9.5< $\log L$<11. In the higher luminosity range ($\log L$ >11) the space densities of Mkn (our determination) and BG samples have almost the same behaviour and evidently that space density of Mkn galaxies derived by Xu et al. [2] is underestimated. We find that 40% of the bright IRAS galaxies of far-infrared luminosity higher than $10^{10.5} L_{\odot}$ are Markarian galaxies. It should be noted that there is no break in the far-IR luminosity function of the Mkn sample at $\log L$=11.75 as noted in [2] .

In order to investigate the gas properties of Markaian galaxies we have selected a subsample of objects with flux density at 60 μm f(60) > 2.5 Jy (82 galaxies) from our original sample. Below we will present results of this study.

3. *Data and results.* Parameters of the 82 galaxies are given in Table 1, which have been extracted from the "Catalogue of Principal Galaxies" (PGC) [17] and from the literature, cited above. Most of HI data are from our observations carried out at Nançay* [12-14]. Additional morphological data of galaxies concerning their fine structure and environment were added according to [18, 19] .The description of Table 1 is as follows:

column 1: Markarian number of the galaxy (increasing right ascension order); column 2: Logarithm of the blue luminosity; column 3: Logarithm of the FIR luminosity, computed by the method of Lonsdale et al. [15]; column 4: The dust mass, computed using the relation $M_d \sim L_{fir} / T_d^5$ [20]; column 5: Logarithm of the HI mass. column 6: Logarithm of the H_2mass. All luminosities and masses are given in solar units. From the literature, there are 24 galaxies which have been observed in the CO line. Using the standard conversion factor $MH_2 = 4.78 L_{CO}$ we have calculated the mass of molecular hydrogen. The direct regression between MH_2 and L_{fir} is:

$$\mathrm{Log} M_{H2} = 0.693 \log L_{fir} + 2.228 \qquad \text{(correlation coefficient = 0.77).}$$

Taking this relation we have estimated the mass of H_2 for the rest 58 galaxies; column 7: Environment and structure of the galaxy. (p): pair of galaxies; (i): isolated galaxy; (ia): interactive galaxy.

*The Nançay Radio Observatory is the Unité Scientifique de Nançay of the Observatoire de Paris, associated as Unité de Service et de Recherche (USR) No. B704 to the French Centre National de Recherche Scientifique (CNRS). The Nançay Observatory also gratefully acknowledges the financial support of the Conseil Régional of the Région Centre in France.

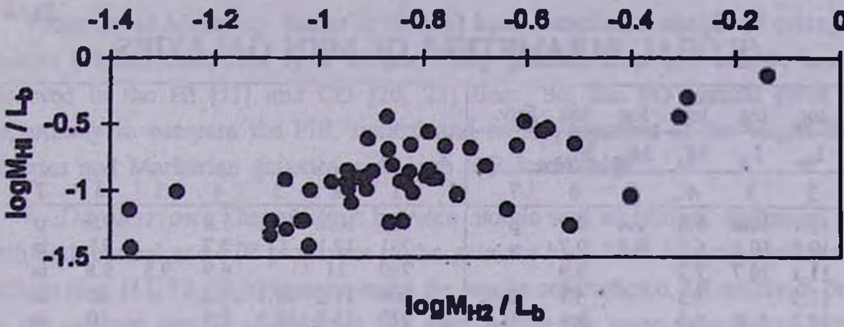

Fig. 2. Relation between atomic (M_{HI} / L_b) and molecular (M_{H2} / L_b) hydrogen mass-luminosity ratios.

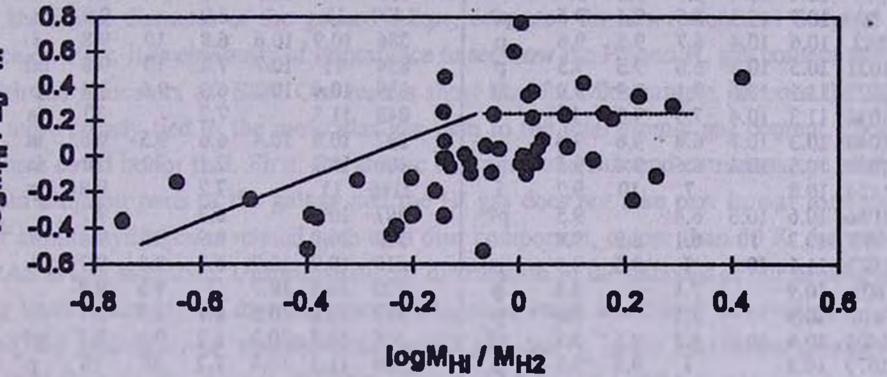

Fig. 3. The HI relative deficiency, expressed by the ratio M_{HI} / L_b, normalized to its mean value, versus M_{HI} / M_{H2} ratio.

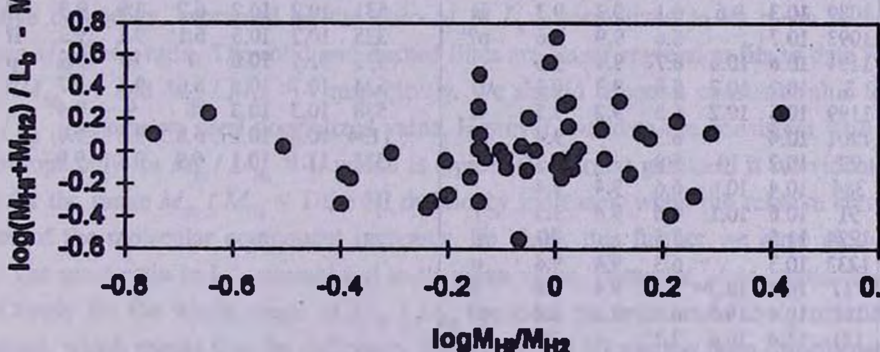

Fig. 4. Total gas mass-luminosity $(M_{HI}+M_{H2})/L_b$ ratio, normalized to its mean value, versus M_{HI} /M_{H2} ratio.

Table 1

GLOBAL PARAMETERS OF MKN GALAXIES

Mkn No.	log L_{IR}	log L_B	log M_d	log M_{HI}	log M_{H2}	Env.
1	2	3	4	5	6	7
334	10.7	10.4	6.3	9.4	9.6	p
545	10.8	10.8	6.9	9.5	9.7	p
947	11.1	10.7	7.2		9.9	
551	11.5		7.3		10	ia
552	10.3	9.9	6.3		9.4	i?
555	10.4	10.5	6.7	9.3	9.4	
353	10.4	10.3	6.4	9.4	9.5	
567	10.9		6.9	10	9.8	i
995	11.4		7.5	11	10	i
575	10.4	10.4	6.7	9.5	9.4	
2	10.7	10.3	6.5	9.4	9.6	p?
582	10.6	10.4	6.7	9.5	9.6	p
1021	10.5	10.5	6.6	9.5	9.5	p
1027	11.1	10.6	7.1	9.9	9.9	ia
1034	11.3	10.4	7.5	9.9	10	
1040	10.3	10.7	6.4	9.6	9.4	
1050	10.5	10.4	6.6	9.4	9.5	
1184	10.8		7	10	9.7	i
1066	10.6	10.3	6.4		9.5	p?
603	10.3	10	6.1	8.9	9.4	
1073	11.1	10.9	7	9.5	9.9	p
609	10.9		7.1		9.8	p
610	10.9		7.1		9.8	p
1405	10.6	10.9	6.7	9.5	9.5	p?
1079	10.8		7	9.8	9.7	p
617	11.3	10.4	6.9	9.4	10	ia
618	10.9		6.9		9.8	
1087	10.8	10.6	6.7	9.9	9.7	
1088	10.6	10.6	6.6	9.4	9.6	
1089	10.3	9.6	6.1	9.3	9.3	ia
1093	10.7		6.6	9.9	9.6	p?
1194	10.6	10.6	6.7	9.4	9.6	
3	10.2	10.2	5.8	9.3	9.3	p
1199	10.5	10.2	6.3	9.2	9.5	ia
1201	10.4		6.3		9.4	p?
73	10.2	10	5.9		9.3	
384	10.4	10.4	6.6	9.4	9.4	
91	10.6	10.1	6.6	9.4	9.5	i
1224	11.5		7.5		10	p
1233	10.3		6.3	9.4	9.4	p
717	10.6	10.3	6.3	9.4	9.6	i
161	10.4	10.5	6.4	9.6	9.4	p?
171	11.4	10.6	7.1		10	ia
1304	10.5	10	6.2	9.5	9.5	ia
761	10.5	10.1	6.6	9.6	9.5	p
201	10.6	10.1	6.3	8.8	9.6	
766	10.2	10.1	5.8		9.3	p
231	12.1	11	7.7		11	ia
789	11		6.9	9.5	9.8	ia
266	11.2	10.7	7.2		10	ia
273	11.9	10.9	7.5		10	ia
796	10.6		6.7	9.7	9.6	p?
1361	10.6		6.3		9.6	
1365	10.6	10.2	6.5	9.4	9.5	
799	10.5	10.4	6.7	9.5	9.5	ia
673	11	10.7	7.2	9.8	9.9	ia
1490	11		6.9		9.9	i
286	10.9	10.6	6.8	10	9.8	i
834	11	10.7	7.2	10	9.8	ia?
839	10.4	10.2	6.3	9.6	9.4	p
848	11.5		7.2		10	ia
297	10.6	10.4	6.6	9.5	9.6	ia
496	11.2		7.1	10	10	ia
1116	11		7.2		9.8	p
897	10.8		6.7		9.7	
512	10.9		6.9	10	9.8	i
518	10.9	10.7	6.8	9.8	9.7	i
520	10.9	10.7	7	9.8	9.8	
917	10.8	10.5	6.7	9.7	9.7	
308	10.5	10.3	6.2	9.8	9.5	p?
309	11.2	10.8	7.2	10	10	p
928	11.1		6.9		9.9	ia
319	10.9	10.8	7	9.8	9.8	
321	10.9	11.1	7.3	10	9.8	
323	10.4	10.4	6.9	9.4	9.4	i?
531	10.2	10.2	6.2	8.9	9.3	i?
325	10.2	10.3	6.1	9.1	9.3	i?
533	11.1	10.8	7	10	9.9	p
534	10.7	10.6	6.6	9.5	9.7	p
538	10.3	10.3	6	9	9.4	
1134	10.6	10.1	6.8	9.5	9.6	
331	11.1	10.1	6.9	9.9	9.9	i

From the IRAS survey, Soifer et al. [21] have compiled a sample of extragalactic sources brighter than 5.24 Jy at 60 μm. Many galaxies from this sample have been observed in the HI [11] and CO [20, 22] lines. So, the BG sample gives a best opportunity to compare the FIR, optical and radio properties of the bright infrared galaxies and Markarian galaxies with high FIR luminosity.

4. *Discussion*. The relations between atomic and molecular hydrogen masses with both optical and FIR properties of the galaxies have been investigated by various authors (e.g. [11, 12, 23]). In some cases the results contradicted. Of course, it depends on the selected sample of galaxies, but even within the same sample low luminous galaxies show different relation between FIR luminosity and HI content with respect to luminous ones [23]. It is generally accepted that the SFA is increasing with dust temperature. Another indicators of the SFA are L_{fir} (or L_{fir}/A_0^2) and L_{fir}/L_b, where A_0 is the linear diameter of the galaxy in kpc, corrected for absorption and deduced to face-on view. It is obviously of importance to see how the HI and H_2 gas content varies with the indicators of SFA. Our results show that for Mkn sample galaxies the SFA is more closely tied to the molecular gas than to the total atomic gas content. Some causes could be for that. First, the atomic hydrogen and infrared emissions are arising from different parts of the galaxy and the HI gas does not take part in star formation (or atomic hydrogen is related with cold dust component, colder than 30 K, for which IRAS is less sensitive). Unfortunately, HI distribution in the galaxies of our sample has not been measured, so that this comparison must await additional observations. Second, the probability of transformation of HI gas into H_2 in the Markarian galaxies is higher than in the normal galaxies. Figure 2 shows the tight correlation between M_{HI}/L_b and M_{H2}/L_b implying that there is a possibility for transformation of HI gas into H_2. To investigate this property in more detail we have plotted (Fig. 3) the HI relative deficiency, expressed by the ratio M_{HI}/L_b, normalized to its mean value, versus M_{HI}/M_{H2} ratio. The solid and dashed lines are linear regression fits to data for $M_{HI}/M_{H2} < 1$ and $M_{HI}/M_{H2} > 1$ respectively. We should expect a constant value for M_{HI}/L_b, because we used normalized value. However, our data are consistent with a zero slope only for $M_{HI}/M_{H2} > 1$, which is typical for normal galaxies. It is evidente, that for the range $M_{HI}/M_{H2} < 1$ the HI deficiency increases, when the relative abundance of the molecular component increases. To check this further we have plotted total gas mass ratio to L_b, normalized to its mean value, versus M_{HI}/M_{H2} ratio (Fig. 4). Clearly for the whole range of M_{HI}/M_{H2} the total gas mass ratio to L_b remains constant, which means that the deficiency disappears and HI gas has been transformed into H_2. When it is considered the ratio M_{HI}/A_{02} normalized to its mean value as a HI deficiency, the result is the same. This result has been obtained previously in

[12,24] for the luminous infrared galaxies. We have estimated that HI gas mass for the range $M_{HI} / M_{H2} < 1$ is smaller than that of the range $M_{HI} / M_{H2} > 1$ for 70%, which means that up to 70% of the HI mass can be converted into H_2 gas mass. It should be noted that for galaxies of our sample M_{HI} / M_{H2} ratio does not depend on the morphological type of the galaxy.

Below we will consider isolated galaxies (14 objects) and galaxies with complex environment (i.e. paired, interactive, 35 objects) separately for Mkn sample. In these statistics galaxies with ambiguous environment have not been included. The mean global parameters of galaxies in two subsamples ("isolated" and "complex") do not differ significantly, except M_{HI} and M_{H2}. According to our results the M_{H2} is 2 times higher in the galaxies with complex environment than in the isolated ones. On the contrary, the HI mass is 2 times higher in the isolated galaxies than in the "complex" galaxies. There is no HI deficiency in the isolated galaxies and it appears in the "complex" galaxies only. Our sample of 82 galaxies contains 16 Seyfert type galaxies. Main results of our study were not changed when Seyfert galaxies were excluded.

5. *Conclusion*. We have presented far-infrared luminosity function of Markarian galaxies derived from flux-limited complete sample of galaxies. The space density of Markarian galaxies comprise about 40% of luminous ($>10^{10.5} L_{\odot}$) IRAS galaxies. There is an absence of correlation between HI content of Markarian galaxies and star formation activities. On the contrary, the H_2 content of Markarian galaxies is well correlated with star formation activities. It is argued that tight correlation between HI and H_2 contents is a consequence of transformation of atomic hydrogen into molecular. The rate of conversion of atomic hydrogen into molecular hydrogen depends from the environment of the galaxy.

Finally, it should be noted that more observations, specifically with high angular resolusion of HI, in mm-wavelengths and in optics are needed for the Mkn galaxies with high FIR luminosities in order to address the questions raised in this study. Namely, a) The environment and galactic properties; b) The spatial distribution of the dust and gas components in these galaxies.

ОБИЛИЕ ГАЗА В ГАЛАКТИКАХ МАРКАРЯНА, ЯРКИХ В ИНФРАКРАСНОЙ ОБЛАСТИ

Р.КАНДАЛЯН, Ж.-М.МАРТИН, Л.БОТИНЕЛЛИ, Л.ГУГЕНАЙМ

Представлены особенности атомарного и молекулярного водородного газа для полной выборки галактик Маркаряна с плотностью потока на 60 мкм выше 1.95 Ян. Приводится уточненная функция светимости галактик Маркаряна в далекой инфракрасной области и ее сравнение с другими выборками. Найдено, что 40% ярких IRAS -галактик со светимостью выше $10^{10.5}L_{\odot}$ в далекой инфракрасной области являются галактиками Маркаряна. Нет корреляции между обилием HI и активностью звездообразования в галактиках Маркаряна, показывая, что звездообразование в этих объектах имеет сложную структуру и простым образом не зависит от обилия HI. Наоборот, обилие H_2 в галактиках Маркаряна хорошо коррелирует с активностью звездообрвзования. Установленно, что тесная корреляция между обилиями HI и H_2 является следствием превращения атомарного водорода в молекулярный.

REFERENCES

1. *B.E.Markarian, V.A.Lipovetskii, D.A.Stepanian*, Astrofizika, 17, 619, 1981.
2. *C.Xu, G.De Zotti, A.Franceschin, L.Danese*, Astron. Astrophys., 196, 59, 1988.
3. *J.M.Jackson, R.L.Snell, P.T.P. Ho, A.H.Barrett*, Astrophys. J. , 337, 680, 1989.
4. *E.Krugel, H.Steppe, R.Chini*, Astron. Astrophys., 229, 17, 1990.
5. Y.*Taniguchi, O.Kameya, N.Nakai*, in «The Interstellar Medium in External Galaxies», ed. D.J. Hollenbach and H.A. Thronson Jr. (NASA Conf. Publ. No 3084), p. 56, 1990.
6. *R.Chini, E.Krugel, H.Steppe*, Astron. Astrophys., 255, 87, 1992.
7. *P.Biermann, J.N.Clarke, K.J.Fricke*, Astron. Astrophys., 75, 19, 1979.
8. *J.R.Fisher, R.B.Tully*, Astrophys. J. Suppl. Ser., 47, 139, 1981.
9. *I.F.Mirabel, A.S.Wilson*, Astrophys. J., 277, 92, 1984.
10. *J.M.Jackson, A.H.Barrett, J.T.Armstrong, P.T.P.Ho*, Astron. J., 93, 531, 1987.
11. *I.F.Mirabel, D.B.Sanders*, Astrophys. J., 335,104, 1988.

12. *J.-M.Martin, L.Bottinelli, M.Dennefeld, L.Gouguenheim*, Astron. Astrophys., 245, 393, 1991.
13. *R.A.Kandalian, J.-M. Martin, L.Bottinelli, L.Gouguenheim*, Astron. Astrophys., in press, 1995.
14. *R.A.Kandalian, J.-M.Martin, L.Bottinelli, L.Gouguenheim*, The 11th IAP meeting "The Interplay Between Massive Star Formation, the ISM and Galaxy Evolution", Paris, 1995.
15. *C.J.Lonsdale, G.Helou, J.C.Good, W.Rice*, Catalogued Galaxies and Quasars Observed in the IRAS Survey, Jet Propulsion Laboratory, Pasadena, 1985.
16. *B.T.Soifer, D.B.Sanders, B.F.Madore, G.Neugebauer, G.E.Danielson, J.H.Elias, C.J.Lonsdale, W.L.Rice*, Astrophys. J., 320, 238, 1987.
17. *G.Paturel, P.Fouqué, L.Bottinelli, L.Gouguenheim*, «Catalogue of Principal Galaxies», 1989.
18. *W.C.Keel, E.T.M. van Soest*, Astron. Astrophys. Suppl. Ser., 94, 553, 1992.
19. *J.M.Mazzarella, T.A.Boroson*, Astrophys.J. Suppl. Ser., 85, 27, 1993.
20. *D.B.Sanders, N.Z.Scovile, B.T.Soifer*, Astrophys. J., 370, 158, 1991.
21. *B.T.Soifer, L.Boehmer, G.Neugebauer, D.B.Sanders*, Astron. J., 98, 766, 1989.
22. *C.G.Tinney, N.Z.Scoville, D.B.Sanders, B.T.Soifer*, Astrophys. J., 362, 473, 1990.
23. *J.S.Young, S.Xie, J.D.P.Kenney, W.L.Rice*, Astrophys. J. Suppl. Ser., 70, 699, 1989.
24. *I.F.Mirabel, D.B.Sanders*, Astrophys. J., 340, L35, 1989.

АСТРОФИЗИКА

ТОМ 38 НОЯБРЬ, 1995 ВЫПУСК 4

PERSPECTIVES OF THE ROT 54/32/2.6 IN ASTRONOMY

J.M.MARTIN, C.ROSOLEN

ARPEGES, Observatoire de Paris-Meudon-Nançay,
Pl. J. Janssen, F-92195 Meudon cedex, France

Perspectives for the Radio-Optical-Telescope 54/32/2.6 are given for the scientific research in radioastronomy. Its characteristics and potential scientific fields are summarized in the frame of the present french-armenian collaboration. A 3-phase upgrade plan including a detailed technical evaluation of the antenna is presented.

1. *Introduction.* The Radio-Optical-Telescope 54/32/2.6 (ROT) is located in Orgov (Armenia) and has been operated for the first time in 1986 [1]. Since this is one of the largest millimeter radiotelescopes of the world, the ROT can be a scientifically productive instrument if it is upgraded and made available to the astronomy community.

A preliminary technical evaluation of its characteristics has started in October 1994 with the visit of the Institute of Radiophysics Measurements (Prof. P. Herouni) and of the Byurakan Observatory (Dr. A. Petrossian) by J.-M. Martin and C. Rosolen [2].

2. *The ROT and some radiotelescopes which are available to french astronomers in the world.*

2.1. *The ROT:*

- useful diameter : 32 meters
- surface accuracy : 70/100 μm ==> working wavelength : λ = 30 mm — 3 mm (2 mm)
- site relatively dry in the mountain
- low background radio-noise and also the antenna is well protected against radio interferences.

2.2. *French radiotelescopes:*

- IRAM (Veleta):	30 m,	λ = 3 mm — 1 mm
- IRAM (Bure):	5 x 15 m,	λ = 3 mm — 1 mm
- NANCAY (NRT):	200 x 35 m,	λ = 22 cm — 9 cm

2.3. *Main single-dish radiotelescopes used by french astronomers:*

Name	Diameter	Typical working wavelength
SEST (ESO, Chile)	15 m	3 mm — 1 mm
JCMT (Hawaii)	15 m	mm/up to 0.5 mm
KITT PEAK (USA)	20 m	1 cm — 3 mm
ONSALA (Sweden)	20 m	1 cm — 3 mm
NRO (Japan)	45 m	3 cm — 3 mm
NRAO (Green Bank, USA)	43 m	up to 1 cm
EFFELSBERG (Germany)	100 m	50 cm — 6 mm
ARECIBO (USA)	300 m	50 cm — 3 cm
MEDICINA (Italy)	32 m	21 cm — 6 mm
PARKES (Australia)	64 m	50 cm — 3 cm
JODRELL BANK (UK)	76 m	50 cm — 5 cm
etc...		
Under construction :		
GBT (USA; 1998)	100 m	50 cm — 3 mm
Mexican-US antenna (2000?)	45 m	(sub?)millimeter
VLBI antennas (Russia; ?)	64 m	?

3. *Possible scientific fields for the ROT.*

- Cosmology : evolution of galaxies, physics of galaxies at large z; gravitational lenses, jets (VLBI).
- Physics of galaxies : gas and dust content, physical processes in galaxies, nuclear activity.
- Physics of our Galaxy : star forming regions, young stellar objects, molecular clouds.
- Evolved stars : OH/IR stars, C stars, evolution of the envelopes, variability.
- Pulsars (rather prospective) : spectra of extremely strong pulsars.
- Solar System : search of new molecules in comets and planetary atmospheres.

4. *How to work with the ROT?*

- Observation of large samples of objects : active galaxies, blue compact galaxies, evolved stars

==> large amount of telescope time needed.

==> collaboration with the Byurakan observatory and Orgov institute staffs needed.

==> New catalogues, new reference samples.

- Variability studies :
  * In continuum (quasars)
  * in spectroscopy (stars, clouds...)

  ==> long term projects.

  ==> also large amount of telescope time and collaborations are needed.
- VLBI : the ROT could be associated with the European VLBI network, to extend its u-v coverage.

5. *The ROT's upgrade is necessary.* Due to the very long stop of the telescope (1990-1995). For the upgrade to be done, 3 phases can be identified.

5.1. FIRST PHASE: 1995-1996

In order to obtain a good technical evaluation and expertise for the upgrade.

Started in 1995 with funds from Ministère des Affaires Etrangères and from the PICS n°147.

- collaboration between the Radiophysics Measurements Institute and the Byurakan Observatory
- correction of the main reflector
- pointing and guiding system of the radiotelescope
- hardware and software for the radiotelescope control
- tests and upgrade of the interfaces
- 1 cm receiver
- tests of the complete instrument
- measurements on radiosources in order to determine the efficiency, pointing accuracy, stability, etc...
- decision to start phase 2.

5.2. SECOND PHASE: 1996-1997

According to the measurements done in phase 1.

- detailed definition of the technical improvements, according to the scientific and cost requirements. (working wavelentgh, receivers)
- evaluation of the global conditions for the scientific exploitation in the future
- collaboration with other countries
- identification of the main scientific programs

- fundings, official agreements, etc...
- decision to start phase 3.

5.3. THIRD PHASE: 1997-1998

- Upgrade of the radiotelescope *according to* phase 2.
- construction of the receivers
- preparation of the scientific programs, scientific collaborations, fundings...
- implementation of the data-analysis system
- organisation of the local staff and of the scientific commities
- start of operations.

6. *Conclusion.* With a strong collaboration between the Institute of Radiophysics Measurements and the Byurakan Observatory, the upgrade of the ROT would provide to the armenian and international astronomical communities a very interesting and powerful radiotelescope. The ROT should be dedicated to long term scientific projects, which could involve complementary observational work done with the Byurakan Observatory 2.6m telescope.

ПЕРСПЕКТИВЫ РОТ 54/32/2.6 В АСТРОНОМИИ

Ж.М.МАРТИН, К.РОЗОЛЕН

Изложены перспективы радио-оптического телескопа 54/32/2.6 для научных исследований в радиоастрономии. Кратко описаны его характерироситики и потенциальные научные области применения в рамках настоящего франко-армянского сотрудничества. Представлен план восстановления в три этапа, включая детальную техническую оценку антенны.

REFERENCES

1. *P.Herouni*, 1989, in the Sixth International Conference on Antennas and Propagation ICAP 89, Conf. Pub. N. 301
2. *J.M.Martin, C.Rosolen*, 1994, Report "Mission en Arménie, du 13 au 20 octobre 1994".

АСТРОФИЗИКА

ТОМ 38 НОЯБРЬ, 1995 ВЫПУСК 4

A SEARCH OF ENVIRONMENTAL EFFECTS ON THE PHYSICAL CHARACTERISTICS OF GALAXIES IN GROUPS

A.P.MAHTESSIAN[1], V.H.MOVSESSIAN[1],
E.Ye.KHACHIKIAN[1], H.TIERSCH[2]

1 Byurakan Astrophysical Observatory
2 University of Potsdam, Astrophysikalisches Institut, Potsdam, Germany

The characteristics of galaxies within the galaxy groups are investigated from point of view of the influence of the surroundings.

1. *Introduction.* The observed physical characteristics may be determined either by primordial conditions during the epoch of galaxy formation or by the influence of the surroundings after the formation of the galaxies. To get an insight into their formation and evolution the correlation between the observed physical characteristics of the galaxies and their surroundings should be investigated.

Mahtessian [1-4] investigated the characteristics of the galaxies depending on the surrounding density and the morphological content of the group using a sample of galaxy groups of Karachentsev [5]. It was found that the characteristic parameters of the galaxies are stronger correlated with the morphological composition of the group than with its density.

In this report an investigation of environmental influences on some physical characteristics of galaxies in galaxy groups, which have been identified by Mahtessian [4,6,7] is presented.

All galaxies which do not belong to these groups are assigned to the sample of single galaxies.

2. *Preparing the sample for the statistical analysis.* Our sample is limited by the distance (see [4,7,8]). Using H=100 km/s/Mpc the greatest distance is 80 Mpc and the smallest one is 3 Mpc.

The morphological types of the galaxies are taken from [14].

The Seyfert galaxies are taken from the catalogues [15] and [16].

The Markarian galaxies are taken from the catalogue [17].

3. *The dependence of the morphological content of the group, and the rela-tive number of Seyfert and Markarian galaxies on the number of galaxies within the group.* In paper [8] the dependence of the morphological content of the group on the number of member-galaxies within the group is investigated. It is shown that the percentage of the E and S0 galaxies grows, while the percentage of spirals of late types sharply drops along the sequence "single galaxies - double galaxies - galaxy groups". The percentage of early type spirals does not depend on the number of surrounding galaxies.

The dependence of the relative number of Seyfert and Markarian galaxies on the number of member-galaxies within the group is examined in papers [9] and [12]. It was found that the frequency of occurence of Sy1 and Sy2 galaxies in galaxy groups did not differ from the one in the sample of single galaxies, but the frequency of occurence of Sy3 (Liners) was statistically higher in galaxy groups than among the single galaxies.

The frequency of occurence of Sy1 and Sy2 galaxies does not differ in groups with different number of members. Only that of Sy3 grows from member-poor groups to member-rich ones.

The frequency of occurence of Markarian galaxies is statistically lower in galaxy groups than among the single galaxies. The frequency of occurence of Markarian galaxies decreases from member-poor groups to member-rich groups.

4. *The morphological content of the group as a function of group parameters.* The basis for the investigation of the correlation between the morphological content of the group and their parameters is a sample of galaxies which consists of at least five galaxies and no more than eighteen objects.

The investigated groups are divided into two subsamples according to the content of E and S0 galaxies being either smaller or greater than 40%. For these subsamples the mean density of the luminous matter, the velocity dispersion and the mean pairwise distances between the galaxies were calculated.

The statistical analysis shows that there are no significant statistical differences between the analogous parameters of the both subsamples of groups, with high and low relative number of E+S0 galaxies.

5. *The correlation between the characteristic parameters of a group from the availability of Seyfert and Markarian galaxies.* The availability of Seyfert galaxies as a function of group parameters is investigated in [9]. It is shown that the groups, which contain at least one Seyfert galaxy have in the mean signifi-

cantly larger velocity dispersion and smaller crossing time as compared with analogous quantities of groups without Seyferts.

The morphological content has obviously no influence on the existence of Seyfert galaxies in the groups. The group with and without Seyfert galaxies cannot be distinguished in this sense.

There is no correlation between mean pairwise distances and the availability of Seyfert galaxies in the groups.

The availability of Markarian galaxies as a function of group parameters is investigated in [12]. It was not found any obvious correlation between the velocity dispersion, the galaxy density within the group, the morphological content of the group, the crossing time and the availability of Markarian galaxies.

6. *Segregation of galaxies of different morphological types and luminosities or masses into groups*. The investigation of segregation of galaxies belonging to different morphological types and luminosity or mass in terms of their position relative to the centers of the groups and in terms of their peculiar radial velocities within the groups are presented in [10,11].

We investigate the groups of galaxies with from six to 18 members. In each of groups we are interested in the following transformation of the physical parameters of the galaxies:

a) The peculiar radial velocities within the group are devided to the dispersion of the velocities of the galaxies. The new parameter δV (thus obtained) will have in all groups a distribution with identical unit dispersion.

b) The distances of the galaxies to the geometric center of the group are devided to their mean values with respect to each group. The new parameter δRc (thus obtained) will have in all groups a mean value equal to unit.

After these transformations, all groups are collected together into a single unified group in which each galaxy occurs with its own new parameters δV and δRc.

Our investigation leads to the following conclusions:

The mean distances of the galaxies relative to the center of the groups gradually increase from elliptical to lenticular and spiral galaxies. However, galaxies classified as early or late type spirals are not distinguishable on the basis of this parameter.

The peculiar radial velocities of the elliptical, lenticular and spiral galaxies in the groups are statistically indistinguishable. However, spiral galaxies of early and late subtypes are distinguishable in terms of this parameter. The former subtype exhibit a smaller mean peculiar radial velocity than the latter subtype.

The most luminous and massive galaxies, on an average, are closer to the center of the group, while the faintest and lightest galaxies, are farther. The galaxies with intermediate luminosities or masses occupy an intermediate position.

The segregation of galaxies of different luminosity or mass in terms of their mean peculiar radial velocities manifests itself less strongly.

Acknowledgements. This research was supported by grant ESO C&EE No. A-04-069.

ВЛИЯНИЕ ОКРУЖЕНИЯ НА ФИЗИЧЕСКИЕ ХАРАКТЕРИСТИКИ ГАЛАКТИК В ГРУППАХ

А.П.МАГТЕСЯН, В.Г.МОВСЕСЯН, Э.Е.ХАЧИКЯН, Г.ТИРШ

Изучены физические характеристики групп галактик в зависимости от характеристик их окружения.

REFERENCES

1. *A.P.Mahtessian*, Soob. Byurakn. Obs., 53, 102, 1982.
2. *A.P.Mahtessian*, Abstracts of the Conference of young physicists, Yerevan, p. 96, 1983.
3. *A.P.Mahtessian*, Soob. Byurakan. Obs., 57, 13, 1985.
4. *A.P.Mahtessian*, Ph.D. thesis, Yerevan, 1989.
5. *I.D.Karachentsev*, Problemy kosm. fiz., 5, 201, 1970.
6. *A.P.Mahtessian*, Astrofizika, 28, 255, 1988.
7. *A.P.Mahtessian*, Soob. Byurakan. Obs., 65, 1992 (in press).
8. *A.P.Mahtessian, V.H.Movsessian, E.Ye.Khachikian, H.Tiersch*, Astron. Nachr., 316, 143, 1995.
9. *A.P.Mahtessian, E.Ye.Khachikian, H.Tiersch*, Astron. Nachr., 316, 1995 (in press).
10. *A.P.Mahtessian, V.H.Movsessian*, Astrofizika, 37, 301, 1994.
11. *A.P.Mahtessian, V.H.Movsessian*, Pisma v Astron. J., 21, 1995 (in press).
12. *A.P.Mahtessian, V.H.Movsessian, V.M.Mahtessian*, in preparation.
13. *M.J.Geller, J.P.Huchra*, Astrophys. J. Suppl. Ser., 52, 61, 1983.

14. *J.Huchra, M.Devis, D.Latham, J.Tonry,* Astrophys. J. Suppl. Ser., 52, 88, 1983.
15. *V.A.Lipovetsky, S.I.Neizvestny, O.M.Neizvestnaya,* Soob. Spec. Astrofiz. Obs., 55, 5, 1987.
16. *M.-P.Veron-Cetti, P.Veron,* ESO Scientific Report Nr 7, 1989.
17. *B.E.Markarian, V.A.Lipovetsky, J.A.Stepanian, L.K.Erastova, A.I.Shapovalova,* Soob. Spec. Astrofiz. Obs., 62, 5, 1989.

АСТРОФИЗИКА

ТОМ 38 НОЯБРЬ, 1995 ВЫПУСК 4

THE ESO NEARBY ABELL CLUSTER SURVEY (ENACS)

A.MAZURE, P.KATGERT, R.DEN HARTOG, A.BIVIANO, P.DUBATH, E.ESCALERA, P.FOCARDI, D.GERBAL, G.GIURICIN, B.JONES, O.LE FÈVRE, M.MOLES, J.PEREA, G.RHEE

Laboratoire d'Astronomie Spatiale, Marseille, France and Sterrewacht Leiden, Netherlands and Institut d'Astrophysique de Paris, France and Observatoire de Genève, Switzerland and Lick Observatory, Univ. of California, Santa Cruz, USA and Dipartimento di Astronomia, Università di Trieste, Italy and Royal Observatory, Edinburgh, UK and Dipartimento di Astronomia, Università di Bologna, Italy and DAEC, Observatoire de Paris, Universitè Paris 7, CNRS (UA 173), France and SISSA, Trieste, Italy and Nordita, Copenhagen, Denmark and Instituto de Astrofísica de Andalucía, CSIC, Granada, Spain and Department of Physics, University of Nevada, Las Vegas, USA.

A statistically reliable distribution of velocity dispersions free from biases and systematic errors for a sample of ACO clusters is obtained. This distribution is compared with other data and model predictions.

1. *Introduction.* The present-day distribution of cluster masses contains information about important details of the formation of large-scale structure in the Universe. In principle, the distribution of present cluster masses constrains the form and amplitude of the spectrum of initial fluctuations, via the tail of high-amplitude fluctuations from which the clusters have formed, as well as the cosmological parameters that influence the formation process. Recently, several authors have attempted to use either the distribution of cluster mass estimates, or of gauges of the mass (such as the global velocity dispersion, or the temperature of the X-ray gas) to constrain parameters in cosmological scenarios. For constraining the *slope* of the spectrum of initial fluctuations through the slope of the mass distribution, unbiased estimates of the mass (or of a relevant mass gauge) are required. The latter always require assumptions about either the shape of the galaxy orbits, the shape of tne mass distribution, or about the distribution of the gas temperature. Therefore gauges of the total mass that are based

on directly observable parameters, such as global velocity dispersions or central X-ray temperatures, are sometimes preferable. However, the use of such mass gauges also requires a lot of care. Global velocity dispersions, although fairly easily obtained, can be affected by projection effects and contamination by field galaxies.

More fundamentally, the velocity dispersion of the galaxies may be a biased estimator of the cluster potential (or mass) as a result of dynamical friction and other relaxation processes. In principle, the determination of the X-ray temperatures is more straightforward. However, temperature estimates may be affected by cooling flows, small-scale inhomogeneities, bulk motions or galactic winds. Also, temperature estimates of high accuracy require high spectral resolution and are therefore less easy to obtain.

To obtain useful constraints on the *amplitude* of the fluctuation spectrum, it is essential that the completeness of the cluster sample in the chosen volume is accurately known. The completeness of cluster samples constructed from galaxy catalogues obtained with automatic scanning machines is, in principle, easier to discuss than that of the ACO catalogue, which until recently was the only source of cluster samples. In theory, one is primarily interested in the completeness with respect to a well-defined limit in mass. In practice, cluster samples based on optical catalogues can be defined only with respect to richness, and the relation between richness and mass seems to be very broad. A further complication is that all optical cluster catalogues suffer from superposition effects, which can only be resolved through extensive spectroscopy. Cluster samples based on X-ray surveys do not suffer from superposition effects, but they are (of necessity) flux-limited, and the extraction of volume-limited samples with well-defined luminosity limits requires follow-up spectroscopy. The large spread in the relation between X-ray luminosity and X-ray temperature implies that, as with the optical samples, the construction of cluster samples with a well-defined mass limit from X-ray surveys is not at all trivial. We discuss here the distribution of velocity dispersions, for a volume-limited sample of rich ACO clusters with known completeness. The discussion is based on the result of our ESO Nearby Abell Cluster Survey which has yielded 5634 reliable galaxy redshifts in the direction of 107 rich, nearby ACO clusters with redshifts out to about 0.1. We have supplemented our data with about 1000 redshifts from the literature for galaxies in 37 clusters.

2. *The Southern ACO R≥1 Cluster Sample.* The ENACS was designed to establish, in combination with data already available in the literature, a database for a complete sample of $R \geq 1$ ACO clusters, out to a redshift of $z = 0.1$, in a solid angle of 2.55 sr around the SGP, defined by $b \leq -30$ and $-70 \leq \delta \leq 0$. For our sample we selected clusters which at the time either had a known spectroscopic redshift $z \leq 0.1$,

or which had $m_{10} \leq 16.9$. Judging from the m_{10}-z relation the clusters with $m_{10} \leq 16.9$ should include most of the $z \leq 0.1$ clusters. With this selection, the contamination from $z > 0.1$ clusters would clearly be non-negligible due to the spread in the m_{10}-z relation.

At present, after completion of our project and with other new data in the literature, the region defined above contains 128 $R \geq 1$ ACO clusters with a measured or estimated redshift $z \leq 0.1$. A spectroscopically confirmed redshift $z \leq 0.1$ is available for 122 clusters, while for the remaining 6 a redshift ≤ 0.1 has been estimated on the basis of photometry.

We have first shown that the 128 clusters form a sample that can be used for statistical analysis. We have estimated the completeness of our cluster sample with respect to redshift from the distribution of the number of clusters in 10 concentric shells, each with a volume equal to one-tenth of the total volume out to $z = 0.1$. It appears that the sample of 128 clusters has essentially uniform density, except for a possibnle ($\approx 2\sigma$) "excess" near $z = 0.06$, and an apparent "shortage" of clusters in the outermost bins. The "excess" is at least partly due to the fact that several of the clusters in the Horologium-Reticulum and the Pisces-Cetus superclusters are in our cluster sample.

3. *The estimation of the velocity dispersions.* For a determination of the distribution of cluster velocity dispersions, one must address several points. First, it is very important that the individual estimates of the global velocity dispersions are as unbiased as possible, as any bias may systematically after the shape and amplitude of the distribution. Before calculating the global velocity dispersion we have taken special care to remove fore- and background galaxies that cannot be members of the system on physical grounds. Leaving such non-members in the system will in general lead to an overestimation of the global velocity dispersion.

4. *Comparison with other data.* The main result is that our upper limit on the occurence of clusters with σ_V above 1200 km/s is mush more severe than any previous result for optical data, namely that the space density of such clusters is less than one in our survey volume of $1.8 \times 10^7\ h^{-3}\ Mpc^3$. It turns out that this is almost entirely due to our removal from the redshift data of those interlopers that can only be recognized on the basis of the combination of radial velocity and projected position within the cluster.

We compare also our result with distributions of the cluster X-ray temperature T_X. It transforming the T_X scale into σ_V scale we assumed that $\sigma_V^2 = (kT_X/\mu m_H)$, where μ and m_H have theire usual meaning. The agreement is excellent for σ_V above 800 km/s. Both the amplitude and the slope agree very well, and to us this suggest that the removal of interlopers is necessary, and that our removal procedure is adequate. It also suggests that the velocity dispersions in excess of 1200 km/s, found by others, must indeed almost all be overestimates caused by interlopers. Interestingly, the two results start to diverge below ≈800 km/s. Although one cannot claim that $n(>T_x)$ is very well determined in that range there is at least no contradiction with the remark that our $n(>\sigma_v)$ must start to become underestimated below ≈800 km/s as a result of the richness limit of our cluster sample.

The extremely good agreement between our $n(>\sigma_v)$ and the $n(>T_x)$ for σ_v above 800 km/s and for an assumed value of $\beta = \sigma_v^2 / (kT_x / \mu m_H) = 1$ strongly suggests that X-ray temperatures and velocity dispersions statistically measure the same cluster property. On the basis of the data we conclude that the *average* value of β must lie between 0.7 and 1.1.

5. *Comparison with selected model predictions.* Our result confirms previous conclusions that the distributions of the velocity dispersions or masses of rich clusters do not support $\Omega = 1$ CDM models with low values of the bias parameter. The high values of the bias parameter, that one infers from the comparison are in conflict with the results for the normalization of the $\Omega = 1$ CDM models on larger scales, from comparisons with e.g. the COBE data.

The important conclusion is therefore that, for σ_v above 800 km/s our observed distribution $n(>\sigma_v)$ provides a very powerful constraint for cosmological scenarios of structure formation. It will not be too long before detailed predictions based on the currently fashionable (or order) alternative scenarios (be it low-density, titled-spectrum, vacuum-dominated or neutrino-enriched CDM) can be compared, in a proper way, to the observational constraints. Even though it is worthwhile to try and obtain unbiased estimates of $n(>\sigma_v)$ for σ_v below 800 km/s, it would seem that the high $-\sigma_v$ tail of the distribution has the largest discriminating power.

6. *Conclusions.* We have obtained a statistically reliable distribution of velocity dispersions which, for σ_v above 800 km/s, is free from biases and systematic errors.

The observed distribution $n(>\sigma_v)$ offers a reliable constraint for cosmological scenarios, provided model predictions are based on line-of-sight velocity dispersions for all galaxies inside the turn-around radius and inside a projected aperture of $1.0h^{-1}$ Mpc, and provided the clusters are selected according to a richness limit that mimics the limit that defines the observed cluster sample.

The sample of ACO clusters with $|b| > 30$, $C_{ACO} \geq 50$ and $z \leq 0.1$ is ≈85% complete. We find that the density of clusters with an apparent richness $C_{ACO} \geq 50$ is $8.6 \pm 0.6 \times 10^{-6}$ h^3 Mpc^{-3}.

The space density of clusters with σ_v above 1200 km/s is less than 0.54×10^{-7} h^3 Mpc^{-3}. This is in accordance with the limits from the space density of hot

X-ray clusters. From the good agreement between $n(>\sigma_v)$ and $n(>T_X)$ we conclude that $\beta = \sigma_v^2 / (kT_X/\mu m_H) \approx 1$ and that X-ray temperature and velocity dispersion are statistically measuring the same cluster property.

For the low values of the bias parameter ($b \approx 1.0$) that are implied by the large-scale normalization of the standard $\Omega = 1$ CDM scenario for structure formation this model appears to predict too many clusters with high velocity dispersions. Approximate agreement between observations and the $\Omega = 1$ CDM model can be obtained for bias parameters in the range 2 to 3.

ОБЗОР ESO БЛИЗКИХ СКОПЛЕНИЙ ЭЙБЕЛЛА

А.МАЗУР, П.КАТТЕРТ, Р. ДЕН ХАРТОГ, А.БИВИАНО. П.ДУБАТ, Е.ЭСКАЛЕРА, П.ФОКАРДИ, Д.ЖЕРБАЛ, Дж.ДЖИУРИЧИН, Б.ДЖОНС, О. ЛЕ ФЕВР, М.МОЛЕ, Дж.ПЕРЕА, Г.РИ

Для выборки АСО скоплений получено статистически надежное распределение дисперсий скоростей, свободное от отклонений и систематических ошибок. Это распределение было сравнено с другими данными и модельными предсказаниями.

АСТРОФИЗИКА

ТОМ 38 НОЯБРЬ, 1995 ВЫПУСК 4

ON THE INTERNAL STRUCTURE OF SUPERMASSIVE COMPACT CELESTIAL BODIES

G.T.TER-KAZARIAN, K.L.YERKNAPETIAN

Byurakan Astrophysical Observatory, Armenia 378433.
E-mail address: byur@mav.yerphi.am

The conceptual part of the physics of baryonic protomatter and the alternative approach to understanding of the internal structure of highly compact stationary supermassive celestial bodies have been previously suggested in [1-5]. There are a number of advantages to this approach, which differs in principle from the standard black hole accretion models and is in good agreement with the observational data from active galactic nuclei. In order to be more consistent and convinced in the correctness of previously drawn statements, in our research it has been advantageous to verify them by expansion of the basic ideas with the appropriate and consistent theoretical constructions backed up by detailed numerical studies of the models, which are physically more realistic, with the spherical-symmetric distribution of matter in many-phase stratified states. Multiple integrations in the aftermath prove the validity of the previous physical scenario and correctness of drawn statements that *the process of inner distortion of the space-time continuum just serves as the eligible mechanism counteracting to collapse.*

1. *Background and Significance.* There is a sufficiently large number of observational data in astrophysics, which prove the presence in the Universe of highly compact supermassive formations existing in the stable stationary state for a long time compared to the age of the Universe. In spite of the considerable progress achieved over the last twenty years in astrophysics in regard to the extensive program of systematic surveys of those well-defined celestial sources of immense power of radiation, our understanding of their internal constitution and environment close to their cores still remains far from being complete. Moreover, we are only at the very beginning of a deeper understanding of the physical properties of supervenes matter, which are uncertain by now and there is still a long way to go.

The most important astrophysical phenomenon such as active galactic nuclei (AGN's) with super-Eddington luminosity has been in central part of those investigations, since they display most clearly the nonthermal behavior that is believed to exist in their cores. Over the entire subsequent period the standard black hole accretion models have became a generally acceptable paradigm as the view on those objects. The fact that accretion processes really take place in AGN's seemed to be proven for certain by many observations. But with in respect to standard models, one should note that this approach to understanding of physics of superdense equilibrium configurations based on the main idea of black holes suffers from some grave shortcomings and it can no longer support itself against the inner inconsistency from the theoretical point of view as well as astrophysical observations. First among them: the fate of collapsing sphere, with respect to the proper coordinate system that is being used, remains indefinite. The theory breaks down inside the black hole, where static observers cannot exist, because they are inexorably drawn into the central singularity. Then, it is impossible to calculate corresponding integral characteristics of the supermassive objects. But the main deficiency is the fact that the observed time-scale for flux variations of some AGN's are inconsistent with contemporary black hole accretion models. That is, on the base of the diagram of the minimum variability time-scale against the bolometric luminosity of 60 sources (AGN's) it has been shown that a few BL Lac objects -B2 1308+72,3C 66A, OJ 287, AO 02335+16 and quasars - 3C 345, 3C 446, 3C454.3, LB 9743 remained in forbidden zone (particularly the initial three of them). Therefore, the creation of the new viable theoretical constructions to overcome all these shortcomings and for the explanation of an abundant spectra of observational data is the problem of paramount significance.

As a matter of fact during increasing the mass of configuration, it achieves (irrespective of the gravitational theory which is being used) the critical turning point beyond which the gravitational forces of compression become dominant (a stage of relativistic collapse). Moreover, it is enough to add from the outside a small amount of energy nearby the critical point in order to begin a process of irresistible infinite catastrophic compression of configuration under the pressure of grand forces. The big problem as it was seen at the outset was how to get a concrete mechanism for the supermassive objects, which could provide a proportional increase of internal pressure of degenerate Fermi gas with the sharp increase of the gravitational forces . Only due to the validity of hydrostatic equilibrium, the supermassive formation really could remain in the stable state for a long time, even up to the limit of masses much greater than solar mass.

2. *Preliminary Studies*. The novel viewpoint came up recently to overcome the above-mentioned difficulties of the contemporary theory [1-5], where outlined the main principles of an alternative approach to understanding of internal structure of stationary supermassive cosmic objects. A simple way of effecting a reconciliation is

to assume that the considerable changes of the properties of the space-time continuum take place in the density range above nucleus, that is at short distances below some length scale is about 0.4fm. This hypothesis, which actually needs in further confirmation, seemed could lead to substantial impact on progress in considered field. This idea comes from the theory of distortion of space-time continuum [5-7], in which a perception of space and time has been suggested by means of new concepts. While the problems and dynamics of the processes, which are of the interest of Special and General Relativity, Quantum Field Theory have been studied from a specific novel point of view. The spatial-time concepts have been properly substituted by the appropriate new ones. The general theory of distortion of the space-time continuum has been suggested, which predicts the new important phenomena existing below the threshold length scale. Two regimes are distinguished: First one is the curvature of the space-time continuum, which is considered as the familiar regime of distortion and leads to the new gravitational theory. The latter is in good agreement with the general relativity up to the limit of neutron stars. But this theory should begin to manifest its virtues around the threshold length, where the second regime should be switched on. Second regime is a quite new one, which is called *the inner distortion of the space-time continuum* (IDST). At the short distances equal or less than 0.4fm, along with many other processes, in particular, the considerable changes of the space-time continuum take place, the metric undergoes the phase transition of second kind, and as a direct consequence of it the matter, which is found in this continuum also undergoes the phase transition of second kind. Each particle goes off from the mass shell. The shift of mass at rest, the energy-momentum spectra of the particles upwards along the energy scale took place. *The new phase state of matter, which is found in the inner distorted space-time continuum, we called a protomatter.* The study of these processes and the laws of phase transitions is the main subject of suggested theory, which is of decisive importance for more deeper understanding of the physics of superdense matter. Latter will have to be considered anew and will have to be adjusted to fit this novel viewpoint. To facilitate our altered approach it seems well to present below some formal matters which one will have to know in order to understand the structure of theory. So far as displayed at short distances new phenomena relate directly to IDST, they hold irrespective to concrete model of configuration. This allows oneself to carry out -the numerical calculations in the most simple case of equilibrium one-component configurations of degenerate ideal neutron gas in presence of one-dimensional space-like inner distortion of space-time continuum. It has been shown, that *due too IDST in the central region of superdense core of neutron protomatter, the internal pressure rises proportional with sharp increase of gravitational forces of compression in near* *about 18-20 order of magnitude with respect to the central pressure of neutron star. This counteracts the catastrophic compression of central region. Hence, the stable equilibrium remains valid in outward layers too, even up to the limit of masses much greater than solar mass. As the models of AGN's one has considered the configurations consisting of such cores surrounded by accretion disks. The principle difference from standard models is the fact that central cores are in stable equilibrium state with the certain radial distribution of density and pressure of matter, and a number of integral characteristics. The important effect of metric singularity cut-off has been established, due to which the metric singularity ceased to be significant no longer. The rigorous restriction on the upper limit of possible values of the total masses of equilibrium configurations is obtained ($M \lesssim 3.5\times10^{9}M$), which is in good agreement with the observational data from AGN's. It seems that a decisive significance has the metric singularity cut-off effect for the BL Lac objects OJ 287, 3C 66A and B2 1308+32, hence their observed sizes are less than the sizes of corresponding spheres of even horizon.* This may serve as a strong indication that suggested approach is preferable to the standard models.

3. *Research Design and Methods.* The foregoing theory involves a drastic revision of our ideas of space and time and structure of superdense cores of suppermassive celestial bodies. In order to be more consistent and convinced in the correctness of previously drawn statements, in our research it would be advantageous to verify them by appropriate expansion of the basic ideas to models, which are physically more realistic, with the spherical-symmetric distribution of matter in many-phase stratified states. The layering of considered configurations is a consequence of the onset of different regimes in the equation of state. We consider the most general configurations of two classes. They including the same shells, which are made of cold catalyzed matter formed after nuclear burning in the density range below neutron drip $\rho_{dr}=4.3\times10^{11}$ gcm^{-3}. The latter is consisted of surface ($\rho\leq10^{6}\,gcm^{-3}$), of outer crust ($10^{6}\,gcm^{-3}\leq\beta<\rho_{dr}$) and inner crust . This is made of separated nuclei in β equilibrium with the electron gas. The pressure is dominated by degenerate electrons that become fully relativistic above b. A considerable amount of those nuclear composition is changing along the radial direction step-by-step away from the state of lowest energy up to more neutron-rich larger nuclei depending of the pressure of relativistic electrons, which combine with bound nuclear protons to form neutrons (inverse β - decay). Increasing the density above ρ_{dr} leads more free neutrons emerge in a medium, until nuclei dissolve by merging together. It is well known that the nuclear matter at high density range above nucleus still remained not so well understood. A large number of representative models for the nuclear equation of state are available in literature, but they

all are subject to many uncertainties, including such exotic processes as a neutron and proton superfluidity, a pion condensation, a phase transition to quark matter and so on. For the simplicity, above the density $4.54\times10^{12}\mathrm{gcm}^{-3}$ the first class configurations are now thought to be composed of two phases of ideal cold n-p-e gas. The latter is a mixture of neutrons, protons and electrons in complete inverse β – decay equilibrium. The first phase state covers the intermediate density domain $4.54\times10^{12}\mathrm{gcm}^{-3} \leq \rho<\rho_d=2.617\times10^{16}\mathrm{gcm}^{-3}$, which is the regular n-p-e gas in absence of IDST. The second phase state is the n-p-e protomatter above the density $\rho\geq\rho_d$ with short distances between the nucleons $r_{NN}\leq0.4\mathrm{fm}$ *in* the presence of IDST. This regime needs in a special theoretical study. For the second class configurations we consider an onset of melting down of hadrons at the density about $\rho_{fl}=4.09\times10^{14}\mathrm{gcm}^{-3}$. to which the nucleon-nucleon distances $r_{NN}\leq1.6fm$ are corresponded, and nuclear matter consequently turns to quark matter. In the domain of $\rho_{fl}\leq\rho<\rho_{as}=m_n(0.25\mathrm{fm})^3=1.072\times1017\mathrm{gcm}^{-3}$ where m_n neutron mass at rest, 0.25fm is the string thickness, we should consider two phase states of string flip-flop regimes:

1) the regular string flip-flop at the densities $\rho_{fl}\leq\rho<\rho_d$ (to which the distances $0.46\mathrm{fm}<r_{NN}\leq1.6\mathrm{fm}$ are corresponded) and the IDST is absent. There is a kind of tunneling effect in which the strings stretch themselves violating energy conservation, and after touching each other they switch to the other configuration.;

2) the string flip-flop regime in presence of IDST at the densities $r_{fl}\leq r<r_{as}$ or distances $0.25\mathrm{fm}<r_{NN}\leq0.4\mathrm{fm}$. That is, the system is made of the quark protomatter in complete b - equilibrium with rearrangement of string connections joining them. Here we concerned with the individual particle approximation (Hartree approximation). The Hartree potential is almost linearly proportional to the string length. The Y shape string is the most convenient for the calculation, just because the center of it almost coincides with the gravity center. The medium is made of the fully relativistic quarks of *u, d, s* flavors, in complete b - equilibrium. Finally, at the densities above the r^3r_{as} the system is made of the quarks in one bag, in complete b - equilibrium under the weak interactions, and gluons including the effects of Quantum Chromodynamics (QCD) perturbative interactions in the presence of IDST. The QCD vacuum is generally believed to have a complicated structure is intimately connected to the glue-glue interaction. The confinement of quarks is a natural feature of the exercising a pressure on the surface of the local region of the perturbative vacuum to which quarks are confined. This is just the main idea of bag model: the quarks are assumed to be confined in a bag and the stability of the hadron is ensured by the vacuum pressure and the surface tension. Due to the screening of strong forces, the quark field is considered to be free inside the bag and to interact strongly only in the surface region.

The surface energy is estimated to be proportional to quark density. The medium is made of quark protomatter in overall color singlet ground state, which can be considered as the non-interacting relativistic Fermi gas found in the inner distorted spacetime continuum. The last two domains need in special theoretical treatment. In achievement of the major specific goal of our approach, with the appropriate and consistent theoretical constructions backed up by detailed numerical studies, we have justified the previously drawn statements in the case of considered above modified realistic models of superdense configurations.

Each configuration is defined by two parameters of central values of concentration of particles and the inner distortion field. Hence the central value of gravitational potential is being found by means of multiple integrations through with the subsidiary sewing condition of smoothness of matching of internal and external geometries.

Multiple integrations in the sequel prove the validity of the previous physical scenario, and convince us in the correctness of drawn statements. The all obtained previously results concerning to the integral characteristics of AGN's really have high enough accuracy. That is the modification of the models in the sense of form of state equation actually could not lead to the perceptible corrections in the domain of AGN's. Meanwhile we proved the validity of already cleared up physical scenario, according to which the process of IDST just serves as the eligible mechanism counteracting to collapse.

4. Beyond Geometry and Particles. One final observation is worth recording. All research works presented above, in fact, are only some part of more extensive program, the major goal of which is to achieve at last the consistent high energy physics. Certainly, the principle problems of the physics of superdense matter could not be solved separately, without consistent high energy physics. In view of all this, as the first stage, the fundamental question that guides our discussion in the theory of goyaks (goyak in Armenian means an existence ; an existing structure. This term has been firstly used in [6]) [8,9] is how did the geometry and particles come into being? To explore this query the theory of goyaks reveals primordial deeper structures underlying fundamental concepts of contemporary physics. It address itself to the primecause of origin of geometry and basic concepts of particle physics, such as the fundamental fields with the spins and various quantum numbers, internal symmetries and so forth; also basic principles of Relativity, Quantum, Gauge and Color Confinement, which, as it was proven, all are derivative and come into being simultaneously. The substance out of which the geometry and particles are made is the set of new physical structures-the goyaks, which are involved into reciprocal linkage establishing processes. It is appropriate to turn to them as the primordial deeper structures.

The most promising aspect of our approach so far is the fact that many of the important anticipated properties, fundamental concepts and principles of particle physics are appeared quite naturally in the framework of suggested theory. In pursuing the original problem further we have elaborated a new mathematical framework, which is, in fact, a still wider generalization of familiar methods of secondary quantization with appropriate expansion over the geometric objects.

One interesting offshoot of this generalization directly leads to the formalism of operator manifold, which, consequently yields the quantization of geometry. This approach differs in principle from all earlier studies. The theory of goyaks predicts a class of possible models of internal symmetries, which utilize the idea of gauge symmetry and reproduce the known phenomenology of electromagnetic, weak and strong interactions. In order to save writing in [8,9] we guess it worthwhile to leave the other concepts such as the flavors and so forth with associated aspects of particle physics for the further publications. Surely this is an important subject for separate research. Here we focused our attention mainly on developing the mathematical foundations for our viewpoint. Hence our discussion has been rather general and abstract. Of course, much remains to be done for a larger contribution into the particle physics. However, we believe that the more realistic final theory of particles and interactions can be found within the context of the theory of goyaks. We hope that all these seminal works would entail support of the large number of researchers from all over the world.

ВНУТРЕННЕЕ СТРОЕНИЕ СВЕРХМАССИВНЫХ КОМПАКТНЫХ НЕБЕСНЫХ ТЕЛ

Г.ТЕР-КАЗАРЯН, К.ЕРКНАПЕТЯН

Концептуальная часть физики барионного протовещества и новый подход к пониманию внутреннего строения сверхплотных, сверхмассивных стабильных небесных тел, первоначально были предложены в [1-5]. Этот подход принципиально отличается от стандартных моделей черных дыр и хорошо согласуется с результатами наблюдений Активных Галактических Ядер. Для последовательности и проверки первоначальных выводов исследованы физически более реалистические модели устойчивых сверхмассивных конфигураций теоретическими и численными методами. Результаты подтверждают, что процесс внутреннего искажения прост-

ранства-времени действительно является приемлемым механизмом, противодействующим коллапсу.

REFERENCES

1. *G.Ter-Kazarian*, Dokl.Akad.Nauk, SSSR, 309,No1, 97, 1989.
2. *G.Ter-Kazarian*, Astrophysica, 31, No2, 345-358, 1989.
3. *G.Ter-Kazarian*, Astrophysica, 33, No1, 143, 1990.
4. *G.Ter-Kazarian*,1991, Astrophysica, 33, No2, 401, 1991.
5. *G.Ter-Kazarian*, Astrophysics and Space Sci., 194, No1, 1, 1992.
6. *G.Ter-Kazarian*, "Selected Questions of Theoretical and Mathematical Physics", VINITI, N5322-B86, Moscow, 61, 1986.
7. *G.Ter-Kazarian*, Comm.Byurakan Obs., No62, 1, 1989.
8. *G.Ter-Kazarian*, I.C.T.P. Preprint, Trieste, Italy IC/94/290, 1, 1994.
9. *G.Ter-Kazarian*, hep-th/9510110 , 1995 (revised version of [8]), submitted to Int'l J. of Theor. Phys.

АСТРОФИЗИКА

ТОМ 38 НОЯБРЬ, 1995 ВЫПУСК 4

SOME SIMILARITIES OF EXPANSION PHENOMENA IN THE VICINITY OF THE EARTH AND IN THE UNIVERSE AS A WHOLE

H.A.HARUTYUNIAN

Byurakan Astrophysical Observatory, Armenia

Some expansion phenomena in the immediate vicinity of the Earth and their influuence on the Earth's angular momentum are considered. It is pointed that the tidal mechanism which is traditionally used to explain the lunar retreat is actually unfounded. These expansion effects are compared with Hubble expansion of the Universe and their similarity is shown. A way for the solution of the lunar retreat paradox is suggested using the tidal effects and Hubble expansion combined. An increase of the Earth-Sun distance is predicted and the rate of this removal is estimated.

1. *Introduction.* A vast quantity of observational data available at present time makes very difficult to orient oneself in it. In this situation a lot of hypotheses appear with a purpose to explain the formation and evolution of cosmic objects. All of these hypotheses and corresponding theories are based on the observational data which are widely accepted or at least on their suitable part. For most of them the discovery of the galaxy recession law [1] serves as a decisive factor till nowdays. On the other hand the simplest physical interpretation of the Universe expansion has brought to the idea of Big Bang. The microwave background radiation discovered later was taken for the predicted by the theory relict radiation and became a corner-stone in the physical picture of Big Bang cosmology.

However the existence of some uncertainties in the description of initial physical conditions as well as the appearance of new and more precise observational data in the last decades made the fundamental idea of the grand explosion and the theories based on it vulnerable. In this connection one can refer to the paper by Burbidge [2] as one of the firsts, in which it is confirmed, that the evidence in favour of a Big Bang cosmology is much less definite than is widely realized. The need to coordinate the theories with observational data compels some authors to take under the doubt even the validity of the application of Doppler principle for the interpretation of redshift in the spectra of galaxies. Therefore some other physical mechanisms connected with conceptions of a steady-state Universe and almost forgotten at present time are regenerating periodically (e.g. [3]). Other cosmological models suggest something between Big Bang and steady-state Universe, trying to find new ways for more realistic interpretation of data (e.g. [4] and references therein).

The main purpose of this paper is to call attention on some observational facts connected with expansion phenomena which have not been discussed seriously earlier or simply have been neglected. However these data exist and their importance becomes higher with the increase of the observational accuracy.

2. *Expansion phenomena in the vicinity of the Earth.* One of the most interesting and exiting expansion phenomena is connected with the increase of the radius of lunar orbit, which does not have a well founded explanation yet. The present rate of lunar retiring from the Earth obtained by lunar laser ranging is 3.82±0.07 cm/year [5] (compare also with the value 3.7±0.2 cm/year obtained less than one decade ago [6,7]). As a rule the effect of lunar retreat is explained by a tidal interaction between the Earth and Moon. It is accepted that as a result of such interaction the Moon takes away some portion of the Earth's angular momentum.

It is known, on the other hand, that the Earth rotation speed decelerates by about 1.7 ms per century [8]. Thus one can calculate the annual change of lunar orbit taking into account the conservation of the Earth-Moon system's angular momentum of inertia and Kepler's third law.

For a rotating homogeneous ball of radius R and mass M the angular momentum can be expressed in the following form

$$I = \frac{4\pi}{5}\frac{MR^2}{T} \tag{1}$$

where T is the period of rotation. If a more realistic model of Earth interior is used, one can find a similar expression, which differs from the given by a factor of about 0.8. Usually it is considered that the ratio of the Moon's orbital momentum

$$I_M = 2\pi\frac{ma^2}{p} \tag{2}$$

(where m, a and p are the mass, orbital radius and rotation period respectively) to the Earth's spin angular momentum is equal to 4.83 [9], which corresponds to the value of above mentioned factor of about 0.83. Then if the Earth-Moon system is accounted to be an isolated one, we may write the following conservation law

$$0.83\frac{4\pi}{5}\frac{MR^2}{T}+2\pi\frac{ma^2}{p}+\frac{4\pi}{5}\frac{mr^2}{p}=\text{const} \tag{3}$$

where r is the radius of the Moon.

Further one can easily find that the third term at the left side of the given expression (3) is neglectibly small in comparison with the other two terms. Then a simple calculation shows, that even if the portion of the angular momentum lost by the Earth is completely passed to the Moon, it can provide an increase of lunar orbit radius only of about 3.0-3.1 cm per year.

It means that the tidal effects are unable to explain the rate of lunar removal. In the recent paper [10] this difficulty is remembered indirectly by the following note: "The average change in the length of the day over the past 2500 years is 1.7ms/cent. This is about 25 percent less than the change expected on the basis of tidal friction alone (2.3ms/cent)". This difficulty is not new but exists for a long time. It is worth to mention that with the times researchers contrive to decrease the necessary value of the Earth's rotation deceleration. On the other hand due to the simultaneous increase of measurements accuracy the observed value itself becomes lower. As to the rate of lunar retreat, it's measured value increases with higher accuracy of measurements complicating the situation as well. So the mentioned difficulties seem to be unsurmountable for the traditional mechanism of explanation.

We would like to refer to two other papers published respectively 20 and 10 years ago to show that nothing was changed in the understanding of the problem though the accuracy of measurements was highly increased. First of them asserts: "The total tidal acceleration of the earth is estimated to result in a 3.7ms/cy increase in the length of day. The most recent discussion of the ancient eclipse records indicates an observed increase in the length of day only 2.5ms/cy" [11]. The second one affirms approximately the same [12]: "Calculations show, that the basic part of the Earth deceleration, which is 3.5 ms per century, is caused by oceanic tides (actually the deceleration is less, about 2 ms per century so far as simultaneously an acceleration due to an unknown reason by about 1.5 ms per century occurs)". However such an explanation with "an acceleration due to an unknown reason" was adopted of course because of the lack of any better idea. By the way, one can find a very useful review on the difficulties of the tidal mechanism in [13].

3. *Expansion of the Earth.* For a long time, since the end of the last century, another phenomenon of expansion which was connected with an increase of Earth's

radius has been under consideration. A brief chronology of the establishment of this phenomenon one can find in Egyed's paper [14]. To be more correct it must be mentioned that there have been various hypotheses argueing the Earth's contraction and pulsation phenomena as well. However, as far as we know only the expansion hypothesis has obtained a quantitative confirmation. Egyed was the first who has suggested a method for immediate calculation of the possible change of Earth's radius [15]. Using palaegeographical data he has found a cumulative increase of this radius and estimated it to be 0.4-0.66 mm/year with average value of about 0.5 mm/year. Later the problem was discussed in more details from various points of view (see, [9,16-18]). As it was mentioned by Wesson there were about twenty estimates of the rate of increase of the Earth radius in 1973 which had showed an annual expansion rate of about 0.5-0.6 mm [19].

But, if the Earth's expansion effect is a reality, one can calculate the Earth rotation speed deceleration due to the radius increase itself. Using the expression (1) one can estimate the rate of the Earth's speed deceleration to be equal to 1.3 ms/century. On the other hand, if the existence of the Earth's expansion is adopted the mentioned difficulties for the explanation of lunar orbit increase by tidal effects grow into a catastrophe, because only a small value of angular momentum corresponding to the Earth's rotation deceleration rate of 0.4 ms/century remains to be passed to the Moon. That is one of the reasons why the effect of the Earth expansion is excluded from the consideration. Certainly it does not mean that tidal effects have not any influence on the deceleration of the Earth rotation speed and retreat of the Moon, but we may confirm at least that they have only a minor role.

At first sight the situation seems to be more complicated if the Earth's expansion effect is taken into account as well. Instead of the unsoluble problem of lunar orbit radius increase, we have one more.

4. *Comparison with the Universe expansion.* One of the most marvellous facts established by the astronomy of our century is undoubtedly the discovery of the Universe expansion law by Hubble [1]. And obviously any independent phenomenon which can be considered as directly or indirectly connected with the expansion of the Universe could be very important for understanding of the real essence of the observed phenomenon. Especially as nobody knows what is the true reason of the recession of galaxies.

As it is known the expansion of the Universe at least for moderate cosmological distances is described by the Hubble law

$$v = Hr \qquad (4)$$

where v is the recession velocity for a galaxy which is at the distance r and H is Hubble constant, which is estimated to be equal to 50-100 km/sec per Mpc.

It is easy to see, that one can interpret the relation (4) as a slow increase of the cosmological scale of distances (lengths). Then we may rewrite this law, at least in a first approximation, as follows:

$$r = r_0[1 + \varepsilon(t - t_0)], \tag{5}$$

where r_0 is the distance (length) between two points for an arbitrary choosen time moment $t=t_0$ and shows the increase of the unit length for the unit time (the Hubble constant). If one will use the Hubble parameter's value H=75 km/s per Mpc (see, [20-21]), then one can find

$$\varepsilon = 7.6 \cdot 10^{-11} \text{year}^{-1}. \tag{6}$$

Further, one can use the relation (5) to compare the expansion phenomena observed in the immediate vicinity of the Earth with that of the Universe. Undoubtedly this suggestion to use the Hubble expansion law for the vicinity of the Earth will meet an unfriendly attitude of cosmologists and will become a target of attacks by a part of them. That is inevitable because existing theories (which never took into account this phenomenon) do not allow such a method of approach. We will not consider this question in more detail here, because this is a point for a separate discussion. That is why we would like to present only the striking results of such comparison. In any case the facts exist and they must be interpreted and taken into account.

Let us at first calculate the Earth's radius change. Such calculation first has been done by MacDougall et al [22] and undeservedly forgotten. Taking the value of radius R=6378 km, we can easily find

$$\Delta R = 0.48 \text{ mm / yr} \tag{7}$$

which is in a good accordance with the value given by Egyed [15] and other authors (see, also [19]).

The change of lunar orbital radius due to this mechanism could be estimated as well. Using the same value of the parameter ε from (6), one can find, that the Earth-Moon distance increases by about 3 cm per year. It means, that the formula (5), rewritten from the Hubble law, gives for the lunar retreat rate the same value obtained as an upper limit provided by the tidal mechanism. But in this case in addition the part of the Earth's angular momentum corresponding to the planet's rotation deceleration rate of 0.4ms per century remains in the reserve. Simple calculations show that this value can provide a rate of lunar retreat of order 0.7-0.8 cm per year. So we find that the universal (Hubble) expansion and tidal mechanism effects together provide a result (3.7-3.8 cm per year) which is very close to the observational value.Then one can conclude, that three observed values (the Earth's radius annual increase, the Earth's rotation speed deceleration rate and the rate of lunar retreat) are in a good agreement with Hubble's law.

What does it mean? Such conformity between observed values cannot be a result of a pure chance. The probability of such coincidence is very small. Moreover with the increase of the accuracy of measurements agreement between the considered values becomes better. Then the more naturally conclusion could be one, which is in favour of the correctness of the formula (5) for the vicinity of the Earth.

This problem in our view has two main aspects for further discussion and investigations. First one is connected with the confirmation of reality of the mentioned universal expansion and the correction of the formula (5). The second one is connected with the interpretation of really existing phenomenon and investigation of its consequences.

In any case the mentioned expansion mechanism is one which gives a fruitful opportunity to explain both expansion phenomena in the immediate vicinity of the Earth and of the Universe as a whole.

5. *Discussion and conclusions*. There are at least three observational values, which are in a good quantitative accordance with the expansion of the Universe. Taking into account the fundamental significance of the suggested unversal expansion effect for the construction of a cosmological conception, it is necessary to discuss all available possibilities of verification of the phenomenon under the question. If the phenomenon exists really, as a result of some physical mechanisms it will undoubtedly exhibit itself in various physical regularities. One needs to find and study the objects or phenomena, where it can be discovered. Moreover, it is clear that such an insignificant effect, especially for moderate geometrical distances, could be found only in systems which are considered to be "steady-state" from the classical point of view.

For this purpose one can suggest our planetary system. Thus, the simplest way to check the correctness of the formula (5) is to examine the motion of the planets. One can easily find, for example, the changes of the planets' orbital radii using the formula (5) and then calculate from Kepler's third law the lengthenig of their revolution period. Such calculation for the Sun-Earth distance gives an increase of about 11.4 meter per year, and consequently the year must become longer by 3.6 ms/yr. For Uranus and Neptune one can obtain 18.3 km and 56.4 km for the orbital radii changes and the extension of the "year" - 25 sec and 1 min 49 sec per period.

The author wishes to thank Prof. V. Ambartsumian for many useful discussions and late Prof. G. de Vaucouleurs for reading of the first version of this paper and interest. I am grateful to the administration of the IAP which made possible my work in France and enrichment of this article by new data.

НЕКОТОРЫЕ АНАЛОГИИ МЕЖДУ ЯВЛЕНИЯМИ РАСШИРЕНИЯ В ОКРЕСТНОСТЯХ ЗЕМЛИ И ВО ВСЕЛЕННОЙ

Г.А.АРУТЮНЯН

Рассматриваются явления расширения, наблюдаемые в непосредственных окрестностях Земли, а также их влияние на изменение углового момента Земли. Показывается, что приливной механизм, традиционно используемый для объяснения удаления Луны от Земли, в действительности несостоятелен. Эти явления расширения сопоставлены с хаббловским расширением и показано, что они аналогичны с последним. Предложен метод для решения парадокса удаления Луны, для чего совместно применяются хабболовское расширение и приливной механизм. Предсказывается увеличение расстояния Земля-Солнце, а также оценивается скорость этого удаления.

REFERENCES

1. *E.Hubble,* Proc. Nat. Acad. Sci. USA, v.15, 29, 1929.
2. *G.Burbidge,* Nature, v.233, 36, 1971.
3. *P.A.La'Violette,* Astrophys. J., v.301, 544, 1986.
4. *F.Hoyl, G.Burbidge, J.V. Narlikar,* Astrophys. J., v.410, 437, 1994.
5. *J.O.Dickey et al,* Science, v.265, 482, 1994.
6. *X.X.Newhall, J.G.Williams, J.O.Dickey,* The Earth's Rotation and Reference Frames For Geodesy and Geodynamics, ed. A.K.Babcock, J.A.Wilkins, Kluwer, Dordrecht, 159, 1988.
7. *G.E.Williams,* J. Phys. Earth, v.38, 475, 1990.

8. *J.O.Dickey,* Highlights of Astronomy, ed. I.Appenzeller, v.10, 17, 1995.
9. *S.K.Runcorn,* Nature, v.204, 823, 1964.
10. Reports on Astronomy, Transactions of the IAU, v.XXIIA, p.183, Kluwer, Dordrecht, 1995.
11. *K.Lambeck, J.Geophys,* Res., v.80, 2917, 1975.
12. *M.Ya.Marov,* The Planets of the Solar System, Nauka, Moscaw, 1986 (in Russian).
13. *W.H.Munk, Q.J.Roy.* Astr. Soc., v.9, 352, 1968.
14. *L.Egyed,* Nature, v.197, 1059, 1963.
15. *L.Egyed,* Nature, v.178, 534, 1956.
16. *L.Egyed,* Nature, v.190, 1097, 1961.
17. *A.Cox, R.R.Doell,* Nature, v.189, 45, 1961.
18. *K.M.Creer,* Nature, v.205, 539, 1964.
19. *P.S.Wesson, Q.J.Roy.* Astr. Soc., v.14, 9, 1973.
20. *S. van den Bergh,* PASP, v.106, 1113, 1994.
21. *R.C.Kennicutt, W.L.Freedman, J.R.Mould,* Astron. J., v.110, 1476, 1995.
22. *J.MacDougall, R.Butler, P.Kronberg, A.Sandqvist,* Nature, v.199, 1080, 1963.

АСТРОФИЗИКА

ТОМ 38 НОЯБРЬ, 1995 ВЫПУСК 4

EXAMPLES OF CLUSTERING AROUND HIGH REDSHIFT RADIO-GALAXIES

J.M.DELTORN, O.LE FÈVRE

LAEC, Observatoire de Paris-Meudon
delton @obspm.fr, lefevre @obspm.fr

1. *Introduction.* Motivated by the interest of high redshift galaxy clusters, in such different fields as the study of large scale structures formation or the birth and evolution of galaxies, various observational campaigns are know carried out in order to enlarge our knowledge of an Universe twice younger than today. Moreover, at such large redshifts, the prevalence of clusters and other large scale structures is yet unknown and the evolution of these structures may well be at a critical stage, where observations can directly constrain cosmological models.

However only a handful of clusters are known at z>0.8. Indeed, finding cluster candidates at redshifts close to one is by no means an easy task: perturbed by a large fraction of foreground galaxies it is not possible to merely rely on projected number over-densities to define clusters. We consider here the fact that at z<0.5 one third of bright radio galaxies and QSOs lie within rich clusters (Hill & Lilly, 1991; Yee & Ellingson, 1993), and we extend this methodology to z>0.8. The extensive survey of radio-galaxies environments, both using IR and optical as well as multi-slit spectroscopy, should then allow the indentification of cluster candidates.

We present here the succesful indentification of galaxy clusters around two powerful radio-galaxies, 3C265 (z=0.81) and 3C184 (z=0.996). A more detailed analysis of these observations can be found in Le Fèvre & Deltorn, 1995.

2. *Clustering indentification*

2.1. Observations and reductions. V and I (resp. 600 and 1200s) exposures were obtained for a 10'×10' field centered around 3C265 at the CFHT using the MOS spectrograph imaging mode. Similarly we observed 3C184 in R, I and K' bands (resp.

900, 2400 and 2700s). Standard CCD image processing was conducted using the IRAF software, producing a catalog of 1684 objects for 3C184 and 956 objects for 3C265. The completeness limit in the *I* band for each catalog is respectively 22.5 and 22. Additional images were obtained using a narrow band filter centered on the redshifted [OII] line (3600s for 3C184 and 3900s for 3C265).

Multi-slit spectroscopy was obtained with MOS (3×4800s with a 37 slit mask for 3C184 and 3×3600s with a 39 slit mask for 3C265), with a resolution of 0.355nm in the dispersion). The measured galaxies were selected in function of their flux excess in the [OII] filter, and such that their magnitude was comprised between the magnitude of the radio-galaxy and 22. Spectra were processed using the MULTIRED package implemented in IRAF (Le Fèvre et al., 1995).

2.2 Galaxy density excess in redshift space. Two galaxies within 150 and 1140 km/s from the radio-galaxy were found in the 3C184 field (out of 14 secure measured redshifts). As for 3C265, four galaxies have velocities less than 900km/s from the radio-galaxy (out of 24). Fig. 1 presents the redshift distribution for both fields, compared with field galaxy redshift distribution from the CFRS (Crampton et al, 1995). From a random sample of field galaxies, we would expect 0.03 galaxies out of 14 at z=0.996 and 0.1 out of 24 at z=0.81. Although the small number of observed redshifts prevents us from robust statisitical tests, these probabilities give good confidence on the reality of the observed over-densities.

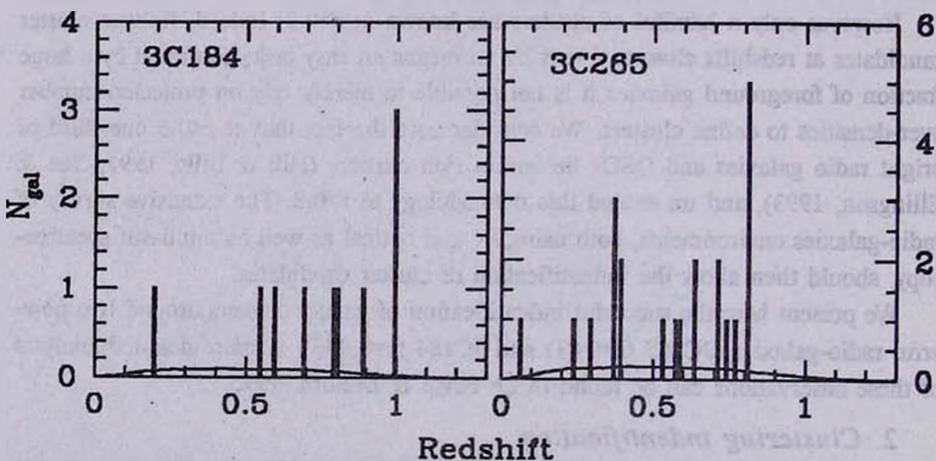

Fig. 1. Redshifts distribution respectively in the 3C184 field (left) and the 3C265 field (right). The continuous line represents the CFRS redshift distribution for I<22, plotted with the same redshift bin as the 3C184 and 3C265 distributions (i.e. 1500km/s).

2.3. Sky projected density excess. Using the photometric catalogs constructed for the two fields we compute both a projected number density map (Dressler, 1980) and the excess of galaxies with *V-I* >1 (for the 3C265 field) and *R-I* >0.2 (3C184) which should be predominantly at z>0.5 (bruzual & Charlot, 1993). Fig. 2 shows the radial density excess plots around 3C184 and 3C265.

The excess of galaxies is respectively 2.7 and 3.4, corresponding to 8σ and 12σ above the mean galaxy background. Boh radio-galaxies therefore lie in significant projected galaxy over-densities. The number of galaxies brighter than m_3+2 and within 0.5h^{-1}Mpc from 3C184 and 3C265 is $N_{0.5}$=10 and 20 resp.We also observe a projected multi-modal morphology that might indicate a young dynamical state of the clusters; however the importance of contamination from foreground galaxies at such redshifts prevents us from drawing any strong conclusion as for the real clusters structures.

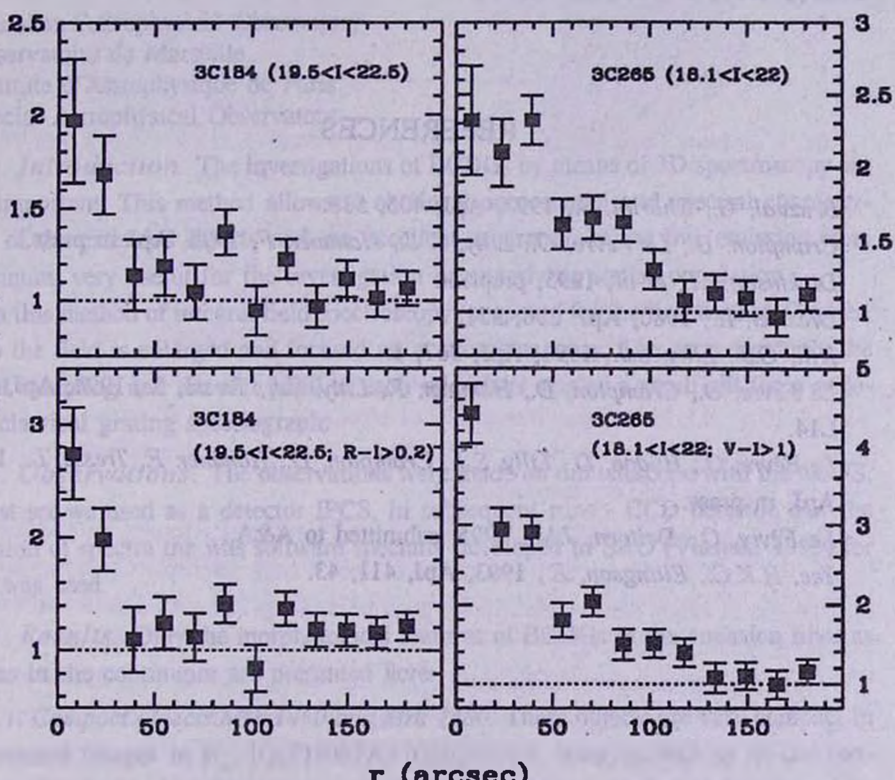

Fig. 2. Projected galaxy density excess around 3C184 (left) and 3C265 field (right). The number of galaxies has been computed in 15.7 arcsec wide rings, and normalized to the mean background galaxy density.

3. *Conclusion*. Indications of clustering around two high redshift 3C radio galaxies have been presented. based on the measured galaxy density excess both in redshift space and in projection on the sky. More velocity measurement are needed in order to investigate the detailed properties of the clusters and of the galaxies in these environments. These two examples nevertheless add to the still quite poor, but growing, list of very high redshift structure candidates (Le Fèvre et al, 1994; Dickinson et al, 1995). As more examples of clustering of galaxies are identified at $z \approx 1$ and above, direct comparisons with large scale structure evolution theories will become possible.

Примеры скоплений галактик вокруг радиогалактик с большими красными смещениями. Представлены результаты отождествления скоплений галактик вокруг двух радиогалактик, 3C265(z=0.81) и 3C184(z=0.996).

REFERENCES

Bruzual, G., Charlot, S., 1993, ApJ, 405, 538.

Crampton, D., Le Fèvre, O., Lilly, S. J., Hammer, F, 1995, ApJ in press.

Dickinson, M., et al, 1995, preprint.

Dressler, A., 1980, ApJ, 236, 351.

Hill, G.J., Lilly, S.J., 1991, ApJ, 367, 1.

Le Fèvre, O., Crampton, D., Hammer, F., Lilly, S.J., Tresse, L., 1994, ApJ, 424, L14.

Le Fèvre, O., Hudon, D., Lilly, S.J., Crampton, D., Hammer, F., Tresse, L., 1995, ApJ, in press.

Le Fèvre, O., Deltorn, J.M., 1995, submitted to A&A..

Yee, H.K.C., Ellingson, E., 1993, ApJ, 411, 43.

А С Т Р О Ф И З И К А

ТОМ 38 НОЯБРЬ, 1995 ВЫПУСК 4

SOME RESULTS OF OBSERVATIONS OF BCDGS WITH MULTI-PUPIL SPECTROGRAPH ON 6M TELESCOPE

T.A.MOVSESSIAN[1], A.R.PETROSSIAN[1], G.COMTE[2], D.KUNTH[3], S.N.DODONOV[4]

1 Byurakan Astrophysical Observatory
2 Observatoire de Marseille
3 Institute d'Astrophysique de Paris
4 Special Astrophysical Observatory

1. *Introduction.* The investigations of BCDGs by means of 3D spectroscopy are very important. This method allows to obtain at once spatial and spectral characteristics of the extended objects with an excellent separation of the line emission from continuum, very useful for the investigation of underlying stellar population.

In this method of integral field spectroscopy (proposed for the first time by Courtès, 1980) the field is enlarged and focused on a microlens array. The array produces the spatial sampling and the exit pupil of each microlens acts as a small slit for a wide-field classical grating spectrograph.

2. *Observations.* The observations were made on 6m telescope with the MPFS. In first set we used as a detector IPCS, in subsequent runs - CCD detector. For the reduction of spectra the was software specially developed in SAO (Vlasjuk, 1995) for MPS was used.

3. *Results.* Only the morphological features of BCDGs in the emission lines as well as in the continuum are presented here.

3.1. Compact objects Mrk 1450 and Mrk 1480. These objects are very compact in the restored images in H_α, [OIII]5007A, [OIII]4959A, lines as well as in the continuum (Fig. 1a,b). But the images in continuum are more extended and shallow. The larger size observed in the continuum could be caused by an extended envelope of old stellar population which is redder than the starforming region.

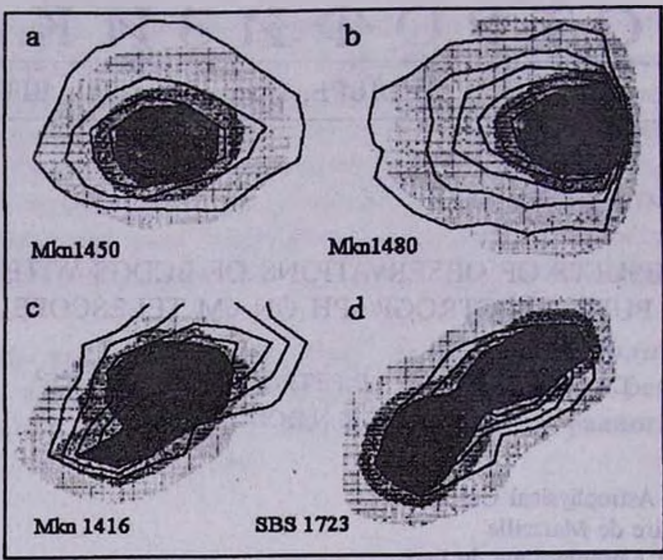

Fig. 1. Intensity maps in [OIII]5007A line (grey) superposed on continuum (isophotes).

3.2. Double objects. In the case of some double objects (Mrk 1416, Mrk 1426, SBS 1723) (Fig. 1 c,d) the peaks of the emission regions coincide with the continuum peaks. The more interesting objects are the galaxies SBS 1154 and Mrk 324 with noticeable separation between emission and continuum regions.

SBS 1154. It represents a striking case of separation of emission and continuum regions (Fig. 2a). It has two emission lobes separated by about 12 arcsec and a double continuum peak located between them. There is no observable difference of radial velocity between the two emission lobes.

Mrk 324. Opposite to the double-structured continuum image, in the emission lines (H_α, [OIII]) (Fig. 2 b,c). Images obtained in both spectral regions show color differences between the two continuum peaks, implying that we observe two different stellar populations (Fig. 2b).

The restored image in [SII] lines show the filamentary structure non-congruent with images in Ha and [OIII] lines. This filament could be caused by a shock wave which may be triggered by star formation processes, or by a chain of supernovae remnants. These hypotheses are consistent with the detection of a faint [OI] 6300 A line in this galaxy.

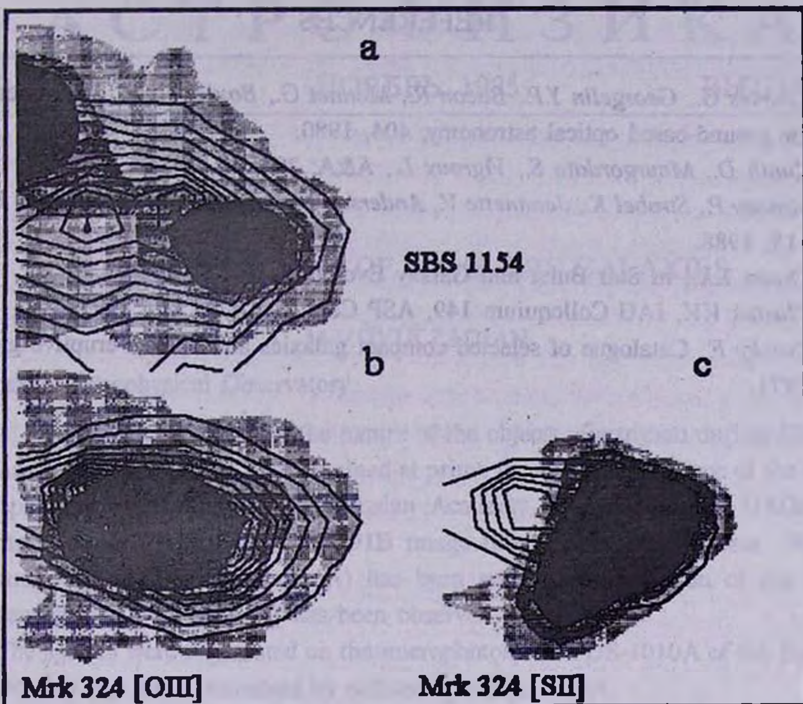

Fig. 2. Intensity maps in [OIII]5007A line (a and b) (grey) and [SII]6716+6731A (c) superposed on continuum (isophotes).

Некоторые результаты наблюдений голубых компактных карликовых галактик на 6м телескопе с многозрачковым спектрографом. **Представлены результаты наблюдений голубых компактных карликовых галактик с мультизрачковом спектрографом на 6-метровом телескопе САО РАН. Приводятся восстановленные изображения семи галактик в эмиссионных линиях и континууме. В ряде случаев наблюдается пространственное несовпадение областей, излучающих в линиях и в континууме.**

REFERENCES

Courtes G., Georgelin Y.P., Bacon R., Monnet G., Boulesteix J., Instrumentation for ground-based optical astronomy, 404, 1980.

Kunth D., Maurgordato S., Vigroux L., A&A, 204, 10, 1988.

Massey P., Strobel K., Jeannette V., Anderson B., Anderson E., Astrophys. J., 328, 315, 1988.

Thuan T.X., in Star Burst and Galaxy Evolution, p. 129, 1987.

Vlasiuk V.V., IAU Colloquium 149, ASP Conf. Ser. vol. 71, 1995.

Zwicky F., Catalogue of selected compact galaxies and of post-eruptive galaxies, 1971.

АСТРОФИЗИКА

ТОМ 38 НОЯБРЬ, 1995 ВЫПУСК 4

SPECTROSCOPY OF SOME SBS GALAXIES

M.V.GYULZADIAN

Byurakan Astrophysical Observatory

1. For the determination of the nature of the objects, discovered during SBS their medium resolution spectra were obtained at prime focus of 6m telescope of the Special Astrophysical Observatory of the Russian Academy of Sciences with UAGS spectrograph connected with the UMK-91B image tube. A dispersion about 90A/mm (spectral resolution is about of 5A) has been used. For calibration of the spectra standard star BD+33°2642 [1] has been observed.

The spectra were registrated on the microphotometer PDS-1010A of the Byurakan Observatory and were processed by software package AIDA.

2. *Results. a) Objects description.* *SBS1122+610*. According to [2] it is a "starlike, blue object". In the spectra of the galaxy [SII] λλ6731,6717, [NII] λ6584, H_α, [OIII] λλ5007, 4959, H_β, HeII λ4686, [OII] λ3727, weak [OIII] λ4363, H_γ emission lines and absorption lines of H and K CaII were identified.

SBS1133+597. According to [2] it is a "starlike, blue object". In the spectra of the galaxy [SII] λ6731, 6717, [NII] λ6584, H_α, [OIII] λ5007, 4959, H_β, [OII] λ3727 were identified.

Table 1

SBS	α(1950)	δ(1950)	Vr (km/s)	SIZE	m	SURVEY TYPE	M
1122+610	$11^h\ 22^m.11$	+61° 03'	9866	5"	$18^m.5$	se	$-17^m.4$
1133+597	1133.8	+59 43	2280	13 x8"	17.5	sd2e	-15.2
1139+601	11 39.9	+60 06	12638	9 x6"	18.0	se	-18. 4

SBS1139+601. It is a spherical, blue object [2]. Emission lines [SII] λλ6731, 6717, [NII] λ6584, H_α, [OIII] λλ5007, 4959, H_β, weak [OIII] λ4363, H_γ, [OII] λ3727 were observed.

Table 1 lists the integral parameters of the studied SBS galaxies. Column 1 gives SBS designation [2]. Column 2 and 3 give right ascensions and declination of the objects. Column 4 gives galactocentric radial velocities. Column 5 and 6 give measured on POSS size and apparent blue magnitudes of the galaxies. Column 7 gives Markarian spectral type [3] and column 8 gives corrected for extinction absolute blue magnitudes of the galaxies for H=75km s^{-1} Mpc^{-1}.

b) Line widths. The full widths at half maximum (FWHM) of the strongest emission lines in spectra of galaxies were measured. Obtained data are corrected for instrumental profile. Averaged by strongest emission lines FWHMs are presented in Table 2.

Table 2

Physical parameters	SBS		
.	1122+610	1133+597	1139+601
Te	5710±740	-	11621±+1003
ne	$3.9x10^3$	-	-
FWHM(km/s)	413±80	159±74	433±90
[OIII]5007/H_β	2	1.5	0.32
[NII]/H_α	0.21	0.33	0.32
[SII]/H_α	0.21	0.33	0.24
12+LOG(O/H)	8.66	-	8.24
12+LOG(N/H)	7.49	7.65	7.64
EW(H_β)	14.1	5.96	4.21
<E>	0.097	-	0.06
[OII]λ3727/0[III]λ5007	0.97	-	3.15

c) *Emission line ratios. Photoionization mechanism and chemical abundance.* To determine physical conditions, the excitation mechanism and estimate heavy element abundances in the objects selected line ratios, in particular [NII]/H_α, [SII]/H_α, [OII] λ3727/[OIII] λ5007 were calculated. Results are presented in Table 2. The position of all three galaxies on two dimensional diagrams of ([OIII]/H_β versus [OII]/[OIII] and [NII]/H_α versus [OII]/[OIII]) agrees well with the position occupied with HII galaxies [3].

On the Classification diagrams of Veilluex and Osterbrock [4] two galaxies, SBS1122+610 and SBS1139+601, lie in the region of NELGs, third one, SBS1133+597 lies in the region of HII galaxies.

It is important to note, that for all three galaxies the observed [SII]/H_α ratios are rather large compared to more conventional HII regions. The oxygen and nitrogen abundances in the galaxies are determined according to the empirical relations described by Petrosian [5]. [OIII]+[OII]/H and [NII]/H line intensity ratios were used. The results are given in Table 2. The oxygen and nitrogen abundances for SBS1122+610 correspond to that for HII regions in Sc/m galaxies [5].

For SBS1139+601 abundances correspond to HII Nuc [5]. For SBS1122+610 the oxygen abundance corresponds to HII regions in giant irregular galaxies.

3. *Conclusions*. On the base of FWHM of emission lines observed in the spectra of SBS1122+610 and SBS1139+601, the position of emission lines in Baldwin et al. [3], Veilleux and Osterbrock [4] diagrams show that these galaxies are NELGs. SBS1133+597 is HII galaxy.

I am grateful to Dr. A. Petrosian for helpful discussion and Dr. J. Stepanian for making available the spectra.

Спектроскопия некоторых SBS галактик. Представлены результаты спектроскопии трех галактик из Второго Бюраканского Обзора. Спектры получены в первичном фокусе 6-и метрового телескопа САО АН России со спектрографом UAGS и ЭОП УМК-91В в диапазоне λλ3700-7400. Изучение этих спектров показывало, что все три объекта являются галактиками с узкими эмиссионными линиями.

REFERENCES

1. *R.P.S.Stone*, Astrophys.J.,218,767, 1977.
2. *B.E.Markarian and J.Stepanian*, Astrofisica, 19, 637, 1983.
3. *J.A.Baldwin, M.M.Philips, R.Terlevich*, P. A. S. P. , 93, 5, 1981.
4. *S.Veilleux and D.Osterbrock*, Astrophys. J. Supl. Ser. , 63, 295, 1987.
5. *A.Petrosian*, Comm. Byurakan Observatory, 61, 15, 1989.

АСТРОФИЗИКА

ТОМ 38 НОЯБРЬ, 1995 ВЫПУСК 4

PHOTOMETRY AND SPECTROSCOPY OF TWO COMPACT GROUPS OF GALAXIES SH 354 AND SH 355

H.TIERSCH[1,4], H.OLEAK[1], D.STOLL[1,4], S.NEIZVESTNY[2], A.S.AMIRKHANIAN[3], A.G.EGIKIAN[3]

1 University of Potsdam, Astrophysikalisches Institut Potsdam, Germany
2 Special Astrophysical Observatory, Nizhny Arkhys, Russia
3 Byurakan Astrophysical Observatory, Armenia
4 Viziting astronomers at the German-Spanish Astronomical Center, Calar Alto, Spain

Among the dense groups so called compact groups of galaxies are known. Shahbazian in 1957 [1] discovered a very dense aggregate of red objects later recognized as galaxies [2]. The concept of the compact groups of compact galaxies was then introduced by Shahbazian and her colleagues at the Byurakan Astrophysical Observatory, and ten lists of 377 groups were published from the search of the Palomar Sky Atlas prints [3 and refereces therein].

Not many Shahbazian compact groups of galaxies have been investigated photometrically and spectroscopically till quite recently [4-7]. For this reason a program has been started in the University of Potsdam, Potsdam Astrophysikalisches Institut (WIP-project "Astronomy") in cooperation with other observatories to obtain photometric and spectroscopic properties of the Shahbazian group members [8,9]. In this study the results of high resolution CCD *B, V, R* photometry and long-slit spectroscopy of galaxies in two compact groups Sh 354 and Sh 355 are presented.

Photometric and spectroscopic CCD observations have been taken out at the German-Spanish Astronomical Center in Calar Alto (Almeria, Spain) using the 1.23m and 2.2m telescopes. The data reduction procedure was made with MIDAS system at Potsdam Astrophysikalisches Institut.

The radial velocities for the members of the compact groups of galaxies Shahbazian 354 and 355 are determined. The dispersions of the radial velocities of these two compact groups are equal to 360 and 227km/s, respectively. Moreover the CCD apparent magnitudes of galaxies in colours *B, V, R* and absolute those of in *V* as well as the mass to luminosity ratios are obtained. The latters are approximately equal to 235 and 69 $M_{\odot}/L_{\odot}$ for the groups Sh 354 and Sh 355, respectively.

Compact groups of galaxies represent the most dense galaxy systems in the Universe. The space number densities of galaxies in these two groups are as high as 10^3 gal/Mpc^3 and 10^4 gal/Mpc^3 for Sh 354 and Sh 355, respectively, even higher than the densities in the centers of rich clusters. The crossing time of $\sim 10^8$ years for two groups is small compared with the Hubble age.

Galaxy number 7 in Shahbazian 354 is projected AGN (probably QSO-like) object with redshift z=0.1805. The mean redshift of Sh 354 has been found to be z=0.0707.

Object number 4 in Shahbazian 355 is Seyfert 1 type active galaxy. Its redshift (z=0.0941) makes Sh 355/4 a physical member of the group.

This work is supported by a grant of the "Deutsche Forschungs-gemeinschaft".

Фотометрия и спектроскопия двух компактных групп Sh 354 и Sh 355. На основе CCD фотометрических и спектроскопических наблюдений с высоким разрешением, проведенных на 1.23м и 2.2м телескопах обсерватории Калар Альто для галактик компактных групп Sh 354 и Sh 355 определены лучевые скорости, видимые и абсолютные *B, V, R* звездные величины, а также отношения масса-светимость, которые оказались равными 235 $M_{\odot}/L_{\odot}$ и 69 $M_{\odot}/L_{\odot}$, соответсвенно.

REFERENCES

1. *R.K.Shahbazian*, Astron. Tsirk. SSSR, No.177, 11, 1957.
2. *L.B.Robinson, E.J.Wampler*, Astrophys. J. Lett. 179, L135, 1973.
3. *F.W.Baier, H.Tiersch*, Astrofizika, 15, 33, 1979.
4. *A.S.Amirkhanian, A.G.Egikian*, Astrofizika, 27, 395, 1987.
5. *C.R.Lynds, E.Ye.Khachikian, A.S.Amirkhanian*, Pisma v Astron. J., 16, No.3, 195, 1990.
6. *K.Kodaira. M.Sekiguchi, H.Sugai, M.Doi*, Publ. Astron. Soc. Japan, 43, 169, 1991.
7. *A. del Olmo, M.Moles*, Astron. Astrophys., 245, 27, 1991.
8. *H.Tiersch, H.Oleak, D.Stoll, H.Bohringen*, in H.T.MacGillivray et al.: Astronomy from Wide-Field Imaging, Kluwer, Dordrecht, p.623, 1994.
9. *H.Oleak, D.Stoll, H.Tiersch, H.T.MacGillivray*, Astron. J., 109, 1485, 1995.

АСТРОФИЗИКА

ТОМ 38 НОЯБРЬ, 1995 ВЫПУСК 4

TWO GALAXIES WITH UV EXCESS

A.A.YEGHIAZARIAN

Byurakan Astrophysical Observatory

The direct plates of the galaxies No.49 and No.50 with UV excess from the Kazarian list [1] were obtained in the primary focus of the 2.6 m telescope at Byurakan Observatory, on ORWO type blue plates with 25 minute exposure time (original scale is 1 mm = 20").

The galaxy No.50 is a homogeneous elliptical galaxy.

The galaxy No.49 = MCG 11-19-30 [2] is a spiral galaxy with a bright binary nucleus. Spiral arms of the galaxy, with condensations extend northwards and southwards from the central area. The diameter of the nuclear region is 7". There are a quasi-stellar condensation with 2" diameter on the northern arm at a distance of 8" from the center and 2 condensations on the southern arm at almost the same distance, 2".5 in diameter, which are less compact and less bright than the previous one [3].

The spectra of these galaxies were obtained in 1982 by means of 6 m telescope of SAO with SP-160 and image tube with 20 minutes exposure (60 A/mm dispersion, 3000 - 7000 AA). Later on the spectra of these galaxies were obtained in 1983 by means of 6 m telescope of SAO with SP-160 and bicameral image tube in three spectral regions (65 A/mm dispersion, 3000 - 7000 AA).

There are $H\alpha$; He I $\lambda\lambda$ 5876, 4926; H_β; He II λ 4686; $H\gamma$; H_δ; $H\varepsilon$ emission lines and [S II] $\lambda\lambda$ 6731, 6717, 4976 / 4967; [N II] $\lambda\lambda$ 6584, 6548, 5755; [O III] $\lambda\lambda$ 5007, 4959, 4363; [He III] $\lambda\lambda$ 3968, 3869; [O II] λ 3727 bright forbidden lines in the bright and narrow continuous spectrum of the galaxy No.49. Besides that the [N II], H_α, H_β and [O II] lines get out of borders of the continuous spectrum and reach the visible borders of the galaxy [4].

The redshift of the galaxy No. 49 is 0.0298.

The northern quasi-stellar condensation of the galaxy No.49 has rather bright emission lines in the very weak continuous spectrum. The diameter is equal to 1 kpc.

Probably it is a H II region in the galaxy [5].

The galaxy No. 49 is physically associated with the galaxy No. 50.

The spectra of the galaxy No. 50 mainly show absorption lines. The redshift of the galaxy is 0.0299.

The separation of galaxies No. 49 and No. 50 in projection is 150 kpc.

It is important to note that the profiles of emission lines in the spectrum of the galaxy No. 49 are different. The forbidden lines are narrower but the emission lines of Balmer series of the hydrogen are wider. The velocity of the Doppler width of the nuclear region referring to the forbidden lines is about 400 km/sec. and referring to the hydrogen lines is about 1200 km/sec.

The last time the spectra of the nucleus of the galaxy No.49 were obtained in 1990 by means of the 6 m telescope in SAO using 1000 canal TV scanner in 2 spectral regions. The spectrum of the eastern component of the nucleus is typical for nuclear spectra, while the spectrum of the western component resembles a spectrum of H II region.

The further research of these galaxies will help to understand better their nature.

Две галактики с ультрафиолетовым избытком. Приводятся результаты исследования двух физически связанных галактик с УФ избытком No. 49 и No. 50 из списка Казаряна. Двухядерная спиральная галактика No. 49 имеет спектр с линиями излучения высокого возбуждения, а эллиптическая галактика No. 50 - спектр с линиями поглощения.

REFERENCES

1. *M.A.Kazarian*, Astrophysika, 5, 15, 1979.
2. *B.A.Vorontsov-Veliaminov, A.A.Krasnogorskaia*, Morphology Catalogue of Galaxies v. 1, 1962.
3. *A.A.Yeghiazarian*, Astrophysika, 19, 631, 1983.
4. *A.A.Yeghiazarian*, Dissertation, Yerevan, 1987.
5. *A.A.Yeghiazarian, E.Ye.Khachikian*, Soob. Byurakan Obs. 3, 60, 1989.

АСТРОФИЗИКА

ТОМ 38 НОЯБРЬ, 1995 ВЫПУСК 4

THE MAGNETIC FIELDS AND RADIO JET IN GIANT RADIO GALAXIES

M.A.HOVHANNISSIAN

Byurakan Astrophysical Observatory

The study of giant radio galaxies by the scintillation method [1-4] at the102 MHz frequency enables us to estimate the strength of magnetic field and also the density of relativistic electrons in compact radio sources. Using formulae $\theta = 4.3' 10^{16} S^{1/2} \nu^{-5/4} H_{\perp}^{1/4} (1+z)^{1/4}$ [5] the strength of magnetic field $H_{\perp}$ is estimated, where θ is the angular size of the source, S is the maximum flux density at ν frequency, and z is the redshift.

One readily may determine the energies of magnetic field and relativistic electrons by estimated values of $H_{\perp}$ and the density of electrons. Comparison of these energies (see Table 1) shows that in the radio galaxy DA240 the strength of magnetic field is in 6 order of magnitude greater than the energy of relativistic electrons [1]. In the DA240 the relativistic electrons can be easily captured by magnetic field and consequently emit isotropic radiation. In this case the radio jet cannot be formed.

In the NGC1275 the energy of magnetic field is in 8 order of magnitude less than the energy of electrons [2], and the relativistic electrons easily can pass through the galaxy into the intergalactic medium. Hence the radiation in the radio-range is absent far from the core. In this case the radio jet will not be observed.

Table 1

RESULTS OF THE OBSERVATIONS

Source name	E_H(erg)	E_e(erg)	θ(arcsec)	L(pc)	Jet
DA240	10^{56}	10^{50}	0.07	40	no
NGC1275	10^{47}	10^{55}	0.03	11	no
NGC315	10^{50}	10^{49}	0.002	1	yes
3C31	10^{51}	10^{50}	0.002	1	yes

In NGC315 and 3C31 the energy of magnetic field is comparable with the energy of electrons [3,4], and the electrons are gathered in the galaxy and around it. But the magnetic field prevents electrons to pass through the galaxy, which are captured by magnetic field radiating in radio-range.

If the magnetic field has a fixed direction or electrons are being ejected by galaxy core in fixed direction, then the radio jets can be formed. The interaction of electrons with the vicinity can form compact radio sources at the edge of radio jet.

Thus, we can draw the statement, that in the radio galaxies,where the energies of magnetic field and relativistic electrons are comparable, the radio jets can be formed, otherwise they do not form.

Магнитные поля и радиоджеты в гигантских радиогалактиках. Если энергия магнитного поля близка к энергии релятивистических электронов, то могут образоваться радиоджеты. В других случаях джеты не формируются.

REFERENCES

1. *V.S.Artyukh, M.A.Hovhannissian,* Pisma Astron Zh., 14, 706, 1988.
2. *V.S.Artyukh, M.A.Hovhannissian,* Astron. Zh., 70, 443, 1993.
3. *V.S.Artyukh, M.A.Hovhannissian, S.A.Tyul'bashev,* Pisma Astron. Zh., 20, 178, 1994.
4. *V.S.Artyukh, M.A.Hovhannissian S.A.Tyul'bashev,* Pisma Astron. Zh., 20, 258, 1994.
5. *V.I.Slish,* Nature, 199, 682, 1963.

АСТРОФИЗИКА

ТОМ 38 НОЯБРЬ, 1995 ВЫПУСК 4

A NEW SAMPLE OF CANDIDATES GPS SOURCES

G.A.OHANIAN

Byurakan Astrophysical Observatory, Armenia

Three types of extragalactic radio sources are well-known. (I) Extended sources with steep spectra, $\alpha > 0.5$ ($S \sim \nu^{-\alpha}$) and sizes > 100 kpc. (II) Compact nuclear sources with flat spectra, $\alpha < 0.5$ and sizes < 1 pc. (III) Compact sources with steep spectrum (CSS), $\alpha > 0.5$, with linear sizes smaller than a galaxy typical diameter (~25 kpc). The size of CSS sources are in order of typical sizes of the optical narrow emission line region (~1 kpc). The spectra of many CSS sources has turnover at low frequency, near 100 MHz.

Recently high attention has been devoted to the so-called "gigahertz peaked spectrum" (GPS) radio sources with exhibit a clear peak near 1 GHz (0.5-5 GHz). The nature of these sources and their relationship to compact and extended radio sources is not clear yet. The properties of these objects, as stressed by O'Dea et al [1] are: (I) peaked radio spectra with narrow spectral shape and steep high frequency spectrum, (II) low radio polarization, (III) high radio luminosity ($\sim 10^{45}$ erg s^{-1}) (IV) very compact radio structure.

It is now clear, that the family of GPS sources is a mix of galaxies and quasars. They frequently are associated with high redshift objects [2, 3]. The great potential of GPS sources to discover high z objects is the major motivation for enlarging of the sample of GPS sources. First list of 25 GPS objects has been published by Gopal Krishna et al [3]. Later publications by different authors [1,4-8] enlarged the number of candidates GPS to 141.

In the present paper we extend the lists of candidate GPS sources, using a sample of 39 sources selected from first 10 published Ooty lists ([9] and references therein). The spectra of the Ooty radio sources have been determined by observing them simultaneously at 968, 2300, 3660, 3950 and 7700 MHz, with the RATAN-600 radio telescope, which gave an adequately large frequency range 24:1.

The measurements of the flux densities at 968, 2300, 3660, 3950 and 7700 MHz were carried out by myself at RATAN-600 for 307 of the total 930 Ooty radio sources ($b^{II} > 10°$). The observed sample has a median value of S_{327}=0.7 Jy and an optical identification rate of 56%. The optical identifications have been done on the base of prints of the Palomar Observatory Sky Survey (POSS). Optical positions of all the objects were measured with an accuracy of 0.5 arcsec, and their photographic magnitudes are accurate within 1^m [9]. The spectra of these sources were derived by combining our RATAN-600 flux densities with the S_{327} taken from the Ooty lists using additional flux densities available from the literature. All flux densities were converted to the scale of Baars et al [10]. Details of these observations and the spectra of Ooty radio sources are presented by Ohanian and Panajian [11, 12] and Ohanian [13]. We found that among these 307 sources 39 (13%) can be candidates of GPS sources (S_{327med} = 0.5 Jy). Five of them were included in the Gopal Krishna et al sample [3]. The sources, whose peaked spectrum may be due to confusion, are excluding from the sample. Our sample of GPS sources, together with data published by other authors, enlarged the number of known GPS source candidates to 175 objects.

The 327 MHz flux densities of a observed sample of 307 sources lie in the range of 0.2-4.3 Jy with a median value of 0.7 Jy. 136 (44%) of them are EF (m_{pg}>21^m on the POSS prints). The magnitudes of remaining optical identified objects lie in the range of 11-21^m, with a median value of 19^m . The fluxes of 39 candidate GPS sources lie in the range of 0.25-2.4 Jy with a median value of 0.5 Jy. 19 (48.7%) of them are EF, the magnitudes of remaining optical identified objects lie in the range of 16-21^m with a median value of 19.5^m. The comparison these values for observing sample and for 39 candidate GPS sources show, what GPS type objects are frequently found among the fainter objects both in radio and optical range. This can be another indication that sample of GPS type sources might be rich by objects at high redshifts.

From observed sample of 307 sources 9 are identified as BG (blue galaxies), 4 (44.4%) of them are GPS sources. From 25 identified RG (red galaxies) the GPS type of sources are default. We have examined the spectra of fainter radio sources ($S_{1.4GHz}$< 50mJy) from Leiden - Berkeley Deep Survey (LBDS) presented by Oort [14]. It is shown, that from 13 blue radio galaxies (z =0.3-0.7), 8 (61.5%) appear to be GPS sources. From 6 red radio galaxies only one (16.7%) is true GPS source. It seems, that GPS type sources to be frequently associated with galaxies of blue colour.

Новая выборка радиоисточников с пиком в спектре в гигагерц диапазоне. Представлена новая выборка радиоисточников с пиком в спектре в Гегагерц диапазоне (ГПС). Наша выборка, вместе

с данными, опубликованными другими авторами, увеличивает число кандидатов в ГПС до 175.

REFERENCES

1. *C.P.O'Dea, S.A.Baum, C.Stanghellini*, Astrophys. J., 380, 66, 1991.
2. *C.P.O'Dea*, Mon. Notic. Roy. Astron. Soc., 245, 20p, 1990.
3. *Gopal Krishna, A.R.Patnaik, H.Steppe*, Astron. and Astrophys., 123, 107, 1983.
4. *T.A.Th. Spoelstra, A.R.Patnaik, Gopal Krishna*, Astron. and Astrophys., 152, 38, 1985.
5. *C.Stanghellini, C.P.O'Dea, S.A.Baum, R.Fanti*, in Proc. Dwingelos Workshop on CSS and GPS Source, ed. C.Fanti, C.P.O'Dea, R.T.Schilizzi (Bologna Instituto di Radioastronomia) 55, 1990.
6. *Gopal Krishna, T.A.Th. Spoelstra*, Astron. and Astrophys., 271, 101, 1993.
7. *J.C.Cersosimo, M.Lebron Santos, S.I.Cintron, Z.M.Quiniento*, Astrophys. J. Suppl. Ser., 95, 157, 1994.
8. *G.Snellen, M.Zhang, R.T.Schilizzi, H.J.A.Rottgering, A.G. de Bruyn, G.K.Miley*, Astron. and Astrophys., 300, 359, 1995.
9. *A.K.Singal*, Astron. and Astrophys., Suppl. Ser., 69, 91, 1987.
10. *J.W.M.Baars, R.Gentel, I.I.K.Pauliny-Toth, A.Witzel*, Astron and Astrophys., 61, 99, 1977.
11. *G.A.Ohanian, V.G.Panajian*, , Sobsh. Byur. Obs., 54, 10, 1982.
12. *G.A.Ohanian, V.G.Panajian*, Sobsh. Byur. Obs. , 57, 28, 1984.
13. *G.A.Ohanian*, 1995 (in preparation).
14. *J.A.Oort*, Astron and Astrophys., 192, 42, 1988.

АСТРОФИЗИКА

ТОМ 38 НОЯБРЬ, 1995 ВЫПУСК 4

A SAMPLE OF GIGAHERTZ-PEAKED SPECTRUM CANDIDATE RADIO SOURCES

V.G.PANAJYAN

Gigahertz-peaked spectrum (GPS) radio sources are a subset of more general class of compact peaked spectrum radio sources. The sources of this class have narrow peak in their spectra around 1 GHz and fall off in flux density at high and low frequencies. The turnover of the spectra signifies the presence of synchrotron self-absorbtion of the radiation. The first sample of GPS extragalactic radio sources was completed by Gopal-Krishna et al. [1]. During past more than ten years new lists of GPS radio sources were completed by Spoelstra, Patnaik and Gopal-Krishna [2], Gopal-Krishna and Spoelstra [3], O'Dea, Baum,and Stanghellini [4], Cersosimo, Lebron-Santos and Cintron [5], Snelen, Zhang et al.[6]. There are now at least 131 GPS known radio sources.The median peak flux density of sources in the last sample [6] is 0.7 Jy. Investigation of fainter sample of GPS sources might give information on the evolution of distant GPS radio sources. Here we present a sample of faint GPS candidate radio sources, the median peak flux density of which is 0.20Jy.

The sources of our sample were selected from the "A new catalog of 30.239 1.4 GHz sources" [7]. The observations of this catalog were carried out by means ef the 91m telescope in Green Bank, West Virginia. The minimum flux density of the catalogued radio sources at 1.4 GHz is 100 mJy. For the great part of radio sources it contains:coordinates for epoch 1950.0, flux densities (peak flux densities for unresolved sources, and integrated flux densities for resolved sources), high and low spectral indices α_{hi} and α_{lo} ($\alpha_{hi} = \alpha_{(1.4\text{-}4.85)GHz}$, $\alpha_{lo} = \alpha_{(0.365\text{-}1.4)GHz}$), where the flux density $S \sim \nu^{\alpha}$ and ν is the frequency.In the [7] to calculate the α_{hi} and α_{lo} the flux densities at 4.85 GHz from [8] and at 0.365 GHz Texas interferometer observations were used.

To select GPS radio sources from the "A new catalog of 30.239 1.4 GHz sources" we used the criteria : 1) $\alpha_{hi} < -0.5$, 2) $\alpha_{lo} > 0$, 3) $|b_{II}| > 10^{\circ}$, where b_{II} is galactic latitude of sources. We inspect each candidate of GPS sources by means of their flux

Table

GPS CANDIDATE SOURCES

IAU name	RA(1950) h m s	Dec(1950) o ' "	S^{20}_{GB} mJy	S^{6}_{GB} mJy	S^{75}_{B3} mJy	α_{hi}	α_{lo}	$\alpha_{(0.4-1.4)}$
0002+4040	00 02 35	40 40 57	164	27	<100	-2	-	>0.4
0004+4118	00 04 18	41 18 26	253	141	190	-1	-	0.23
0024+4129	00 24 34	41 29 03	174	68	150	-1	-	0.12
0055+3845	00 55 47	38 45 59	161	83	<100	-1	-	>0.38
0158+4159	01 58 44	41 59 30	260	-	<100	-1	-	>0.77
0235+4622	02 35 16	46 22 25	208	58	160	-1	-	0.21
0253+4154	02 53 03	41 54 27	159	44	140	-1	-	0.1
0321+4458	03 21 36	44 58 11	254	27	<100	-2	-	>0.75
0706+4602	07 06 31	46 02 13	423	102	260	-1	0.2	0.4
0747+4238	07 47 46	42 38 57	143	28	<100	-1	-	>0.29
0801+4344	08 01 26	43 44 18	364	130	160	-1	-	0.67
0825+3832	08 25 01	38 32 39	354	127	260	-1	0.3	0.25
0833+4641	08 33 20	46 41 40	155	26	<100	-1	-	>0.36
0834+3932	08 34 47	39 32 55	235	112	<100	-1	-	>0.69
0932+3849	09 32 54	38 49 38	157	89	130	-1	-	0.15
0934+4333	09 34 18	43 33 58	143	47	<100	-1	-	>0.29
0937+4703	09 37 34	47 03 31	173	35	100	-1	-	>0.45
1055+4320	10 55 12	43 20 53	692	240	420	-1	-	0.4
1122+4015	11 22 45	40 15 00	199	91	<100	-1	-	>0.56
1333+4017	13 33 20	40 17 06	424	43	270	-2	-	0.37
1446+4732	14 46 41	47 32 48	160	34	110	-1	-	0.3
1447+4233	14 47 28	42 33 26	148	118	<100	—	-	>0.32
1526+4402	15 26 07	44 02 02	163	93	<100	-1	-	>0.39
1528+3808	15 28 24	38 08 54	100	162	<100	—	-	-
2356+3833	23 56 59	38 33 58	642	437	300	-0	0.7	0.62

densities at 408 MHz from the B3 catalog [9], because of the interferometer used for Texas survey underestimates the flux densities of sources larger than 15". The selected GPS candidate sources are listed in Table 1, where column (1) shows IAU name of the sources, columns (2) and (3) show the right ascension α and the declinations δ for epoch 1950.0, columns (4), (5) and (6) show the flux densities at 1.4 GHz, 4.85 GHz and 408 MHz respectively , columns (7), (8) and (9) show spectral indices $\alpha_{(1.4\text{-}4.85)GHz}$, $\alpha_{(0.365\text{-}1.4)GHz}$ and $\alpha_{(0.408\text{-}1.4)GHz}$, where $\alpha_{(0.408\text{-}1.4)GHz}$ are calculated by us using flux densities from the GB [7] and B3 catalogues.

The peak frequencies of the spectra all of sources in our sample are around 1.4 GHz, excluding the sources 1528+3808 and 2356+3833. The median values of the α_{hi} and α_{lo} are -1.0 and +0.23 respectively and the median of the peak flux densities of our sample is 0.2 Jy. Two sources 1447 + 4233 and 1528 + 3808 are galaxies and are identified with sources from the *IRAS* Point Source Catalog version 2 [10].The distance of the source 1447 + 4233 is 945.1 Mpc (the Hubble constant H=50 km/s Mpc, q_0=1/2), but the distance of the second source is unknown. The dominant energy sources of the both galaxies are "monster" [10].

Список радиоисточников, имеющих пик вблизи 1ГГц. Представляется список радиоисточников, имеющих пик в своих непрерывных спектрах вблизи 1 ГГц.

REFERENCES

Gopal-krishna, A.R.Patnaik, H.Steppe, Astron. Astrophys.,123, 107,1983.
T.A.T.Spoelstra, A.R.Patnaik, Gopal-Krishna, Astron. Astrophys.,152,38,1985.
C.P.O'Dea, S.A.Baum, C.Stanghellini, Astrophys. J.,380,66,1991.
Gopal-Krishna, T.A.T.Spoelstra, Astron. Astrophys.,271,101.1993.
J.C.Cersosimo, M.Lebron-Santos, S.I.Citron, Astron. Astrophys. Suppl.,95,157,1994.
I.A.G.Snellen, M.Zhang, R.T.Schillizzi et al., Astron. Astrophys.,300,359,1995.
R.L.White, R.H.Becker, Astrophys.J. Suppl.,79,331,1992.
R.H.Becker, R.L.White, A.L.Edwards, Astrophys. J. Suppl.,75, 1, 1991.
A.Ficarra, G.Grueff, G.Tomasetti, Astron. Astrophys. Suppl., 59, 255, 1985.
J.J.Condon, E.Anderson, J.J.Broderick, Astrophys.J.,109, 2318, 1995.

А С Т Р О Ф И З И К А

ТОМ 38 НОЯБРЬ, 1995 ВЫПУСК 4

ON EXPLANATION OF THE DISCRETIZATION OF REDSHIFTS OF QUASARS

R.A. VARDANIAN

Byurakan Astrophysical Observatory

On the base of observational data [1] of quasars and Seyfert 1 galaxies the influence of strong emission lines in their spectra on the distribution of redshifts, and on the diagram of relation between *(U-B)*, *(B-V)* for the quasars and Sy 1 galaxies is considered.

By study of this problem I was using non - standard methods of investigation: median filtration and pair method (choosing a pair of objects with the same absolute magnitudes, however with maximal differences of colours *(B-V)*, *(U-B)* or parameters $Q=(U-B)-(B-V)$).

From the above mentioned analysis the following results have been obtained [2-5].

1. The work [2] gives new evidences of connection of Sy 1 type galaxies and quasars which can be considered in favour of cosmological nature of their redshift.

It is shown that discrete redshifts (z =0.04; 0.12; 0.35; 0.67; 0.96; 1.36; 1.93; 2.61; 3.57) are due to selection effects of strong emission lines of quasars and absorption line OVI(1035A), which fall in the maxima of passband of *U, B , V* filters.

2. It is shown [3] that the differences between observed [6] and expected discrete values of quasars redshifts are negligible ($\Delta z < 0.1$) .

The periodicities calculated from observed and expected redshifts are $\Delta\lg(1+z_A)=0.091\pm0.005$ and $\lg(1+z_v)=0.087\pm0.012$ respectively [3].

On the base of comparison of the observed quasars redshifts with the expected discretization of quasars redshifts is conditioned by the observational selection and their periodicity-by chance.

3. It is shown that the relation $\Delta\ln[1+z]=0.206$ suggested to represent the discretization of redshifts of quasars is conditioned by observational selection and

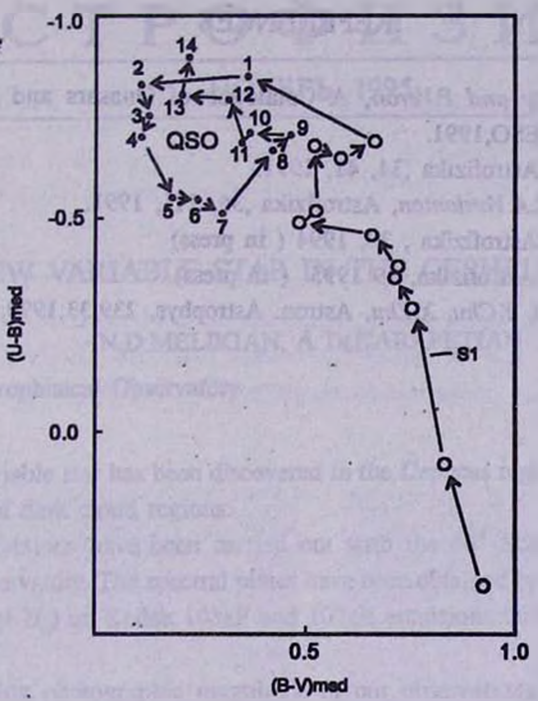

Fig. 1. Colour-colour [$(U - B)$med, $(B - V)$med] diagram for the O - Seyfert 1 (S1) galaxies and • -quasars.

predetermined by using relations of the effective wavelengths of the photometric system *U, B, V, R* and also by the relations of the wavelengths of emission lines Mg II, OIII, CIV Lyα and absorption line OVI (1035 A) of the quasars.

4. It is shown [5] that strong emission lines (MgII, OIII , CIV, Lyα) passing through the maxima of filters *U, B, V* bring to a linear and sometimes (in the z=0.1-1.4 interval) to cyclic changes in the dependence of *U-B* on *B-V* (Fig. 1). In Fig. 1 numbers near the points correcpond to redshifts z = 0.1; 0.2; ... ;1.4 respectively.

The mean values of variations of colours conditioned by strong emission lines (MgII; CIV; Lyα) is equal to about $0^m.15$.

Об объяснении дискретизации красных смещений квазаров. Показано, что соотношение $\Delta \ln[1+z]=0.206$, предложенное для описания дискретизации пространственного распределения квазаров, является следствием наблюдательной селекции.

REFERENCES

M.-P.Veron-Cetty and P.Veron, A Catalogue of Quasars and Active Nuclei, (5-Th edition), ESO,1991.

R.A.Vardanian, Astrofizika ,34, 41, 1991.

L.V.Mirzoyan, R.A.Vardanian, Astrofizika ,35, 211, 1991.

R.A.Vardanian, Astrofizika , 38, 1994 (in press)

R A.Vardanian, Astrofizika, 39 1995 (in press)

V.H.Arp, H.G.Bi, Y.Chu, X.Zhu, Astron. Astrophys, 239,33,1990.

АСТРОФИЗИКА

ТОМ 38 НОЯБРЬ, 1995 ВЫПУСК 4

A NEW VARIABLE STAR IN THE CEPHEUS REGION

N.D.MELIKIAN, A.Ts.KARAPETIAN

Byurakan Astrophisical Observatory

A new variable star has been discovered in the Cepheus region during the spectral observations of dark cloud regions.

The observetions have been carried out with the 40" Schmidt telescope of the Byurakan Observatory. The spectral plates have been obtained by the 4° objective prims (1100 A/mm at H_{α}) on Kodak 103aF and 103aE emulsions through RG610 and RG2 filters.

The limiting photographic magnitude of our observations was about 18.5. The different exposures and epochs of observations have allowed to detect the light variations of stars and variation of intensity of H_{α} emission line during the observational period.

During the period from 1979 to 1989 in the Byurakan Astrophysical Observatory 14 dark clouds regions were observed and about 100 new H_{α} emission stars were discovered in three regions [1-3]. Altogether in these regions a few hundred H_{α} emission stars are known already.

In the next two regions 130 new H_{α} emission stars have been discovered.

In one of these regions a new variable star has been detected on the spectral plates obtained in 1985. In 1985 three plates have been obtained for this region: two plates on August 23 and one in September 8. On the last plate a brightness variation of the star was detected.

In table 1 the following data for this star are presented respectively: coordinates (1950.0), red magnitude of the star (m_r) at minimum of brightness and the amplitude of variation (ΔR).

Table 1

THE DATA FOR THE NEW VERIABLE STAR

α(1950)	δ(1950)	m_r	ΔR
21 10.5	52 55.5	17.5	1.5

In Fig. 1 a, b the star images from the spectral plates obtained in 1985 are shown. As one can see in Fig. 1 b, a very strong H_α emission line exists. On the plates obtained in 1979 the star is again in the minimum without H_α emission.

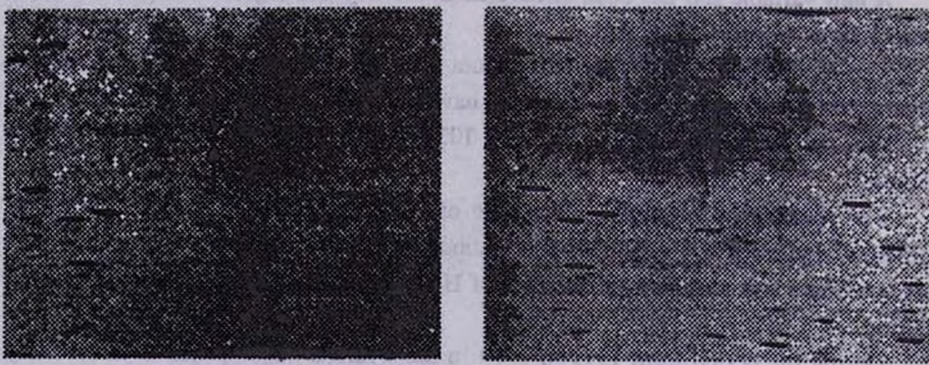

a b

Fig. 1

This star is in Cepheus region. If the distance of the star is the same as for the association Cep OB2 [4], its absolute magnitude will be M_m=8. The star with such an absolute magnitude can be a red dwarf and in all probability it is a flare star.

Новая переменная звезда в области цефея. При спектральных наблюдениях области цефея, была обнаружена новая переменная звезда с амплитудой $\Delta R=1.^m5$. По всей вероятности она является вспыхивающей звездой.

REFERENCES

1. *N.D.Melikian, V.S.Shevchenko, S.Yu.Melnikov,* IBVS, No 3073, 1987.
2. *N.D.Melikian, V.S.Shevchenko,* Astrofizika, 32, 169, 1990.
3. *N.D.Melikian*, Astrofizika, 1994, in press.
4. *S.C.Simonson*, Astrophys. J., 154, 923, 1968.

АСТРОФИЗИКА

ТОМ 38 НОЯБРЬ, 1995 ВЫПУСК 4

FACTORIZATION METHODS IN RADIATIVE TRANSFER THEORY

N.B.YENGIBARIAN, L.G.ARABAJIAN, B.N.YENGIBARIAN

Byurakan Astrophysical Observatory

A wide class of linear and nonlinear problems in Radiative Transfer (RT) theory lead to the integral equation

$$S(\tau) = g(\tau) + \lambda \int_0^\infty K(|\tau - t|)\, S(t)\, dt, \; or \; (\mathrm{I} - \lambda \mathrm{K})\, S = g, \tag{1}$$

where $0<\lambda\leq 1$ is the albedo of scattering .

Let V be the solution of nonlinear factorization equation (NFE)

$$V(\tau) = \lambda K(\tau) + \int_0^\infty V(\tau) V(\tau + t)\, dt; \; t \geq 0 \tag{2}$$

and let $\mathrm{V}_\pm$ be Volterra type operators:

$$(\mathrm{V}_+ f)(\tau) = \int_0^\tau V(\tau - t)\, f(t)\, dt; \; (\mathrm{V}_- f)(\tau) = \int_\tau^\infty V(t - \tau)\, f(t)\, dt.$$

Then there holds the factorization (see [1,2])

$$\mathrm{I}-\lambda\mathrm{K}=(\mathrm{I}-\mathrm{V}_-)(\mathrm{I}-\mathrm{V}_+). \tag{3}$$

In applications to RT the kernel K is usually superposition of exponentials

$$K(\tau) = \int_a^b e^{-|\tau| p}\, G(p)\, dp; \; G \geq 0; \; \int_a^b \frac{G(p)}{p}\, dp = 1 \tag{4}$$

In this case (2) is reduced to Ambartsumian's equation (AE)

$$\varphi(s) = 1 + \varphi(s)\int_a^b \frac{\varphi(p)\,G(p)\,dp}{s+p};\; V(\tau) = \int_a^b e^{-\tau s}\varphi(s)\,G(s)\,ds;$$

$$\int_a^b \frac{\varphi(s)}{s} G(s)\,ds = 1 - \sqrt{1-\lambda}. \qquad (5)$$

Equation (1), including Miln's problem (when g=0, λ=1, S>0) is easily solved by using (3).

In conservative case λ=1, if $\int_0^\infty g(t)\,dt < +\infty$, equation (1) possesses of a solution $S \geq 0$ (see [2,3]).

The results, mentioned above, are generalized to systems of the form (1) (see [4]), which are also widely applied in astrophysics.

In [5] on the basis of these results it is proved that Miln's problem in inhomogeneous medium:

$$S(\tau) = \lambda(\tau)\int_0^\infty K(|\tau - t|)\,S(t)\,dt, S > 0,\ 0 \leq \lambda(\tau) \leq 1,\ \tau \in R^+ , \qquad (6)$$

under conditions $\int_0^\infty t(1-\lambda(t))\,dt < +\infty$ has a solution $S > 0$.

Some methods of solution of the equation (1) by means of repeated factorization are obtained by B.N.Yengibarian recently.The following representation

$$I - \lambda K = (I - U_-)(I - T)(I - U_+),$$

where $U_\pm$ are Volterra operators, and T is the operator of the form K with a simpler structure, lies on the base of these methods.

(a) The split of albedo: Then $I - U_\pm$ are Volterrian factors for $I - \lambda_1 K$, where $0 \leq \lambda_1 \leq \lambda$

(b) Iterative method: Then $U_\pm = K_\pm$ are Volterrian components of K: $K = K_+ + K_-$.The factorization of this type can be repeated several times.

(c) Factorizational interpretation of Chandrasekhar method of discrete ordinates

(MDO). Let the kernel K, in accordance with the MDO, be reduced to a finite sum

$$K(\tau) \approx T(\tau) = \sum_{m=1}^{n} a_m e^{-s_m|\tau|}$$

Then the operator I-λK may be represented in the form

$$\mathrm{I} - \lambda\mathrm{K} = \left(\mathrm{I} - \mathrm{U}_1^-\right)\ldots\left(\mathrm{I} - \mathrm{U}_n^-\right)\left(\mathrm{I} - \mathrm{U}_n^+\right)\ldots\left(\mathrm{I} - \mathrm{U}_1^+\right)$$

where $\mathrm{U}_m^{\pm}$ are "simplest" Volterrian operators with kernels

$$b_m e^{-s_m\tau},\ b_m > 0.$$

Факторизационные методы в теории переноса излучения. **Приводятся факторизационные методы авторов, применяемые при решении и изучении интегральных уравнений переноса в однородном и неоднородном полупространстве. К числу этих ФМ относятся метод нелинейных уравнений факторизации и методы многократной факторизации.**

REFERENCES

1. *N.B.Yengibarian, A.A.Arutyunyan*, M., Mat. Sb., 97, 35, 1975.
2. *L.G.Arabadzhyan, N.B.Yengibarian*, M., Itogy Nauki i Tech. 22, 175, 1984.
3. *L.G.Arabadzhyan*, Izv. Akad. Nauk Arm. SSR. Ser. Math, 16, 65, 1981.
4. *N.B.Yengibarian, L.G.Arabadzhyan*, M., Math. Sb. 124, 189, 1984.
5. *L.G.Arabadzhyan*, Minsk, Diff. Eq. 23, 1618, 1987.

А С Т Р О Ф И З И К А

ТОМ 38 НОЯБРЬ, 1995 ВЫПУСК 4

DIRECT AND INVERSE PROBLEMS OF RADIATIVE TRANSFER

N.B.YENGIBARIAN, M.G.MOURADIAN

Byurakan Astrophysical Observatory

The operator approach to the linear problems of Radiative Transfer (RT) and corresponding apparatus of analytical semigroups (see [1,2]) are very flexible and general means for solution of Direct and Inverse problems of RT, which are of a great importance in astrophysics . Here we present some results, which are mainly taken from [3].

The integral differential equation of stationary RT in a homogeneous slab $\Pi(\tau_0)$ of thickness $\tau_0 \le +\infty$ admits of the following operator representation

$$\pm\frac{dJ^{\pm}}{d\tau} = -AJ^{\pm} + L^{+}J^{\pm} + L^{-}J^{m} \qquad (1)$$

where the vector functions J^{+} and J^{-} describe the radiation intensities at a depth τ in directions of increasing and decreasing τ respectively. $J^{\pm}$ may depend on the direction ω, frequency ν and etc. A and $J^{\pm}$ are operators: A describes absorption of radiation by infinite thin slab and $J^{\pm}$ describe redistribution by ω , ν of emitted radiation.

Let $R(\tau_0)$ and $T(\tau_0)$ be the reflection and transmission operators for a slab $\Pi(\tau_0)$.

Problem 1. By given of $R(\tau_0)$ and $T(\tau_0)$ to find $R_m = R(m\tau_0)$ and $T_m = T(m\tau_0)$, $m \ge 2$.

This problem can be solved by multiple application of well known formulas of addition of layers.

Here we describe a more effective approach to this problem.

Let $W = W(\tau_0)$ is the Canonic solution (CS) of the equation

$$W = (R+TW)(T+RW). \qquad (2)$$

The CS is the limit of natural iteration W_n, with $W_0 = 0$. We have $W \ge 0$ $||W|| \le$

1 and

$$\rho=R+TW,\ X=T+RW \tag{3}$$

where $\rho=R(\infty)$, and $X(\tau)=\exp(-G\tau)$ is the semigroup of operators with generator

$$G=-A+L^{+}+L^{-}\rho,\ \ X(0)=I.$$

We have

$$X(m\tau_o)=X_m(\tau_o) \tag{4}$$

R_m and T_m may be determined by formulae

$$R_m=(\rho-X_m)W_m(I-W^2_m)^{-1},\ T_m=(I-\rho)X_m(I-W^2_m)^{-1} \tag{5}$$

where $W_m=\rho X(m\tau_o)$.

Problem 2. (Division slab in half). By given of $R(\tau_o)$, $T(\tau_o)$ to find $R\left(\frac{\tau_0}{2}\right), T\left(\frac{\tau_0}{2}\right)$.

Problem 3. By given of $R(\tau_o)$, $T(\tau_o)$ to find local properties of the medium.
Solution of the problem 2. We determine W, ρ and X from (2), (3), then we extract the root from $X(\tau_o)$: $X(\tau_o/2)=[X(\tau_o)]^{1/2}$. Operators $R\left(\frac{\tau_0}{2}\right), T\left(\frac{\tau_0}{2}\right)$ are determined from (5) at $m=1/2$.

Solution of the problem 3. Applicating n times repeated operation of division in half the operators $R(2^{-n}\tau_o)$ and $T(2^{-n}\tau_o)$ are created, which for enough large n, describe local properties of the medium. The operators A and $L^{\pm}$ participating in (1) may be found by means of them.

The operator $\rho=R_\infty$ is the CS of Ambartsumian's equation

$$A\rho+\rho A=L^{-}+\rho L^{+}+L^{+}\rho+\rho L^{-}\rho. \tag{6}$$

At $L^{+}=L^{-}=L$ we obtain

$$L=(I+\rho)^{-1}(A\rho+\rho A)(I+\rho)^{-1} \tag{7}$$

The formula (7) solves inverse problem 4.

Problem 4. By given ρ to determine $L(L=L_{+}=L^{-})$.

From Eq. (7) and well known connection between A and L may be determined A and L by iteration way.

In work [4] a matrix representation of L^* in case of coherent anisotropy scattering were found.

Above mentioned results may be applied to the problems of distance probe for atmosphere of earth and other planets.

Прямые и обратные задачи переноса излучения. На основании операторного подхода к линейным задачам переноса (ЛЗП) и соответствующего аппарата аналитических полугрупп предлагаются некоторые методы решения ЛЗП и задач по восстановлению локальных оптических свойств плоского слоя по наблюдаемым характеристикам всей среды.

REFERENCES

1. *A.Shimitzu, K.Aoki,* Applic. of invariant embedding, Acad. Press. New York. 1972.
2. *N.B.Yengibarian, M.A.Mnatsakanian,* Docl. Acad. Sc. USSR, 217, 3, 1974.
3. *N.B.Yengibarian M.G.Mouradian,* DAN Arm. SSR, 36, 122, 1988.
4. *M.G.Mouradian,* Comput. Math. and Math. Phys; 33, No.2, 241, 1993.

АСТРОФИЗИКА

ТОМ 38 НОЯБРЬ, 1995 ВЫПУСК 4

NEW APPROACHES TO SOME CLASSIC METHODS OF RADIATIVE TRANSFER

N.B.YENGIBARIAN, E.A.MELKONYAN

Byurakan Astrophysical Observatory

1. *About the Method of Discrete Ordinate (MDO).* Let us consider the well known integral Equation of Radiative Transfer (RT).

$$S(\tau) = S_0(\tau) + \frac{\lambda}{2}\int_0^{\tau_0} K(|\tau - t|)\, S(t)\, dt \tag{1}$$

where

$$K(\tau) = E_1(\tau) = \int_1^{\infty} e^{-\tau s}\frac{ds}{s}$$

Application of MDO leads to the following reduction

$$K(\tau) \approx T(\tau) = \sum_{m=1}^{n} a_m e^{-|\tau| s_m} \tag{2}$$

where $\frac{1}{s_m}$ are the positive roots of Legendre polynomial $P_{2n}(\eta)$ and $a_m > 0$.

Such choice of nodes of discretization (2) does not correspond to the essence of the problem.

Let S be the solution of (1) when K is replaced by T. For deviation $\|S-\tilde{S}\|$ we have the estimate

$$\|S-\tilde{S}\| \le (1-\lambda)^{-1}(1-\lambda-\delta)^{-1}\delta\|S_0\|$$

where

$$\delta = \delta(s_1, s_2, \ldots s_n, a_1, a_2, \ldots a_n) = 2\int_0^\infty |K(\tau) - T(\tau)|\, d\tau.$$

In [4] the problem of minimization of δ for fixed n, when K is arbitrary superposition of exponentials

$$K(\tau) = \int_a^b e^{-|\tau|s}\, G(s)\, ds, \quad G \geq 0$$

was solved.

2. *About the Method of Spheric Harmonics (MSH).* Consider the problem of anisotropic scattering. MSH is based on the reduction

$$g(\mu) \approx \tilde{g}(\mu) = \sum_{m=0}^{n} c_m P_m(\mu)$$

where $g(\mu)$ is the indicatrix of scattering, P_m are Legandre polinomials, and c_m are the corresponding Fourier coefficients. It was shown that the choice of this coefficients, based on requirement of minimization of quantity

$$\delta = \delta(c_0, c_1, \ldots c_n) = \int_{-1}^{1} \left[g(\mu) - \sum_{m=0}^{n} c_m P_m(\mu) \right]^{-1} d\mu$$

is more effective. The problem of minimization of δ for fixed n can be solved by numerical methods.

3. *About Principle of Invariance (PI).* Consider the general linear Transfer Equation in homogeneous half-space $\Pi(0,+\infty)$ (see [5]).

$$\pm \frac{d\mathbf{J}^{\pm}}{d\tau} = -\mathbf{A}\mathbf{J}^{\pm} + \mathbf{L}^{+}\mathbf{J}^{\pm} + \mathbf{L}^{-}\mathbf{J}^{\pm} \qquad (3)$$

where the vectors $\mathbf{J}^{+}$ and $\mathbf{J}^{-}$ are the desired radiation intensities at the optical depth τ in directions of increasing and decreasing τ respectively.

The operators A and $\mathbf{J}^{\pm}$ describe the absorption and redistribution of radiat n by infinite thin slab.

Ambartsumian's equation corresponding to (3) has the form

$$A\rho + \rho A = L^- + \rho L^+ + L^+\rho + \rho L^-\rho \tag{4}$$

where ρ is the operator of reflection from $\Pi(0,+\infty)$. It was shown, that the Eq. (4) has always unique physical solution (PS), which is the limit of iterations ρ_n , determined by

$$A\rho_{n+1} + \rho_{n+1}A = L^- + \rho_n L^+ + L^+\rho_n + \rho_n L^-\rho_n,\ \rho_0 = 0.$$

PS is the minimal positive solution of (4).

Новые подходы к некоторым классическим методам теории переноса излучения. Предлагаются новые, математически обоснованные, подходы к Принципу инвариантности Амбарцумяна, методу дискретных ординат Чандрасекара и методу Сферических гармоник.

REFERENCES

1. *V.A.Ambartsumian,* S.c. Works I , Yerevan, 1960.
2. *S. Chandrasekhar,* Radiative Transfer, Oxford, 1950.
3. *V. V.Sobolev,* Radiative Transfer, Moscow, 1956, (in Russian).
4. *N.B.Yengibarian, E.A.Melkonian,* DAN SSSR, 292, 322, 1987.
5. *N.B.Yengibarian, E.A.Melkonian,* Principle of invariance and its Applic., Proc. of the 1981 Sympossium in Byurakan, Yerevan, 1989.

АСТРОФИЗИКА

ТОМ 38 НОЯБРЬ, 1995 ВЫПУСК 4

KONISHI - KANEKO MAP AND FEIGENBAUM UNIVERSALITY

V.G.GURZADYAN, A.MELKONYAN, K.OGANESSYAN

Department of Theoretical Physics, Yerevan Physics Institute

The study of chaotic properties of N - body gravitating systems has become one of essential problems of stellar dynamics [1]. An interesting possibility of study of N - body dynamics is provided by the iterated maps [2, 3]. From this point of view the demonstrated by Inagaki [2] agreement of Konishi - Kaneko map with the thermodynamic formalism and the results of numerical simulations, is of particular importance.

The Konishi - Kaneco map is defined as follows [4,5]:

$$p_i^{n+1} = p_i^n + k\sum_{j=1}^{N}\sin 2\pi\left(x_j^n - x_i^n\right), \tag{1}$$

$$x_i^{n+1} = x_i^n + p_i^{n+1};(mod\, 1). \tag{2}$$

This system describes 1 - dimentional N - body system with a pontential of interaction which is free of singularity and is attractive if $k>0$.

To study the possibility of existing of period - doubling bifurcations, first, we have to check the necessary condition, i.e. the negativity of the Schwartzian derivation:

$$Sf = f'''/f'' - 3/2\left(f''/f'\right)^2 < 0. \tag{3}$$

This condition is fulfilled for Eqs. (1) and (2) since $f'''/f'<0$ for any value of k.

The numerical calculation were performed as follows. The point is to observe via computer analysis the period - doubling befurcations and to calculate the scaling defined by the Feigenbaum number δ for Konishi - Kaneko map. To obtain the bifurcation scale δ we have to find out the values of period - doubling bifurcation points which must satisfy the conditions

$$\sum_{j}^{N}\left|x_j^{n+1}-x_j^{n}\right|<\varepsilon,\left(2^1=2\right);\ \sum_{j}^{N}\left|x_j^{n+2}-x_j^{n}\right|<\varepsilon,\ \sum_{j}^{N}\left|x_j^{n+3}-x_j^{n+1}\right|<\varepsilon,\left(2^2=4\right);$$

for each k_n, n=1,2,..., respectively. The ε is the accuracy of the obtained values of k_n.

Our numerical calculation of k_1 e. g. for N=10 $\varepsilon=10^{-5}$, and 10^{-4} for k_2 and k_3. These calculations were enough to find out the Feigenbaum universal number δ=8.72... (cf. [3]). The result of calculations for N=10 are given in Table 1.

Table 1

k_1	k_2	k_3	δ
0.015000...	0.015196...	0.01521822...	8.82...
0.015000...	0.015194...:	0.01521622...	8.78...
0.015000...	0.01519368...	0.01521590...	8.71584...
0.015000...	0.01519368...	0.01521578...	8.76359...
0.015000...	0.01519368...	0.01521593...	8.70490...
0.015000...	0.01519368...	0.01521591...	8.71219...
0.015000...	0.01519368...	0.01521589...	8.71950...
0.015000...	0.01519368...	0.01521587...	8.72682...
0.015000...	0.01519368...	0.015215885...	8.72315...
0.015000...	0.01519368...	0.015215889...	8.71950...
0.015000...	0.01519368...	0.015215887...	8.72315...

The results for other values of N are absolutely identical with those for N=10, though with different accuracy ε. We have noticed a clear decrease in the accuracy with the increase of the number of particles.

Using the obtained values of k_n and the formula

$$k_\infty=\left(\delta\, k_{n+1}-k_n\right)/\left(\delta-1\right), \tag{4}$$

we also estimate the k_∞, from which the chaotic behavior of the system is established and map (sequence) never repeats itself:

$$k_\infty = 0.1307....$$

At $k>k_\infty$ the system should have positive Lyapunov numbers. This fact supports the results in [5] on the estimation of Lyapunov numbers.

Thus, we showed the existence of period - doubling bifurcations and numerically calculated the Feigenbaum number for the Konishi - Kaneko map. The period - doubling points correspond to the phase transitions of second order and can enable the study of such systems via the methods of thermodynamical formalism.

Система Кониши-Канеко и Фейгенбаум универсальность. Компьютерный анализ системы Кониши-Канеко показывает существование бифуркаций удвоения (периода), что обусловлено соответствующим условием для производной Шварца. Значение контрольного параметра k_∞, соответствующего переходу в хаотическую фазу оценено наряду с универсальными постоянными Фейгенбаума. Подобный факт может быть решающим в порядке исследования хаоса в звездной динамике.

REFERENCES

1. "Ergodic Concepts in Stellar Dynamics", 1994, Eds: Gurzadyan V.G., Pfenniger D, Springer - Verlag.
2. *S.Inagaki*: 1994, in " Ergodic Concepts in Stellar Dynamics ". Eds: Gurzadyan V.G., Pfenniger D., Springer - Verlag, p.105.
3. *S.-Y.Kim*: 1994, Phys. Rev. E. B 50, 1992.
4. *T.Konishi, K.Kaneko*: 1992, J. Phys. A, 25, 6283.
5. *T.Konishi, K.Kaneko*: 1994, in: " Ergodic Concepts in Stellar Dynamics ". Eds: Gurzadyan V.G., Pfenniger D., Springer - Verlag, p.95.

АСТРОФИЗИКА

ТОМ 38 НОЯБРЬ, 1995 ВЫПУСК 4

THE BEHAVIOR OF KS-ENTROPY OF N-BODY SYSTEMS AND RICCI CURVATURE

A.A.MELKONYAN
Yerevan Physics Institute, Yerevan, Armenia

1. The study of various statistical properties of N-body systems can be crucial for the understanding of many astrophysical problems - from the dynamics of the Solar system up to the dynamics of clusters of galaxies [1].

Below will consider two methods of the study of chaotic properties of N-body gravitating systems:

1. Lyapunov exponents and KS-entropy;
2. Ricci curvature.

In the first case the aim is to reveal whether the behavior of the system with given boundary conditions is chaotic or not. In the second case we investigate the "comparative" behavior of two close systems and will estimate their relative instability with respect to each other.

2. Lyapunov numbers show the exponential rate of divergence of close trajectories, and are defined as:

$$\lambda(x,t) = \lim_{t\to\infty} 1/t \ln \frac{d(x_0,t)}{d(x_0,0)},$$

with a spectrum: $\lambda_1 < ... < \lambda_M$, where M is the dimension of the phase space. The existence of the limits and of the order is established by Oseledets theorem.

KS-entropy is the sum of positive Lyapunov exponents and defined as:

$$KS = \sum_{\lambda_i > 0} \lambda_i .$$

To demonstrate the complicated behavior of the chaotic properties of the systems on control parameters even for relatively simple systems, we will consider the following 1D Hamiltonian system:

$$H = \sum_{i=1}^{n} p_i^2 / 2m + \sum_{i=1}^{n}\left(Ax_i^4 - Bx_i^2 + B^2/4A\right) + C/2\sum_{i=1}^{n}\left(x_{i+1} - x_i\right)^2,$$

where A,B,C>0 are positive constants.

Lyapunov numbers and KS-entropy of this system have been calculated using the algorithm by Bennetin et al [2]. Some results of calculations are represented in Fig.1 and Fig.2. It's interesting, that A and B parameters are symmetrical.

Such behavior has been overlooked in some previous studies of this system [3].

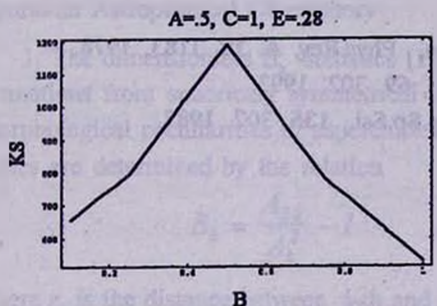

Fig. 1.

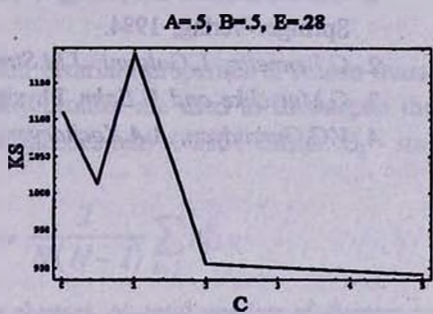

Fig. 2.

3. Ricci curvature is a geometrical method for study relative chaotic behavior of close geodesics, introduced in [4].

Ricci curvature is defined as:

$$r_u(s) = \frac{Riemu^j u^j}{|u|^2}$$

Consider some interval S, and denote r, as:

$$r = 1/3\,Ninf\left[r_u(s)\right].$$

Consider two systems with value of Ricci curvature r_1 and r_2 accordingly within this interval $[0,s_1]$. We will conclude, that first system is less stable with respect second system within this interval, if $r_1 < r_2$ and $r_1 < 0$. Numerical experiments have been performed for various configurations of N-body gravitating systems with fixed values of control parameters (energy, momentum, etc.).

Поведение KS-энтропии систем N-тел и кривизна Ричи. **На отдельных примерах рассмотрены два метода изучения хаотических свойств многомерных нелинейных динамических систем. Представлены результаты расчетов KS-энтропии на примере 1D системы N-тел для различных параметров.**

REFERENCES

1. *V.G.Gurzadyan, D.Pfenniger,* (Eds.) Ergodic Concepts in Stellar Dynamics, Springer-Verlag, 1994.
2. *G.Bennetin, L.Galgani, J.M.Strelcyn,* Phys.Rev. A. 18, 1183, 1978.
3. *G.Mutschke and U.Bahr*, Physica D, 69, 302, 1993.
4. *V.G.Gurzadyan, A.A.Kocharyan*, Ap.Sp.Ssi., 135, 307, 1987.

АСТРОФИЗИКА

ТОМ 38 НОЯБРЬ, 1995 ВЫПУСК 4

INTEGRAL GEOMETRIC METHOD OF MORPHOLOGICAL INVESTIGATION OF EXTRAGALACTIC SYSTEMS

G.A.SAIYAN

Byurakan Astrophysical Observatory

1. The dimensionless B_k -statistics [1,2] and invariant properties of Radon transformations from sphericaly symmetrical density profiles are used to investigate the morphological peculiarities of superclusters of galaxies and A 2151 cluster. B_k - statistics are determined by the relation

$$B_k = \frac{A_{2k}}{A_k^2} - 1 \qquad A_k = \frac{2}{N(N-1)} \sum_{i=j} r_{ij}^k$$

where r_{ij} is the distance between i-th and j-th clusters, N- total number of clusters in supercluster. A_k - statistics are related with certain aspects of integral geometry [2], particularly with Blashke problem on the characterization of convex bodies in - n-dimensional Euclidean space [3]. A_k - statistics are approximations (at $N \to \infty$) of the functionals. That is they are - k-order moments of pair distribution (distance between two points) inside of body or random chord length distribution in the case of point arrangement on its surface.

Extrema of the functionals (and consequently A_k, B_k - statistics) are necessary characteristics of bodies and may be used to determine of geometrical forms of complicated astrophysical systems. One can calculate analyticaly (at $N \to \infty$, see Table 1) and numericaly for final N the values of B_k- statistics for a few special geometrical configurations. These values must be compared with observational ones. We studied morphology of 16 superclusters of galaxies from West list [4]. The number of clusters in selected superclusters satisfies the condition $N > 4$. For our purpose we used a compilation of redshifts and velocity dispersions for Abell clusters [5]

Table 1

Figure/statistics	B_1	B_2	B_3	B_4
ball	0.134	0.429	0.837	1.357
sphere	0.125	0.333	0.562	0.800
circle	0.220	0.670	1.289	2.041
circumference	0.234	0.500	0.735	0.941
straight chain	0.500	1.400	2.571	4.000

Here we present preliminary results of statistical analysis and numerical simulations for different values of N. Superclusters seemed to have quite different morphological properties.Some of them are flattened systems (probabaly pancake or disk - shaped, SC 8, N = 7) or flattened and elongated simultaneously, for example SC 12, N=4 (clusters are numerated according to West list). Having close to spherical forms the superclusters are also existed (SC 11, N=5).

2. *To investigate the large scale asymmetry of any system of objects first* of all it is necessary to select those signs which allows to distinguish sphericaly symmetric systems amongst the others. Such signs have to be invariant under the projective transformations of the system or under the special transformations which forms subclass in the class of projective transformations. We considered Radon transformation $F(p)$ of space density $f(r)$ in n - dimensional spherical volume. Function $F(p)$ is an integral along the hyperplane, which intersects this sphere at the p - distance from the center. One can show that ortogonal projections of sphericaly symmetric distributions on the linear subspaces of Euclidean space all have the same Radon transformation which equaled to linear density. This result has a simple consequence - the mass of the sphere on the one side from hyperplane is independent of its orientation. Taking into account this property one can show the presence of eastern asymmetry of central region as well as northeast to south-west elongation in distribution of galaxies in the cluster A 2151, the structure of which was already investigated by isodensitometric method [6].

The publication of more detailed paper about discussed problems should follow.

Интегрально-геометрический метод морфологического исследования внегалактических систем. С помощью моментов парного распределения и преобразования Радона от пространственной плотности исследуются конфигурации сверхскоплений галактик, а также тонкая структура скопления Abell 2151.

REFERENCES

1. *J.M.Koudryavtsev.*, Vestnik LGU,N 15, 74, 1985
2. *G.A.Saiyan.*, Astron. Zhourn., 68, 5, 1036, 1991.
3. *L.Santalo.*, Integral Geometry and Geometric Probability., M,Nauka" (in Russian), 1983, p. 360.
4. *M.F.Struble, H.J.Rood.*, Ap.J.Suppl.Ser., 63, 543, 1987.
5. *M.J.West.*, Ap.J., 347, 610, 1989.
6. *D.Maccagni, B.Garilli, M.Tarenghi*, Ap.J., 109, 465, 1995.

CONTENTS

continued

~~400 դր.~~
700 դր.

CONTENTS